# Decomposition and Fire Retardancy of Naturally Occurring Mixtures of Huntite and Hydromagnesite.

**by**

**Luke Hollingbery**

A thesis submitted in partial fulfilment for the requirements of the degree of
**Doctor of Philosophy**
at the
**University of Central Lancashire**
In collaboration with
**Minelco**

**July 2011**

I declare that while registered as a candidate for the research degree, I have not been a registered candidate or enrolled student for another award of the University or other academic or professional institution.

I declare that no material contained in this thesis has been used in any other submission for an academic award and is solely my own work.

Signature of Candidate_____

*(Mr Luke Hollingbery)*

Type of Award *Doctor of Philosophy*

Name of School *Centre of Fire and Hazards Science in the School of Forensic and Investigative Sciences.*

# Abstract

Mixtures of the two minerals huntite and hydromagnesite have been successfully used as a fire retardant additive in polymers for many years. The onset of decomposition of hydromagnesite is at a higher temperature than that of aluminium hydroxide but lower than that of magnesium hydroxide, the two most commonly used mineral fire retardants. This makes it an ideal addition to the range of materials available to polymer compounders for improving fire retardant properties.

In comparison to the better known mineral fire retardants there has been little published research on the fire retardant properties of huntite and hydromagnesite. What has been published has often been commercially orientated and the limited quantity of scientific literature does not fully explain the fire retardant mechanism of these blends of minerals, often dismissing huntite as having no useful fire retardant action other than diluting the solid phase fuel.

Standard thermal analysis techniques (thermal gravimetric analysis, differential scanning calorimetry, Fourier transform infra-red analysis) have been used to characterise the thermal decomposition of huntite and hydromagnesite from a source in Turkey. This has lead to an understanding of the decomposition mechanism of the minerals in terms of mass loss, enthalpy of decomposition, and evolved gases between room temperature and 1000°C. Hydromagnesite endothermically decomposes between about 220°C and 500°C, initially releasing water followed by carbon dioxide. The rate of heating and partial pressure of carbon dioxide in the atmosphere can influence the mechanism of carbon dioxide release. Huntite endothermically decomposes between about 450°C and 800°C releasing carbon dioxide in two stages.

The use of the cone calorimeter to study the rate of heat release during combustion of ethylene vinyl acetate based polymer compounds has lead to an understanding of how

both huntite and hydromagnesite affect the burning processes at different stages of the fire. By varying the ratio of the two minerals, hydromagnesite has been shown to increase the time to ignition and reduce the initial peak in rate of heat release, while huntite has been shown to reduce the rate of heat release later in the fire.

It has been shown that huntite is far from being an inactive diluent filler. The endothermic decomposition of huntite in the later stages of the fire reduces the heat reaching underlying polymer and continues to dilute the flame with inert carbon dioxide. The platy huntite particles have been shown to align themselves in such a way that they can hinder the escape of volatiles from the decomposing polymer and also physically reinforce the inorganic ash residue.

# Table of Contents

# Index of Figures

# Index of Tables

# Acknowledgements

I would like to thank the following for their assistance given in many varied ways and without which this thesis would not have been possible:

Professor T. Richard Hull from the Centre of Fire and Hazards Science at the University of Central Lancashire for his support as PhD Director of Studies for this work. His guidance and encouragement throughout this process has been invaluable.

Dr. Anna Stec for her help as second academic supervisor of this work.

Minelco for their financial support. In particular Mr Ian Yates of Minelco GmbH for his personal enthusiastic support in initiating this PhD research and allowing me to achieve my ambition of increasing our knowledge (and hopefully sales) of huntite and hydromagnesite by studying at PhD level. Mr Stefan Viering for his constant supply of challenging ideas and theories on the subject of fire retardancy and the use of mineral fillers in general. Miss Patthrapa Ngamkanokwan for her work in the laboratory over the last few years that has allowed me to concentrate more of my time on this subject. Mrs Seleena Creedon for her help with the printing of this thesis and various posters for conferences and other materials related to this work. Mr Gareth Brown for his unique methods of obtaining the samples of the natural pure hydromagnesite used in this work.

All members of the Centre for Fire and Hazards Science that have helped me over the past few years. Firstly Mr Steve Harris for his much appreciated efforts in maintaining and fixing the cone calorimeter on many occasions. Of course my fellow students, particularly Jen, Parina, Cameron and Artur for the help and encouragement they all offered at various times. Mr Dave Kind for his endless enthusiasm and long conversations during shared car journeys up and down the M6.

My parents and step-parents for bringing me up to work hard, study hard to improve myself, and have a fascination with science.

Finally, but by no means least to my wife Heidi for pushing me onward and constantly reminding me that I can do this at the times when I was fed up and struggling to motivate myself. Thanks also to Heidi for recently falling pregnant with our first child, I love you.

# 1. Introduction

## 1.1 Introduction to Minelco and the minerals huntite and hydromagnesite

Minelco is a subsidiary of the Swedish government owned company, Luossavaara-Kiirunavaara AB (LKAB). The main business of LKAB, which was founded in 1890, is the mining of magnetite ($Fe_3O_4$), at one of the world's largest underground mines. LKAB's mines are located within the Arctic Circle in the far north of Sweden. The main market for this iron ore is the iron and steel industry; however a small quantity of magnetite is supplied to other industries including the polymer industry. Originally LKAB's subsidiary, Minelco, was setup to deal with these markets. Minelco processes the magnetite into a fine power that has useful properties for the polymer market. It has a high density (5.1 $gcm^{-3}$), is electrically and thermally conductive, and responds to microwave heating. Typical applications for the material are sound deadening in the automotive market, cosmetics, building and construction, electrical appliances, magnetic paints, and many more.

In 2002 LKAB acquired the Frank and Schulte Fillers and Minerals division from Stinnes AG. Microfine Minerals was part of the Frank and Schulte Fillers and Minerals division and was renamed under the Minelco brand. Microfine Minerals already had a portfolio of minerals used in the polymer, construction, coatings, and other industries. Minelco is now an international company with processing and / or office facilities in the UK, USA, Sweden, Finland, Germany, The Netherlands, Spain, Greece, Turkey, Hong Kong, and China. As part of Minelco's strategy of controlling the supply chain from the mine to the end user, Minelco owns and mines its own sources of selected minerals, most notably phlogopite mica from Finland and mixtures of huntite and hydromagnesite from Turkey. It also processes and trades a wide range of other minerals including: talc, wollastonite, muscovite mica, expandable graphite, ground aluminium hydroxide,

marble, dolomite, chalk, barytes, magnetite, bentonite, chromite, and olivine amongst many others. These minerals are used in a wide range of applications as diverse as refractories, construction, road surface markings, water treatment, surface coatings, oil drilling, and many polymer applications both to enhance fire retardancy and to improve other physical properties or simply for decorative effect.

As one of Minelco's 'selected' minerals, blends of huntite and hydromagnesite are of great importance to the company. Minelco has invested in purchasing a large source of the mineral and therefore needs to see maximum return on this investment. Therefore a high level of research and development investment is available for understanding and developing the product in order to open up new markets and grow existing ones.

UltraCarb is the brand name under which Minelco sells the mixed mineral as a fire retardant. It comprises of varying proportions of huntite and hydromagnesite. Its main application is in the wire and cable industries as an alternative to ATH in PVC, halogen free, and rubber applications. However is also finds use as a fire retardant in other applications including roofing membranes and other polymer applications where fire retardancy is important. The minerals have other industrial uses but the focus of this work is fire retardancy. The purpose of this work is to study and gain an in depth understanding of the thermal decomposition mechanisms of huntite and hydromagnesite and how the individual minerals function together to provide a fire retardant action in polymers. Using this understanding will allow the performance of huntite and hydromagnesite in its current applications to be optimised in terms of the mix of minerals and particle sizes. The overall aim of the project is to use the knowledge gained to develop new improved grades and open up new areas of application in order to grow the Minelco business.

## 1.2 Introduction to fire

Man has known how to create and control fire for thousands of years. In its controlled form it is a useful tool bringing heat and power. When it is out of control it is a destructive killer, therefore the study of fire and how to control and prevent unwanted

fires is of great importance. In order for any combustible material to burn there are three things that are required.

1. Fuel
2. Heat
3. Oxygen

If any one of these components is missing or in limited supply a fire is unsustainable and will not propagate. If there is no fuel, there is nothing to burn. If there is no oxygen, fire cannot be sustained. If there is no heat, decomposition and volatilisation of combustible products will not occur. Each of these components has a direct effect on the fire; therefore no two fires will ever be exactly the same. Different fuel sources, oxygen supply, and heat input will all contribute to exactly how the fire progresses. Once the fire is in progress there is feedback into each of these components as follows:

- The fuel is depleted as the fire progresses and consumes materials.
- How well ventilated and how developed the fire is determines the oxygen concentration.
- The heat input to the fire varies from the initial heat source throughout the fire as the fire develops and generates its own heat dependant on the amount and type of fuel, and the supply of oxygen.

This is often represented as a triangle (Figure 1) , known as 'the fire triangle', which illustrates the point that removing or restricting any of the three components will lead to a diminishing or extinguishing of the fire.

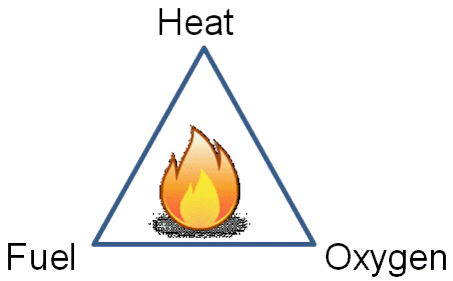


Figure 1: The fire triangle

A full scale uncontrolled fire develops through a series of stages from the initial ignition source through to the burning of a whole item, room, or building.

The initial source could be something as simple as a discarded cigarette, an electrical fault, an unattended candle, or any other heat source with enough heat output to ignite nearby combustible materials. For example, an electrical fault in a TV or stereo causing the copper wires to heat up could lead to the insulation layers on the wires reaching a high enough temperature for them to start to decompose and combust. In turn the small flame from the combustion of the insulation on the wire could then ignite the circuit board, and then the casing of the TV itself. A fully burning TV would have enough radiant heat to spread the fire to surrounding furniture, curtains, waste paper baskets etc. Once the radiant heat within the room reaches a high enough level most of the items within the room will begin to chemically decompose emitting decomposition gases. These gases will rise and accumulate near the ceiling in the room. These gases may react slowly with oxygen resulting in heating but once the temperature reaches about 700°C they will ignite with the flames emitting thermal radiation. This sudden ignition of the decomposition gases results in flashover. The resulting radiant heat will cause wide spread pyrolysis of all exposed fuel surfaces leading to spread of fire to the whole room. Once flashover has occurred the fire is in its fully developed state, the entire room in which the fire started will be blazing and the fire will spread to neighbouring rooms, ultimately engulfing the whole building. In these circumstances the fire can spread faster than people can run and the objectives of the fire fighters change from extinguishment to containment within a particular building or enclosure. Ultimately the aim of fire retardancy is to prevent these highly destructive conditions from occurring.

Finally the fire will enter its end stages as the amount of combustible material is reduced and the rate of fire growth decreases. The fire will slow and eventually self extinguish once all of the combustible material has been consumed.

It is for these reasons that studying fire retardants is important. Once flashover has occurred it is too late and no fire retardant will prevent a polymer from burning.

Slowing down or preventing the initial ignition, of for example a TV with an electrical fault, is possible. This may prevent to fire from occurring or if the fire does occur may give any occupants of the building vital extra seconds to escape.

## 1.3 Polymer structures

Brydson[1] defines a polymer as "a large molecule built up by repetition of small, simple chemical units". The repeat unit is known as the monomer, when the repeat units form a chain the chain is known as a polymer. For example polyethylene is built of many ethylene monomer units as illustrated in Figure 2.

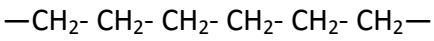


Figure 2: Molecular structure of polyethylene

In commercial use the length of polymer chains is commonly between 1000 and 10000 repeat units. Many different polymers with differing physical and chemical properties can be produced by the addition of chemical side groups or though modification of the main chain.

Some typical polymers illustrating the replacement of hydrogen atoms with side groups or other elements are polypropylene and polyvinylchloride[2]. In polypropylene one of the hydrogen atoms of the polyethylene monomer is replaced by a methyl group giving a repeat unit as show in Figure 3, PVC replaces a hydrogen atom with chlorine to give a repeat unit as shown in Figure 4.

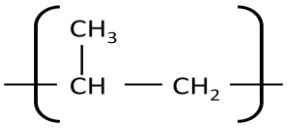


Figure 3: Polypropylene repeat unit

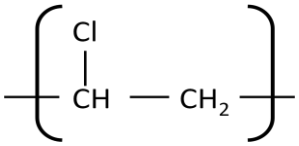


Figure 4: Polyvinylchloride repeat unit

Modification of the carbon backbone of the polymer chain with other groups and elements can result in polymers such as polyethylene terephthalate (Figure 5), which incorporates a benzene ring and oxygen atoms, and silicone rubber (Figure 6) in which the carbon atoms are completely replaced by silicon and oxygen atoms.

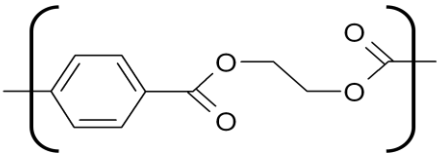


Figure 5: Polyethylene terephthalate repeat unit

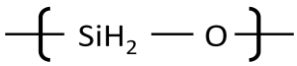


Figure 6: Silicone rubber repeat unit

By modifying the backbone and side groups in this way a huge array of polymers can be created, each with differing properties.

Most polymers are melt processed to create polymer blends or to incorporate other additives such as fire retardants, fillers, stabilisers, and colours. Hydromagnesite, a mineral used to fire retard polymers, begins to endothermically decompose at about 220°C (this will be discussed in more detail later), which means that the polymers that can be fire retarded by hydromagnesite are currently limited to those that can be processed below this temperature. This means that hydromagnesite is commonly used in polymers such as polyolefins, ethylene vinyl acetate (EVA) and polyvinylchloride. EVA is widely used in the wire and cable industry for producing insulation and sheathing compounds. It is a flexible polymer and also has the ability to accept high loading levels of fire retardant fillers such as hydromagnesite, aluminium hydroxide, or magnesium hydroxide. Ethylene vinyl acetate is a copolymer of ethylene and vinyl

acetate, the molecular structure is shown in Figure 7. The amount of vinyl acetate within the copolymer can vary[3] up to a total content of about 70%. As the vinyl acetate content increases the polymer becomes less crystalline and more rubbery, although above 70% content the copolymer stiffens and becomes brittle.

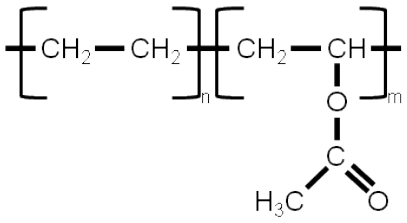


Figure 7: Molecular structure of ethylene vinyl acetate copolymer

## 1.4 Decomposition of polymers

Polymers are becoming used in ever increasing volumes due to their versatility and excellent properties for a wide range of applications. One drawback of many polymers is that they are highly flammable leading to an increased fire risk wherever they are used.

When a thermoplastic polymer is heated it will usually soften and become mouldable. This process is essential for the processing of polymers and is partly what makes polymers so versatile. Thermoset polymers will initially flow and then the action of the heat will initiate a chemical process known as crosslinking which produces chemical links between the polymer chains. Once these crosslinks have been formed the polymer will no longer soften to the point of becoming mouldable even at high temperatures. During normal processing polymers are kept below their decomposition temperature, but in a fire situation the polymer can begin to decompose. The American Society for Testing and Materials (ASTM) defines a number of terms[4] relating to polymer decomposition and combustion; among the terms defined are decomposition and degradation. Degradation is defined as “a process whereby the action of heat or elevated temperature on a material, product, or assembly causes a loss of physical, mechanical, or electrical properties”. Decomposition is defined as “a

process of extensive chemical species change caused by heat". During combustion of polymers thermal decomposition is an important process. Thermal decomposition is the correct term to use because this involves the generation of volatile decomposition products, therefore the chemical species is changing due to heat. In a fire decomposition of a polymer can be caused either by an external heat source, or by the heat generated from the combustion of the decomposition products of the polymer within the flame. The way in which a polymer decomposes depends on a number of factors but there are four main mechanisms by which they decompose[5-7] these are discussed below.

### 1.4.1 Random chain scission

Random chain scission is the random breaking of bonds in the polymer backbone, resulting in two shorter polymer chains and a smaller proportion of monomer units where the random scission occurs at the end of the chain. This creates free radicals at the break in the chain (Figure 8).

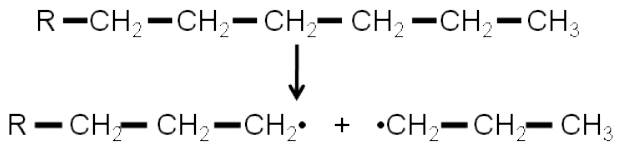

Figure 8: Random break in the polymer chain creating free radicals

These free radicals further propagate the decomposition by either intra or inter-molecular hydrogen transfer creating further chain scission and free radicals. The free radical takes a hydrogen atom either from another random point in the same polymer chain (Figure 9) or a neighbouring polymer chain (Figure 10) causing the creation of a double bond, further fragmentation and the formation of an additional free radical. This process continues in the solid phase until fragments are produced which are small enough to be volatile and escape through the decomposing polymer to enter the gas phase. As shown in Figure 9 and Figure 10 polyethylene decomposes by random chain scission.

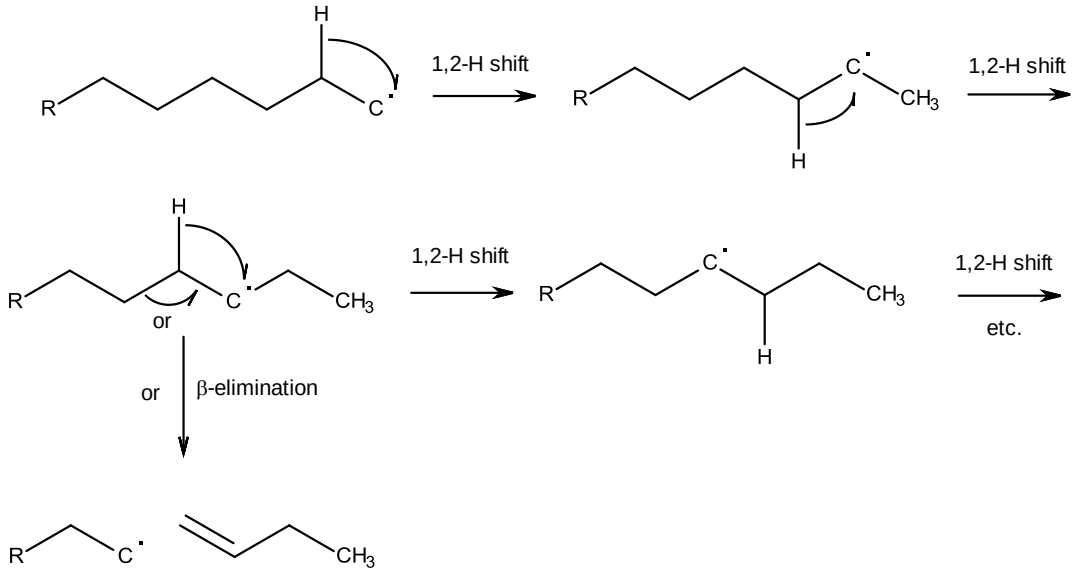


Figure 9: Intramolecular hydrogen transfer

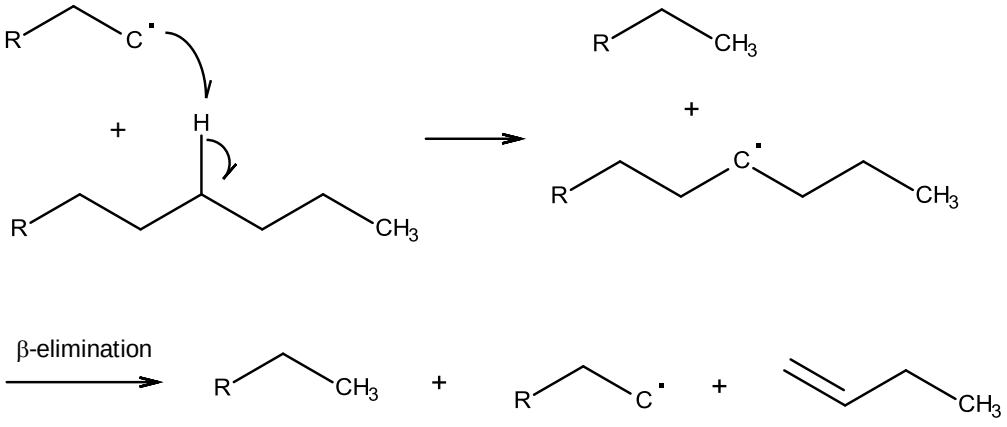


Figure 10: Intermolecular hydrogen transfer

### 1.4.2 End chain scission (unzipping)

End chain scission, also known as unzipping occurs when chain scission occurs only at the end of the polymer chain resulting in the decomposition of the polymer into its monomer units rather than the mixture of chain lengths produced from random chain

scission. The mechanism does not involve hydrogen transfer it is simply the depolymerisation of the polymer back into its monomer units (Figure 11).

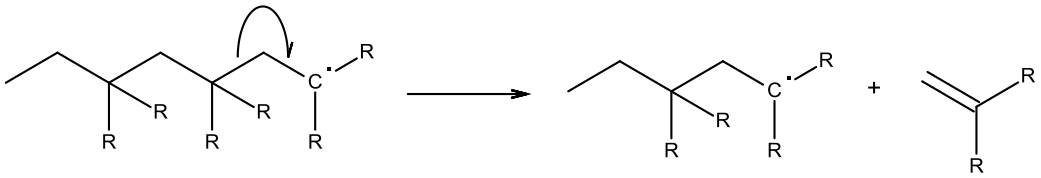


Figure 11: End chain scission (unzipping)

Polymethylmethacrylate (Figure 12) is an example of a polymer that thermally decomposes by unzipping, because the methyl group directly attached to the carbon backbone stabilises the free radical on the $CR_2\cdot$ end group which then transfers along the chain.

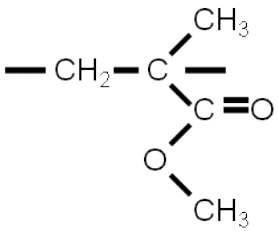


Figure 12: Monomer unit of polymethylmethacrylate

### 1.4.3 Chain stripping

Chain stripping involves the elimination of small molecules from the side groups attached to the main polymer chain. These eliminated molecules are often small enough to be volatile, such as in PVC where hydrogen chloride (HCl) is stripped from the polymer.

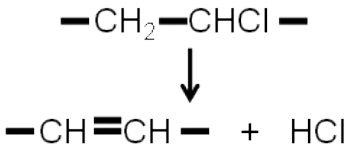


Figure 13: Stripping of HCl from polyvinylchloride

This type of decomposition is important in char formation. After the elimination of side groups the polymer has a higher proportion of carbon content. This carbon rich residue may break down at higher temperatures by chain scission or may crosslink to form a protective char.

### 1.4.4 Crosslinking

Crosslinking of the polymer chains can also occur during polymer decomposition. It sometimes occurs after chain stripping reactions. Bonds form between two adjacent polymer chains increasing the molecular weight of the decomposing fragments. Crosslinking therefore helps to reduce the production of volatile products, lessening the amount of flammable products being fed to the flame. Crosslinks also increase the melting temperature of the polymer, helping to keep more of the mass within the solid phase rather than in the gaseous phase. These processes work to counteract the chain scission processes that are producing volatile products and sustaining the flame. Crosslinking is also an important part of char formation in some polymers. Formation of a carbonaceous char insulates and isolates polymer below the char from the heat and the flame.

### 1.4.5 Decomposition of ethylene vinyl acetate

In reality polymers may show a combination of the decomposition mechanisms discussed above. EVA is a perfect example, exhibiting a complex decomposition mechanism that has been studied and described by several authors[8-11].

EVA decomposes through two steps, it has been shown that initially a chain stripping mechanism causes elimination of the acetate side groups[10]. Good correlation has been shown between mass losses measured by thermogravimetric analysis (TGA) and

the vinyl acetate content quoted by the polymer producers. Fourier transform infra-red (FTIR) analysis of the pyrolysis products has confirmed[9] that EVA thermally decomposes by deacetylation releasing acetic acid at temperatures between 360°C and 450°C. The result is a residue of polyethylene containing unsaturated polyene sequences where loss of acetate groups has occurred. Decomposition by random chain scission of this polymer chain occurs between 450°C and 550°C evolving 1-butene, ethylene, methane, and carbon dioxide. During the degradation process rapid autocatalytic crosslinking has also been shown[11] to occur through the polyene segments. This crosslinking process has been linked[8] to the formation of a protective char layer on the surface of EVA during thermal decomposition.

## 1.5 Methods of studying decomposition

There are many methods used for the study of thermal decomposition of polymers some of the more common methods[6] are discussed below.

### 1.5.1 Thermogravimetric analysis (TGA)

Thermogravimetric analysis (TGA) is a commonly used technique for studying the thermal decomposition and associated mass losses of many materials including polymers. It continuously measures and records the mass of a small, milligram size, sample as it is heated at a set heating rate. Experiments can be carried out under various atmospheres, such as nitrogen, air or other atmospheres that may affect the decomposition mechanism. The results are usually presented as a graph showing percentage mass loss against temperature. This allows studies to be made of how materials decompose, whether they simply lose all of their mass at one temperature, or whether they pass through several stages of mass loss at different temperatures.

DTG or differential thermogravimetry is the same technique as TGA. The results are processed slightly differently, instead of simply measuring mass loss the results are differentiated to give the rate of mass loss. This is useful for determining at what

temperatures decompositions are occurring most rapidly and can help separate two steps of a decomposition that my occur at similar temperatures.

TGA and DTG are useful for characterising mineral fire retardants. The temperature at which the mineral becomes active, decomposing to give off inert gases such as carbon dioxide or water, can be determined by measuring the mass loss. TGA and DTA can also be useful in analysing whether the decomposition reactions of fire retardant additives coincide with those of the polymers being used and are therefore likely to be effective.

### 1.5.2 Simultaneous thermogravimetric analysis with Fourier transform infra-red analysis (STA-FTIR)

Whilst TGA is a useful technique in its own right it tells us nothing about the chemistry of the decompositions that are causing the mass losses. Fourier transform infra-red spectroscopy (FTIR) is a technique used to analyse and identify materials by their infra-red absorption spectra. The technique can be used to identify gas phase molecules as well as solid or liquid samples. Therefore, by analysing the gas stream that leaves the TGA furnace, the gaseous decomposition products of the sample can be identified and linked with mass losses in the sample occurring at specific temperatures.

This technique can be used to study the evolution of common decomposition products, such as carbon dioxide or water, or more specific products such as carbon monoxide, or hydrogen chloride during the decomposition of polymer compounds. It can also be used in the study of decomposing minerals such as huntite and hydromagnesite in order to identify the chemical changes at each stage of the decomposition.

### 1.5.3 Differential thermal analysis (DTA) and differential scanning calorimetry (DSC)

Differential scanning calorimetry (DSC) and differential thermal analysis (DTA) are two similar techniques that measure how much heat is taken in (endothermic) or given out (exothermic) when certain physical or chemical changes occur within a sample. These can be changes that do not affect the sample mass such as melting or crystallisation, or they can include decompositions resulting in mass losses that can be measured by TGA.

DSC works by heating a sample at a set heating rate and simultaneously comparing this to an inert reference material. The difference in energy input needed to keep the two samples at the same temperature is measured by the equipment and used to calculate the heat of reaction for any change or decomposition that occurs. DTA is very similar but the difference in temperature of the two samples is measured, instead of measuring the differences in energy input required to keep the two samples at the same temperature. These types of equipment are usually calibrated using samples with well known melting points and heats of fusion to allow for the accurate analysis of unknown materials.

Simultaneous TGA-DTA equipment measures the mass loss and the exotherm or endotherms associated with these mass losses. DSC and DTA, alone and in combination with TGA, provide useful analysis tools for studying the decomposition mechanisms of polymers and mineral fire retardants.

## 1.6 Flaming combustion

So far only the decomposition of the polymer in the condensed phase has been discussed in detail. This decomposition is an essential part of the burning process because it is this that generates the supply of volatiles to the gas phase that sustains the flame, which is a purely gas phase process. Volatiles generated from the decomposition of the condensed phase will freely mix with the surrounding air. If the temperature is high enough, or there is a source of ignition such as a spark, ignition of the gases will occur creating a flame when a critical concentration is reached. Once a

flame has established itself it will feed back heat into the polymer causing further decomposition and creating more volatiles which feed into the flame. If the rate of polymer decomposition is sufficiently high, a self sustaining flame will develop. Depending on the rate of polymer decomposition the flame will either grow in size spreading the fire or it will diminish and the fire will reduce.

### 1.6.1 The flame

An often used example to illustrate the initiation and development of a flame is that of a burning candle[12-14].

There are two types of flame: the premixed flame, and the diffusion flame. A premixed flame is one in which the gaseous fuel and oxygen are already mixed such as a Bunsen burner or gas stove flame. This ensures the ready availability of oxygen resulting in complete combustion. Moreover, the absence of soot particles minimises the radiant heat component of heat transfer resulting in a blue flame with almost 100% convective heat transfer. A diffusion flame is one in which the oxygen diffuses into the gaseous fuel from the surrounding air; a candle flame is an example of this.

For the candle flame to burn the candle wax must melt and move up the wick by capillary action. As the wax moves up the wick it decomposes into volatile hydrocarbons due to the heat from the flame. These volatile decomposition products leave the wick and enter the gas phase. As the flame relies on diffusion of oxygen from the surrounding atmosphere there is very little oxygen at the centre of the flame, near the wick. As the decomposition gases diffuse outwards from the wick they meet oxygen diffusing inwards. At this point exothermic oxidation reactions take place feeding heat back to the wax causing further melting and the continuation of the cycle. As there is little or no oxygen at the centre of the flame some of the hydrocarbon fragments can aromatize and form soot particles, these particles start to glow, due to the heat of the flame, giving the luminescence seen in the outer parts of the flame. If the flame is small and there is sufficient oxygen available the final combustion products from the flame will be only carbon dioxide and water. If there is insufficient

access to oxygen, carbon monoxide and other products of incomplete combustion will be present.

The principles of the candle flame can be applied to any burning polymeric item[14]. The polymer itself must first decompose to evolve volatile gases which then ignite forming a flame which feeds back heat into the solid phase. Therefore the burning process is both a solid and gas phase process, although the heat generation is usually located entirely in the gas phase. The decomposition of the polymer is an endothermic process requiring energy in order to break chemical bonds leading to the decomposition of the polymer. The exothermic reactions in the gas phase must therefore generate enough energy to sustain the endothermic decompositions taking place in the condensed phase. If this is true the fire will grow, if the exothermic reactions do not generate enough energy the fire will dwindle and die.

### 1.6.2 Free radical reactions in the flame

In order to understand the chemistry of diffusion flames the combustion of ethane can be considered as a simple model (Figure 14)[14].

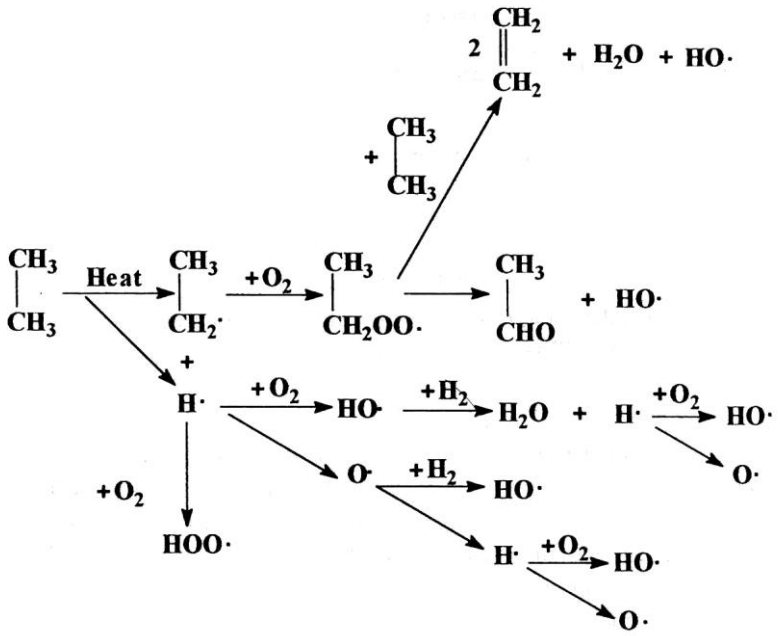


Figure 14: Combustion of ethane[14]

The heat of the flame initiates the decomposition of ethane to produce a hydrogen free radical. This hydrogen radical then starts an exothermic chain reaction with the oxygen diffusing into the flame to produce a cascade of hydrogen and hydroxide radicals resulting in rapid spread of the flame front.

In a more simplified form the important chain reaction involved in flame spread can be represented as the two reactions shown in Figure 15. Each reaction produces a free radical which feeds the other reaction.

$$H\bullet + O_2 \rightarrow OH\bullet + O\bullet$$

$$O\bullet + H_2 \rightarrow OH\bullet + H\bullet$$

Figure 15: Hydrogen and oxygen free radical reactions

Both reactions shown in Figure 15 produce a hydroxide radical which can also react with carbon monoxide (Figure 16), oxidizing it to form carbon dioxide. This oxidation reaction is highly exothermic and provides the greatest amount of exothermic energy to the flame[15].

$$OH\bullet + CO \rightarrow CO_2 + H\bullet$$

Figure 16: Conversion of carbon monoxide to carbon dioxide

## 1.7 Methods of studying flaming combustion

There are many methods commonly used for studying the flaming decomposition of polymers. Some are relatively simple and produce one, apparently easy to understand, number such as the limiting oxygen index allowing ease of ignition to be ranked for different materials. Others such as the NBS smoke chamber only measure the optical density of the smoke emissions. The cone calorimeter makes a wide variety of measurements on one burning sample providing large amounts of data. A few of the more common test methods are discussed below.

### 1.7.1 Limiting oxygen index

The limiting oxygen index test is described in BS ISO 4589-2 and ASTM D2863[16,17]. The oxygen index of any material is defined as “the minimum concentration of oxygen, by volume percentage, in a mixture of oxygen and nitrogen introduced at 23°C ± 2°C that will just support combustion of a material under specified test conditions”[16,17]. The test was first described[18] in 1966 as a new method for assessing the flammability of polymers. It was used[18,19] to study the flammability of polymers and fire retardant mechanisms by using atmospheres of oxygen and nitrogen in

combination with other gases. For example by adding chlorine into the gas mixture it was concluded that halogens function by inhibiting the gas phase reactions within the flame.

The test is conducted by igniting the top edge of a vertically mounted sample in a controlled flow of oxygen and nitrogen. The ratio of oxygen and nitrogen can be varied until the minimum concentration of oxygen required to just support burning is determined. Igniting the top surface of a sample in a candle-like fashion was found[18] to give very reproducible results. By igniting the top surface the heat feedback by convection is minimised since heat rises. This means that a higher concentration of oxygen is required to support combustion as compared to inverted tests such as the UL94 vertical test where the lower edge of a sample is ignited causing greater heat feed back to the decomposing polymer.

The test is commonly used and produces a single, seemingly, easily understood number. Its popularity is also partly to do with its precision and high reproducibility between different workers and different laboratories[20]. It makes no measure of heat release, smoke, or toxic gas emission so a high oxygen index does not mean good performance in all aspects of fire. It is a measure of how dependent the flame is on oxygen concentration. It must also be taken into consideration that the test uses unrealistically high oxygen concentrations. In a real fire situation oxygen concentrations are usually lower than 21% due to consumption of oxygen by the fire.

The test has been shown to be almost independent of gas flow rate between 30 and 120 mm $s^{-1}$ [18,19], however it is temperature dependant. If the temperature of the sample is increased the limiting oxygen index is reduced[20], but not necessarily in a linear fashion. This has lead to the development of a temperature index test method[21] in which the temperature at which the oxygen index is reduced to that of ambient air is determined. Using a combination of the oxygen index and the temperature index it is easier to appreciate why materials with an oxygen index greater than 21% still burn in real fire situations. The additional radiant heat from the fire lowers the oxygen index of these materials until it reaches that of the available oxygen in the surrounding air and combustion occurs.

A good example of heating the sample reducing oxygen index is the fact the oxygen index of coal has been reported[22] to be 44% at room temperature. Such a high oxygen index might lead to the conclusion that coal must therefore be very fire retardant, but clearly this is not the case. If coal is added to an already burning fire the temperature of the coal increases reducing its oxygen index causing it to ignite. Once the coal has been ignited it emits a large quantity of heat energy and easily sustains burning as more coal is added to the fire. It has been reported[23] that the temperature index of coal is only 150°C, which is much lower than most fire retarded polymers.

### 1.7.2 UL94

The UL94 test is an Underwriters Laboratory test but similar tests are also described in ASTM D635[24], ASTM D3801[25], BS2782-1:Method 140A:1992 (ISO 1210)[26]. The test method measures the linear burning rate of a vertically or horizontally mounted sample. In the test the standardised burner flame is applied to the bottom edge of a vertically mounted sample for 10 seconds, or the end of a horizontally mounted sample. The burning characteristics are assessed and given a V or HB rating as follows:

**V-0 (Vertical Burn)**

Burning stops within 10 seconds after two applications of ten seconds each of a flame to a test bar. Flaming drips are not allowed.

**V-1 (Vertical Burn)**

Burning stops within 60 seconds after two applications of ten seconds each of a flame to a test bar. Flaming drips are not allowed.

**V-2 (Vertical Burn)**

Burning stops within 60 seconds after two applications of ten seconds each of a flame to a test bar. Flaming drips are allowed.

**H-B (Horizontal Burn)**

Slow horizontal burning on a 3mm thick specimen, with a burning rate less than 3 inches per minute or extinguishes before the 5 inch mark. H-B rated materials are considered 'self-extinguishing'.

### 1.7.3 Cone calorimeter

There are several standard test methods for the cone calorimeter[27-29], including ISO5660, ASTM E1354. There are also a number of useful papers[30-34] giving information on the development and running of the cone calorimeter and interpretation of data. The cone calorimeter is commonly used as a research tool for studying the combustion of polymers and other materials under well-ventilated conditions. It provides data on the heat release, smoke generation, and mass loss rate of burning materials along with a variety of other parameters related to the combustion of the sample.

The sample, a 10cm x 10cm square plaque of up to 50mm thick is mounted horizontally on a load cell beneath a conical shaped radiant heater. In certain circumstances the sample can be mounted vertically but this can give the added complication of the sample melting and / or dripping away from the heat source. A controlled heat flux of up to 100 $kWm^{-2}$ is applied to the sample allowing the simulation of various stages of a real fire. Heat fluxes of 35 or 50 $kWm^{-2}$ simulate the conditions found in a developing fire, while higher heat fluxes simulate the conditions found in a more fully developed fire. According to Schartel[33] the surface of a non-combustible ceramic plate has been measured at 300 - 520°C for heat fluxes of 15 - 35 $kWm^{-2}$ which is high enough to ignite most combustible organic materials. 50 $kWm^{-2}$, and 70 $kWm^{-2}$ have been shown to cause a surface temperatures of about 610°C and 700°C.

The radiant heat initiates decomposition of the sample and a spark provides the source of ignition causing combustion of the decomposition gases when they reach a high enough concentration. The heat release rate is measured using the principles of

oxygen consumption calorimetry. It is based on the assumption[27] that the heat of combustion is proportional to the amount of oxygen consumed during combustion. It has been shown[35] that approximately 13.1 MJ of heat energy is released for each kilogram of oxygen consumed from a fire involving conventional organic fuels. Measurements of the oxygen concentration in the exhaust gas are made to calculate the heat release. The cone calorimeter creates a lot of data and interpretation[32,33] of this can take some time to fully understand.

In addition to heat release the cone calorimeter calculates smoke release by measuring the obscuration of a laser light source through the exhaust ducting. Mass loss of the sample, time to ignition and extinction, and carbon monoxide and carbon dioxide production can also be measured.

Graphs of heat release rate against time (Figure 17) measured by the cone calorimeter give rise to some characteristic behaviours[33] depending on the size and burning behaviour of the sample.

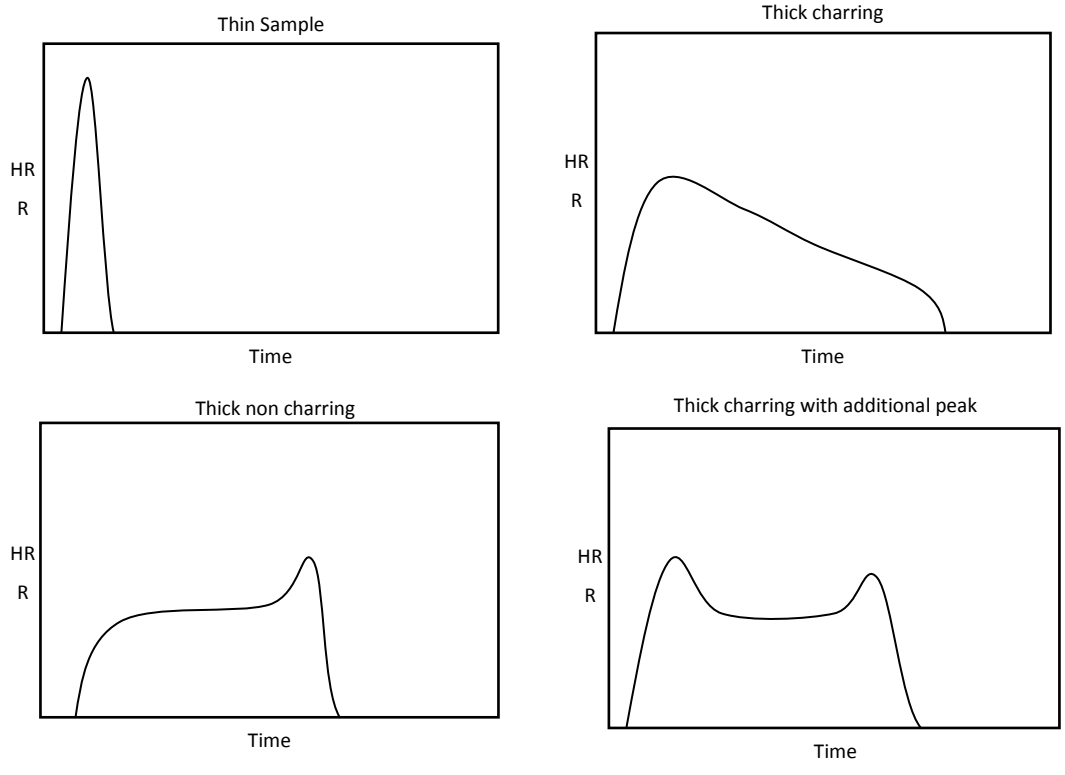


Figure 17: Characteristic behaviours of materials in the cone calorimeter

A thermally thin sample will simply have one sharp peak as the sample burns and quickly exhausts the fuel supply.

A thermally thick non-charring material will reach a steady burning state followed by a final peak in heat release. During the period of steady state combustion the thickness of the underlying sample conducts heat with a steady flow of away from the surface. As the sample thins this steady conduction of heat away from the surface is reduced and results in an increase in a peak in the heat release before extinction of the flame.

A thermally thick char forming material will show an initial increase in heat release followed by a steady reduction. The steady reduction in heat release is a result of the increasing char layer protecting the underlying sample from the heat flux and therefore reducing the rate of burning.

In some cases a char forming sample can show a second peak for the same reason as the final peak in the thick non-charring sample.

## 1.8 Smoke

The term smoke can be difficult to define, does it include combustion gases, or is it simply the cloud of soot particles emitted from the fire? The ASTM definition[4] of smoke is “airborne solid and liquid particulates and gases evolved when a material undergoes pyrolysis or combustion”. British Standards define it as simply the “visible part of fire effluent”[36]. One of the main concerns with smoke is that is reduces visibility for anyone trying to escape the fire, in these terms it is the particulates that absorb or scatter light that are the main concern.

Smoke formation is not an inherent property of a polymer[14,37], it depends on the conditions of burning. Oxygen concentration, ventilation, heat flux, and sample geometry are just some of the influencing factors. Therefore any tests carried out to measure smoke only give an indication of smoke production under those precise conditions, they do not necessarily have any relationship to smoke production in a real fire situation. For this reason the smoke results from one particular smoke test may not correlate with the smoke results from another type of test.

As discussed previously the burning of polymers occurs through diffusion flames. Therefore, complete combustion of the decomposition products to carbon dioxide and water does not readily occur since the supply of oxygen will be limited. This is the reason that oxygen supply and ventilation has a major effect on smoke production, making prediction from laboratory scale test results to actual smoke in a real fire situation impossible. Visible smoke is a result of incomplete combustion leading to the formation of carbon and soot particles[14]. In a diffusion flame with a limited oxygen supply some of the decomposition products from the polymer can form polybenzenoid structures which form soot. This explains why aromatic polymers such as polystyrene burn with a lot of smoke. Purely aliphatic polymers generally produce low levels of smoke, while those with aromatic groups, or polyenic polymers, which can cyclise to form aromatic products, generally produce more smoke.

## 1.9 Methods of measuring smoke

As discussed above, the actual amount of smoke produced is not an intrinsic material property and is dependent on several factors including the test conditions and type of test used. There are several methods for measuring smoke; a couple of the more common methods are described below. It should be remembered that although some materials have clearly different tendencies to form smoke, there is unlikely to be any obvious correlation between results measured using different methods or even different conditions in the same method.

### 1.9.1 Smoke density chamber

The smoke density chamber is described in ASTM E662[38], BS6401[39], and ISO5659-2[40], it is one of the few tests specifically designed for measuring smoke. Most other tests, such as the cone calorimeter, measure smoke along with other characteristics of the burning sample. The test works by measuring the obscuration of a light beam shone vertically through an enclosed chamber. A sample of 75mm x 75mm and up to 25mm thick is mounted vertically in front of or below (ISO 5659-2) an infra-red heater with a heat flux of 25 $kWm^{-2}$. ISO 5659-2 also allows for tests to be carried out using a

heat flux of 50 $kWm^{-2}$. The sample is either pyrolysed through smouldering or combusted in flaming mode. To ensure that flaming combustion occurs in flaming mode a small pilot burner is mounted in front of the sample. The equipment records the level of light obscuration as the smoke accumulates in the chamber throughout the test. The smoke is not exhausted from the chamber until the test is completed. Results are usually presented as a graph of light obscuration over the time period of the test, and as a specific optical density.

### 1.9.2 Cone calorimeter

The use of the cone calorimeter for studying combustion has already been discussed in section 1.7.3. As well as measuring heat release, the cone calorimeter can also be used to measure smoke. It does not accumulate the smoke in a chamber like the smoke density chamber. Instead the optical obscuration is measured by passing a laser beam through the exhaust duct. This method gives a measure of the amount of smoke being generated at any particular instant during well-ventilated burning, rather than a cumulative value as measured by the smoke density chamber.

## 1.10 Fire retardancy and fire retardants

Polymers are generally flammable and therefore methods of reducing the fire hazard of articles manufactured from polymers are of great importance. There are a variety of methods for improving the fire retardancy of a polymer and a number of materials which significantly improve fire retardant properties of a polymer when mixed with the polymer. There are several review papers[41-44] which cover the range of fire retardants commonly used today. The principle behind most fire retardants is to try and slow the development of the fire in its early stages by limiting at least one of the essential elements of every fire: oxygen, fuel or heat.

The supply of oxygen, heat, and fuel to the fire can be controlled or reduced through either chemical or physical means depending on the fire retardant used. Whichever mechanism is employed the overall objective is always to reduce the severity of the

fire in one or more ways. Simple dilution of the polymer with inert fillers such as chalk reduces the fuel supply. Use of active fillers that dilute the supply of oxygen and combustible gases through the release of non-combustible gases is a well known method. The release of these inert gases is through endothermic decomposition of the additive which reduces the supply of heat to the decomposing polymer. This in turn slows the supply of flammable decomposition products to the gas phase. The free radical chemistry of the flame can be disrupted through the use of halogens, this leads to lower heat generation and therefore less feedback of heat into the polymer and the surrounding area. The surface of products can be protected through the formation of a carbonaceous char, which insulates and protects the polymer from further decomposition. These are all proven methods for which commercially available products are already in the market and are discussed below.

### 1.10.1 Halogens

Halogens act as fire retardants[37] by interfering with the free radical reactions occurring in the flame. Hydrogen halides released by the decomposition of halogen containing materials, such as PVC, react with the hydrogen radicals and hydroxide radicals in the flame forming molecular hydrogen or water and a halide radical as shown in Figure 18. This removal of hydrogen radicals and hydroxide radicals from the flame reduces the rate of combustion.

$$HX + H\bullet \rightarrow H_2 + X\bullet$$

$$HX + OH\bullet \rightarrow H_2O + X\bullet$$

$$X = \text{halogen}$$

Figure 18: Reaction of hydrogen halide with hydroxide and hydrogen radicals

The removal of the hydroxide radicals has a significant effect on reducing the temperature of the flame because it reduces the availability of the free radical for the highly exothermic conversion of carbon monoxide to carbon dioxide[20] shown in

Figure 16. Less generation of heat in the flame has the effect of feeding less heat to the polymer and therefore slowing the whole degradation and combustion process. The less reactive halide radicals regenerate the hydrogen halide by abstracting hydrogen from the decomposing polymer fragments. In addition the loss of the halide radicals from the polymer results in unsaturation which may act as a precursor to crosslinking and the formation of a carbonaceous char.

The effectiveness of halogens as fire retardants increases in the order: F < Cl < Br < I. In practice bromine and chlorine are the only halogens that find general use as fire retardants as fluorine is too ineffective and iodine is thermally unstable at polymer processing temperatures[37].

Antimony trioxide ($Sb_2O_3$) shows no fire retardant action on its own but is a well known synergist, increasing the effectiveness[45] of halogen containing fire retardants. It has been shown to function through the conversion of antimony trioxide to antimony trihalide which then acts as a very effective trap for hydrogen radicals and hydroxide radicals[46].

The action of the antimony halide as a free radical trap is through the following reactions[47].

$$SbX_3 + H\bullet \rightarrow SbX_2 + HX$$

$$SbX_2 + H\bullet \rightarrow SbX + HX$$

$$SbX + H\bullet \rightarrow Sb + HX$$

$$Sb + O\bullet \rightarrow SbO$$

$$Sb + OH\bullet \rightarrow SbOH$$

**X=halogen**

**Figure 19: Mechanism of antimony halide as a free radical trap**[47]

The SbO and SbOH go on to trap further hydrogen and hydroxide free radicals as shown in Figure 20.

$$SbO + H\bullet \rightarrow SbOH$$

$$SbOH + H\bullet \rightarrow SbO + H_2$$

$$SbOH + OH\bullet \rightarrow SbO + H_2O$$

Figure 20: Action of SbO and SbOH as further radical traps

Therefore the action of antimony with a halogen is very effective at inhibiting the free radical reactions generating heat within a flame.

### 1.10.2 Borates

The use of borates as fire retardants has been known since the late 1800's when Joseph Louis Gay-Lussac investigated their use as a treatment for cotton. The formation of a glassy borate skin was found to inhibit combustion of the cotton[20].

Mixtures of boric acid and borax (sodium borate) function as fire retardants by decomposing endothermically with the release of water forming a glassy residue on the surface of the substrate.

$$2H_3BO_3 \xrightarrow{130 - 200°C} 2HBO_2 + 2H_2O \xrightarrow{260 - 270°C} B_2O_3 + 2H_2O$$

Figure 21: Thermal decomposition of boric acid

The mixture dissolves in the water generated during decomposition, swelling to form foam before dehydrating a second time to form a glassy melt which acts as a shield between the substrate and the flame. This shield effect reduces the amount of oxygen reaching the surface therefore reducing the oxidation of carbon in the substrate and increasing char formation[43].

Zinc borates have been shown to be able to partially or completely replace antimony trioxide[48] in halogen containing systems in terms of fire performance. The mechanism is somewhat different than the gas phase reactions that occur with antimony trioxide, zinc borate functions in the condensed phase creating a glassy surface barrier. Zinc borate also functions as a smoke suppressant, and afterglow suppressant. In electrical applications another benefit of zinc borate is the ability to improve surface electrical breakdown characteristics.

Synergism has been reported[41] between both ATH and magnesium hydroxide with zinc borate. Improved char formation leads to lower peak heat release in cone calorimeter tests.

### 1.10.3 Phosphorus

There are a large range of phosphorus containing fire retardants, partly due to the fact that so many phosphorus containing molecules show a fire retarding action. The various forms of phosphorus can be incorporated into polymers either through adding phosphorus containing additives such as red phosphorus, phosphates, phosphites, etc. or through copolymerising with phosphorus containing molecules. Some phosphorus containing fire retardants work in the condensed phase[43] by increasing the carbonaceous char yield while others show gas phase flame inhibiting action[49]. Phosphorus influences the decomposition of the polymer to favour the production or carbon rather than carbon monoxide or dioxide. The fire retardant mechanisms of phosphorus are still not fully explained, although the use of phosphorus containing compounds is widely known.

### 1.10.4 Silicon

Small additions of silicon containing compounds (such as silicones, silicas, silicates, organosilanes and silsesquioxanes) have been reported to improve fire retardancy through both improved char formation[50] and radical trapping in the vapour phase[43].

It has also been reported[51] that silicone polymer, or silicon dioxide, can interact with zinc borate to form borosilicate glass at the combustion temperatures of polymers. This has been suggested as a mechanism for improved fire properties seen in mixtures of magnesium hydroxide with talc (a silicon containing mineral) and zinc borate[48,50,51].

### 1.10.5 Nitrogen

Nitrogen containing fire retardants are usually used in the form of melamine variants. In the condensed phase they can form crosslinked structures promoting char formation and releasing ammonia which dilutes the gas phase[45].

### 1.10.6 Metal hydroxide and carbonate fire retardants

The main focus of this thesis is on mineral fire retardants, therefore they will be discussed both here in outline and in more detail in the following chapter. They generally take the form of metal hydroxides. Aluminium hydroxide (ATH) and magnesium hydroxide (MDH) are the most commonly used[44] materials in this category. Metal hydroxides function as fire retardants by releasing water vapour though endothermic decomposition. They therefore cool the condensed phase though endothermic decomposition, dilute the combustible decomposition products in the vapour phase with non combustible water and form an inorganic residue which can act as a protective layer on the polymer surface.

#### *1.10.6.1 Aluminium hydroxide*

Aluminium hydroxide is known by several names, especially in industry, including: aluminium trihydroxide, aluminium trihydrate, alumina trihydrate or simply ATH. Chemically the correct name is aluminium hydroxide, the use of the name alumina trihydrate implies the structure, $Al_2O_3 \cdot 3H_2O$, which is incorrect but is the origin of the widely used abbreviation ATH. Aluminium hydroxide is the most widely used fire

retardant and the most commonly used metal hydrate fire retardant[41,52]. In simple terms it decomposes according to the reaction shown in Figure 22.

$$2Al(OH)_3 \rightarrow Al_2O_3 + 3H_2O$$

Figure 22: Thermal decomposition of aluminium hydroxide

It has been reported[53] that under certain conditions the stable intermediate boehmite, AlO(OH), can form. This mechanism is favoured under increased partial pressures of water. It may therefore be favoured when ATH particles are encapsulated within a polymer matrix. In this situation water from the decomposition of the ATH particles may become entrapped around the particle leading to locally high water partial pressures. Boehmite has a decomposition temperature of about 500°C and therefore this decomposition mechanism is thought to be detrimental to the fire retardant effectiveness of ATH. Formation of boehmite also increases with increasing particle size probably due to the water molecules become entrapped within the larger particles. This has been suggested as a reason for finer particle sizes have significantly improved fire retardant action.

The thermal decomposition enthalpy of ATH is quoted at values between 1170 and 1300 $Jg^{-1}$ by various authors[15,52,54]. The evolution of approximately 35% of the mass of ATH as water vapour through endothermic decomposition is the mechanism by which ATH provides a fire retardant action. The decomposition starts to occur at about 180 - 200°C[54]. The decomposition temperature of ATH is a limitation on its use because it cannot be used in polymers that are processed at or above this temperature.

High loading levels, typically at least 60% by weight, of ATH are usually required in order to achieve good fire retardant properties[41]. Such high loading levels will have a negative effect on the mechanical properties of the compound and this is an important consideration with all the metal hydroxide / mineral filler fire retardants.

#### 1.10.6.2 Magnesium hydroxide

Magnesium hydroxide is used less commonly than ATH. It works through a very similar mechanism to ATH, decomposing through an endothermic reaction to give off water as shown in Figure 23.

$$Mg(OH)_2 \rightarrow MgO + H_2O$$

Figure 23: Thermal decomposition of magnesium hydroxide

The enthalpy of thermal decomposition is quoted at values between 1244 and 1450 $Jg^{-1}$ by various authors[15,52,55,56]. It starts to decompose at about 300 - 330°C giving off about 31% of its mass as water[55]. Magnesium hydroxide is believed to decompose directly to magnesium oxide without passing through any stable intermediates as seen with ATH. However there are several theories[55,57,58] as to the exact mechanism of decomposition of the crystal structure. Hornsby[59] states that initially the magnesium oxide decomposition product maintains the original hexagonal structure of the magnesium hydroxide crystals. As the temperature rises sudden crystallisation of cubic magnesium oxide causes the structure to fragment as the magnesium oxide crystals form.

The higher decomposition temperature of magnesium hydroxide means that it can be used with some polymers, such as polyamides[56], where ATH cannot due to the processing temperatures required.

As with ATH, high loading levels of 50 – 65% by weight of MDH are usually required to achieve good fire retardant properties.

Hornsby[59-61] has proposed that magnesium hydroxide works as a fire retardant through five main mechanisms:

1. endothermic decomposition which helps to reduce the thermal decomposition of the polymer
2. release of water vapour diluting the vapour phase
3. the heat capacity of both the magnesium hydroxide and the decomposition product, magnesium oxide, further reduces the thermal energy available to degrade the polymer

4. the decomposition products promote char formation and therefore insulate the substrate from the heat source
5. the high loading level of magnesium hydroxide acts as a solid phase diluent

Hornsby also states[59] that the high surface area of the active magnesium oxide decomposition product acts as a smoke suppressant by absorbing carbonaceous decomposition products and may also catalyse their oxidation. The fact that both magnesium hydroxide and aluminium hydroxide act as smoke suppressants was shown[60] in a comparison of polypropylene compounds filled with ATH, MDH and calcium carbonate. Both the MDH, and ATH showed lower smoke production than the calcium carbonate filled compound meaning that the action was more than a simple dilution effect of the polymer.

Hornsby[60] rules out a redox reaction between carbon and the metal oxide as the reason for smoke reduction since both aluminium and magnesium oxides are refractory materials and cannot be reduced by carbon under combustion conditions. The reduction, by carbon, of the water produced by the decomposition of the hydroxide is also ruled out[59,60] since this reaction will only occur at temperatures and pressures in excess of those seen during polymer combustion. Hornsby suggests that the most likely mechanism for smoke suppression by magnesium oxides is the deposition of carbon on the surface of the active magnesium oxide during combustion. The carbon products subsequently volatilise on exposure to oxygen due to the dissociation of oxygen on the oxide surface at temperatures of 400°C - 500°C. The oxygen radicals then react with carbon, forming oxides.

It has also been reported[51,62] that mixtures of magnesium hydroxide, talc, and zinc borate can give synergistic effects. It is claimed that the platy talc particles form a mass transfer barrier on the surface of the decomposing polymer therefore protecting the underlying polymer.

#### *1.10.6.3 Huntite and hydromagnesite*

This natural mixture of minerals is an alternative to aluminium hydroxide and magnesium hydroxide as a fire retardant. It is the main focus of this thesis and as such is discussed in detail in the following chapter.

# 2. The thermal decomposition and fire retardant action of huntite and hydromagnesite

Naturally occurring mixtures of huntite and hydromagnesite have found important industrial use. Their endothermic decomposition over a temperature range similar to that of commonly used polymers and their release of water and carbon dioxide, has led to such mixtures being successfully used as fire retardants. They have replaced aluminium hydroxide and magnesium hydroxide in many applications. The reports from literature presented below show the current understanding of the thermal decomposition mechanism of both minerals, their combination in natural mixtures and the implications for their fire retardant action. It also shows that both minerals contribute to the reduction in flammability of polymers although the extent of these interactions has not been fully investigated. However, the fire retardant mechanism of these minerals appears more complicated than either aluminium hydroxide or magnesium hydroxide.

## 2.1 Industrial use of mineral fillers as fire retardants

The largest group of mineral fire retardants are metal hydroxides. Their endothermic decomposition and associated release of inert gases or water vapour, above the processing temperature but below the thermal decomposition temperature of polymers suppresses the ignition, while the accumulation of a solid inert residue on the surface of the burning polymer reduces the heat release rate. Although ATH and magnesium hydroxide (previously discussed in section 1.10.6) are the most well known mineral fire retardants, Rothon[54] has identified a number of minerals (Table 1) that could be of potential benefit in polymers. Each decomposes endothermically with the

evolution of either carbon dioxide, water or both. Of these minerals, hydromagnesite is the one that has probably seen most commercial interest. Hydromagnesite is naturally occurring in mixtures with huntite. Its onset of decomposition is at a slightly higher temperature than that of ATH making it suitable for polymers where ATH has been traditionally used, as well as in polymers where ATH becomes unsuitable due to higher processing temperatures.

| **Mineral** | **Approximate onset of Decomposition (°C)** |
|---|---|
| Nesquehonite ($MgCO_3 \cdot 3H_2O$) | 70 – 100 |
| Gypsum ($CaSO_4 \cdot 2H_2O$) | 60 – 130 |
| Magnesium phosphate octahydrate ($Mg_3[PO_4]_2 \cdot 8H_2O$) | 140 – 150 |
| Aluminium hydroxide ($Al[OH]_3$) | 180 – 200 |
| Hydromagnesite ($Mg_5[CO_3]_4[OH]_2 \cdot 4H_2O$) | 220 – 240 |
| Dawsonite ($NaAl[OH]_2CO_3$) | 240 – 260 |
| Magnesium hydroxide ($Mg[OH]_2$) | 300 – 320 |
| Magnesium carbonate subhydrate ($MgO \cdot CO_{2[0.96]}H_2O_{[0.3]}$) | 340 – 350 |
| Boehmite ($AlO[OH]$) | 340 – 350 |
| Calcium hydroxide ($Ca[OH]_2$) | 430 – 450 |

**Table 1: Minerals with potential fire retardant benefits, and their decomposition temperatures**[54]

Hydromagnesite has been shown[63-69] to decompose endothermically releasing water and carbon dioxide over a temperature range of approximately 220°C to 550°C (Figure 24).

$$Mg_5(CO_3)_4(OH)_2 \cdot 4H_2O \rightarrow 5MgO + 4CO_2 + 5H_2O$$

**Figure 24: Thermal decomposition of hydromagnesite**

This endothermic decomposition and release of inert gases gives hydromagnesite its fire retardant properties.

Huntite also decomposes endothermically[70-73] releasing carbon dioxide over a temperature range of approximately 450°C to 800°C (Figure 25).

$$Mg_3Ca(CO_3)_4 \rightarrow 3MgO + CaO + 4CO_2$$

Figure 25: Thermal decomposition of huntite

While this is too hot to coincide with major polymer decomposition and fuel production stages occurring around ignition, its platy morphology reinforces the formation of a thermally protective barrier layer which may reduce the rate of burning.

The structure of these minerals, their thermal decomposition and their fire retardant action will be discussed in detail in this chapter.

## 2.2 Sources of huntite and hydromagnesite

Hydromagnesite is a naturally occurring mineral and has been found in a number of locations around the world, it is the third most common[74] carbonate found in caves, after calcite and aragonite. Commercial extraction of hydromagnesite is not from caves, as there are locations where larger quantities occur at the surface, in mixtures with another carbonate mineral, huntite. Huntite is rarer than hydromagnesite, although it is also found in caves[75] as flowstone.

Georgiades[76] reported some of the history of one such deposit of mixed hydromagnesite and huntite in Greece. It had been known by local people as a source of material for whitewashing their houses for many centuries. Then in the mid 20$^{th}$ century it began to be used as a filler for shoe soles. It was ground using the local granite mills designed for wheat. Georgiades started investigating commercial exploitation of the minerals in 1978 and commenced worldwide sales in 1986. The Greek deposit is still operated commercially, although the world's largest known reserves are in Turkey, operated commercially by Minelco. Stamatakis[77] has carried out some evaluation on a source of hydromagnesite in British Columbia[78,79] and concluded that it is composed mainly of hydromagnesite with minor amounts of

magnesite but no huntite. The whiteness and decomposition properties are reported to be similar to commercially mined minerals from Greece, leading to the conclusion that this source of hydromagnesite might be suitable for use as a fire retardant.

Since hydromagnesite is a carbonate, it has been proposed that its production could be used to convert the greenhouse gas carbon dioxide into a solid carbonate. A slurry of magnesium hydroxide can be converted[80] into hydromagnesite by bubbling carbon dioxide through the slurry.

A method for the conversion of serpentine ($Mg_3Si_2O_5(OH)_4$) into hydromagnesite has been investigated[81] as a way of trapping carbon dioxide and preventing its accumulation in the atmosphere. The process involves production of magnesium chloride from serpentine through the reaction shown in Figure 26.

$$Mg_3Si_2O_5(OH)_4 + 6HCl \rightarrow 3MgCl_2 + 2SiO_2 + 5H_2O$$

Figure 26: Reaction of serpentine with hydrochloric acid to produce magnesium chloride

The magnesium chloride is then converted to hydromagnesite in the presence of sodium hydroxide and carbon dioxide (Figure 27).

$$5MgCl_2 + 10NaOH + 4CO_2 \rightarrow 10NaCl + Mg_5(OH)_2(CO_3)_4 \cdot 4H_2O$$

Figure 27: Conversion of magnesium chloride into hydromagnesite in the presence of sodium hydroxide and carbon dioxide

These studies are primarily driven by the desire to trap carbon dioxide in a stable form. However, the suitability of both synthetic and natural hydromagnesite as a fire retardant for polymers could improve the cost effectiveness of the plan and lead to a future commercial source of hydromagnesite. There has also been interest in the literature[80,82-86] in synthetic hydromagnesite as a fire retardant.

## 2.3 Chemical formula and crystal structure of hydromagnesite

There is some variation in the chemical formula reported for hydromagnesite. Rothon inadvertently illustrates this in his well regarded book[55] on particulate filled polymer composites. The following formula (Figure 28) is shown in one chapter[53] by Hancock and Rothon:

$$4MgCO_3 \cdot Mg(OH)_2 \cdot 3H_2O$$

Figure 28: Chemical formula for hydromagnesite containing three water molecules

while in a later chapter[54], by Rothon alone, the formula shown in Figure 29 is given. This formula is also given by Frost[82] and Winchell[87].

$$Mg_5[(CO_3)_4(OH)_2] \cdot 4H_2O$$

Figure 29: Chemical formula for hydromagnesite containing four water molecules

This formula has the equivalent composition to the formula shown in Figure 30:

$$4MgCO_3 \cdot Mg(OH)_2 \cdot 4H_2O$$

Figure 30: Alternative way of writing the chemical formula for hydromagnesite with four water molecules

Therefore the amount of water of crystallisation differs, 4 moles are shown in the formula given by Frost[82] and Winchell[87] compared to only 3 moles in formula reported by Hancock and Rothon[53].

In the 1970's Todor[64] also made the point that in various mineralogical handbooks two formulae are given, one with three water molecules and one with four.

Botha[80] introduces a third variation observing that hydromagnesite is a hydrated basic magnesium carbonate that can be synthesised in two forms, referred to as light and heavy magnesium carbonate with 4 and 5 water molecules respectively, adding a third variation.

In 1972 Robie reported[88] that the geometry of the hydromagnesite unit cell was still in question with some authors[89] taking $Mg_4(CO_3)_3(OH)_2{\cdot}3H_2O$ as the correct form while others[87] considered it to be $Mg_5(CO_3)_4(OH)_2{\cdot}4H_2O$. Robie's own measurements using specific gravity, chemical and X-ray analysis lead him to the conclusion that the correct formula for a sample of hydromagnesite from Hindubagh, Pakistan contained four water molecules. A further sample of hydromagnesite from Soghan, Iran, analysed by Bariand[90] in 1973 confirmed that the formula contained 4 water molecules in agreement with Robie[88], Winchell[87], and with Todor's[64] findings from thermal analysis. This now appears to be accepted and is the formula given by the Mineralogical Society of America in their Handbook of Mineralogy[74].

Various studies[91-96] have been made on the crystalline structure of hydromagnesite. Murdoch[93] concludes that it is a monoclinic crystal with a pseudo-orthorhombic structure. Akao[96] first published a crystal structure of hydromagnesite in 1974. It was determined using 3-dimensional X-ray data. The structure was shown to be based on a three dimensional framework of $MgO_6$ octahedra with the magnesium atom surrounded by the six oxygen atoms. The octahedra share oxygen atoms with the surrounding octahedra forming a 3-dimensional structure. The octahedra consist of two distinct structures. The first contains a magnesium atom surrounded by four oxygen atoms from carbonate ions, the fifth from a hydroxyl ion and the sixth from a water molecule. The second structure contains four carbonate ions and two hydroxyl ions. The strong C-O bonds of the carbonate ion reinforce the crystal by forming a triangular structure with three oxygen atoms from three different octahedra. In a subsequent publication[95] in 1977 Akao further developed understanding of the structure by determining in greater detail the positions of the remaining water molecules and the hydroxyl group. The hydroxyl group was shown to be shared between three $MgO_6$ octahedra and does not take part in any hydrogen bonding, while the water molecules are located at unshared corners of the $MgO_6$ octahedron and form a network of hydrogen bonds. The water molecules are arranged so that the oxygen atoms are tetrahedrally surrounded by two hydrogen atoms, one magnesium atom and one hydrogen from a neighbouring water molecule. This hydrogen atom from the neighbouring water molecule forms a hydrogen bond, causing the water

molecules to form a chain. The chain consists of one hydrogen atom in each water molecule forming a hydrogen bond to its neighbouring water molecule and the other hydrogen atom forming a hydrogen bond with oxygen in the carbonate groups. The three dimensional structures has been characterised in the excellent works of Akao[95,96] where detailed tables of interatomic distances, bond angles, diagrams of the crystal structures and in depth discussion and comment is given.

The American Mineralogist Crystal Structure Database[97,98] collates mineralogical structural data. This data can be freely downloaded and the crystal structure displayed using XtalDraw[99] (a free to download program), this allows the structure to be rotated in three dimensions on the screen. This database quotes the structural data as described by Akao[95] and gives a structure of hydromagnesite as shown in Figure 31.

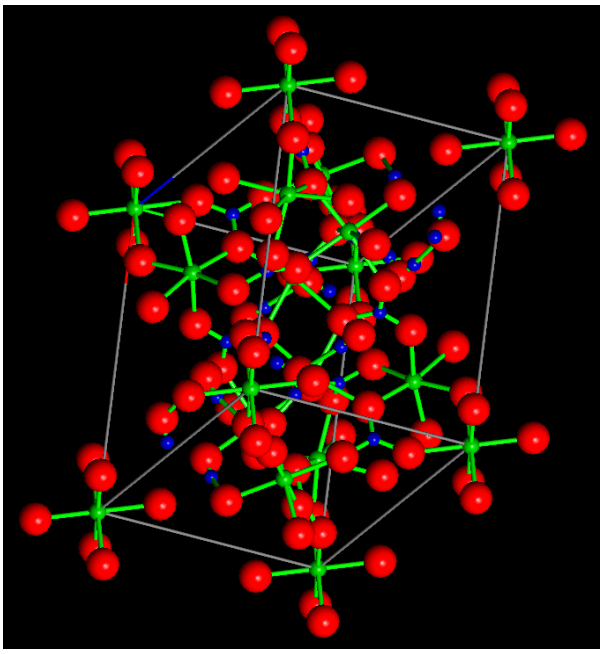

**Figure 31: Crystal structure of hydromagnesite as given in the American Mineralogist Crystal Structure Database**[97,98]

## 2.4 Endothermic decomposition of hydromagnesite

In the 1950's Beck [63] published information on the decomposition characteristics of a range of carbonate minerals including natural hydromagnesite from California. Beck quoted the chemical formula as $Mg_4(CO_3)_3(OH)_2{\cdot}3H_2O$. He noted that the

hydromagnesite went through a series of endothermic decompositions releasing water and carbon dioxide and published DTA curves to accompany his observations.

Todor[64] published one of the earliest attempts to characterise the decomposition mechanism of hydromagnesite. Between 210°C and 395°C, the four water molecules are released (Figure 32).

$$Mg_5(CO_3)_4(OH)_2{\cdot}4H_2O \rightarrow Mg_5(CO_3)_4(OH)_2 + 4H_2O$$

Figure 32: Loss of water molecule from hydromagnesite to form a magnesiumhydroxycarbonate

Immediately following the loss of the four water molecules, between 395°C and 460°C, the loss of a carbon dioxide molecule occurs, followed by a reorganisation of the crystal structure. Todor does not give any detail on what this reorganisation involves. Between 460°C and 515°C a fifth molecule of water is released due to the decomposition of the hydroxide group and a further carbon dioxide molecule is released (Figure 33).

$$Mg_5(CO_3)_4(OH)_2 \rightarrow 2MgCO_3 + 3MgO + 2CO_2 + H_2O$$

Figure 33: Decomposition of magnesiumhydroxycarbonate to from a magnesium carbonate

Finally over the temperature range of 515°C to 640°C a further two carbon dioxide molecules are released to leave a magnesium oxide residue (Figure 34).

$$2MgCO_3 \rightarrow 2MgO + 2CO_2$$

Figure 34: Decomposition of magnesium carbonate to form magnesium oxide

Todor notes that the complicated decomposition mechanism may have lead to some of the confusion over the actual chemical structure of hydromagnesite. However this precise mechanism and order of events is not in agreement with that of more recent work, as discussed below.

Padeste[100] showed that hydromagnesite decomposes through different mechanisms depending on the surrounding atmosphere. In the absence of carbon dioxide only two decomposition stages were observed; the loss of the crystalline water, followed by the combined dehydroxylation and decarbonation. However, under carbon dioxide the dehydroxylation and decarbonation were thought to occur separately, giving three steps.

In the late 1970's Sawada published a number of papers[65-69] investigating in detail the decomposition of hydromagnesite. These investigations included the effect of different gaseous atmospheres at varying partial pressures on the decomposition of hydromagnesite. He confirmed that under a nitrogen atmosphere the decomposition of hydromagnesite occurs through only two steps. Increasing the partial pressure of carbon dioxide was found to strongly influence the decomposition[65], separating the single loss of carbon dioxide between 350°C and 500°C into three distinct losses at 350°C - 500°C, 500°C - 520°C and 530°C - 650°C. The first and third losses of carbon dioxide were found to be endothermic, while the middle loss was exothermic. This effect was also observed on increasing the heating rate. Low heating rates gave only one decarbonation step which split into two and which were then separated by a third sharp exothermic decomposition at even higher heating rates, presumably due to the local increase in the partial pressure of carbon dioxide in the bulk of the solid.

Further study[66] under helium also showed dehydration below 300°C followed by a single decarbonation step between 300°C and 500°C, while XRD analysis showed an amorphous structure, with no indication of magnesium carbonate crystals. Above 500°C, magnesium oxide was detected by XRD with the peaks becoming sharper and stronger at higher temperatures. When the same decomposition was carried out under helium and carbon dioxide ($P_{CO2}$=0.5 atm) the dehydration below 300°C was unaffected. Samples examined using XRD after the occurrence of the exotherm at about 520°C showed the presence of crystalline magnesium carbonate. It is therefore concluded that under conditions of high partial pressure of carbon dioxide, or high heating rates, exothermic crystallisation of magnesium carbonate occurs at about 520°C. The magnesium carbonate then decomposes through decarbonation to

magnesium oxide, between 530°C and 650°C. This led Sawada to propose two types of decomposition for hydromagnesite[67]

Type I: $P_{CO2}$ < 0.1 atm - The amorphous carbonate formed after dehydration decomposes directly to magnesium oxide.

Type II: $P_{CO2}$ ~ 1 atm – The amorphous carbonate formed after dehydration partially decarbonates followed by exothermic crystallisation of magnesium carbonate at about 520°C. The magnesium carbonate then itself decarbonates to magnesium oxide between about 530°C and 650°C.

Having investigated the effects of carbon dioxide partial pressures at atmospheric pressure Sawada went on to investigate the decomposition of hydromagnesite under high pressure atmospheres[67]. Increasing pressures of nitrogen, argon, and carbon dioxide had no effect on the dehydration temperature up to 50 atm. Increasing pressures of argon, and nitrogen had minimal effect on the temperature of the exothermic crystallisation of magnesium carbonate and subsequent decarbonation. Increasing pressures of carbon dioxide had a significant effect. The temperature of the exothermic crystallisation of magnesium carbonate was linearly reduced by about 30°C as the pressure was increased from 1 to 50 atm, while the peak of decomposition of the resultant magnesium carbonate increased to just less than 700°C. At pressures of carbon dioxide above about 10 atm a third decomposition mechanism was identified. This was given the classification of Type III by Sawada, in which a second exotherm occurred at a slightly lower temperature than the Type II exotherm. An intermediate phase is formed before the occurrence of the Type II exotherm and the formation of crystalline magnesium carbonate.

These differing mechanisms have implications for the decomposition mechanism of hydromagnesite in polymer compounds for two reasons. First, the heating rate in a fire situation is likely to be high and the self generated carbon dioxide atmosphere will both contribute to the formation of the crystalline magnesium carbonate and associated higher decomposition temperature of the Type II decomposition mechanism. Second, in a hydromagnesite-polymer composite the local partial pressure of carbon dioxide during hydromagnesite decomposition is likely to be much higher

than atmospheric pressure due to the tortuous route from the surface of the hydromagnesite crystal to the polymer-gas interface on the surface.

## 2.5 Comparison of synthetic hydromagnesite with naturally occurring blends of huntite and hydromagnesite

More recently Haurie *et al*.[84] studied the use of synthetic hydromagnesite with the chemical formula shown in Figure 35.

$$Mg_5(CO_3)_4(OH)_2{\cdot}4H_2O$$

**Figure 35: Chemical formula of synthetic hydromagnesite studied by Haurie *et al*.**

It had a total decomposition endotherm of 800 $Jg^{-1}$ associated with the loss of carbon dioxide and water. Decomposition studies using TGA/DTA at 10°C $min^{-1}$ in air showed that it decomposed in three steps as follows:

200 - 250°C release of water of crystallisation

380 - 450°C release of water from decomposition of the hydroxides

510 - 550°C release of carbon dioxide from decomposition of the carbonate

The three decomposition stages detected in the synthetic hydromagnesite were also detected in mixtures of natural hydromagnesite and huntite (UltraCarb) although the temperatures varied slightly. In addition two peaks at 540 - 600°C and 725 - 780°C due to decomposition of huntite were observed.

The synthesis and three step decomposition of hydromagnesite is also discussed by Botha[80]. The second study[101] discusses the decomposition of hydromagnesite and then goes on to investigate the re-hydration of hydromagnesite that has been dehydrated and dehydroxylated at 325°C. It was found that over an 11 week period the dehydrated hydromagnesite reverted back to its original form. During the first 7 days water was taken up by physical surface absorption and the reappearance of hydroxyl groups in the crystal lattice was also observed. These observations were

confirmed with FTIR and the appearance of DTA peaks at about 100°C and 246°C. Over the 11 week period FTIR analysis showed water molecules integrating into the crystal lattice. Changes in the carbonate FTIR spectra showed that there was interaction between these groups and the water molecules as they realigned themselves into the crystal structure. This may well have been due to hydrogen bonding of the water molecules to the carbonate groups as discussed by Akao[95].

One work[82] differs from most others in the decomposition temperatures reported. Frost reports that a 5°C $min^{-1}$ heating rate gives decomposition temperatures of 135, 184, 412 and 474°C for hydromagnesite that he synthesised. The first two decompositions at 135 and 184°C are attributed to loss of water of crystallisation in two steps, each giving a loss of two water molecules. The third decomposition at 412°C is attributed to dehydroxylation. Decarbonation is said to occur at 412°C and 474°C. These conclusions are all drawn through comparisons of theoretical mass losses compared to the mass losses measured using TGA, no analysis of the gases emitted during the decomposition appears to have been made. Comparing with other authors' work[63,80,84,85,101] the first two decompositions seem to occur at very low temperatures. Frost comments on this, referring to the fact that Beck[63] found decomposition temperatures between 275 and 325°C for loss of water, and loss of carbon dioxide at 485°C and again at 565 - 600°C. Frost appears to question the validity of Beck's results at this stage, stating that "the results of Beck are so significantly different that the measurement is open to question". The difference in the higher temperature decompositions appears to arise from the fact that Frost did not find the exotherm that Beck had reported. However several workers[65-69,100,102] have published work showing the conditions needed for the exotherm to occur. One of these conditions being a heating rate of greater than 18°C $min^{-1}$. It is therefore unsurprising that no exotherm was seen by Frost at heating rates of 5°C $min^{-1}$. Beck does not state what heating rate he used, however the strong exotherm that was detected suggests it was fairly fast.

Frost[82] also used controlled rate thermal analysis to study the decomposition of this sample of synthetic hydromagnesite. This method involved using a variable heating rate, up to a maximum of 1°C $min^{-1}$, in order to maintain a constant decomposition

rate of 0.1mg $min^{-1}$. These very slow heating rates showed that the sample went through five stages of decomposition with mass losses at 100°C and 145°C being attributed to dehydration. Dehydroxylation was shown to occur at 203°C followed by isothermal loss of carbon dioxide at 370°C. At 409°C a second brief isothermal was measured, Frost suggests this may be due to the recrystallisation of magnesium oxide as suggested by Beck[63]. Comparison of these results with those achieved at a fixed 5°C $min^{-1}$ clearly illustrates how the decomposition of hydromagnesite is affected by the rate of heating. There is no one true decomposition mechanism for the mineral and no "correct" method for measuring the decomposition, but a number of mechanisms depending on the test conditions.

Frost's work was carried out using synthetic hydromagnesite produced in his own laboratory. He reported that the hydromagnesite produced was characterised for phase specificity using XRD and chemical composition using EDX (energy dispersive X-ray analysis, a technique for identifying chemical composition using a scanning electron microscope) although details of these analysis are not shown. Perhaps, as the TGA decomposition temperatures suggest, the product produced was not true hydromagnesite. Frost's own calculations based on measured mass losses leads him to conclude (in an appendix not discussed within the text) that the formula for the hydromagnesite that he had synthesised was $Mg_5(CO_3)_4(OH)_2{\cdot}2H_2O$. This may well explain the disagreement between the decomposition temperatures reported in the work and that of other authors. Clearly the material that he synthesised was not true hydromagnesite as it did not contain enough water. As the work of Botha[101] showed the process of hydration can take some weeks at ambient conditions and would certainly influence the crystal structure[95,96] since the water molecules form a network of hydrogen bonding with the carbonate ions. This oversight has to throw doubt on the validity of any comparisons made between this work and that of previous authors.

## 2.6 Exothermic event in the decomposition of hydromagnesite

The overall decomposition of hydromagnesite is endothermic, enhancing the fire retardant action of the mineral. However under some conditions an exothermic event has been recorded in hydromagnesite at a little over 500°C. This has led to some discussion about its source and mechanism. Some researchers appear to have missed it completely while others have devoted entire papers to it. It is clear that the event is highly dependent on test conditions which explains why there are differing reports as to its importance and mechanism. The appearance of an exotherm during the thermal decomposition of minerals used as fire retardants is not unique to hydromagnesite. Magnesium hydroxide has also been reported[103] to show an exotherm at about 507°C. This is due to crystallisation of cubic magnesium oxide from the hexagonal magnesium hydroxide crystals after dehydroxylation.

In Beck's[63] work from the 1950's, comparing the decomposition of a quantity of carbonate minerals using differential thermal analysis, an exothermic event in the decomposition of hydromagnesite was reported. This exotherm was reported to result from '*the formation of amorphous (?) MgO which inverts to cubic MgO at 510°C*'. The question mark in parenthesis suggests that Beck was not sure whether the magnesium oxide was actually amorphous at this stage.

In the early 1970's Todor[64] made the observation that an exotherm could be detected at a range of temperatures between 385°C and 460°C. Most other researchers, as discussed below, are in agreement that the exotherm occurs between about 510°C and 530°C. However, Todor gives no details of the test conditions that gave this wide temperature range, so it is difficult to comment on their validity.

Further investigation in the 1970's by Sawada[65] confirms that an exothermic event occurs under certain specific conditions. The conditions favouring the exotherm include a high partial pressure of carbon dioxide, dense packing of the sample and a high heating rate. The exotherm was not seen at a heating rate of 10°C $min^{-1}$ but was seen at 20°C $min^{-1}$. In a later paper again by Sawada[69] further investigation into the exotherm confirms that it is due to the crystallisation of magnesium carbonate from the amorphous phase.

Padeste's work [100] from 1991 gives a detailed analysis of the decomposition of hydromagnesite under nitrogen and carbon dioxide atmospheres. Under nitrogen only two decomposition stages are observed in hydromagnesite, under carbon dioxide the second decomposition stage resolves itself into two separate stages separated by an exotherm. It is reported that the exotherm is caused by the crystallisation of magnesium carbonate after the loss of the hydroxide group. X-ray diffraction (XRD) was used to confirm that this crystallisation occurred.

More recently, in 2001, Khan[102] carried out some investigation into the exothermic peak in the decomposition of hydromagnesite. This work again confirmed the presence of the exotherm under certain conditions. DTA analysis revealed, in a nitrogen atmosphere, that no exotherm was observed for heating rates of less than 18°C $min^{-1}$ but at 18.5°C $min^{-1}$ or faster an exotherm was seen at about 525°C. The size of the exotherm increased as the heating rate was increased above 18.5°C $min^{-1}$. The magnitude of the exotherm was reported to increase and also occur at a lower heating rate as the sample size was increased. Khan also investigated the effect of a carbon dioxide atmosphere, this gas caused the exotherm to be observed at much lower heating rates and with smaller sample sizes. Although Sawada[65] did not report any exotherm in a nitrogen atmosphere, his conclusion that carbon dioxide and high heating rates are required is consistent with this work. Khan also suggests that the exotherm is due to mechanical stress within the crystal structure caused by the release of carbon dioxide which becomes trapped. This trapped gas is then suddenly released resulting in a small 'explosion within the sample'. The mechanical breakdown of the crystallite and the release of heat energy associated with the explosive release of the carbon dioxide is given as the cause of the exotherm. This theory is based on the fact that a sudden mass loss is associated with the exotherm and that electron microscopy shows that the magnesium oxide residue appears more "fluffy and dispersed" in samples that have been through the exothermic decomposition than those that are decomposed without the exothermic event. Such sudden eruptions, especially close to ignition temperatures, could extinguish early flaming increasing the ignition resistance of polymers using hydromagnesite compounds as fire retardant additives.

Clearly an exothermic event does occur during the decomposition of hydromagnesite under certain conditions but at least two different theories about its origin have been proposed. Sawada's work[65-69] is the most detailed and appears the most reliable. Therefore the explanation of the exotherm being due to the crystallization of magnesium carbonate seems a likely explanation. Sawada attributes the sudden mass loss to a sudden increase in the rate of decarbonation, caused by the exotherm.

Inglethorpe[104] carried out one of the more recent investigations into the decomposition of hydromagnesite and huntite. Following a review of the work of earlier researchers and his own investigations, in air, he concluded that the decomposition of hydromagnesite contains four stages as follows:

1) endothermic loss of water of crystallisation
2) endothermic dehydroxylation and formation of amorphous magnesium carbonate
3) exothermic crystallisation of magnesium carbonate
4) endothermic decarbonation of magnesium carbonate

This scheme provides a good summary of the findings of all other researchers.

In none of these studies was the effect of the exothermic event on fire retardancy studied. In fact Inglethorpe[104] is the only researcher to comment on the fact that the exotherm could have a detrimental effect on fire retardant properties. All of these studies were carried out on the mineral alone, not on polymer compound containing the minerals. The existence of the exothermic event occurring in a burning polymer containing hydromagnesite has not been reported. Inglethorpe is the only researcher to comment on this, suggesting that such a detrimental effect is only likely in polymer compounds with high loading levels of the minerals. In the case of commercially available mixtures of hydromagnesite and huntite, the temperature range of the endothermic decomposition of the huntite overlaps the hydromagnesite exotherm. This will remove some of the heat generated by the crystallisation of the magnesium carbonate.

## 2.7 Influence of particle size, milling and surface coating on the decomposition mechanism

In much of the work discussed no information is given on the particle size of the mineral powders. This could have an influence on the decomposition due to thermal conduction within the particles and may explain some of the differences in decomposition temperatures and mechanisms reported at apparently similar test conditions. Haurie[85] has carried out some studies into the effect of particle size reduction through different milling processes on the thermal decomposition characteristics of synthetic hydromagnesite. It was found that mechanical milling methods could cause an increase in the decomposition rate between 400°C and 500°C and reduce the exothermic crystallisation of magnesium carbonate. This was suggested to result from the milling action causing defects in the crystal lattice resulting in the early release of carbon dioxide. Particle size reduction using an air jet mill did not cause significant changes in the decomposition profile of the hydromagnesite. Haurie makes the comment that these changes could influence the fire retardant efficiency of the synthetic hydromagnesite but that further work is needed to investigate this.

Earlier work by Haurie[83] showed that coating of synthetic hydromagnesite with stearic acid, which is frequently used as compatibiliser to aid dispersion of the filler within a polymer, also has an effect on the decomposition of the mineral. Levels of 3% and above influence the decomposition in the region of 350–450°C causing a faster rate of decomposition. A similar effect has been reported for magnesium hydroxide[53] where stearate coating has been shown to increase the rate of decomposition, suggesting that the acid protonates the hydroxide with the release of water. Haurie states that the TGA tests were carried out under an oxygen atmosphere at a heating rate of 10°C $min^{-1}$. The decomposition profile for the uncoated hydromagnesite shows the same distinctive three step decomposition reported by Sawada[67] as Type II decomposition, even though the test was carried out under oxygen with a low heating rate. As the stearic acid coating level was increased to 4.5% the decomposition profile as measured by TGA gradually became more like the Sawada's Type I decomposition. The rate and magnitude of the decomposition

between about 350 – 450°C increased and the magnitude of the decomposition above 480°C correspondingly decreased. Haurie shows that XRD shows a stronger, more defined magnesium oxide peak when hydromagnesite coated with 4.5% stearic acid is heated at 400°C for one hour, compared to an uncoated sample. This indicates a higher degree of crystallinity in the magnesium oxide. No attempt to determine the phase changes in terms of formation and decomposition of a crystalline magnesium carbonate during the decomposition were made. However, taking into account Sawada's detailed work[65-68] it would appear that the stearic acid could be preventing the formation of crystalline magnesium carbonate, causing the hydromagnesite to decompose directly to magnesium oxide. A similar effect on the decomposition profile was also seen by Haurie[85] when hydromagnesite was mechanically ground to smaller particle sizes. The method used for coating the stearic acid was a heated high speed mixer. It is possible that similar stresses resulting in defects are being introduced into the crystal structure through the mechanical action of coating the filler, as they are during mechanical grinding.

## 2.8 Structure and decomposition of huntite

The earliest reference to huntite is a paper by George Faust[71] from 1953 in which the discovery of a new mineral in Nevada was announced. Faust acknowledges that the mineral probably had been discovered previously but had been misidentified as impure magnesite by W. E. Ford in 1917. Faust announced that the new mineral was to be named huntite in honour of his former teacher, Walter F. Hunt, Professor of Petrology at the University of Michigan from 1922 until 1933 and editor of American Mineralogist for 35 years[105]. Faust carried out DTA analysis of the newly discovered mineral, huntite, discovering that it went through endothermic decompositions at 644°C and 901°C, these decompositions were attributed to the dissociation of $MgCO_3$ and $CaCO_3$ respectively. It was also shown by chemical analysis that the chemical formula for huntite was $Mg_3Ca(CO_3)_4$.

Dolomite, $MgCa(CO_3)_2$, has a chemical structure that is similar to huntite. Beck[63] showed by DTA that is also decomposes through two endothermic stages at 815°C and

965°C. Dolomite has a high whiteness, and resistance to wearing, weathering, and chemical attack. It is therefore used in applications such as textured wall coatings and white lines on the roads. It has no known fire retardant properties.

The crystal structure of huntite is somewhat simpler than hydromagnesite. In 1962 Graf and Bradley[106] described it as an ordered rhombohedral double carbonate, similar to a deformed face centred cube. The calcium atom is located at the origin with three magnesium atoms at the face centres and three carbonate groups at the edge centres, the final carbonate group is located at the body centre. For detailed information regarding the crystal structure of huntite, including tables of d-spacings, structural factors, interatomic distances and structural diagrams, the reader should refer to Graf and Bradley's work[106].

The American Mineralogist Crystal Structure Database[97,98] gives structural data for huntite as described by Dollase[107] and XtalDraw[99] displays this data as shown in Figure 36.

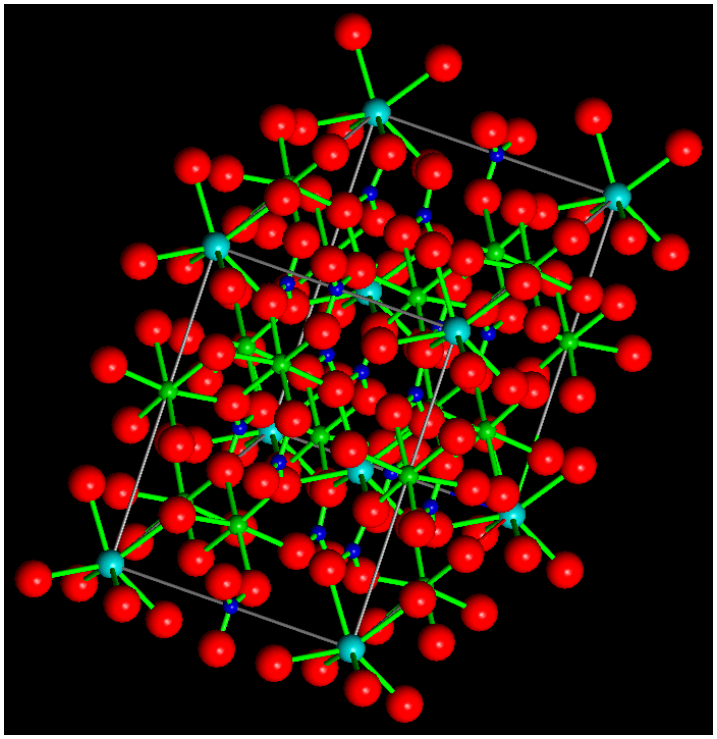

**Figure 36:Crystal structure of huntite as given in the American Mineralogist Crystal Structure Database**[97,98]

In 1966, a white powder was discovered on the wreck of a Roman ship. Barbieri[72] carried out an analysis on the powder identifying it as huntite. DTA analysis confirmed that it went through two endothermic decompositions, one at 650°C and one at 910°C, much the same as the findings of Faust. Barbieri also went into some detail trying to determine whether the huntite had formed from some other mineral such as magnesite due to being submerged in sea water for many years. Their chemical analysis concluded that it was most likely that the huntite was in its original form and that therefore the Romans were in fact trading huntite. The fact that huntite was used in the ancient world is confirmed by Riederer[108] in a paper indentifying pigments used by the ancient Egyptians. A bowl that had been excavated in Nubia and accurately dated to 1600BC was analysed and it was shown that huntite was used as a white pigment. It therefore seems reasonable that the Roman ship (dated to the 3$^{rd}$ century AD) may well have been trading huntite as part of its cargo. There is also evidence[109] that huntite was used as a white pigment in Cambodian manuscripts from the 18$^{th}$ and 19$^{th}$ centuries.

Ozao and Otsuka[70] stated in 1985 that a detailed study of the decomposition of huntite had not yet been carried out. They went on to describe their work in this area, confirming the previously known decompositions shown by Faust[71] and Barbieri[72]. Ozao's DTA curves, measured in at a heating rate of 10°Cmin$^{-1}$ in a carbon dioxide atmosphere, of mechanical mixtures of magnesite ($MgCO_3$) and calcite ($CaCO_3$) were shown to be clearly different to those of huntite ($Mg_3Ca[CO_3]_4$). The distinctive peaks associated with the decomposition of the magnesium carbonate and the calcium carbonate were present in the huntite but they occurred at slightly lower temperatures. This indicates that huntite is not a simple mechanical mixture of the two minerals. XRD analysis showed that at about 620°C huntite has decomposed to leave poorly crystallised magnesium oxide and "magnesian calcite". This is illustrated by Ozao as shown in Figure 37.

$$Mg_3Ca(CO_3)_4 \rightarrow CaCO_3{\cdot}nMgCO_3 + (3-n)MgO + (3-n)CO_2$$

***n* gradually reduces from 0.2 to 0.05 over the temperature range 620°C to 790°C.**

Figure 37: Ozao's proposed mechanism of huntite decomposition to magnesium oxide and "magnesian calcite"

The magnesian calcite gradually decomposes to form further magnesium oxide as the temperature increases to about 790°C and over the same temperature range the magnesium oxide crystallises to leave magnesium oxide and calcite. The remaining magnesian calcite then decomposes to leave magnesium oxide and calcium oxide at about 900°C. Illustrated by Ozao as follows:

$$CaCO_3{\cdot}nMgCO_3 \rightarrow nMgO + CaO + (1+n)CO_2$$

$n < 0.05$

Figure 38: Decomposition of magnesian calcite to magnesium oxide and calcium oxide

More recently Kangal & Guney[73] made some investigations on Turkish huntite. They quote huntite as having a two stage decomposition at 602°C and 622°C, and a further decomposition at 829°C but make no measurements of what these decompositions correspond to in terms of chemical decomposition.

## 2.9 Implications for the suitability of huntite and hydromagnesite as fire retardant additives

It is generally accepted[59-61] that for metal hydroxides to act as effective fire retardant additives in polymer composites the decomposition temperature of the polymer must be closely matched by the endothermic decomposition temperature of the metal hydroxide. The rate of polymer decomposition is therefore slowed because of the heat absorbed by the decomposing metal hydroxide and the released water dilutes the flammable polymer decomposition products. The metal oxide residue also acts as a thermal barrier to further decomposition of the underlying polymer.

A mixture of hydromagnesite and huntite meets all of the above requirements and compared to the commonly used metal hydroxides may well provide some further

benefits. The initial decomposition temperature of hydromagnesite has been shown[63-69,100] to be about 220°C compared to 180 - 200°C for ATH[54]. This gives it the advantage of being able to withstand higher processing temperatures meaning that it is suitable for polymers with higher melt temperatures such as polypropylene where ATH cannot be used.

When used as a fire retardant additive the rate of temperature increase that hydromagnesite will experience within a burning polymer is likely to be well in excess of the 18.5°Cmin$^{-1}$ that Khan[102] found to be the point at which crystallisation of magnesium carbonate occurs. The hydromagnesite particles will also be held in a self generated carbon dioxide atmosphere, which will also contribute to the decomposition mechanism becoming close to that described by Sawada[67] as type II decomposition. These effects mean that, within a polymer composite, hydromagnesite will be likely to follow the mechanism of releasing water at about 220°C, followed by partial decomposition of the carbonate ions up to 520°C and creation of a high partial pressure of carbon dioxide around the particles. Following the crystallisation of magnesium carbonate the final release of carbon dioxide will occur up to 600°C. This gives hydromagnesite a wide decomposition range making it suitable for reducing flammability of a wider range of polymers.

Initially huntite may appear to have a decomposition temperature that is too high for fire retardancy in polymers. However it is feasible that it may provide some benefit in high temperature polymers such as polyetheretherketone (PEEK). Studies of the decomposition mechanisms[110] of this polymer show that it does not begin to decompose until 575°C. PEEK's melting point of 343°C makes both aluminium hydroxide and magnesium hydroxide unsuitable. Huntite's initial decomposition temperature of about 400°C and endothermic release of carbon dioxide up to 750°C makes it an interesting possible additive for this polymer. Of course only pure huntite would be suitable, any hydromagnesite present would decompose during melt processing.

In mixtures with hydromagnesite, huntite's platy morphology may provide a barrier to the transport of combustible decomposition products to the flame. It may also

enhance mechanical reinforcement of carbonaceous or inorganic char. Once formed into a char layer huntite will also provide additional protection to the underlying polymer through further endothermic decomposition in response to high external heat fluxes. These functions will not be provided by magnesium hydroxide or aluminium hydroxide due to their complete decomposition at lower temperatures.

## 2.10 Action of huntite and hydromagnesite as a fire retardant in halogen free formulations

In terms of fire retardancy the published literature almost exclusively refers to the use of hydromagnesite in polymers. However there have been other proposed uses of this mineral and its natural blends with huntite, such as its use to fight forest fires[111-115] and its use to control the burning rate of cigarette papers[116,117].

The first reports of mixtures of hydromagnesite and huntite as a fire retardant appeared in the trade literature. Microfine Minerals (the name used by Minelco before acquisition and renaming by Sweden's LKAB) published some work in the late 1980's and early 1990's promoting its new blends of hydromagnesite and huntite as a fire retardant mineral under the trade name UltraCarb. An article[118] appeared in the Plastics and Rubber Weekly in 1988 introducing UltraCarb as a new product consisting of a naturally occurring partially hydrated magnesium calcium carbonate. It was also stated that it could be used as an alternative to already known mineral fire retardants such as ATH and magnesium hydroxide. A similar article[119] appeared in European Plastics News the same year giving details of UltraCarb as a new mineral with claims that it could provide fire retardant and smoke suppressant properties for 'most types of plastics'. Two years later an article[120] in Modern Plastics International described UltraCarb as a 'flame retardant, smoke suppressor which is a mixture of huntite and hydromagnesite'. It goes on to explain that it absorbs heat by forming metal oxides, carbon dioxide and water and gives information on its use in ethylene vinyl acetate copolymer (EVA).

Most published research supports the view that hydromagnesite is the more effective fire retardant of the two minerals (hydromagnesite and huntite), therefore less effort

has been spent analysing possible fire retardant mechanisms of huntite. Kirschbaum [121,122] states that because of its high decomposition temperature, over 400°C, huntite is not a very effective fire retardant on its own. He goes on to say that a combination of hydromagnesite with huntite has equal fire retardant performance to metal hydroxides such as ATH provided the hydromagnesite to huntite ratio is greater than 40%. This implies that if huntite is ineffective as a fire retardant in a blend with hydromagnesite, then hydromagnesite must be a very effective fire retardant since the mixture is still as effective as ATH. Alternatively huntite is contributing some as yet unidentified fire retardant behaviour. As the ratio of hydromagnesite to huntite increases to 40% there is a steady increase in oxygen index but at around 40% the oxygen index plateaus with no further significant increase, even at ratios of 100% hydromagnesite[122]. Again, this suggests that the huntite is having some fire retardant effect because it has been shown[54] that ATH increases limiting oxygen index (LOI) significantly when loading levels in a polymer are raised from 40% to 60%. It appears that in a mixture of hydromagnesite and huntite that the fire retardant effect of hydromagnesite is balanced by the effect of huntite once the ratio of hydromagnesite to huntite reaches 40%. In EVA, blends of hydromagnesite and huntite containing more than 40% hydromagnesite are shown to give an oxygen index of 35 – 36% at a 60% loading level. Kirschbaum also reports that natural blends of hydromagnesite and huntite have a similar endothermicity to aluminium hydroxide and magnesium hydroxide. Kirschbaum also gives brief details[121] of how blends of hydromagnesite and huntite can increase oxygen index when used as a partial replacement for ATH in ethylene propylene diene monomer rubber (EPDM) and can be used to produce a polybutylene terephthalate (PBT) compound suitable for the electrical and electronics industry with a UL94 V0 rating in the Bunsen burner test. This shows that the combination of hydromagnesite and huntite can be more effective than ATH adding to the evidence that huntite is providing some form of fire retardant action.

Georgiades[76] reported that blends of hydromagnesite and huntite containing less than 40% of hydromagnesite struggled to achieve a UL94 V0 rating at reasonable loading levels in polypropylene and EVA. Georgiades reports that studies of mixtures of

the minerals containing between 10% and 67% hydromagnesite showed that there was no significant difference in the fire retardant effect once the hydromagnesite content exceeded 42%. No details are given as to what test was used to determine the fire retardancy of the compounds. It is also reported that a 50/50 mixture of the minerals and a mixture with a higher proportion of huntite are efficient smoke suppressors. This is the first positive evidence of the action that huntite is providing in terms of fire retardancy. Unfortunately these comments are made but no data is presented to back up the claims so it is impossible to draw any further conclusions.

Very little detailed research has been published on the influence of the hydromagnesite/huntite ratio of natural blends on fire retardancy in polymer compounds. Clemens[123] appears to have published the first and so far perhaps the most detailed investigation into the effect of the ratio of the two minerals. The work was conducted using polypropylene and in agreement with previously reported work the hydromagnesite component imparted significantly greater fire retardant effect than the huntite. However, fire retardancy was measured in terms of oxygen index and UL94. No measurements of smoke, heat release or other aspects of fire and combustion were examined. It was also found that huntite was much more effective than hydromagnesite at nucleating crystallisation of polypropylene. This effect was observed to give compounds improved impact properties when a higher proportion of huntite was used. A similar reinforcing nature of huntite particles was reported by Geogiades[76] and attributed to the platy nature of the huntite particles.

The work, discussed above, by Kirschbaum, Clemens, and Georgiades, while providing useful guidelines to the industrial use and applications of natural blends of hydromagnesite and huntite, has been more application oriented rather than making detailed studies of their fire retardant mechanisms. These publications appear to be more focussed on promotion of the use of these materials by the company commercialising the minerals.

Basfar[124] has shown that peroxide crosslinking of EVA containing hydromagnesite and huntite (UltraCarb LH15X) increases elongation at break significantly over a range of filler loading levels from 90 to 180 phr. At 120 phr the elongation at break was

increased from less than 200% to over 500% by crosslinking. At the same time tensile strength was shown to increase, although the magnitude of the improvement diminished with increasing filler loading levels, at 180 phr crosslinking had no effect on tensile strength, but still improved elongation at break. In comparison, peroxide crosslinking of magnesium hydroxide filled EVA showed only small increases in elongation at break (approx. 200% to 250% at 120 phr loading). However, crosslinking provided a consistent increase in tensile strength over the same range of loading levels. Peroxide crosslinking consistently increased the LOI of EVA filled with hydromagnesite and huntite by 3 – 4 percentage points over the range of loading levels (e.g approx. 29 – 33% at 120 phr loading and approx. 36 – 40% at 150 phr loading). The LOI values of the uncrosslinked magnesium hydroxide filled EVA were approximately equivalent to the values achieved with the crosslinked EVA containing hydromagnesite and huntite. However, peroxide crosslinking the magnesium hydroxide filled EVA consistently reduced the LOI values by about 3 – 4 percentage points. Similarly opposing trends were reported in cone calorimeter results; peak heat release rates were reduced from 383 $kWm^{-2}$ to 301 $kWm^{-2}$ when EVA filled with 150 phr of magnesium hydroxide was crosslinked. However, EVA filled with 150 phr of hydromagnesite and huntite showed an increase in peak heat release rate from 310 $kWm^{-2}$ to 379 $kWm^{-2}$. Time to ignition was increased in both the EVA filled with magnesium hydroxide, and hydromagnesite and huntite when the compounds were crosslinked. Crosslinking with ionising radiation was shown to have similar effects as peroxide crosslinking on mechanical properties with both types of fire retardant mineral, but the effect on fire properties was not reported. Basfar states that it is not clear why the crosslinked EVA filled with huntite and hydromagnesite has such different mechanical properties compared to the crosslinked magnesium hydroxide filled EVA, but notes that further work is planned to examine these effects.

### 2.11 Fire retardancy of synthetic magnesium carbonate hydroxide pentahydrate

Rigolo[125] carried out some comparisons in polypropylene between a synthetic magnesium carbonate hydroxide pentahydrate (MCHP) and the commonly used fire

retardants ATH and magnesium hydroxide. The MCHP was a reagent grade supplied from Aldrich Chemicals. MCHP is quoted as having the chemical formula shown in Figure 39.

$$(MgCO_3)_4 \cdot Mg(OH)_2 \cdot 5H_2O$$

Figure 39: Chemical formula of synthetic magnesium carbonate hydroxide pentahydrate

This formula is very similar to hydromagnesite having only one extra water molecule and is the formula given by Botha[80] as heavy basic magnesium carbonate. Rigolo found it to be more effective than magnesium hydroxide in terms of oxygen index and UL94 vertical burn tests. A 60% loading of MCHP in polypropylene gave an oxygen index of 28% with a UL94 V0 rating. Both the ATH and magnesium hydroxide used in this study absorb more energy per unit mass through their endothermic decompositions than MCHP. Therefore the effectiveness of MCHP is attributed to the large loss of water and the formation of a thicker and more impermeable inorganic residue than is formed by either ATH or magnesium hydroxide. For all fillers at loadings of less than 40%, the polymer could flow away from the flame, at levels of greater than 40% the samples retained their shape during burning and formed inorganic residues. In a UL94 vertical burn test a 50% loading level of MCHP was required to prevent dripping and achieve a V0 rating, however magnesium hydroxide required a 60% loading level to achieve the same rating. Investigation was also made into the temperature of the sample during the oxygen index test. This was done using a thermocouple embedded into the oxygen index samples at a set distance from the tip. The temperature profile was then measured as the flame front approached. It was found that MCHP filled PP took considerably longer to reach its maximum burning temperature than ATH filled PP, indicating a slower burn rate. Magnesium hydroxide gave a similar time to peak temperature as MCHP. This longer time to reach maximum burning temperature was used to show that the rate of burning of an MCHP filled PP is slower than that of an ATH filled PP. It was also observed that the temperature measured by the thermocouple in the MCHP filled polypropylene remained high for up to 90 seconds after the flame had extinguished and was accompanied by an afterglow. It is possible

that this is due to the catalytic conversion of carbon to carbon dioxide by the magnesium oxide decomposition product of the MCHP. These findings are not necessarily indicative of the results that could be expected with natural hydromagnesite due to the higher water content of the MCHP or blends with huntite, as no measurements were shown for these materials. Mixtures of magnesium hydroxide and magnesium carbonate in the same ratios as seen in MCHP were found to be less effective fire retardants than MCHP. This indicates that the 5 water molecules and also possibly the combined crystalline structure of the components in MCHP is vital for the efficient fire retardant mechanism of MCHP.

### 2.12 Influence of stearic acid coating on the fire retardancy of mixtures of huntite and hydromagnesite

Haurie[83] reported that in EVA a 2 wt% coating of stearic acid on synthetic hydromagnesite increased oxygen index to 32.9% compared to 24.5% for an uncoated sample, although a 4 wt% coating reduced the oxygen index back to 29.2%. However, it should also be noted that the loading level of hydromagnesite in EVA varied over this test series. The uncoated sample was used at a 50 wt% loading, while the 2 and 4 wt% coated samples was used at 57 wt% loading. The increased loading level will have certainly also improved the oxygen index value, however the presence of stearic acid is also likely to have several effects. It will help to ensure good dispersion of the hydromagnesite, improving fire retardancy. Also its presence will slightly increase the available fuel, reducing the hydromagnesite loading. Haurie observed that the stearic acid coating increased the rate of hydromagnesite decomposition between 350°C and 450°C. In comparison to a commercially available 1% stearic acid coated mixture of hydromagnesite and huntite (UltraCarb C5-10) the oxygen index of the EVA containing 1 wt% stearic acid coated synthetic hydromagnesite was lower (31.9% compared to 34.7%), although it should be noted that the loading level of the synthetic material was again reduced (55 wt% compared to 63 wt%) compared to the UltraCarb C5-10. It was also noted that higher levels of stearic acid gave an improvement in tensile strength and elongation at break. Electron microscope pictures clearly show the effect of coating on improving the interaction of the polymer with the synthetic

hydromagnesite particle surface. The coated samples show clear adhesion of the polymer matrix to the surface of the particles, whereas the uncoated samples sit in voids within the matrix.

### 2.13 Fire retardant behaviour of huntite/hydromagnesite blends in mixtures with aluminium hydroxide

Haurie[84] has also looked at magnesium hydroxide, synthetic hydromagnesite and natural hydromagnesite/huntite blends, each in a 50/50 mix with ATH. This work was done in a 75/25 LDPE/EVA blend. Oxygen index tests showed that all three fire retardants improved the oxygen index from the 18.7% measured for the polymer blend alone. The ATH/synthetic hydromagnesite blend had a slightly higher oxygen index than the ATH/[hydromagnesite/huntite] blend, 28.6% compared to 27.1%. The ATH/magnesium hydroxide blend sat between the two at 28.1%. Cone calorimeter tests at 50 $kWm^{-2}$ showed that all three blends gave peak heat release rates of about 180 $kWm^{-2}$. However, there were differences between the burning and ash formation characteristics. The blend containing synthetic hydromagnesite had a slower reduction in heat release after the peak than either the magnesium hydroxide or the blend of natural hydromagnesite and huntite. The synthetic hydromagnesite blend also showed a second peak in heat release rate at between 450 and 550 seconds. The blend containing hydromagnesite and huntite also showed a second peak around 600 – 800 seconds but it was broader and less intense than the second peak in the formulation containing the synthetic hydromagnesite. These second peaks were attributed to the collapse of the ash structure and the release of the entrapped gases. In the case of the synthetic hydromagnesite the ash had shown a large volume expansion which then collapsed completely. The sample containing natural hydromagnesite and huntite showed some expansion but did not suffer the same collapse. Haurie makes no comment on why this should be. It is possible that the platy huntite particles are providing some reinforcement to the ash structure helping to prevent the overexpansion of the structure and providing support to prevent the collapse. This kind of action by huntite may well add to the fire retardant effect of the mixture of hydromagnesite and huntite. This less obvious fire retardant action may have been

overlooked in the past, leading to the misconception that huntite is an ineffective part of the blend in fire retardant terms. Smoke emission was also measured using the cone calorimeter in relation to the unfilled polymer; the synthetic hydromagnesite blend increased average specific extinction area and the total smoke released, while the magnesium hydroxide and blend of natural hydromagnesite and huntite reduced both of these parameters. Again Haurie doesn't comment but this could indicate that the huntite portion of the hydromagnesite/huntite mixture is performing a useful function. This agrees with Georgiades's observation[76] that huntite reduces smoke. If the huntite is reinforcing the char it will reduce the transport of flammable gases to the flame, therefore reducing heat release and smoke emissions. The synthetic hydromagnesite does not have this functionality, therefore the heat release rate is higher, and there is a second peak in heat release and smoke, as the ash loses integrity, collapsing with the release of entrapped gases.

### 2.14 Fire retardant behaviour of huntite/hydromagnesite blends in mixtures with glass frits

Kandola[126] investigated partial substitution of mixtures of hydromagnesite and huntite, and ATH with glass frits at replacement levels up to 50% in a vinyl ester resin. Glass frits are small friable glass particles made up of mixtures of silicon dioxide mixed with other metal oxides. In a fire situation the frits melt, flow and mix into a hard thermally insulating fire barrier. A number of patents[127-132] published over the past 10 years claim fire retardant benefits for the use of glass frits in a number of polymer systems. Kandola reported that partial replacement of a mixture of hydromagnesite and huntite with glass frits at levels up to 33% reduced the oxygen index by up to 1.5 percentage points, but a 50% replacement gave an oxygen index value similar that of the mixture of hydromagnesite and huntite alone. Partial replacement of ATH with the glass frit reduced the LOI at all levels of replacement up to 50%. Cone calorimeter results showed that replacement of both ATH, and mixtures of hydromagnesite and huntite, with glass frits lead to an increase in peak heat release rate and increased smoke production. Pictures of the char residues shows that addition of the glass frits has the positive effect of producing a more coherent char structure with less cracks in

the surface. This might be expected to help protect the underlying polymer during the burning process, unfortunately the oxygen index and cone calorimeter results do not show such benefits and no explanation is given as to why this might be.

## 2.15 Heat release studies by cone calorimetry

Morgan[133] has made some cone calorimeter studies of the effectiveness of various magnesium carbonate based fire retardants including a blend of natural hydromagnesite and huntite, synthetic hydromagnesite, magnesium carbonate, calcium carbonate and magnesium hydroxide. The work was all completed in ethylene vinyl acetate (EVA) and ethylene ethyl acrylate (EEA). There appears to be some misunderstanding about the decomposition of hydromagnesite. It is stated that "since hydromagnesite has a release temperature of 320 - 350°C, we used $Mg(OH)_2$ as the hydroxide control sample". It has been shown by many authors[63,65-69,84,85,100,101] that hydromagnesite decomposes over a range of about 220 - 550°C. Morgan also states that in his electron micrographs the hydromagnesite particles "can be clearly seen amongst the larger huntite particles". This is incorrect; in the type of blends of natural hydromagnesite and huntite used in this work the huntite particles are naturally much smaller than the hydromagnesite particles.

Morgan found that in EVA, magnesium hydroxide and synthetic hydromagnesite were approximately equal in their ability to reduce peak heat release rates and extend the time to reach the peak heat release rate to a greater extent than the other fire retardant fillers included in the study. Magnesium carbonate was found to be less effective than calcium carbonate at improving these parameters, although in EEA this situation was reversed. This finding was unexpected since magnesium carbonate decomposes endothermically to produce carbon dioxide at a lower temperature than calcium carbonate. It was found that the magnesium carbonate was not decomposing under the 35 $kWm^{-2}$ heat flux, therefore under higher heat fluxes magnesium carbonate may become more effective. The fact that the magnesium carbonate was not decomposed means that the difference in performance could simply be down to differences in the densities of the minerals. Calcium carbonate has a density of

approximately 2.8g $cm^{-3}$ compared to approximately 2.96g $cm^{-3}$ for magnesium carbonate. This means that in the calcium carbonate filled compound about 5.5% additional volume of polymer would have been replaced by inert mineral. However, calcium carbonate has a heat capacity of 0.84$JK^{-1}g^{-1}$[134] compared to 0.89$JK^{-1}g^{-1}$[135] for magnesium carbonate. Comparison of synthetic hydromagnesite with a blend of natural hydromagnesite and huntite in EVA was made. It was stated that the ratio of hydromagnesite to huntite was unknown in the natural blend and therefore the effect of each component cannot be explained. However, it is clear that the dilution of the natural hydromagnesite with an unknown quantity of huntite has had the positive effect of reducing the peak heat release rate, at the cost of reducing the time to ignition, when compared to the synthetic hydromagnesite. However the peak heat release rates of all the fillers was similar. The reduction in time to peak heat release rate arises because the huntite portion of the blend does not decompose until higher temperatures. Therefore during the pre-ignition stages of the fire a blend with huntite has less of the active component than a purer hydromagnesite.

Comparing the different activity of the fillers in EVA and EEA, Morgan makes the suggestion that the interactions between the differing polymers and the fillers accounts for the different fire retardant effectiveness of the fillers in the various polymers. However, no measurement or suggestion of what these different mechanisms might be is given. In summary it is reported that in EEA, hydromagnesite and magnesium hydroxide give similar HRR responses. However, in EVA, hydromagnesite and magnesium hydroxide have similar peak heat release rates but the time to ignition is much earlier for the hydromagnesite.

Morgan concludes that the huntite in blends of natural hydromagnesite and huntite reduces the effectiveness of this material and comments that the huntite has no more function than simple dilution in the manner of a calcium carbonate. It should be remembered though that all of Morgan's work was carried out at 35 $kWm^{-2}$ and as with magnesium carbonate, huntite will only become active at higher temperatures. The surface temperature for a non combustible board[33] at 35 $kWm^{-2}$ in the cone calorimeter reaches a plateau of around 500°C after 30 minutes. Huntite is also a very platy mineral and may act as a much more effective gas barrier and radiant heat shield

than a blocky calcium carbonate. It appears that Morgan's conclusion that huntite is a simple diluent in combination with hydromagnesite is not justified by the evidence in his paper.

Most researchers make the assumption that huntite contributes less to the fire retardant effect than hydromagnesite and that a higher proportion of hydromagnesite brings benefits for fire retardancy. Very little detailed work has been reported on the fire retardant benefits, if any, that huntite brings to the mixture of minerals. Inglethorpe[104] makes brief comment that huntite may have some beneficial properties in terms of fire retardancy. It is suggested that the small particle size of the huntite, which is typically less than 2 μm compared to the 5 – 20 μm size of the hydromagnesite, may improve the fire retardant effectiveness of the mineral. It is also suggested that the small huntite particles could reduce smoke density by producing a high surface area magnesium oxide. These are simply made as suggestions and no work is presented to either confirm or deny these hypotheses.

## 2.16 Effect of huntite/hydromagnesite mixtures on the burning behaviour of ethylene propylene copolymers

Toure has published two papers detailing the use of mixtures of hydromagnesite and huntite as a fire retardant in an ethylene propylene copolymer. The first[136] of the two studies gives details of the fire retardant effects of a blend of natural hydromagnesite and huntite with a 40:60 ratio. DTA measurements show how the polymer decomposes in nitrogen at between 400°C and 500°C and that the blend of hydromagnesite and huntite has endothermic decompositions above and below the polymer decomposition temperature. Similar measurements in air of the polymer and a polymer compound containing the mineral mixture showed how the exothermic decomposition of the polymer between 320°C and 425°C was pushed to a higher temperature when the minerals were added as a fire retardant. In fire tests, increasing loading level of the blend of hydromagnesite and huntite from 0 to 48.5 wt% increased the oxygen index[16] from 18.3 to 24.0%. The rate of horizontal flame spread measured by the French test NF P 92-504[137] was reduced from 0.64 $mms^{-1}$ to

0.12 $mms^{-1}$ over the same range of loading levels. For loading levels of over 25% no dripping occurred in the French NF P 92-505[137] dripping test. It was noted that a fire retardant effect could be expected from the endothermic decomposition of the hydromagnesite and partial decomposition of the huntite diluting the gas phase with water and carbon dioxide. Due to the fact that the polymer had completely decomposed at 500°C, only partial decomposition of huntite was expected to have a significant fire retardant effect. Any further decomposition of the huntite above this temperature was said to have no effect on fire retardancy of the polymer. This would certainly be true for thermally thin polymer compounds but not valid for thermally thick materials. DTA analysis was carried out on the ash residue to confirm the state of decomposition of the minerals. It is unclear in which test the char was formed but at a loading level of 20.4% the DTA analysis shows that there is no endothermic decomposition in the temperature range 500 - 600°C. This is the temperature range in which huntite is expected to endothermically decompose to magnesium oxide and calcium carbonate, indicating that at least partial degradation of the huntite occurred. However at a 48.5% loading level, a large endotherm is present in this temperature range indicating that the huntite did not decompose during combustion of the polymer. The reason given for this is that the higher loading level provides a more efficient fire retardant action, keeping the temperature of combustion to a lower temperature.

### 2.17 Action of huntite and hydromagnesite as a fire retardant in halogenated formulations

In the second paper[138] by Toure, the combination of natural hydromagnesite and huntite mixtures with antimony trioxide and decabromodiphenyl oxide (DBDPO) in ethylene propylene copolymer are investigated in some detail. The blend of natural hydromagnesite and huntite is investigated as a fire retardant in its own right as is the blend of antimony oxide with DBDPO. Combinations of the two blends are also investigated. The DBDPO and antimony trioxide act in the gas phase and it was thought that this may enhance fire retardancy in combination with the condensed phase

endothermic release of water vapour and carbon dioxide from the hydromagnesite and huntite.

The endothermic decomposition of the blend of natural hydromagnesite and huntite was found to cool the substrate reducing the heat transfer to the solid phase. It was also found to dilute the gaseous phase mainly with water. The fire retardant "efficiency" of the hydromagnesite/huntite blend as measured by TGA/DTA, at 10°Cmin$^{-1}$ in air, was said not to increase steadily with loading level. However, it is important to recognise the value of TGA/DTA in understanding thermal decomposition without mistaking it for a flammability test. The reduced "efficiency" was thought to result from incomplete decomposition of the minerals at higher loading levels, due to the lack of combustible material providing thermal feedback. TGA and DTA measurements on ash residue clearly shows that where higher filler loadings are used less decomposition of the huntite had occurred. It follows that when higher loading levels of a hydromagnesite/huntite mixture are used, the decomposition of the hydromagnesite is so effective at reducing the heat of the substrate that it never reaches a high enough temperature to initiate the higher temperature decompositions of the huntite. It is not stated which test the ash residues were taken from but it was probably oxygen index as results from this test were discussed. The oxygen index test has no external heat source after ignition, relying entirely on self sustaining combustion. Therefore the huntite is less likely to decompose than in a cone calorimeter test or real fire situation where higher external heat fluxes are present.

The argument that the effectiveness of blends of hydromagnesite and huntite does not increase steadily with loading level seems to contradict the results presented. Oxygen index results showed a steady increase with increasing loading level and rate of flame spread was steadily reduced. The lack of any mechanism from the hydromagnesite/huntite blend in the gaseous phase, beyond simple dilution, is also stated as a limitation of metal hydrates and carbonates. Therefore the action of DBDPO and antimony oxide which act as free radical scavengers in the gas phase were investigated as co-additives.

The DBDPO blend with antimony trioxide is shown to work well in its own right before blends with hydromagnesite and huntite are discussed. It is reported that there are

two mechanisms working against the DBDPO and antimony trioxide in these blends. The first is that magnesium oxide (a decomposition product from both hydromagnesite and huntite) is known to slow the production of gaseous halogen compounds from antimony/bromine blends[139]. The second is that the endothermic decomposition of the hydromagnesite/huntite mixture is shown to overlap with the exothermic decomposition of the DBDPO/antimony trioxide blend potentially reducing its effectiveness. Experiments at different loading levels of the two blends show that with a 25% loading of the hydromagnesite/huntite blend and a 20% loading of the DBDPO antimony trioxide blend, the potential antagonisms are overcome. At these levels a compound with an LOI of 26%, a UL94 V0 rating and a flame spread rate of $2mms^{-1}$ is reported.

One useful side effect noted by Toure was that increasing loading levels of the hydromagnesite/huntite blend gave an increase in flexural modulus of the same order as would be expected from lamellar fillers such as talc or mica. The smaller huntite particles have a naturally platy morphology so would be expected to enhance certain physical properties.

The use of UltraCarb as a fire retardant in PVC has been published several times at conferences in the early to mid 1990's [123,140-144] and in the scientific journals[145]. These papers give some very detailed information on the use of hydromagnesite/huntite blends in PVC. In PVC, blends of hydromagnesite and huntite have been shown to increase oxygen index[121] and reduce smoke and acid gas emissions[76]. However, since hydrogen chloride is an active flame quencher in the gas phase, reaction with carbonates and hydroxides can be counter-productive.

Early work by Briggs[142,143] gave details of a number of PVC formulations containing blends of hydromagnesite and huntite. It showed how flammability, smoke, acid gas and carbon monoxide emissions can all be reduced by blends of hydromagnesite and huntite. It is likely that when hydromagnesite and huntite are used in halogen containing polymers that the decomposition mechanism of both minerals will be a combination of the thermal decomposition previously discussed and reaction of acidic hydrogen halide with the carbonate mineral. The altered decomposition mechanism

will lead to earlier release of carbon dioxide from the carbonate groups, with the formation of magnesium and calcium halide, reducing the volume of acid gas released into the atmosphere. Cone calorimeter data shows that time to ignition and rate of heat release are improved as the loading level of hydromagnesite and huntite are increased. NBS smoke chamber measurements show that in non-flaming mode there is a trend to lower smoke at higher loading levels. The fact that blends of hydromagnesite and huntite have a higher onset of decomposition temperature than ATH was said to allow higher extrusion speeds giving an obvious benefit to cable producers looking to increase output. Since the decomposition of PVC begins with chain stripping of hydrogen chloride and the decomposition is auto-catalytic, the presence of hydroxides and carbonates to absorb the hydrogen chloride will also improve its thermal stability. Comparisons of zinc borate and antimony trioxide as co-additives to hydromagnesite and huntite were made. It was shown that mixtures of zinc borate with hydromagnesite and huntite gave PVC compounds with lower flammability, smoke and carbon monoxide emissions compared to compounds filled with blends of chalk and antimony trioxide. A PVC compound containing hydromagnesite and huntite was also shown to give reduced flammability and marginal reductions in smoke and carbon monoxide compared to one using a phthalate plasticiser. The formulations shown in this work were all aimed at the electrical wire and cable market. It was also shown that hydromagnesite and huntite in PVC can improve electrical properties of the compound by slightly increasing resistivity. The usual trend of a reduction in electrical resistivity on the addition of fillers, particularly if the polymer is of low polarity, is less apparent with hydromagnesite/huntite mixtures providing an additional benefit compared to alternatives such as ATH.

From 1992 and 1993 Briggs continued to further develop and optimise PVC formulations containing hydromagnesite and huntite. This culminated in two very detailed papers[144,145] giving details of approximately 50 different PVC formulations showing the use of hydromagnesite and huntite. This develops the initial work described above: combinations of a variety of types of plasticisers and coadditives such as antimony trioxide, zinc borate, zinc stannate, molybdenum trioxide, and a

magnesium zinc complex are detailed on their own and in combination, looking for synergies with hydromagnesite and huntite. Of the two most commonly used plasticisers (diisooctyl phthalate [DOP] and diisodecyl phthalate [DIDP]) DOP was shown to give compounds with higher LOI, lower rates of heat release and lower smoke emissions. A pentaerythritol ester plasticiser was shown to be particularly effective at reducing smoke emissions. The use of precipitated calcium carbonate in combination with UltraCarb was shown to be effective at reducing acid gas emissions at the expense of a reduction in oxygen index. A combination of hydromagnesite and huntite with zinc borate is shown to be a particularly effective method of producing antimony free alternatives to the traditional combination of antimony trioxide and chalk in PVC for the wire and cable industry. The work gives details of how hydromagnesite and huntite can be used to produce formulations with low smoke, high oxygen index, low acid gas emissions, and goes some way to providing formulations that meet specifications such as BS7655: Specification for Insulation and Sheathing Materials for Cables[146].

## 2.18 Fire retardant nanocomposites containing hydromagnesite

The study of fire retardant properties of blends of hydromagnesite with nano clays is still in its infancy. There appears to be currently only two published[86,147] papers in this area.

Laoutid[147] showed that use of a 55% synthetic hydromagnesite, 5% organo modified montmorillonite (oMMT) loading in EVA increased the LOI value to 34% compared to 29% for use of 60% hydromagnesite alone. It was suggested that the increase in LOI was due to reinforcement of the ash residue by the oMMT. This reinforcement of the hydromagnesite residue was also shown to lead to reduced heat release during testing on the cone calorimeter where a stable foamed residue was formed. It was suggested that the oMMT forms a barrier helping to prevent the decomposition volatiles entering the gas phase instead promoting the formation bubbles and possibly some intumescent protection of the underlying polymer. SEM observations showed that sintering of the MgO particles happened at temperatures

between 700°C and 1200°C. XRD analysis of the residues showed that at 700°C MgO was present from the decomposition of the hydromagnesite. At 1200°C there had been some crystallisation of the MgO and also formation of small quantities of forsterite ($Mg_2SiO_4$) indicating that there had been some reaction between the MgO and the montmorillonite at high temperature.

Initially it appears that Haurie[86] found contradictory results to Laoutid[147]. Haurie reports that a blend of hydromagnesite with oMMT gives a reduction in LOI, the opposite of Laoutid's reported increase, however Haurie's total filler content is not kept constant. Confusingly, the comparison is made between an EVA compound containing a blend of 30% ATH and 30% hydromagnesite with an EVA compound containing 27.5% each of ATH and hydromagnesite, and an EVA compound containing 30% ATH, 15% hydromagnesite and 5% oMMT. The total filler content has been reduced from 55% or 60% to only 50% when the oMMT was added making the results and conclusions difficult to fully interpret and understand. An increase in time to ignition and a reduction in peak heat release rate, measured in a cone calorimeter, was attributed to the oMMT. This is clearly true from the results even at the lower total filler content of 50% compared to 55% for the compound not containing the oMMT. In fact the oMMT compound containing 50% total filler content gave time to ignition and peak heat release values between those of the compounds containing total filler contents of 55% and 60% with no oMMT. The heat release rate graphs shown by Haurie are less convincing, they clearly show that the average heat release during the entirety of the test is higher for the compound containing the oMMT, again this could be due to the lower total filler content. Haurie claims the presence of oMMT increased the stability of the char and lead to a higher mechanical cohesion of the ash crust. This comment is similar to the comment made by Laoutid that oMMT reinforces the residue.

## 2.19 Decomposition of huntite and hydromagnesite when incorporated into a polymer compound

The decomposition mechanism of hydromagnesite and huntite was discussed earlier in sections 2.4-2.8 However, it is worth considering the decomposition mechanisms within the confines of a polymer matrix.

Hancock[53] showed evidence for an increase in the decomposition temperature of hydromagnesite when it is incorporated into polypropylene. It was shown by DSC that a mixture of hydromagnesite and huntite has four decomposition endotherms with peaks at 275°C, 440°C, 550°C and 690°C. Hancock's DSC measurement of polypropylene containing 60% by mass of a mixture of hydromagnesite and huntite showed an endothermic peak for the melting of polypropylene at about 180°C but the endothermic peaks associated with decomposition of hydromagnesite appear to have moved to about 350°C, and 450°C. Hancock offers little explanation for these results commenting only that a change in the decomposition profile at about 550°C is caused by 'magnesium carbonate, resulting from alteration of the basic magnesium carbonate'.

Within the confines of a polymer matrix the atmosphere surrounding the decomposing hydromagnesite particles will initially contain mainly water vapour and possibly some early polymer decomposition products. At higher temperatures it will contain a mixture of water vapour, polymer decomposition products, and carbon dioxide. The initial atmosphere will rapidly become saturated with water vapour meaning further evolution of water from the hydromagnesite particle is only possible through expansion of the bubble. This effect may result in water remaining within hydromagnesite particles until a higher temperature than in an open atmosphere. This must be an atmospheric saturation effect (i.e. equilibrium between decomposing hydromagnesite and its surrounding atmosphere) not an influence of the gas pressure within the bubble since Sawada[67] showed that under nitrogen, argon or carbon dioxide at pressures up to 50 atm the loss of water was unaffected.

Above 350°C hydromagnesite further decomposes giving off carbon dioxide which, initially, may become entrapped around the particles. It has been shown[65-

69,100,102,104] that a high partial pressure of carbon dioxide or a high heating rate can cause some of the magnesium carbonate formed during the decomposition of hydromagnesite to crystallise rather than immediately decompose giving off carbon dioxide. Crystalline magnesium carbonate decomposes at a higher temperature than the non-crystalline form, causing the complete decomposition of hydromagnesite to be delayed to a higher temperature. The self generated carbon dioxide atmosphere and high heating rate within a burning polymer is also likely to have this effect. Carbon dioxide in close proximity to the hydromagnesite particle will create a high partial pressure generating favourable conditions for the magnesium carbonate to crystallise. Hancock's work[53] shows a difference in the DSC profile between 500°C and 600°C of hydromagnesite and hydromagnesite incorporated into polypropylene. This is very likely to be due to the formation and decomposition of crystalline magnesium carbonate at the higher temperature.

The decomposition temperatures of the hydromagnesite part of a blend of hydromagnesite and huntite have been reported to be affected in the presence of decabromodiphenyl oxide (DBDPO)[138]. Whilst investigating the interactions of DBDPO, antimony trioxide and a hydromagnesite/huntite blend it was shown that an apparent increase in the dehydration temperature of the hydromagnesite was achieved when a blend of equal proportions of the two additives was created. The reason put forward for this increase in decomposition temperature of the hydromagnesite was that the DBDPO fused endothermically over an approximate temperature range of 200 – 400°C which retards the decomposition of the hydromagnesite. Clearly the decomposition temperatures of DBDPO and hydromagnesite overlap and therefore the decomposition reactions could have influence in each other. Without analysis of the gases evolved it is unclear which components are decomposing over which range of temperatures and the validity of this claim is unclear without further evidence.

While the above effects clearly have implications for the fire retardant mechanism of hydromagnesite it is not certain that any benefit in terms of increased processing temperature can be achieved. In both of the above cases (incorporation of hydromagnesite into PP and mixtures of hydromagnesite and DBDPO), the increase in

decomposition temperature was measured using TGA and DSC, both of which are mechanically static tests. Processing is a dynamic process therefore at temperatures above the decomposition temperature of hydromagnesite decomposition products are more likely to be released from the polymer by the continuous movement and mixing of the polymer during the melt processing. However, it appears that no published investigation has been made into this subject.

## 2.20 Comparison of hydromagnesite, huntite, aluminium hydroxide and magnesium hydroxide

Table 2 compares the physical properties of hydromagnesite, huntite, aluminium hydroxide and magnesium hydroxide in terms of decomposition temperature and enthalpy, volatile content and residual mass.

| **Name** | Aluminium Hydroxide | Magnesium Hydroxide | Hydromagnesite | Huntite | UltraCarb[a] |
|---|---|---|---|---|---|
| **Chemical formula** | $Al(OH)_3$ | $Mg(OH)_2$ | $Mg_5(CO_3)_4(OH)_2{\cdot}4H_2O$ | $Mg_3Ca(CO_3)_4$ | |
| **Onset of decomposition (°C)[b]** | 180 – 200 | 300 – 320 | 220 – 240 | ~ 400[c] | 220–240 |
| **Enthalpy of decomposition ($Jg^{-1}$)[b]** | 1300 | 1450 | 1300 | 980[c] | 990[c] |
| **Volatile content by mass (%)[d]** | | | | | |
| Water | 35 | 31 | 19 | 0 | 11 |
| Carbon dioxide | 0 | 0 | 38 | 50 | 43 |
| Total | 35 | 31 | 57 | 50 | 54 |
| **Volatile content by volume (ltr/100g at 373.15K and 1atm)[d]** | | | | | |
| Water | 59.4 | 52.7 | 32.3 | 0 | 14.2 |
| Carbon dioxide | 0 | 0 | 26.4 | 21.6[e] & 8.7[f] | 21.8 |
| Total | 59.4 | 52.7 | 58.7 | 30.3 | 36.0 |
| **Residue content (%)** | | | | | |
| $Al_2O_3$ | 65 | - | - | - | - |
| MgO | - | 69 | 43 | 34 | 40 |
| CaO | - | - | - | 16 | 6 |

Notes:
a – approx. 60:40 mixture of hydromagnesite and huntite
b – figures taken from Rothon[54]
c – author's own work (see Chapter 4)
d – calculated theoretical values
e – initial decomposition $Mg_3Ca(CO_3)_4 \rightarrow MgO + CaCO_3 + 3CO_2$
f – secondary decomposition $CaCO_3 \rightarrow CaO + CO_2$

**Table 2: Summary of the type and quantity of decomposition products produced by aluminium hydroxide, magnesium hydroxide, hydromagnesite, and huntite.**

The data shows that hydromagnesite has a similar decomposition enthalpy to aluminium hydroxide, although the heat capacity of aluminium hydroxide is slightly higher than hydromagnesite (Table 3) in terms of $Jg^{-1}K^{-1}$. However, hydromagnesite loses a higher proportion by mass on decomposition than aluminium hydroxide but produces about the same volume of volatiles. Aluminium hydroxide produces water as the only volatile decomposition product, whereas hydromagnesite produces a mixture of carbon dioxide and water consisting of approximately 55% water vapour and 45% carbon dioxide by volume. The heat capacities, in terms of $Jmol^{-1}K^{-1}$ shown in Table 3, of water vapour and carbon dioxide are similar. In terms of fire retardant effect the volume of mixed gases and the effect on the heat capacity of the mixed gases entering

a flame from the decomposition of hydromagnesite is likely to be similar to that of the water vapour given off by aluminium hydroxide. Aluminium hydroxide leaves an aluminium oxide residue of approximately 65% of its original mass compared to hydromagnesite which leaves a residue of magnesium oxide of only 43% of its original mass. The heat capacity in terms of $Jg^{-1}K^{-1}$ (Table 3) of aluminium oxide is lower than that of magnesium oxide, however, taking into account the mass of residue formed gives values of $0.50JK^{-1}$ and $0.40JK^{-1}$ for the total mass of residue formed from 1 gram of aluminium hydroxide and 1 gram of hydromagnesite respectively. The fact that aluminium oxide produces a larger quantity of residue with a higher total heat capacity would seem to indicate an advantage in favour of aluminium hydroxide over hydromagnesite in terms of fire retardancy. Another may be the promotion of afterglow by the freshly formed alumina[148]. However, the fact that a number of researchers have found hydromagnesite to perform very similarly in terms of fire retardancy indicates that there must be other factors involved in its fire retardant mechanism. One such factor may be that hydromagnesite decomposes over a wider temperature range than aluminium hydroxide allowing it to continue diluting the flame and cooling the solid phase over a longer time period. In natural mixtures of hydromagnesite and huntite, the presence of huntite results in a lower total volume of volatile decomposition products from the minerals when compared to the same mass of pure hydromagnesite; the actual volume will depend on the ratio of the two minerals. Even so, it has been shown by several researchers, and discussed in this article, that these kinds of mixtures perform very similarly to aluminium hydroxide and magnesium hydroxide in terms of fire retardancy. The huntite portion of the blend must therefore be contributing to the fire retardant action, perhaps as a platy barrier layer but not just through endothermic decomposition.

| | Chemical formula | Heat Capacity ($Jmol^{-1}K^{-1}$) | Heat Capacity ($Jg^{-1}K^{-1}$) |
|---|---|---|---|
| Aluminium hydroxide | $Al(OH)_3$ | 93.1[a] | 1.20 |
| Magnesium hydroxide | $Mg(OH)_2$ | 77.0[a] | 1.33 |
| Hydromagnesite | $Mg_5(CO_3)_4(OH)_2{\cdot}4H_2O$ | 526.6[b] | 1.13 |
| Huntite | $Mg_3Ca(CO_3)_4$ | 310.1[c] | 0.88 |
| Water vapour (measured at 500K) | $H_2O$ | 35.22[d] | 1.96 |
| Carbon dioxide | $CO_2$ | 37.12[d] | 0.77 |
| Aluminium oxide | $Al_2O_3$ | 78.77[d] | 0.77 |
| Magnesium oxide | MgO | 37.01[d] | 0.93 |
| Calcium oxide | CaO | 42.09[d] | 0.75 |

Notes:
a – figures taken from Ashton[149]
b – figures taken from Robie[88]
c – figures taken from Hemingway[150]
d – figures taken from NIST Chemistry WebBook, http://webbook.nist.gov/chemistry

Table 3: Heat capacities at 298K (25°C)

## 2.21 Conclusions

It is clear that the decomposition mechanism of hydromagnesite is complicated and influenced by a number of factors, including heating rate and composition of the atmosphere, especially the partial pressure of carbon dioxide. When contained within a polymer matrix, the carbon dioxide given off by a decomposing hydromagnesite particle is likely, at least initially, to be entrapped within a polymer bubble surrounding the particle. This entrapped carbon dioxide may well create a localised high partial pressure of the gas affecting the mechanism by which decomposition occurs. This could lead to the type of decomposition resulting in the exothermic crystallisation of magnesium carbonate. However, in mixtures of hydromagnesite with huntite the endothermic decomposition of the huntite overlaps with the exothermic event in the hydromagnesite helping to eliminate any negative effect this may have on fire retardancy.

The evidence points to mixtures of hydromagnesite and huntite being more effective than would be expected from the evolution of inert gases and endothermicity. Many

researchers have assumed that huntite is acting merely as a diluent filler. However, blends of hydromagnesite and huntite have been shown many times to have similar fire retardant properties to ATH at the same loading levels. This indicates that the wider decomposition range of hydromagnesite as well as the huntite portion of the mixtures must be contributing to the fire retardancy. Huntite will contribute to the formation of an inorganic residue, its platy nature may also act to reinforce this residue. A further mechanism by which huntite may be contributing is through its full or partial endothermic decomposition at temperatures above 450°C. This would provide cooling to the residue layer further reducing the heat transfer to the underlying polymer.

Mixtures of hydromagnesite and huntite have been shown to provide fire retardant properties as good as or better than ATH or magnesium hydroxide in non-halogen as well as halogen containing compounds. In PVC compounds the carbonate nature of both hydromagnesite and huntite make them reactive with acids reducing the yields of acidic hydrogen chloride gas and promoting the decomposition of the carbonate.

Although blends of hydromagnesite and huntite improve fire properties in a range of polymers the mechanisms by which they function are still not fully understood.

# 3. Experimental Procedures

## 3.1 Materials

### 3.1.1 Huntite and Hydromagnesite

Throughout this work all samples of natural huntite and hydromagnesite were supplied by Minelco from a deposit in south western Turkey. The minerals formed naturally and lay close to the surface; they are mined by open cast techniques. The raw materials are then processed by grinding and classifying to controlled particle size distributions and ratios of the two minerals. Minelco produces a range of standard products of varying mineral ratio, particle size distribution and coatings. These minerals are sold commercially under the tradename UltraCarb.

The major constituents of UltraCarb, huntite and hydromagnesite, can vary in proportion. Commercial grades of the material are obviously tightly controlled for consistency of the product, however it is theoretically possible to study any blend of the two minerals from 100% huntite through to 100% hydromagnesite. In reality it is more difficult to produce grades with a high purity of one mineral since they are formed together in mixtures of varying ratio. Because the minerals are formed naturally they are never 100% pure. Small quantities of other closely related minerals form part of the mixture, these minerals consist of the following:

(Mag) Magnesite $MgCO_3$

(Dol) Dolomite $CaMg(CO_3)_2$

(Cal) Calcite $CaCO_3$

(Arag) Aragonite $CaCO_3$

The grades used to study the effects of the ratios of the two minerals have the following compositions (Table 4). The Minelco QA department regularly check the composition using XRD. These figures are taken from QA test results.

| | **HU** | **HM** | Mag | Dol | Cal | Arag |
|---|---|---|---|---|---|---|
| HU93HM5 | **93%** | **4.9%** | 0.7% | 0.2% | 0.2% | 0.1% |
| HU43HM50 | **43%** | **50%** | 1% | 4% | 0.3% | 0.9% |
| HU41HM57 | **41%** | **57%** | 1.4% | 0.2% | 0.1% | 0% |
| HU24HM67 | **24%** | **67%** | 0.2% | 8.3% | 0% | 0.1% |
| HM100 | **0%** | **100%** | 0% | 0% | 0% | 0% |

**Table 4: Composition of the natural mixtures of huntite and hydromagnesite**

The specific grades used in this work are not necessarily commercially available materials, but were used to study the effects of particle size or mineral ratio. For this reason no commercial grade references are given, instead a system of labelling is used to show the ratio of the minerals. For example the reference HU41HM57 indicates a ratio of 41% huntite and 57% hydromagnesite, and HU93HM5 indicated a ratio of 93% huntite and 5% hydromagnesite.

### 3.1.2 Polymers

Whilst mixtures of huntite and hydromagnesite are used in a variety of polymer systems it was decided for the purposes of this investigation to limit the work to an ethylene vinyl acetate (EVA) copolymer based formulation. EVA is widely used in the wire and cable industry as the basis of halogen free compounds used for sheathing on electrical wiring. PVC is also commonly used due to the inherent fire retardancy of the polymer brought about by its high chlorine content. However, when it does burn it can produce large quantities of choking, black, acidic smoke. This hinders the escape of people through visual impairment and also through the effects of breathing in acidic hydrogen chloride gases. Therefore, there is considerable interest in halogen free polymers such as EVA, that produce less smoke and no hydrogen halides.

EVA based compounds used for wire and cable applications are usually based on mixtures of various polyolefin based polymers in order to meet all of the requirements of this application. A typical UltraCarb containing formulation developed by Minelco for the purposes of testing its products is shown in Table 5.

| **Tradename** | **Supplier** | **Description** | **Quantity (phr)** |
|---|---|---|---|
| Escorene UL00328 | Exxon | Ethylene vinyl acetate (28%) | 55 |
| Exact 8201 | ExxonMobil | Polyolefin elastomer | 30 |
| Fusabond MB226D | DuPont | Maleic anhydride grafted polyethylene | 10 |
| Borealis BS2581 | Borealis | High density polyethylene | 5 |
| Irganox 1010 | Ciba (BASF) | phenolic antioxidant | 1 |
| UltraCarb | Minelco | huntite/hydromagnesite | 160 |
| | | **Total** | **261** |

**Table 5: Typical wire and cable formulation**

Ethylene vinyl acetate (EVA) is a flexible polymer with the ability to accept high filler loadings while still maintaining flexibility and mechanical properties. Its structure is shown in Figure 7 in section 1.3, the quantity of vinyl acetate varies in different grades of this polymer. For this formulation a grade with a 28wt% content of vinyl acetate was chosen as it gives a good balance of mechanical properties and flexibility.

The polyolefin elastomer is a grade of polyethylene that has been commercially produced using metallocene catalysts. These catalysts give the polymer producers enhanced control of the structure of the polymer chains. In this case they have been used to produce a polyethylene that has elastomeric properties. This polymer is used to help maintain flexibility in a highly filled compound such as this one.

Maleic anhydride (Figure 40) is a chemical group that when grafted into a polymer chain, through its carbon double bond, acts as a compatibiliser between the polymer matrix and the inorganic filler particles. It improves the wetting and adhesion of the polymer to the filler surface thereby improving the mechanical properties of the filled compound.

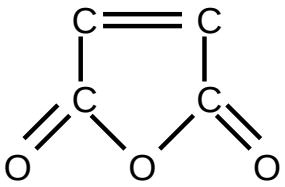


Figure 40: Maleic anhydride molecule

High density polyethylene (HDPE) is added to the compound to increase its resistance to deformation at elevated temperatures. EVA has a very low melting point, according to the data supplied with Escorene UL00328 its peak melt temperature is 71°C. A small addition of HDPE increases the heat resistance of compound which is important because the sheathing of a cable must not soften or deform in warm environments or if the cable generates heat during use.

Antioxidant stabilisers are commonly used to protect the polymer from oxidative degradation during melt processing and during the lifetime of the final product.

It was decided to use this compound formulation for this work since it represents a simple compound with physical and fire performance properties typical of a general purpose wire and cable compound.

### 3.1.3 Other Materials

Other materials used during the course of this investigation include:

Natural calcium carbonate (calcite) supplied by Minelco under the name MicroCarb ST10H

Aluminium hydroxide supplied by Nabaltec under the name Apyral AP40

Magnesium hydroxide supplied by Martinswerk under the name Magnifin H5A

Synthetic hydromagnesite supplied by Solvay under the name Carbomag TL

## 3.2 Compound preparation

Industrially there are many ways of producing a homogeneously mixed polymer compound. These methods can include the use of large scale equipment such as twin screw compounders, internal mixers, Buss co-kneaders, or ring extruders. Each has its own particular set of advantages. On the laboratory scale a two roll mill is commonly used as a way of conveniently producing small quantities of compound.

### 3.2.1 Two roll mill

The two roll mill is relatively simple piece of laboratory equipment consisting of two counter rotating heated rollers. In order to produce compound for this work the temperature of the rollers was set to 140°C. Initially the polymer granules are added to the rolls and allowed to mix and melt. Granules that fall from the rolls are collected and added back to the molten polymer on the rolls. Once the polymers have formed a homogeneous melt the mineral fire retardant is slowly added, allowing it to incorporate into the polymer melt. The molten compound forms a band around one roller making it easy to work with. Because the two rolls rotate at slightly different speeds a shearing action is produced which disperses the mineral particles within the polymer matrix. For mixing huntite and hydromagnesite with EVA based compounds the rollers speeds are typically set at about 15 and 20 rpm. The gap between the rolls is also controllable and is usually adjusted during mixing as the ingredients are added. The ideal gap creates a bank of continuously rolling molten polymer compound in the nip between the two rolls. One disadvantage of a two roll mill is that there is no lateral mixing across the width of the rolls, this is achieved by cutting the band of polymer and folding it back on itself across the width of the rolls. This process of cutting and folding is repeated until a uniform compound is produced; at this point the band is cut and removed from the rolls as a sheet of compound. This sheet can then be cut into granules suitable for further processing using a granulator.

### 3.2.2 Compression moulding

Compression moulding is common laboratory method for shaping the compound produced on a two roll mill (or other compounding method) into test pieces or articles for further testing. The equipment consists of two heated platens in a press. For this work the platens were set to a temperature of 180°C. Compound from the two roll mill was placed in the mould, which consists of two metal plates and a spacer of varying dimensions depending on the size of the plaques required for cone calorimetry, oxygen index or other testing. The mould containing the compound is then placed between the heated platens and a low pressure applied for 2 minutes to allow the assembly to reach the desired temperature. The pressure is then increased to 20 tons and held for a further 5 minutes. During this time the polymer compound is forced to flow, filling the cavity between the spacer and the plates. The mould containing the molten polymer is then transferred to a cold press and held under similar pressure until the material has returned to room temperature (about 5 minutes). Once the compound has cooled it can be removed from the mould.

### 3.2.3 Extrusion

Extrusion is a process by which polymer granules are conveyed along a heated barrel by means of a rotating screw. The action of the heat and the rotating screw creates a homologous polymer melt, the melt flows from the heated barrel into a heated die. There is a pressure increase within the die, caused by the continuous rotation of the screw feeding melt to the die. The pressure within the die causes the polymer to flow from the opening to produce a length of extrudate. For laboratory purposes this is often a simple flat strip of material. Industrially the die can take many forms producing simple shapes such as tubes or pipes, to highly complex extruder and die designs that produce wire or cables containing several layers of polymer around one or more conductive cores.

The current work utilised a Thermo Polylabs single screw extruder. The barrel temperature was set at 160 - 170°C and the die at 175°C. A screw speed of 50 rpm was used to produce a flat strip through a die with a width of 25 mm and a thickness of

1 mm. The extrudate was passed over a set of metallic rollers to cool it to room temperature.

## 3.3 Fire tests

### 3.3.1 Limiting oxygen index – BS EN ISO 4589-2:1999

The limiting oxygen index test is described in more detail in section 1.7.1. The limiting oxygen index figures presented in this thesis were measured using Stanton Redcroft equipment. The oxygen analyser was calibrated to 100% and 0% using oxygen and nitrogen fed from gas cylinders at a flow rate of 18 $lmin^{-1}$. The various oxygen concentrations required during the test were then obtained by independently controlling the flow rates of the two gases through the equipment while keeping the total flow rate at a constant 18 $lmin^{-1}$. All oxygen index measurements given in this thesis were measured to the nearest 0.5% of oxygen required to just support vertical burning.

Samples of 10 mm x 125 mm x 3 mm were cut from compression moulded plaques for this test. A mark was made 50 mm from the end of the sample that would be ignited. The sample was then placed in the holder. A propane gas flame was used to ignite the top surface of sample checking every 5 seconds for ignition of the sample. The flame was applied for a maximum of 30 seconds. Once ignition of the sample occurred the gas burner was removed and the burning characteristics were assessed as follows:

If the sample continued to burn for 180 seconds or the extent of burning exceeded the 50mm mark within 180 seconds it was recorded that self supported combustion occurred at the set oxygen concentration. In this situation the oxygen concentration was reduced and the procedure repeated.

If the sample self extinguished in less than 180 seconds the sample was recorded as self extinguishing at the set oxygen concentration. In this situation the oxygen concentration was increased and the procedure repeated.

The oxygen index value is defined[16] as “the minimum concentration of oxygen, by volume percentage, in a mixture of oxygen and nitrogen introduced at 23°C ± 2°C that will just support combustion of a material under specified test conditions”. Therefore the oxygen index was recorded as the lowest oxygen concentration at which the sample supported combustion during the test. In the case of the materials reported here the oxygen concentration was reported to the nearest 0.5% oxygen concentration.

### 3.3.2 Cone Calorimeter – ASTM E1354 – 08

The cone calorimeter test is described in more detail in section 1.7.3. The equipment used for this work was manufactured by Fire Test Technologies (FTT). Once a day prior to testing the gas analysers and smoke detectors were calibrated. The oxygen analyser was calibrated using nitrogen and ambient air to set the zero and 21.95% oxygen levels. The carbon monoxide and carbon dioxide analyser was calibrated using a source of $CO/CO_2$ with a known concentration of the two gases. The laser smoke detector was calibrated using glass filters of known optical density. Finally methane was burned with a known heat release of 5 kW in order to set the orifice flow constant or C factor within the software.

Once all of the gas calibrations were successfully completed the cone heater was switched on and allowed to warm to the desired heat flux. This was measured using a heat flux meter placed the same distance from the cone heater as the samples are during combustion.

Samples of 100mm x 100mm x 6mm were used for testing. They were wrapped with aluminium foil leaving the upper surface exposed. The samples were then placed on the sample holder and the retainer placed over the sample. The retainer holds the sample in place and reduces the surface area directly exposed the cone heater from $100cm^2$ to $88cm^2$.

Once the sample was in place on the sample holder the spark igniter was moved into position over the sample and the shutters opened exposing the sample to the radiant heat flux. Once ignition occurred the igniter was moved to the side.

During the period of the test the computer records data from the gas analysers and smoke detectors which are later used to calculate rates of heat release, smoke release, etc.

## 3.4 Thermal analysis

### 3.4.1 Thermogravimetric analysis (TGA)

Thermogravimetric analysis is described in more detail in section 1.5.1. The equipment used for this work was a TA Instruments Q5000IR thermogravimetric analyser. Unless otherwise specified tests were carried using a heating rate of 10°Cmin$^{-1}$ in air with a gas flow rate of 50 ml min$^{-1}$. Samples sizes of approximately 10 mg were used and the mass constantly monitored and recorded as the temperature was increased at a controlled rate.

### 3.4.2 Simultaneous thermogravimetric analysis with differential thermal analysis (TGA-DTA)

Simultaneous DTA is described in more detail in section 1.5.3. The equipment used for this work was a TA Instruments SDT2960. Unless otherwise specified tests were carried using a heating rate of 10°Cmin$^{-1}$ in air with a gas flow rate of 50 ml min$^{-1}$. Samples sizes of approximately 10 mg were used and the mass constantly monitored alongside the thermal heat flow as the temperature was increased at a controlled rate.

### 3.4.3 Simultaneous thermogravimetric analysis with Fourier transform infra-red analysis (STA-FTIR)

Simultaneous thermogravimetric analysis with Fourier transform infra-red analysis is described in more detail in section 1.5.2. The equipment used for this work was an STA 780 coupled with a Nicolet Magna IR Spectrometer 550. Samples of approximately 10mg were heated at a controlled heating rate of 10°Cmin$^{-1}$ in air from room temperature up to 1000°C using the TGA instrument. The evolved gases were fed to the FTIR analyser allowing analysis of the gases to be associated with mass losses measured by TGA.

### 3.4.4 Differential scanning calorimetry (DSC)

Differential scanning calorimetry is described in more detail in section 1.5.3. DSC analysis was carried out using a Rheometric Scientific DSC-1500. Samples of approximately 10mg were heated in a nitrogen atmosphere at a heating rate of 10°C$min^{-1}$ unless otherwise stated.

## 3.5 Scanning electron microscopy (SEM)

Electron microscopy was carried out using a LEO Gemini field emission gun scanning electron microscope (FEGSEM). Samples were mounted on a metallic stub and gold coated before analysis with the electron microscope.

# 4. Results and discussion 1 – *Morphology, chemical composition and thermal decomposition of natural Turkish huntite and hydromagnesite*

## 4.1 Morphology of huntite and hydromagnesite

The shape and size of filler particles influences many properties of a polymer compound. They can affect the processing characteristics through increasing viscosity, change mechanical properties and have an effect on the fire retardant properties. For example, platy particles such as mica can very effectively increase flexural stiffness, fibres such as glass or carbon can increase the mechanical strength in the direction of fibre orientation, spherical glass beads can have a very uniform effect in reducing post moulding shrinkage in all directions.

Figure 41 shows an electron microscope image of huntite particles. It can be seen that they resemble tiny platelets with an average diameter (largest dimension) of approximately 1µm or less. The thickness of the plates is clearly in the nanometer range. Particles that have a platelet structure such as this can have a tendency to align themselves along the direction of flow in a molten polymer. This can lead to a mechanically reinforced composite as the structure of the aligned particles adds strength.

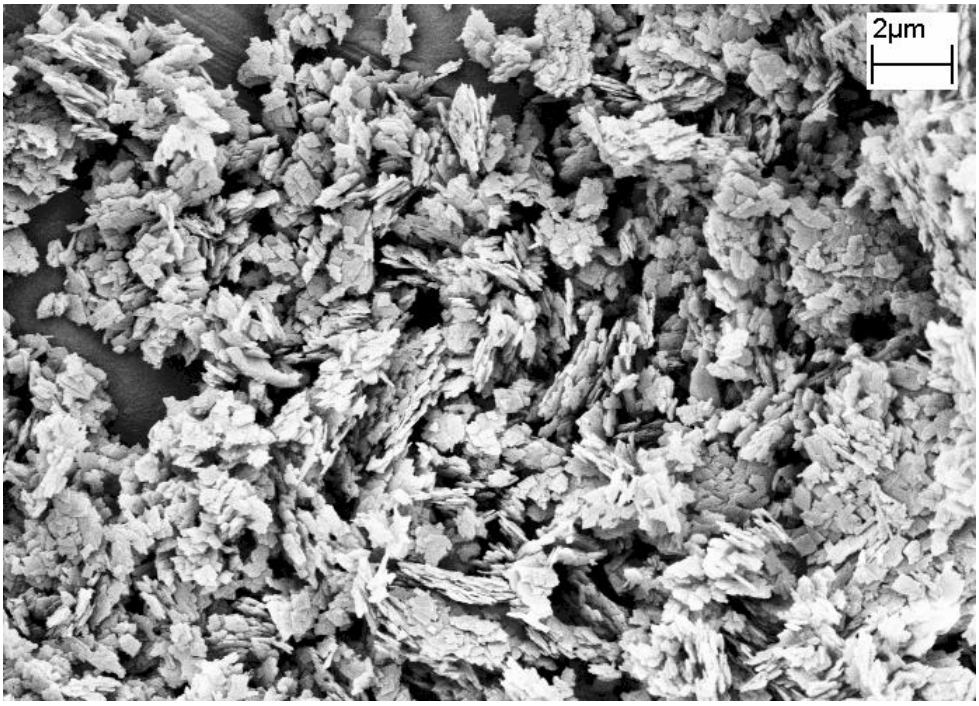


**Figure 41: Huntite particles**

The alignment of particles with this morphology may also help to hinder the escape of flammable decomposition products from a decomposing polymer. This is something that will be discussed in more detail in later sections.

Figure 42 shows a natural mixture of hydromagnesite and huntite where the larger, blockier, hydromagnesite particles can be seen interspersed with smaller platy huntite particles. Because of the way huntite and hydromagnesite naturally form most commercially available material consists of mixtures of varying proportions.

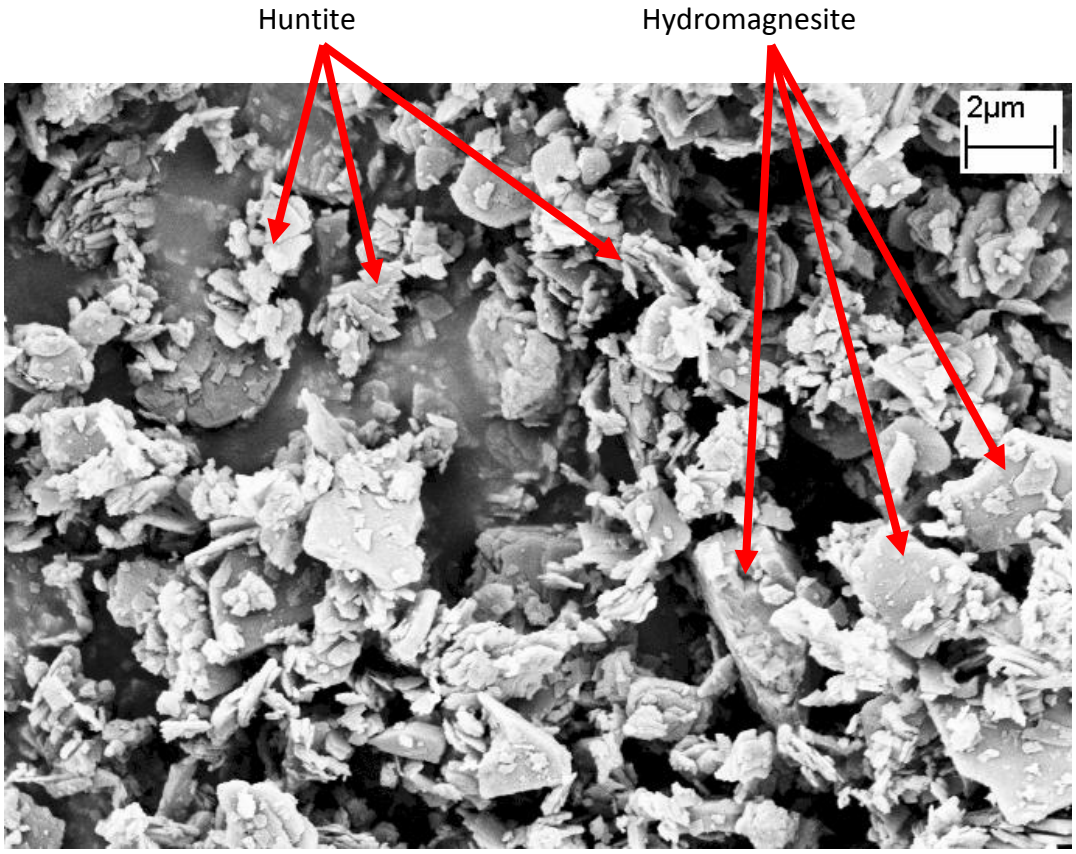


**Figure 42: A mixture of hydromagnesite and huntite particles**

These pictures clearly illustrate that mixtures of huntite and hydromagnesite are more complicated than other mineral fire retardants such as ATH. They are a mixture of two minerals with two clearly different morphologies and distinct particle size distributions.

For comparison Figure 43 shows synthetic hydromagnesite particles (Carbomag TL) this material appears to consist of agglomerates of very small thin plates. The morphology is clearly different to that of naturally formed hydromagnesite. This is probably due to different conditions of temperature and pressure during formation.

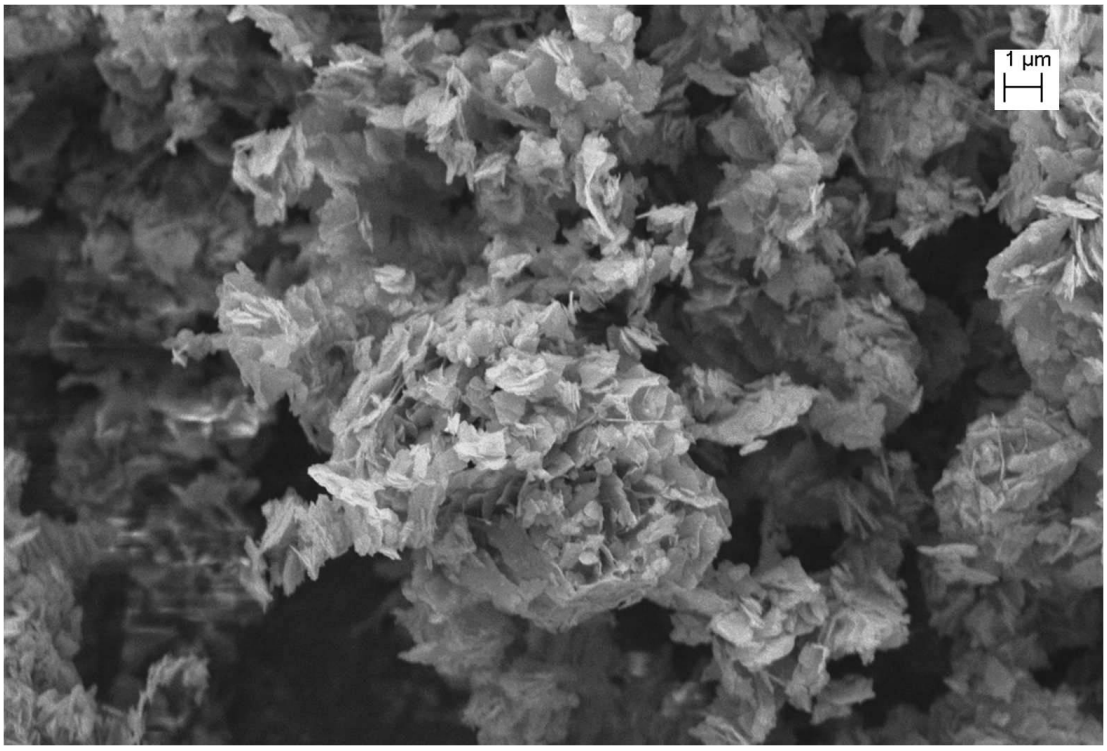


Figure 43: Synthetic hydromagnesite particles

## 4.2 Thermal decomposition of Turkish huntite and hydromagnesite

Both huntite and hydromagnesite thermally decompose, losing mass and giving off water and carbon dioxide. Figure 44 shows a comparison of the thermal decomposition of the two individual minerals with a commercially available mixture of huntite and hydromagnesite (UltraCarb LH15).

Huntite ($Mg_3Ca[CO_3]_4$) decomposes through two stages. The first stage occurs between about 400°C and 630°C with an associated loss in mass of 38%, and the second stage occurs between about 630 and 750°C with a further mass loss of 12% making a total mass loss of 50%. Huntite has a molecular mass of 352. Since it is a carbonate mineral it is likely that its thermal decomposition consists of release of carbon dioxide, which has a molecular mass of 48. Release of 3 carbon dioxide molecules followed by further release of one carbon dioxide molecule gives calculated mass losses of 37.5% and 12.5%, which is in very close agreement with the measured values.

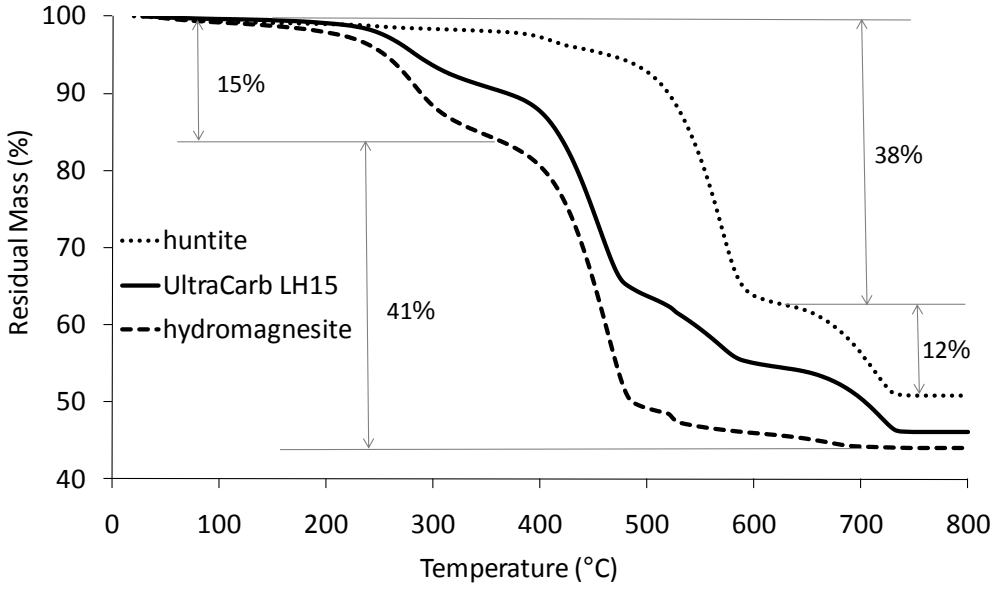


**Figure 44: Thermal decomposition of huntite, hydromagnesite, and a commercially available mixture measured by TGA**

The decomposition of hydromagnesite is more complicated than huntite. There is a mass loss of 15% up to about 350°C and a further loss of 41% by about 700°C. Using hydromagnesite's molecular mass of 466 it can be calculated that loss of the four water molecules (from water of crystallisation) would account for a mass loss of 15.45%. The loss of a further water molecule from the decomposition of the hydroxide ion and loss of four carbon dioxide molecules would account for a further 41.63% (3.86% and 37.77% respectively) mass loss. The figures are close to the measured values, and suggest that the decomposition of the hydroxide ion overlaps the decomposition of the carbonate ions. It is also clear from Figure 44 that the decomposition is not a simple two step mechanism, this will be discussed in more detail later.

The mass loss profile for the natural mixture of huntite and hydromagnesite shows a four step mechanism, which is a combination of the two individual minerals and provides thermal activity over a wide temperature range.

Figure 45 - Figure 47 shows differential scanning calorimetry (DSC) measurements of hydromagnesite, huntite and a mixture of the two minerals. It is clear that the major

decompositions of the minerals are all endothermic, meaning that they have great potential as fire retardants. By comparison with Figure 44 it is also clear that each of the decompositions measured by TGA is associated with an endotherm. The total heat of decomposition of the mixture of huntite and hydromagnesite is approximately -990 $Jg^{-1}$ (see Figure 47). This figure will vary depending on the ratio of the two minerals. Figure 45 clearly shows a small exotherm at about 520°C and some further endothermic changes above this temperature. These areas of the decomposition have been found to be highly dependent on heating rate and have therefore not been taken into account at this stage leading to an underestimation of the total enthalpy change. It will be discussed in detail in section 4.2.3.

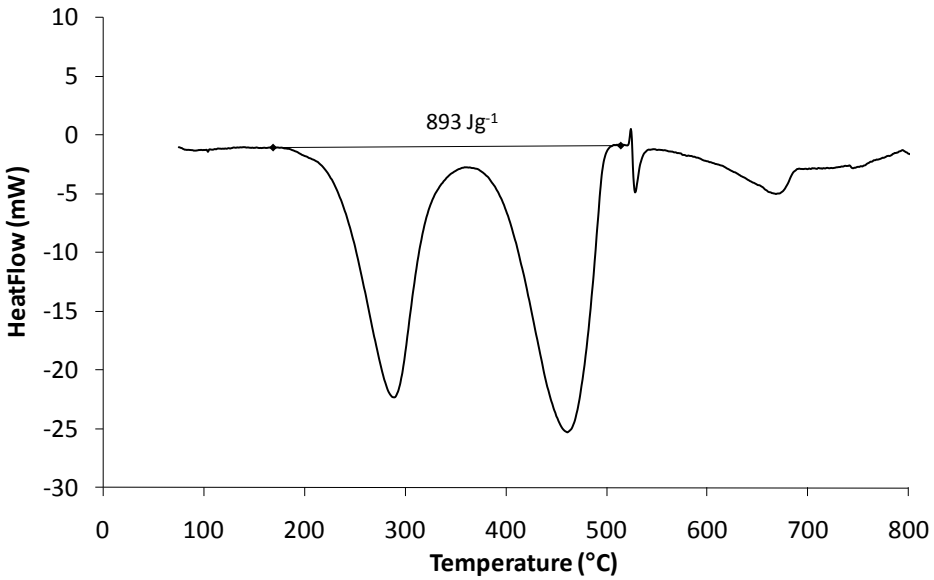


Figure 45: Thermal decomposition of hydromagnesite measured by DSC

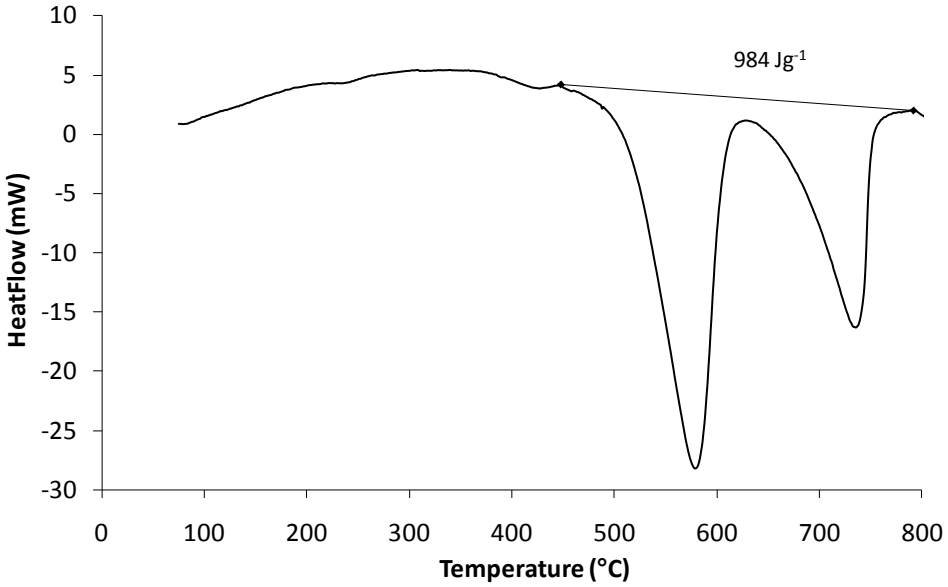


Figure 46: Thermal decomposition of huntite measured by DSC

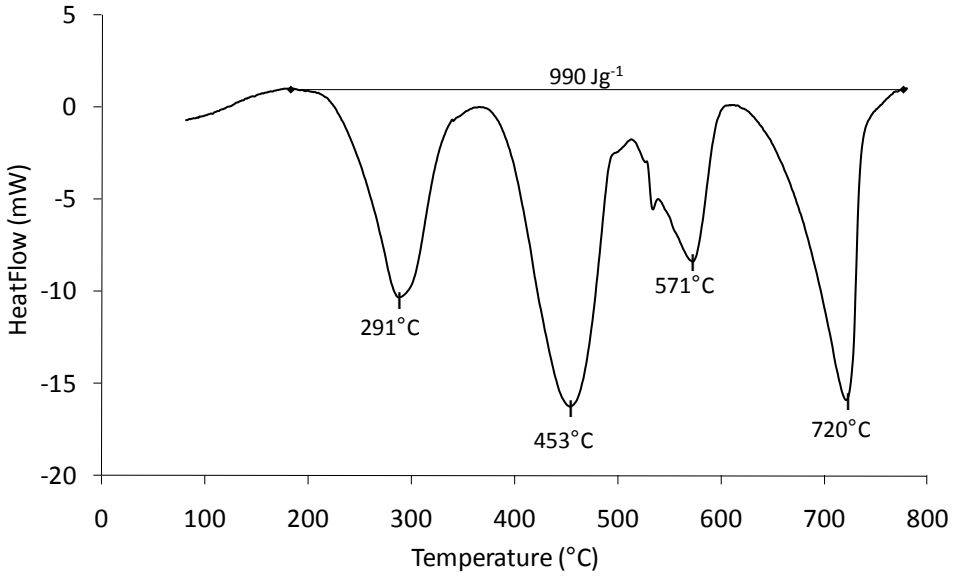


Figure 47: Thermal decomposition of a mixture of natural hydromagnesite and huntite measured by DSC

### 4.2.1 The chemical composition of Turkish hydromagnesite by measurement of its thermal decomposition

Ozao *et. al.*[70] used the fact that the chemical formula for huntite, $Mg_3Ca(CO_3)_4$, can also be written as, $3MgCO_3{\cdot}CaCO_3$, to show by DTA that mechanical mixtures of calcium carbonate and magnesium carbonate have similar although not identical

thermal decomposition characteristics as huntite, this is discussed in more detail in section 4.2.4. A similar analysis can be carried out with hydromagnesite. The chemical formula of hydromagnesite, $Mg_5(CO_3)_4(OH)_2{\cdot}4H_2O$, can also be written as, $4MgCO_3.Mg(OH)_2{\cdot}4H_2O$. Therefore, comparison with magnesium carbonate and magnesium hydroxide in a 4:1 ratio (Figure 48) provides some useful insight into its thermal decomposition. The analysis is not as straightforward as with huntite since hydromagnesite contains four molecules of water of crystallisation which are not present in either magnesium hydroxide or magnesium carbonate.

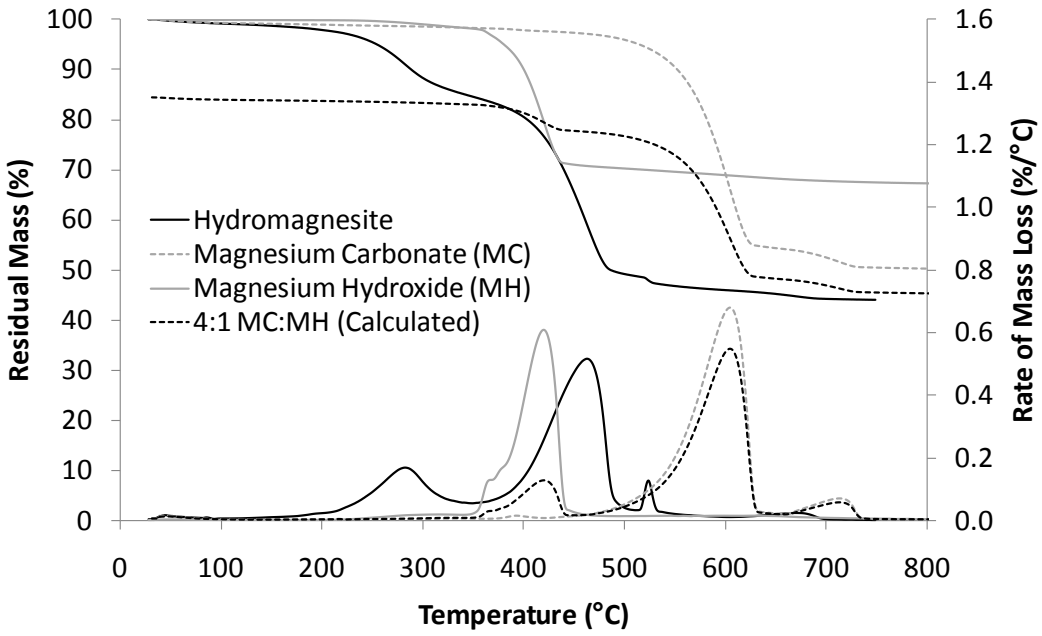


**Figure 48: Comparison of hydromagnesite with magnesium carbonate and magnesium hydroxide using TGA**

It has been shown[65-69,82,90,101,104] that hydromagnesite thermally decomposes by first losing water of crystallisation, followed by decomposition of the hydroxide ion and finally release of carbon dioxide from decomposition of the carbonate ion. Calculation using atomic masses shows that these three decompositions would result in mass losses of 15.45%, 3.86%, and 37.77% respectively and result in a total mass loss of 57.08%.

The decomposition of Turkish hydromagnesite shown in Figure 48 does not clearly separate the three decomposition steps. However at 350°C (the shoulder between the

two major mass losses) the mass loss is 15%, a further mass loss of 41% has occurred by 700°C, giving a total mass loss of 56%. This is very close to the expected total mass loss of 57.08%. The mass loss associated with the decomposition of the hydroxide ion probably occurs somewhere between 330 and 430°C but is overshadowed by the larger mass loss associated with the decomposition of the carbonate ions. This temperature range is also close to the temperature range over which the hydroxide ion in magnesium hydroxide decomposes.

The mass loss profiles of magnesium carbonate and magnesium hydroxide were proportionally summed in a 4:1 ratio. The four water molecules present in hydromagnesite accounting for 15.45% of the mass have been taken into account in the calculation, therefore the line in Figure 48 representing this calculation starts with a total residual mass of 84.55%. As expected from the mass loss profiles of magnesium carbonate and magnesium hydroxide the proportional sum of the two components does not fit closely with that of hydromagnesite in terms of decomposition temperatures. As discussed above the decomposition temperature of magnesium hydroxide coincides closely with that of the apparent loss of the hydroxide ion from hydromagnesite. However, the decomposition temperature of magnesium carbonate does not coincide with that of the decomposition of the carbonate ion from hydromagnesite, although the total mass losses do closely agree. Although the chemical composition of hydromagnesite is similar to a 4:1 mixture of magnesium carbonate and magnesium hydroxide the crystal structure of hydromagnesite [93,95,96] is quite different leading to a more complex decomposition that predicted from simple mixtures.

Comparison of natural hydromagnesite with synthetic hydromagnesite (Figure 49) shows that the total mass losses from the two materials are almost identical, as would be expected. However, the initial onset of decomposition occurs at a lower temperature for synthetic hydromagnesite.

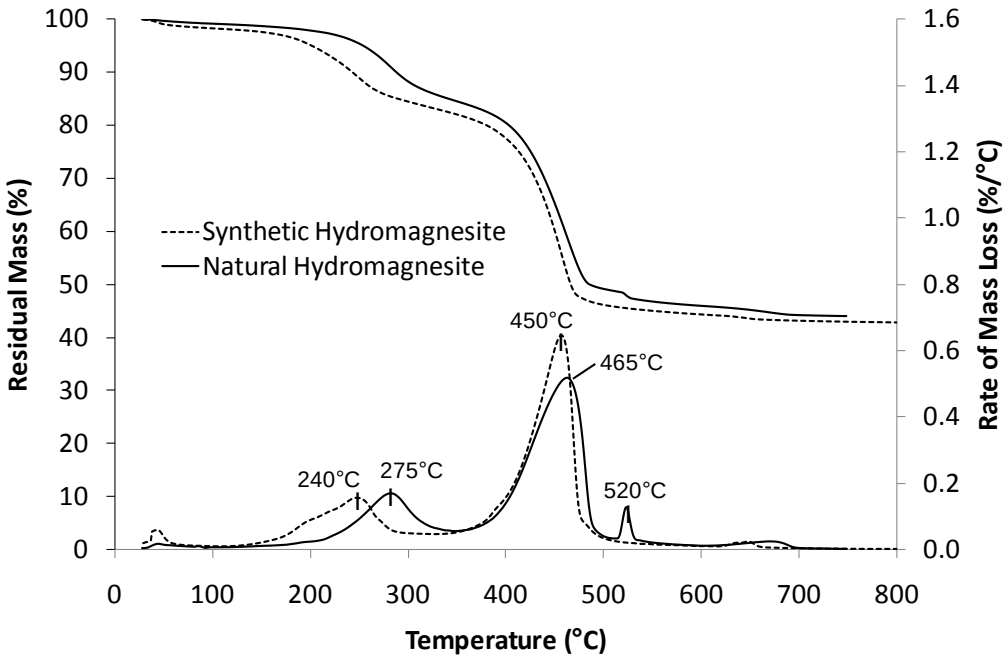


Figure 49: Comparison of natural hydromagnesite with synthetic hydromagnesite using TGA

The maximum rate of mass loss associated with loss of water of crystallisation occurs at about 275°C for natural hydromagnesite and at about 240°C for the synthetic material. The onset of decomposition is also much lower (well below 200°C) for the synthetic material. This is a significant advantage in favour of the natural material in terms of processing in polymer compounds. The lower onset of decomposition of the synthetic material will restrict its use to polymers that are processed below that temperature.

The maximum rate of decomposition associated with the decomposition of the carbonate ions occurs at about 465°C for the natural hydromagnesite and at about 450°C for the synthetic hydromagnesite. Again the decomposition is occurring at a lower temperature in the synthetic material although in this case the difference is smaller and not significant in terms of processing polymers filled with hydromagnesite because it is well above the processing temperature of most polymers.

The additional peak of mass loss at 520°C measured in the natural hydromagnesite but not present in the synthetic hydromagnesite is due to crystallisation of magnesium carbonate during decomposition of the mineral. This will be discussed in more detail in section 4.2.3.

From these results it is clear that the decomposition of synthetic hydromagnesite follows a similar mechanism to that of natural hydromagnesite albeit at slightly lower temperatures. This difference in decomposition temperatures is probably due to variations in the crystal structure between the natural and synthetic materials. It has been reported[151] that the degree of crystallinity of synthetic hydromagnesites can be lower than that found in naturally formed material. This has been attributed to differences in the formation conditions such as temperatures and time scales. The morphology of natural and synthetic hydromagnesite (as shown in Figure 42 and Figure 43) is also very different. The thinner more platy synthetic particles will decompose faster than the larger blocky natural particles due to faster heat transfer to, and easier escape of the decomposition gases from, the centre of the particles. According to the technical datasheet, supplied by Solvay, for the synthetic hydromagnesite, the average particle size ($d_{50}$) is 0.7 µm and the BET surface area is 22 $m^2g^{-1}$. This compares to a $d_{50}$ of 4.9 µm and a BET surface area of 9.7 $m^2g^{-1}$ for the natural hydromagnesite (HM100). This supports the suggestion that part of the difference in the decomposition temperatures could be due to particle morphology.

### 4.2.2 Decomposition mechanism of Turkish hydromagnesite

In order to further confirm the decomposition mechanism of hydromagnesite the decomposition gases generated during TGA analysis were identified using FTIR. This was done in real time allowing the gases indentified to be linked to a specific mass loss and temperature range.

Figure 50 shows the mass loss and Gram Schmidt data for the thermal decomposition of hydromagnesite. Gram Schmidt shows the output of the FTIR detector without linking it to a wavenumber and therefore shows the temperature ranges where evolved gases are detected without identifying them. Unsurprisingly gases are detected in relation to the mass losses measured by TGA with peaks in detector output at 283°C and 460°C. There is a slight offset between the temperatures of maximum rate of mass loss and temperatures where maximum FTIR peak intensities are measured due to the varying mobility of the gases through the heated line to the FTIR

detector. This Gram Schmidt data is therefore valuable in selecting the temperatures for detailed FTIR analysis of the evolved gases.

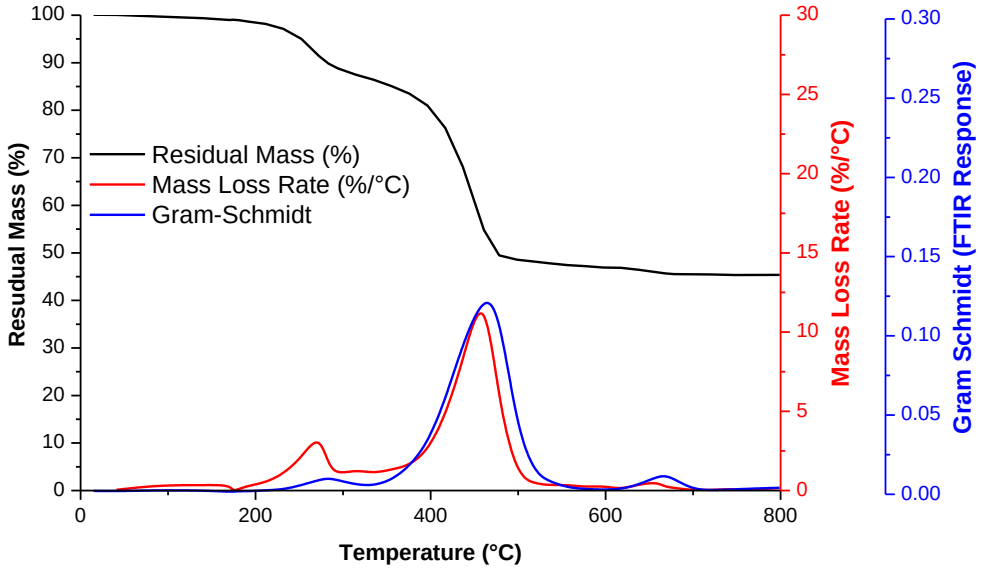


Figure 50: Gram Schmidt data from TGA-FTIR analysis of hydromagnesite

The FTIR spectra of the gases evolved during the decomposition of hydromagnesite are shown in Figure 51. The broad FTIR peaks measured below 350°C at wavenumbers between 2000 and 1200cm$^{-1}$ are characteristic of water. Above 350°C no further water was detected, this confirms that the initial mass loss from hydromagnesite is due to the release of the crystalline water and decomposition of the hydroxide ion. Above 350°C the FTIR spectra are characteristic of carbon dioxide due to decomposition of the carbonate ions. To further clarify, the variation in magnitude of the peaks with temperature at 1308cm$^{-1}$ and 2310cm$^{-1}$ (which correspond to the areas associated with water and carbon dioxide respectively) have been plotted and shown in Figure 52. This breaks the Gram Schmidt data down into its components clearly demonstrating that the first mass loss from hydromagnesite is due to loss of water and the second mass loss is due to loss of carbon dioxide.

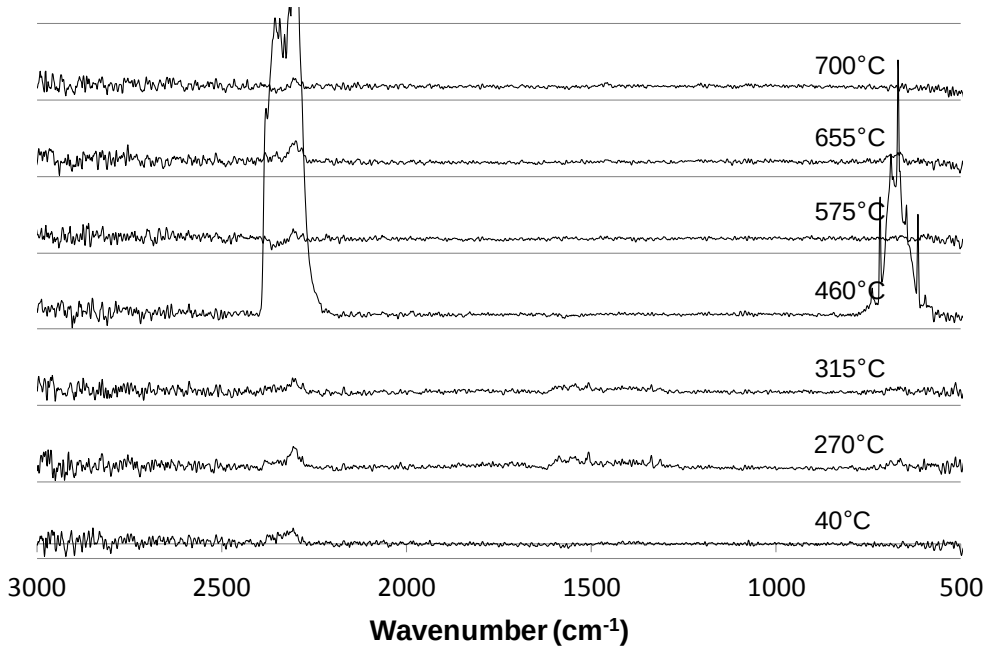


Figure 51: FTIR spectra of gases evolved during the decomposition of hydromagnesite

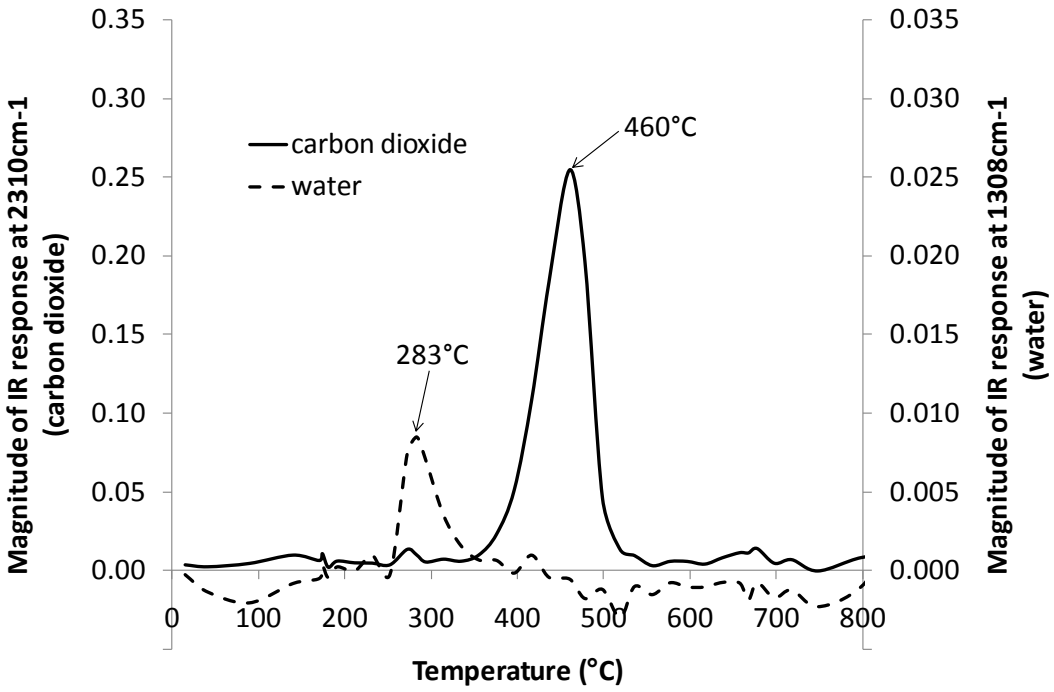


Figure 52: Analysis of gases evolved during the decomposition of hydromagnesite

### 4.2.3 Effect of heating rate on the decomposition of Turkish hydromagnesite

The rate of heating has a significant effect on the decomposition of hydromagnesite. Figure 53 shows how heating rate affects the mass loss profile of hydromagnesite. At a heating rate of 1°Cmin$^{-1}$ there are two clearly defined stages of mass loss with peak mass loss rates at 240°C and 405°C, these are due to the evolution of water and carbon dioxide respectively. Increasing the heating rate to 10°Cmin$^{-1}$ moves these peaks to about 280°C and 455°C respectively and broadens the rate of mass loss peaks. This initial delay is a simple heat transfer effect, at 1°Cmin$^{-1}$ the sample temperature will closely match that of the furnace temperature, at higher heating rates the sample temperature will lag behind the furnace temperature causing the rate of mass loss peaks to move to higher temperatures and also making the peaks less sharp.

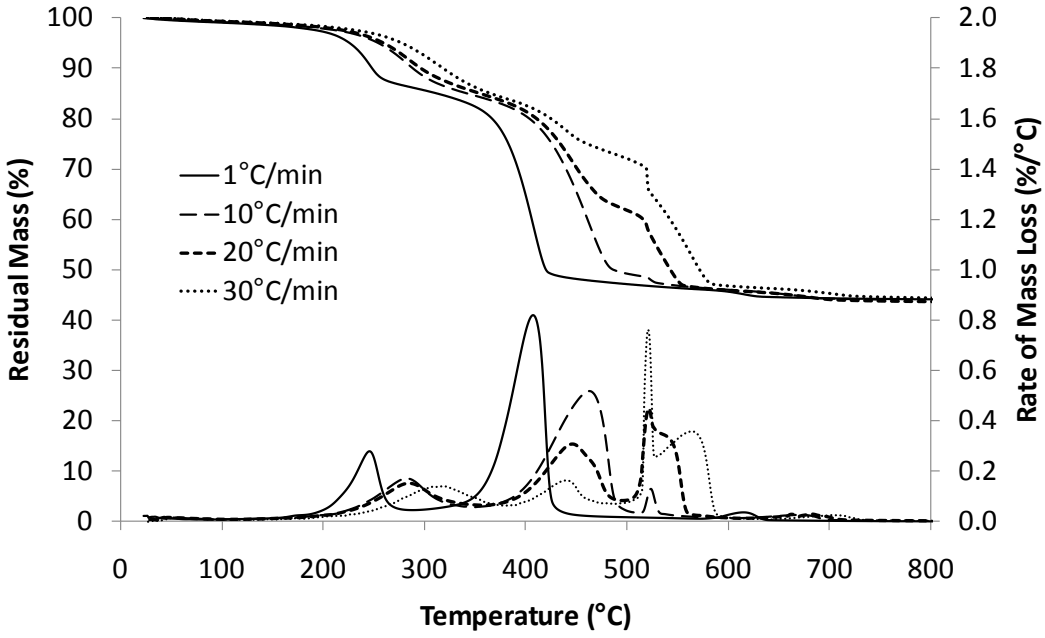


Figure 53: Effect of heating rate on the thermal decomposition of hydromagnesite measured by TGA

Above 450°C more complex differences become apparent. At a heating rate of 1°Cmin$^{-1}$ the mass loss rate has returned to almost zero by 450°C, at a heating rate of 10°Cmin$^{-1}$ the mass loss rate returns to almost zero at about 500°C, but is then followed by another small peak in mass loss rate at 520°C. As the rate of heating is increased further the additional mass loss at 520°C increases and is compensated for

by a reduction in mass loss between 400 and 500°C. This is showing a change in the decomposition mechanism of the carbonate ions. A higher heating rate causes the single stage decomposition to split into two stages.

As the heating rate increases, the release of water apparently moves to a higher temperature due to heat transfer effects. At 30°Cmin$^{-1}$ the release of water is spread over a much wider temperature range than at lower heating rates and the peak rate of water release occurs at a higher temperature. In addition to heat transfer effects as the heating rate increases, the water molecules released within the hydromagnesite particles have less time to diffuse to the surface further spreading the apparent temperature range over which the release occurs. The carbon dioxide release splits into two stages as the heat rate is increased. The release of carbon dioxide initiates at about the same temperature, just less than 400°C, for heating rates between 10 and 30°Cmin$^{-1}$, however less mass is lost and the peak rate of mass loss moves to a lower temperature. At 520°C a sudden mass loss occurs which increases with heating rate. This mass loss is associated with an exotherm (Figure 54) at 520°C followed by an endotherm which both increase with heating rate.

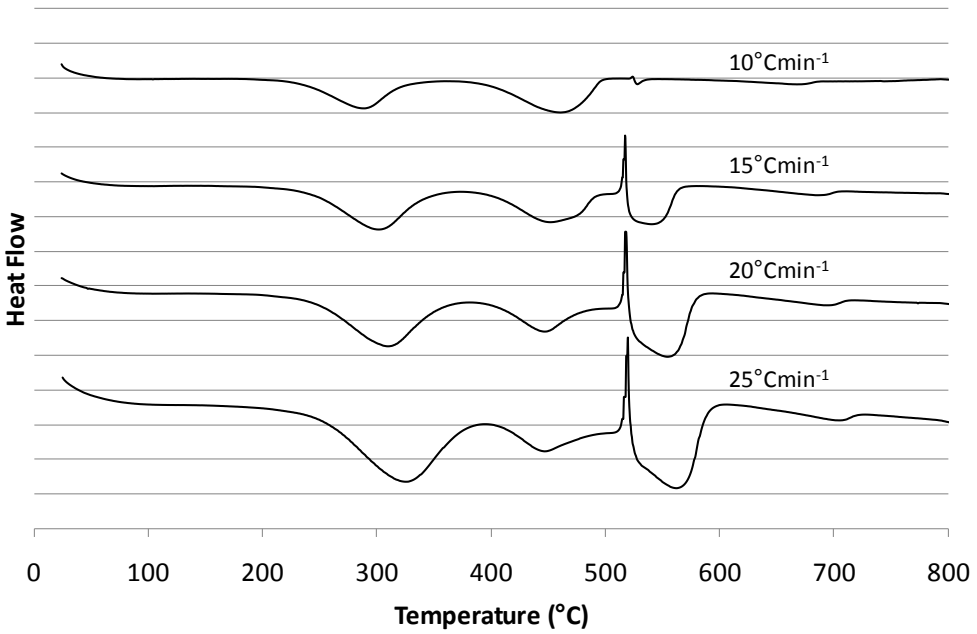


**Figure 54: Effect of heating rate on the thermal decomposition of hydromagnesite measured by DSC**

This effect of heating rate on the decomposition of hydromagnesite has been reported by several authors[65-69,100,102,104]. The partial pressure of carbon dioxide has been shown[66,100] to have a strong influence on the second stage of the carbonate ion decomposition and its associated exotherm. It has also been shown[69,100,104] that the exotherm is due to the formation of crystalline magnesium carbonate after the initial loss of some carbon dioxide. It is likely that at higher heating rates the increase in the partial pressure of carbon dioxide close to the surface, and within, the hydromagnesite particles is greater than at lower heating rates when the gas has more time to disperse. Therefore at higher heating rates a greater degree of crystallisation of magnesium carbonate occurs due to the higher local partial pressure of the self generated carbon dioxide atmosphere. The sudden mass loss at 520°C, visible in Figure 53, has been suggested[102] to be due to 'explosive' release of carbon dioxide trapped within the hydromagnesite particles. Thermal energy due to the mechanical stress caused by entrapped carbon dioxide and its explosive release has also been suggested as a cause for the exotherm. However the appearance of a second stage of mass loss above 520°C suggests that a combination of the two mechanisms is likely.

At slow heating rates hydromagnesite initially releases water of crystallisation followed by decomposition of the hydroxide ion releasing further water. The remaining magnesium carbonate decomposes directly to magnesium oxide by releasing carbon dioxide.

At high heating rates the release of water of crystallisation and decomposition of the hydroxide ion follows the same mechanism as it does at slower heating rates. The resulting magnesium carbonate begins to decompose, releasing carbon dioxide and increasing the partial pressure of carbon dioxide within the hydromagnesite particles and at the particle surface. This causes an increased amount of the carbonate ions to remain intact within the crystal structure until a critical temperature of 520°C is reached. At this temperature the remaining magnesium carbonate recrystallises exothermically to form a more thermally stable structure. The shift in the atomic arrangement of the magnesium carbonate releases entrapped carbon dioxide molecules leading to a sudden mass loss at the recrystallisation temperature. The higher the rate of heating the more pronounced this effect becomes.

### 4.2.4 The chemical composition of Turkish huntite by measurement of its thermal decomposition

As mentioned in section 4.2.1 Ozao *et. al.*[70] used the fact that the chemical formula for huntite, $Mg_3Ca(CO_3)_4$, can also be written as, $3MgCO_3{\cdot}CaCO_3$, to show by DTA that mechanical mixtures of calcium carbonate and magnesium carbonate have similar, although not identical, thermal decomposition characteristics as huntite. That the thermal decomposition is not identical is not surprising since huntite forms its own distinct crystal structure[106]. In a similar way the current sample of Turkish huntite has been compared with calcium carbonate and magnesium carbonate using TGA (Figure 55).

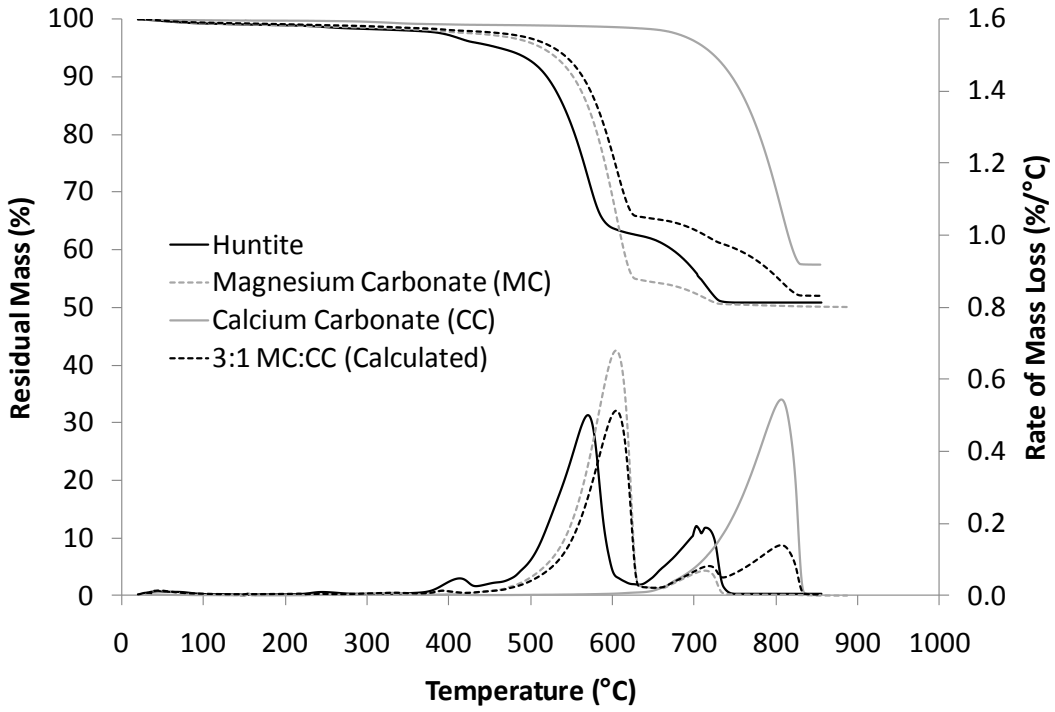


Figure 55: Comparison of huntite with magnesium carbonate and calcium carbonate using TGA

By proportionally summing the mass loss profiles of magnesium carbonate and calcium carbonate in a 3:1 ratio (the same ratio as present in huntite) a calculated mass loss profile has been constructed. This calculated mass loss profile is very similar to that of huntite. The mass losses from magnesium carbonate and calcium carbonate in the

calculated profile correspond well with those of the first and second stages of mass loss from huntite. The mass losses occur at lower temperatures in huntite than in the calculated mass loss profile for the mixture of minerals. This is because huntite is not a mixture of the two minerals but a crystalline substance containing the same ratio of magnesium and calcium atoms, and carbonate ions as a mixture of the two individual minerals. It can therefore be concluded that the decomposition mechanism of huntite must be as follows:

1st stage – between 400 and 630°C, decomposition of the carbonate ions associated with the magnesium atoms, releasing carbon dioxide and leaving a magnesium oxide calcium carbonate residue.

$$Mg_3Ca(CO_3)_4 \rightarrow 3MgO{\cdot}CaCO_3 + 3CO_2$$

The calcium carbonate does not form the same crystal structure as natural calcium carbonate because it decomposes at a lower temperature. This is due to the presence of the magnesium oxide within the structure.

2nd stage – between 630 and 750°C, decomposition of the remaining carbonate ions associated with the calcium atoms, releasing carbon dioxide and leaving a mixed residue of magnesium oxide and calcium oxide.

$$3MgO.CaCO_3 \rightarrow 3MgO{\cdot}CaO + CO_2$$

### 4.2.5 Decomposition mechanism of Turkish huntite

In order to further confirm the decomposition mechanism of huntite the decomposition gases generated during TGA analysis were identified using FTIR. As with the hydromagnesite analysis (section 4.2.2) this was done in real time allowing the gases indentified to be linked to a specific mass loss and temperature range. Figure 56 shows the Gram-Schmidt data from FTIR analysis of the evolved gases from huntite. This shows the output of the FTIR detector without linking it to a wavenumber and therefore shows the temperature ranges where evolved gases are detected, and the relative quantities, without identifying them. Unsurprisingly gases are detected in relation to the two mass losses measured by TGA. There is a slight offset between the temperatures of maximum mass loss rate and temperatures where maximum FTIR peak intensities are measured due to a delay in the evolved gases reaching the FTIR detector.

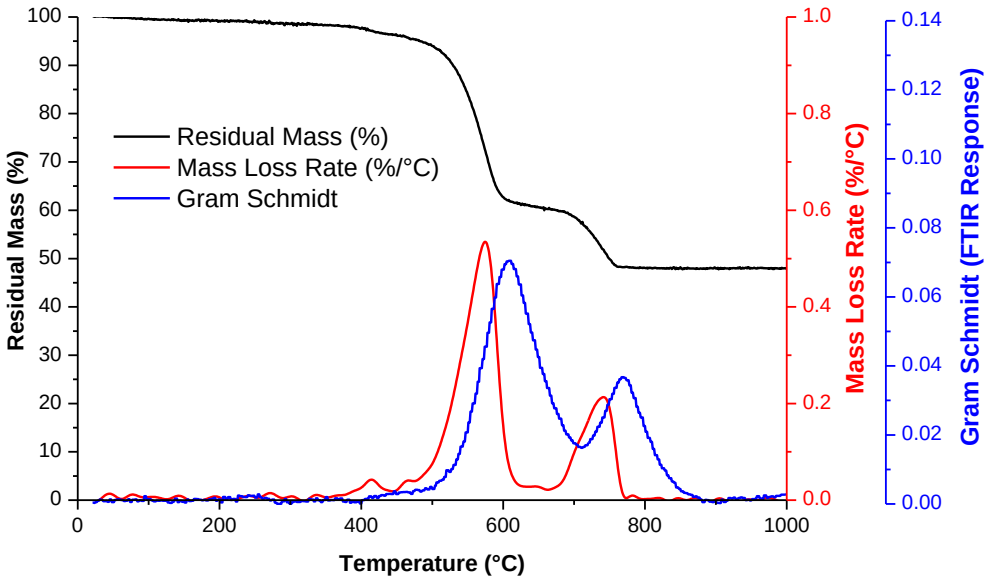


Figure 56: Gram Schmidt data from TGA-FTIR analysis of huntite

Figure 57 shows the FTIR spectra of the evolved gases measured at temperatures determined by the maxima and minima in the Gram Schmidt data from Figure 56. The FTIR peaks that can be seen between 2400 and 2200cm$^{-1}$ and below 750cm$^{-1}$ are characteristic of carbon dioxide. This confirms that the two mass losses measured during the decomposition of huntite are solely due to the decomposition of the carbonate ions and the subsequent release of carbon dioxide.

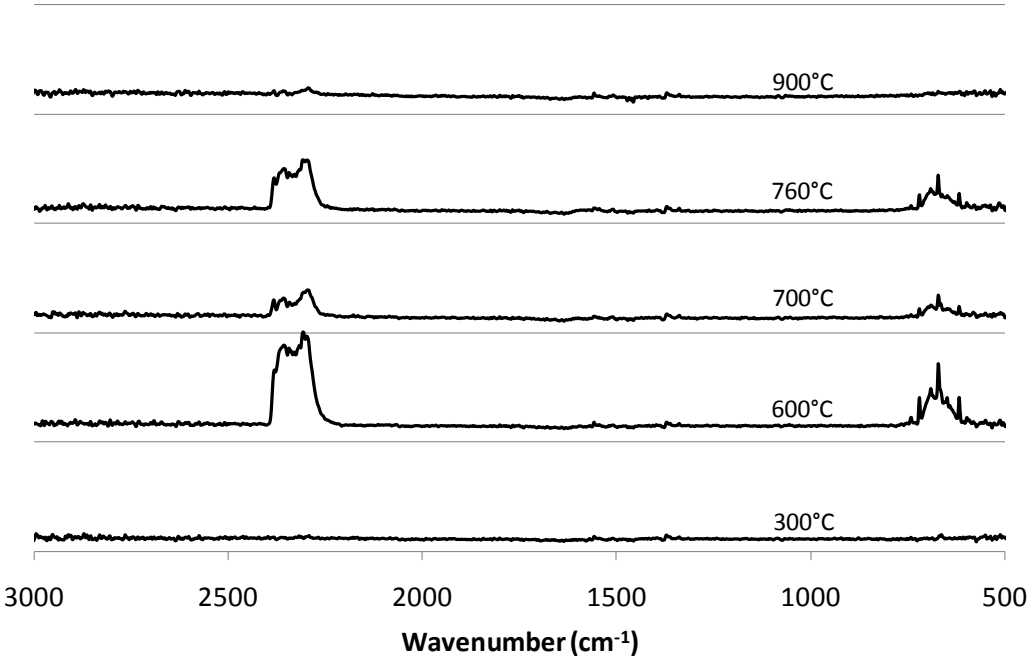


**Figure 57: FTIR spectra of gases evolved during decomposition of huntite**

### 4.3 Thermal decomposition of mixtures of Turkish huntite and hydromagnesite

Huntite and hydromagnesite extracted from Turkey occurs as a natural mixture of the two minerals, and in its use as a fire retardant it is also used as a mixture. Figure 58 shows how the minerals influence each other when mixed together. The thermal decomposition of the two individual minerals (HU93HM5 and HM100) was measured using TGA, along with a manually created 50:50 mixture of the two minerals. The manually created mixture of the two minerals was used to ensure this mixture was directly comparable to the individual huntite and hydromagnesite components. The expected mass loss profile of the mixture of the minerals was calculated by proportionally summing the measured mass loss profiles of the individual minerals.

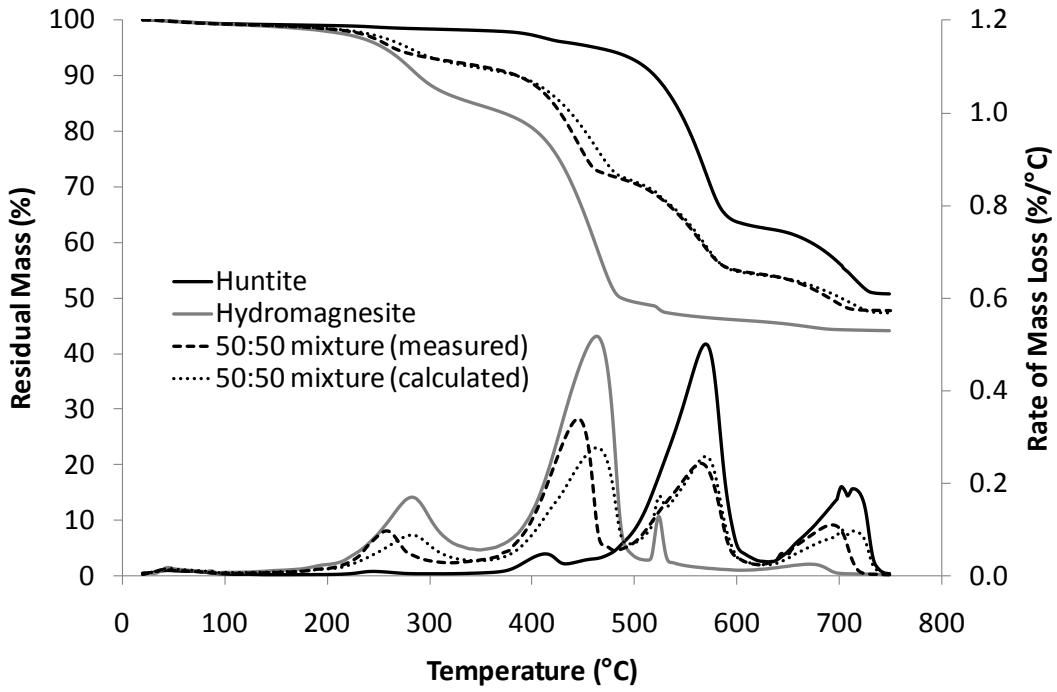


Figure 58: Measured and calculated thermal decomposition of a mixture of huntite and hydromagnesite by TGA

The measured decomposition of the mixture corresponds closely to that of the calculated decomposition profile. Both show decomposition taking place through four stages of mass loss and the mass losses for each stage correspond well with each other. Therefore the decomposition mechanism of the mixture is unaffected by the

presence of the other mineral. However, each stage of the measured decomposition occurs at a lower temperature than calculated.

The hydromagnesite, when measured individually, will have generated a larger endotherm per gram of total material present at any specific temperature than when mixed with huntite this may have slowed the decomposition of hydromagnesite when measured alone. In the mixture over most of the temperature range at which hydromagnesite decomposes the huntite is inert, therefore there is less overall cooling effect in the mixture than in the sample of hydromagnesite alone. This means the mixture will heat more readily than the individual minerals. The effect will be less significant over the temperature range at which huntite decomposes because the hydromagnesite will have decomposed meaning the dilution effect on the huntite portion of the mixture is smaller than it is on the hydromagnesite. This is seen in the difference between measured and calculated decomposition being less for the huntite portion of the mixture than for the hydromagnesite portion. Another possible explanation is that the particle size of the hydromagnesite was reduced during creation of the mixture (see section 4.4 for further discussion on particle size effects). The mixture was created by mixing the two powders in a small sample bag and squeezing the powder in the bag with a shearing finger pressure to make sure a good mixture was obtained.

The calculated rate of mass loss shows that the loss at 520°C, associated with the decomposition of crystallised magnesium carbonate formed from the hydromagnesite, should be detected in the mixture. However, the measured decomposition of the mixture did not show this. In the mixture the hydromagnesite particles are less closely packed due to the presence of huntite particles. Therefore, the partial pressure of carbon dioxide generated from the decomposition of hydromagnesite will be lower in the mixed sample than in the sample of hydromagnesite alone. It has been shown[66,100] that a higher partial pressure of carbon dioxide causes a higher degree of crystallisation. In a mixture of huntite and hydromagnesite crystallisation is less likely to occur, and therefore the predicted mass loss does not occur when the thermal decomposition is measured. As the heating rate is increased crystallisation is more

likely to occur (see Figure 53), but is likely to always be less than predicted from a mixture of the two minerals.

Figure 59 shows how the decomposition of hydromagnesite and huntite compares to theoretical mass losses calculated using atomic masses. There are three decomposition steps associated with the decomposition of hydromagnesite which are marked in Figure 59 as A, B, and C.

(A) - $Mg_5(CO_3)_4(OH)_2{\cdot}4H_2O \rightarrow Mg_5(CO_3)_4(OH)_2 + 4H_2O$

(B) - $Mg_5(CO_3)_4(OH)_2 \rightarrow Mg_4(CO_3)_4 + MgO + H_2O$

(C) - $Mg_4(CO_3)_4 \rightarrow 4MgO + 4CO_2$

These three steps are associated with calculated cumulative mass losses of 15.45%, 19.31% and 57.08% respectively. It can be seen in Figure 59 that these calculated mass losses correspond quite closely to the mass losses measured for hydromagnesite by TGA.

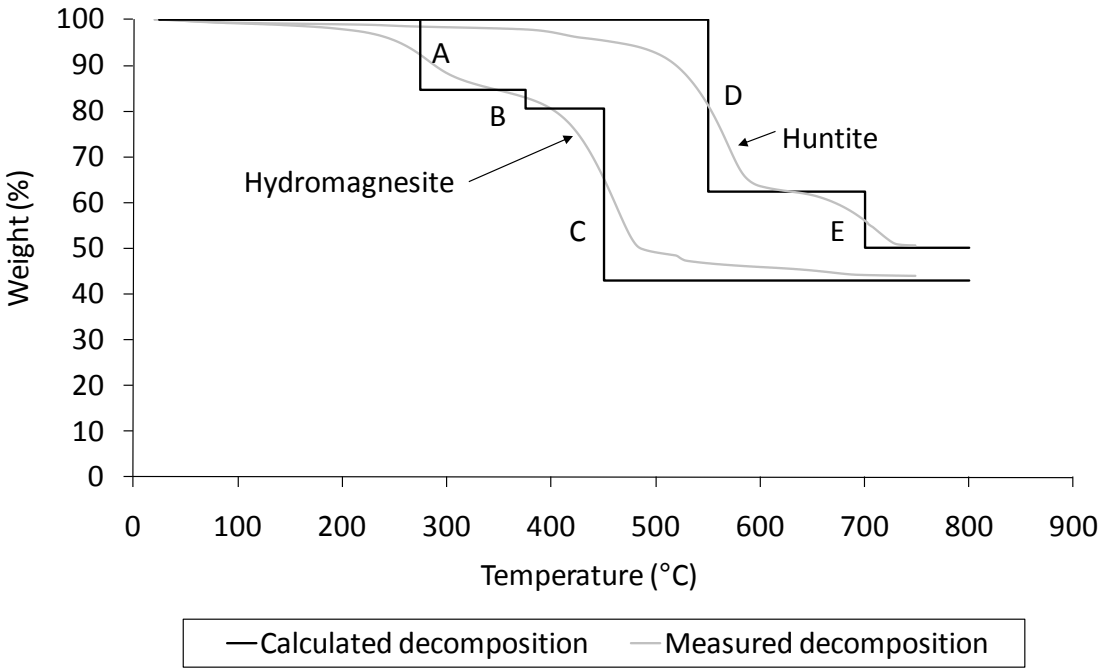


**Hydromagnesite**
A – loss of crystalline water
B – decomposition of hydroxide ion, releasing water
C – decomposition of carbonate ions releasing carbon dioxide
**Huntite**
D – decomposition of carbonate ions associated with Mg
E – decomposition of carbonate ion associated with Ca

**Figure 59: Decomposition of hydromagnesite and huntite compared to the calculated theoretical mass losses**

Huntite has two steps associated with its decomposition; these are marked as D and E in Figure 59.

(D) - $Mg_3Ca(CO_3)_4 \rightarrow CaCO_3 + 3MgO + 3CO_2$

(E) - $CaCO_3 \rightarrow CaO + CO_2$

These two steps are associated with calculated cumulative mass losses of 37.5% and 50.0% respectively. Again, the calculated mass losses correspond quite closely to the mass losses measured for huntite by TGA.

Figure 60 summarises the decomposition mechanisms discussed above, and in the previous sections, in relation to the decomposition of UltraCarb; a natural mixture of hydromagnesite and huntite. The data shown in Figure 60 was measured in air at a

heating rate of 10°C $min^{-1}$. At this heating rate only a minimal amount of crystallisation of magnesium carbonate is expected to occur during the decomposition.

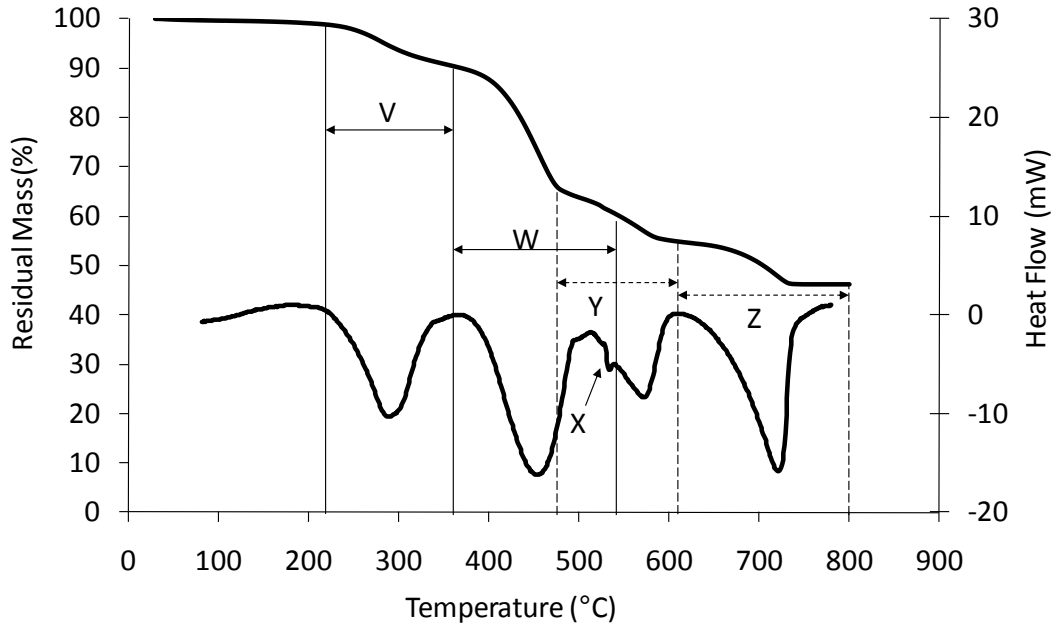


V – Loss of water from hydromagnesite approx. 220°C-350°C
W – Loss of carbon dioxide from hydromagnesite approx. 350°C-550°C
X – Exothermic crystallisation of magnesium carbonate
Y – Initial loss of carbon dioxide from huntite
Z – Secondary loss of carbon dioxide from huntite

**Figure 60: TGA and DSC decomposition of an approximately 60:40 natural mixture of hydromagnesite and huntite**

An initial mass loss and associated endotherm (V) between the temperatures of 220°C and 350°C is due to the loss of water of crystallisation from the hydromagnesite. This is followed by a second step in mass loss. In Figure 59 it is clear that this mass loss, associated with the loss of carbon dioxide from the hydromagnesite, is not complete until about 540°C (W). Therefore, it overlaps with the initial mass loss associated with loss of carbon dioxide from the huntite (Y). The loss of the hydroxyl group from hydromagnesite as water is not detected as a separate mass loss in Figure 60. However, it was reported by Haurie[84] that this loss of water occurs between 380°C and 450°C which would mean that it occurs in the lower half of region W in Figure 60.

This region also covers the temperature range where carbon dioxide is being lost from the hydromagnesite. At about 520°C a slight discontinuity it seen in the DSC data (X). This is the temperature at which the exothermic crystallisation of magnesium carbonate has been reported. The heating rate used for this measurement was 10°C $min^{-1}$ which is why the exotherm is very small, indicating that there is only very minimal crystallisation of magnesium carbonate. It also occurs in the temperature range (Y) at which huntite is endothermically decomposing. Figure 59 shows that above 520°C there is a continued slow loss in mass from hydromagnesite up to about 700°C which is probably slow degradation of the small amount of crystalline magnesium carbonate.

Figure 59 shows that huntite begins to decompose rapidly at about 470°C. This loss in mass with its associated endotherm is complete at about 610°C. The decomposition over this temperature range (Y) is due to the loss of carbon dioxide from the carbonate groups associated with the magnesium ions. A final mass loss and endotherm (Z) between 610°C and 800°C is due to a final loss of carbon dioxide resulting from the decomposition of the carbonate groups associated with the calcium ions.

At 800°C the hydromagnesite has decomposed to leave a magnesium oxide residue and the huntite has decomposed to leave a mixture of calcium oxide and magnesium oxide.

## 4.4 Effect of particle size on the thermal decomposition of mixtures of Turkish huntite and hydromagnesite

Two mixtures of huntite and hydromagnesite were produced at the same time from the same raw material (therefore containing the same proportion of huntite and hydromagnesite). The two mixtures had two different particle size distributions, the first had an average particle size ($d_{50}$) of 1.8µm and the second was finer with a $d_{50}$ of 1.0µm. TGA analysis of the two samples is shown in Figure 61. It is clear that the finer material decomposes slightly earlier than the coarser material. This behaviour is expected because finer particles will conduct heat to the centre of each particle faster than the coarser particles. Therefore the finer particles will show less heat lag behind

the furnace temperature than the coarser particles and will decompose sooner. It will also be easier for gases generated internally to escape because of the shorter path to the surface of the particle.

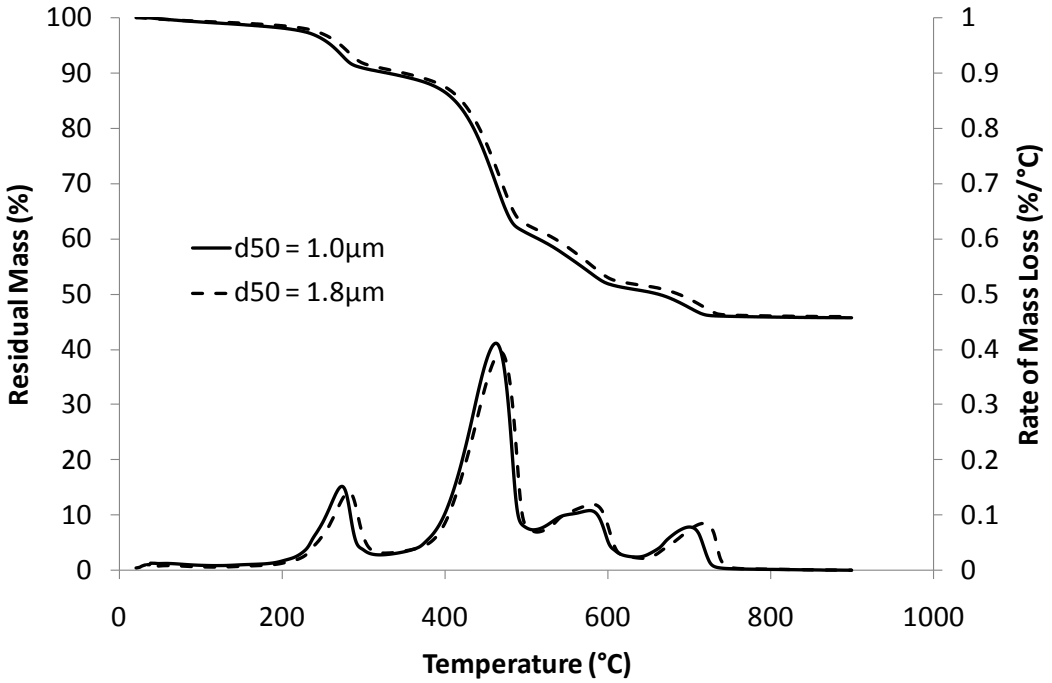


Figure 61: Effect of particle size distribution on the thermal decomposition of a mixture of huntite and hydromagnesite

## 4.5 Comparison of hydromagnesite with aluminium hydroxide and magnesium hydroxide

Thermal mass loss profiles of a mixture of huntite and hydromagnesite, ATH, and magnesium hydroxide as measured by TGA are shown in Figure 62. As can be seen magnesium hydroxide remains stable to a higher temperature than the other two minerals. It begins to decompose at about 330°C and loses mass rapidly up to about 450°C. This decomposition has been studied in detail by other researchers[103,152].

ATH is often quoted[52,54] as having an initial decomposition temperature of 180°C - 200°C. However this graph *appears* to indicate that ATH is stable until well over

200°C. This is not the case as the following further analysis of the data will show. Careful interpretation of TGA data is often needed; the data always indicates that mass losses occur at precisely defined temperatures which can be misleading. In reality there are a number of reasons that can affect the temperature at which a mass loss is measured.

The heating rate is a very important variable in the TGA experiment. The data in Figure 62 is generated by heating the sample at a constant rate of 10°Cmin$^{-1}$. The faster the heating rate the greater the difference between the temperature of the furnace and the temperature of the sample. This means that at faster heating rates mass losses appear to shift to the right (higher temperatures) as the temperature of the sample lags behind that of the furnace. However, 10°Cmin$^{-1}$ is considered a very standard speed at which to conduct this type of test so it still leaves the question open of why ATH appears to be more thermally stable than often quoted.

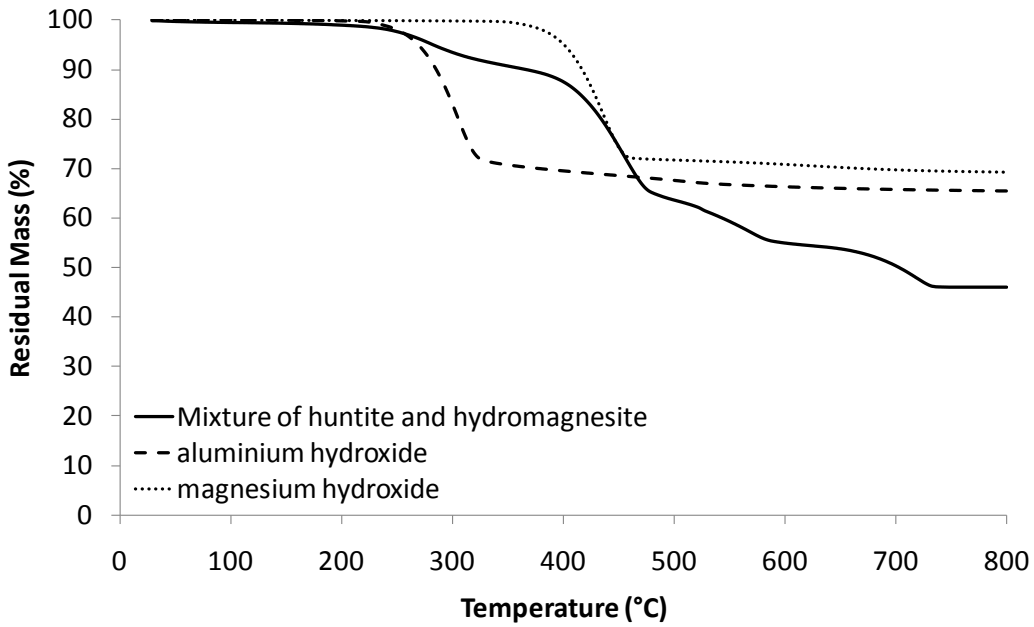


**Figure 62: TGA decomposition of UltraCarb and ATH. Mass loss against temperature at a heating rate of 10°C min$^{-1}$**

Figure 63 shows the results of a TGA experiment carried out using an isothermal method. Instead of heating the sample at a constant heating rate the sample is heated very rapidly to a set temperature and then held at that temperature. This gives the sample time to thermally equilibrate at the desired temperature and time for the rate of mass loss at that temperature to be determined. The samples were held isothermally at 180, 200, 220, and 240°C for 30 minutes. The advantage of this method over the method of using a continuous heating rate is that if a decomposition is occurring slowly at a certain temperature it is given time to happen. Using the continuous heating method causes the mass losses to be associated with higher temperatures simply because they are happening slowly and in that time the temperature of the furnace is increasing.

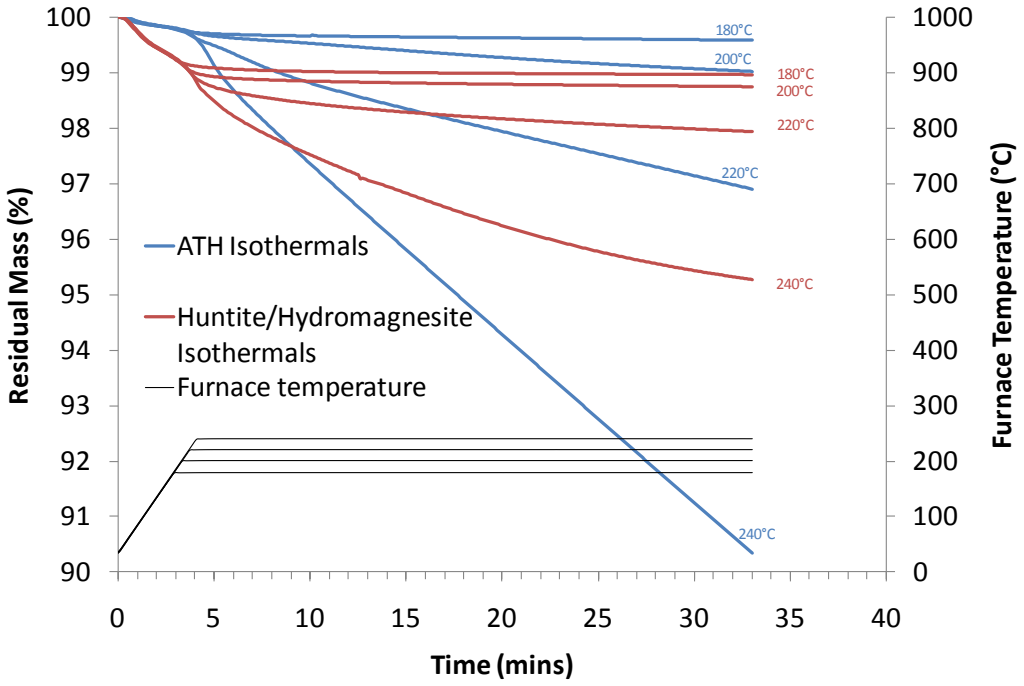


**Figure 63:TGA decomposition of UltraCarb and ATH. Mass loss against time held at a fixed temperature**

In Figure 63 the blue lines represent the mass loss of ATH held isothermally at the four temperatures, the red lines represent the mass loss of the mixture of huntite and hydromagnesite. The 'X' axis in this case shows time held at the desired temperature. The black lines show the furnace temperature against the right hand axis during the experiment (initial rapid heating, followed by isothermal conditions).

It can be seen that during the initial rapid heating phase the mixture of huntite and hydromagnesite lost more mass than ATH. This indicates that there is a driving off of surface moisture or less tightly bound water within the mixture of huntite and hydromagnesite, there is also a mass loss associated with ATH over this initial period. This effect is also visible as the higher mass loss of the mixture of huntite and hydromagnesite, as compared to ATH, at low temperature in Figure 62. This is therefore not an unexpected result. For both ATH and the mixture of huntite and hydromagnesite once the temperature is held at 180°C there is only very slight further loss of mass over a 30 minute period. This indicates that both are stable at 180°C, with no significant decomposition occurring.

At 200°C the mass loss of the mixture of huntite and hydromagnesite again remains very constant once isothermal conditions have been reached, indicating that it is stable at this temperature. However, the ATH sample continues to steadily lose mass once the 200°C isothermal conditions have been reached, indicating that it is slowly decomposing at this temperature. This fits *exactly* with the commonly quoted values of 180 - 200°C for the decomposition temperature of ATH. It is also proof that hydromagnesite is more thermally stable than ATH.

At 220°C hydromagnesite is starting to decompose slowly, and at 240°C more rapidly. At both of these temperatures ATH is decomposing more rapidly than hydromagnesite.

Another way of representing this data is to plot the mass loss against temperature as shown in Figure 64. This gives a similar kind of plot to the standard TGA curve seen in Figure 62. The portions of the graph up until the point at which the data lines become vertical are very similar to the data lines seen in Figure 62. This is because the tests up until this point are the same except that the heating rate in this case is much higher. Once the isothermal temperature is reached, the lines become vertical as the samples are held at the desired temperature and the mass loss is measured over time. In each case the vertical lines are terminated once the sample has been held at the desired temperature for 30 minutes. Therefore the length of the drop from the horizontal portion of the line represents the degree of decomposition at that particular temperature after 30 minutes. At temperatures of 200°C and above that ATH loses more mass during the isothermal stage of the test as compared to the mixture of huntite and hydromagnesite, indicating that the ATH is decomposing faster.

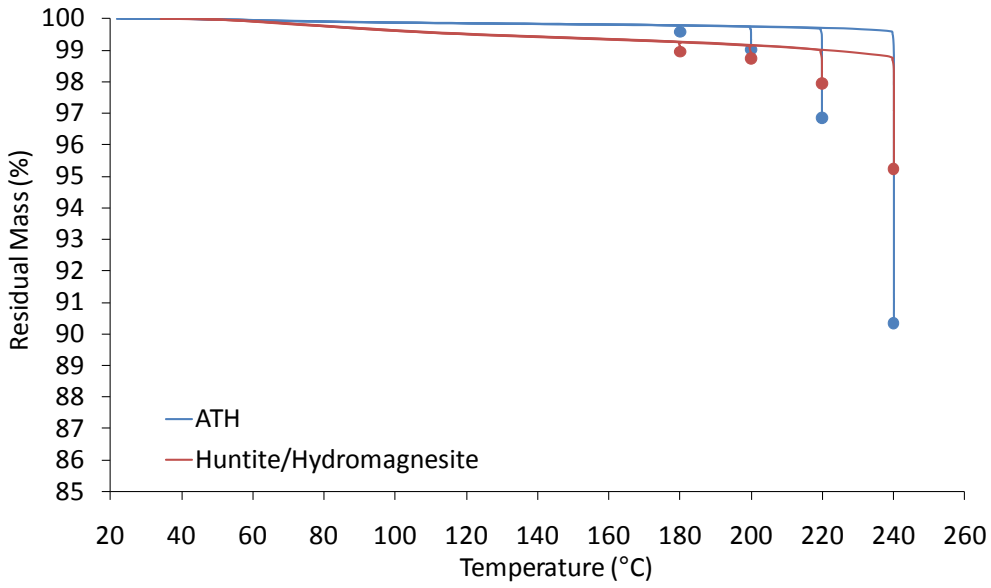


**Figure 64: TGA decomposition of UltraCarb and ATH. Mass loss against temperature held at fixed temperatures**

Figure 65 and Figure 66 show the rate of mass loss for ATH and the mixture of huntite and hydromagnesite against time at four isothermal temperatures. During the initial heating period both ATH and the mixture of huntite and hydromagnesite show a double peak in rate of mass loss. The first peak could well be due to removal of surface moisture and volatiles on the samples. The samples were not dried prior to testing and were stored at ambient conditions so some surface moisture is likely.

Both ATH and the mixture of huntite and hydromagnesite also show a second peak in rate of mass loss which then levels off as the isothermal temperature is reached. This shows that in both materials second phases of mass loss are being entered into which are the early stages of decomposition. Once the isothermal temperature is reached the rate of mass loss drops quickly to a steady level.

The steady rate of mass loss under isothermal conditions is the area of most interest. Figure 65 shows that for the mixture of huntite and hydromagnesite at 180°C and 200°C the rate of mass loss quickly drops to zero, meaning that after the initial loss in mass the mineral is very stable at these temperatures. At 220°C the rate of mass loss for the mixture of huntite and hydromagnesite drops to a very low level showing that extremely slow decomposition of the mineral is occurring at this temperature over the time period. At 240°C the rate of decomposition of the mixture of huntite and hydromagnesite is higher, but it is slowing over the time period.

In contrast Figure 66 shows that at 200°C and above ATH shows a steady rate of decomposition once isothermal conditions have been reached. Also at each temperature the rate of decomposition of the ATH is significantly higher than that of hydromagnesite.

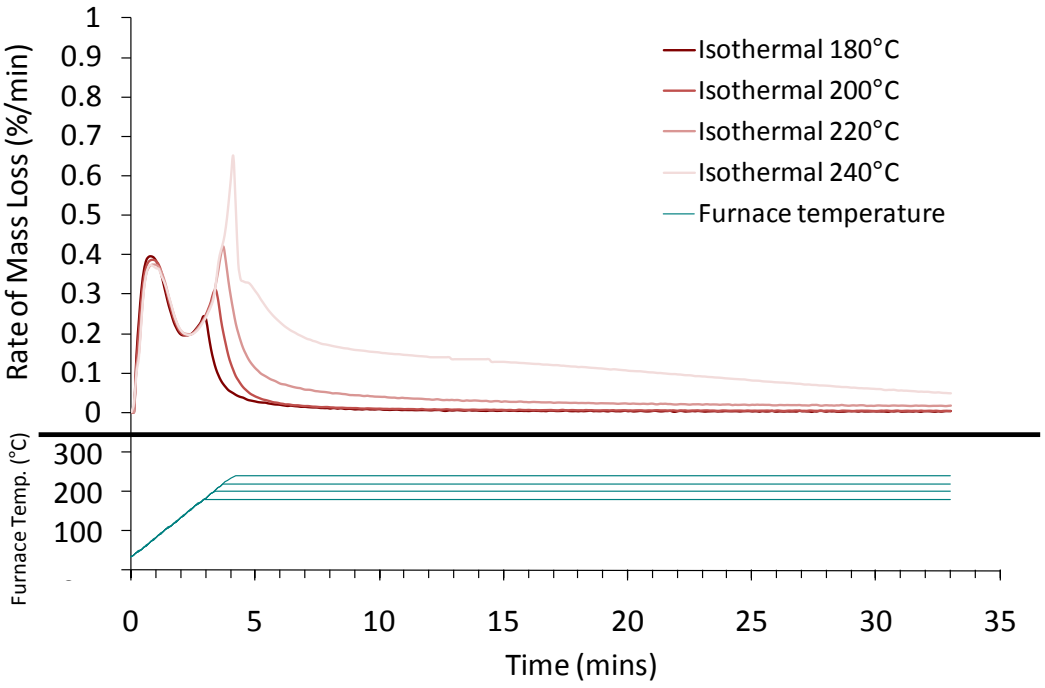


**Figure 65: TGA decomposition of UltraCarb. Rate of mass loss against time**

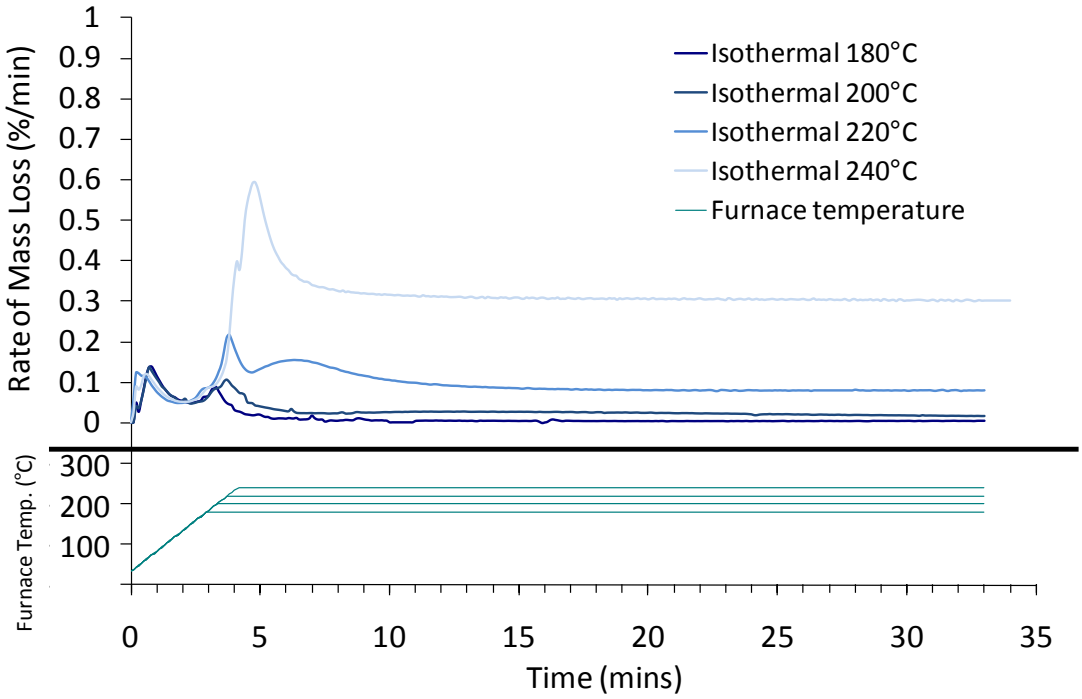


**Figure 66: TGA decomposition of ATH. Rate of mass loss against time**

## 4.6 Summary

The morphology of huntite and hydromagnesite has been shown to be quite different from each other. Huntite particles are generally smaller and more plate-like than the larger blockier hydromagnesite particles.

Both minerals decompose endothermically, with hydromagnesite giving off water and carbon dioxide, and huntite giving off only carbon dioxide. The decomposition of huntite is through a two stage mechanism. Between about 400°C and 630°C the carbon dioxide, from the decomposition of the carbonates associated with the three magnesium ions, is released. This is followed, between 630°C and 750°C, by the release of carbon dioxide from the remaining carbonate ion associated with the calcium ion.

The thermal decomposition of hydromagnesite is more complicated and is significantly affected by the rate of heating. Up to a temperature of about 350°C water of crystallisation is released; above this temperature carbon dioxide is released through a mechanism that varies depending on heating rate and partial pressure of carbon dioxide in the atmosphere surrounding the particles. The two hydroxide ions also decompose to release a further molecule of water. This probably happens at about 330°C but is not clearly visible as a separate stage of decomposition.

At slow heating rates (less than $10°Cmin^{-1}$) the carbonate ions within the hydromagnesite decompose directly to magnesium oxide in a single stage. As the heating rate is increased the single stage spits into two stages, with a clearly defined exotherm and sudden mass loss at 520°C. This is believed to be due to a reorganisation of the crystal structure of the remaining magnesium carbonate, which then goes on to decompose at a higher temperature.

Hydromagnesite has been shown to have a lower degree of decomposition than ATH at temperatures around 200°C. This is beneficial as it means mixtures of huntite and hydromagnesite can be used with polymers that have higher melting temperatures, such as polypropylene, where the decomposition of aluminium hydroxide at the melt processing temperature could cause problems.

# 5. Results and discussion 2 – *The effect of huntite and hydromagnesite as a fire retardant in EVA*

In order to investigate the fire retardant behaviour of huntite and hydromagnesite in a polymer compound the formulation shown in Table 5 in section 3.1.2 was used to prepare samples. The five huntite/hydromagnesite mixtures shown in Table 4 in section 3.1 were used to study the effects of the minerals at a range of ratios. Compounds were mixed on a two roll mill as discussed in section 3.2.1.

The mineral fillers and fire retardants used in this chapter are blends of huntite (HU) and hydromagnesite (HM), aluminium hydroxide (ATH), magnesium hydroxide (MDH) and calcium carbonate (chalk). Throughout this chapter the following labelling method will be used. Where a mineral is being referred to in its pure form the abbreviations shown in Table 4 will be used. Where mixtures of huntite and hydromagnesite are referred to the abbreviation will show the approximate ratio of the two minerals, for example the mixture that contains approximately 41% huntite and 57% hydromagnesite will be abbreviated to HU41HM57. Where the minerals are incorporated into the EVA compound shown in Table 5 this will be indicated by the letters EVA in front of the mineral abbreviation. For example a calcium carbonate filled EVA compound will be represented as EVA.chalk, and a compound containing huntite and hydromagnesite will be represented as EVA.HU41HM57.

## 5.1 Thermogravimetric analysis (TGA) studies

TGA was used to analyse the thermal decomposition of individual components of the compound in air at a heating rate of 10°Cmin$^{-1}$. Each polymer and additive has its own characteristic decomposition mechanism. Individual decomposition profiles can be used to calculate the expected decomposition of a compound containing those components. This is done by proportionally summing the residual masses of the components. The residual masses are multiplied by their weight fractions in the compound, at each temperature. For example, the expected thermal decomposition profile of a simple compound containing 40% EVA and 60% calcium carbonate can be calculated, by summing 60% of the percentage mass loss of calcium carbonate with 40% of the percentage mass loss of EVA at each temperature. The calculated mass loss profile can then be compared with the measured mass loss profile of the compound. Any differences in the two profiles indicate areas where there must be some interaction between the components causing faster or slower decomposition of the compound than calculated. These differences can be caused by actions such as the endothermic decomposition of a mineral slowing the thermal decomposition of a polymer, or the release of an acid from a polymer such as PVC or EVA which if strong enough could react with a carbonate based mineral filler causing it to release carbon dioxide at a lower temperature than it would through thermal decomposition. Therefore, this method can be used to investigate the decomposition mechanism of compounds containing fire retardants and help explain the compound's performance in other fire tests.

### 5.1.1 Thermal decomposition by TGA of the individual components of the EVA compound

Thermal decomposition of the polymers used in the compound were carried out by TGA at a heating rate of 10°Cmin$^{-1}$ in air, the results are shown in Figure 67.

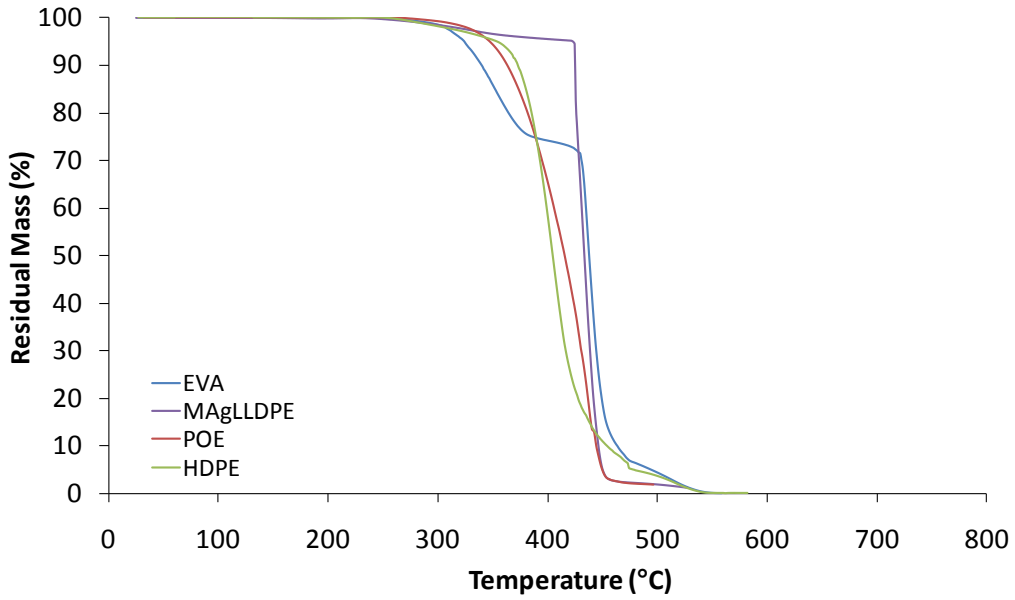


Figure 67: Thermal decomposition of polymers by TGA

The two polyethylene polymers (HDPE, and POE) follow similar mass loss profiles. It has been shown[153,154] that polyethylene follows a decomposition mechanism involving random chain scission (as discussed in section 1.4.1).

The EVA sample follows a two stage decomposition; loss of the vinyl acetate side groups as acetic acid followed by decomposition of the polymer backbone[8-11]. Loss of the vinyl acetate groups may also lead to some crosslinking of the polymer chain resulting in an increased decomposition temperature as compared to the pure polyethylene materials.

Maleic anhydride grafted LLPDE shows a small mass loss before the sudden main mass loss. It has been suggested[155] that the decomposition mechanism of this polymer involves chain scission followed by the formation of hydroxide groups at the end of the

polymer chains through reaction of the free radicals. The hydroxide groups then react with the maleic anhydride groups forming a crosslinked structure which rapidly decomposes at about 425°C.

Irganox 1010 is an antioxidant commonly used in polymer compounds to protect the polymer from early degradation during melt processing and during the lifetime of the product. It is only used at very low addition levels so its mass loss shown in Figure 68 will be negligible in the compound, although it will have an effect on reducing the oxidative decomposition of the polymers.

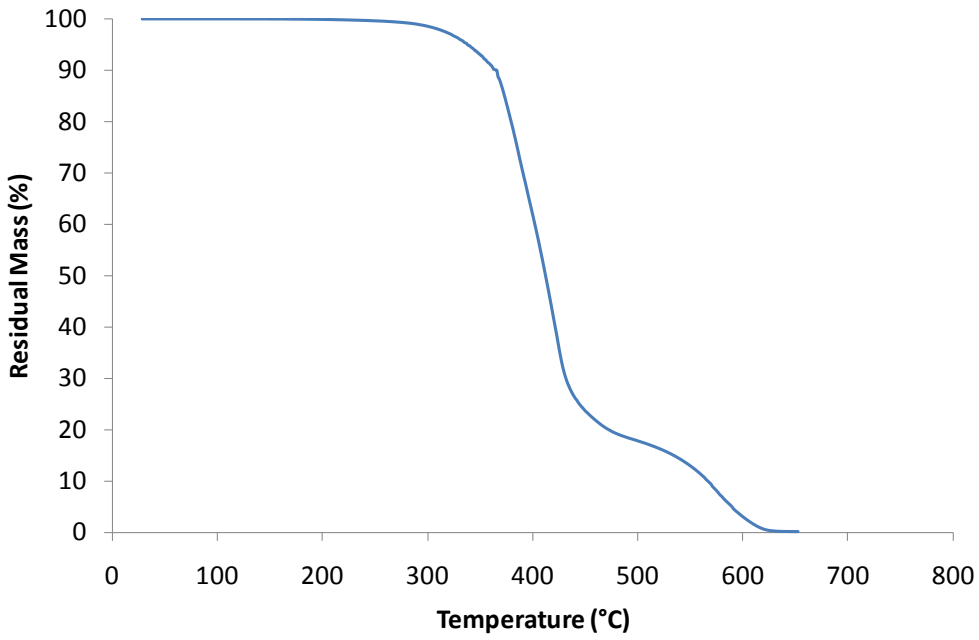


Figure 68: Thermal decomposition of Irganox 1010 by TGA

### 5.1.2 Thermal decomposition by TGA of EVA compounds filled with huntite and hydromagnesite

Comparison of the expected thermal decomposition behaviour from calculation with the measured behaviour of compounds containing the various mineral fire retardants is discussed in this section. Measurements were made using TGA at a heating rate of 10°Cmin$^{-1}$ in air. Mass loss profiles of the compounds were calculated by proportionally summing the mass loss profiles of the individual components and in each case the mass loss profile of the relevant fire retardant filler is shown in proportion for the fact that it is used at a 60% loading level in the compound.

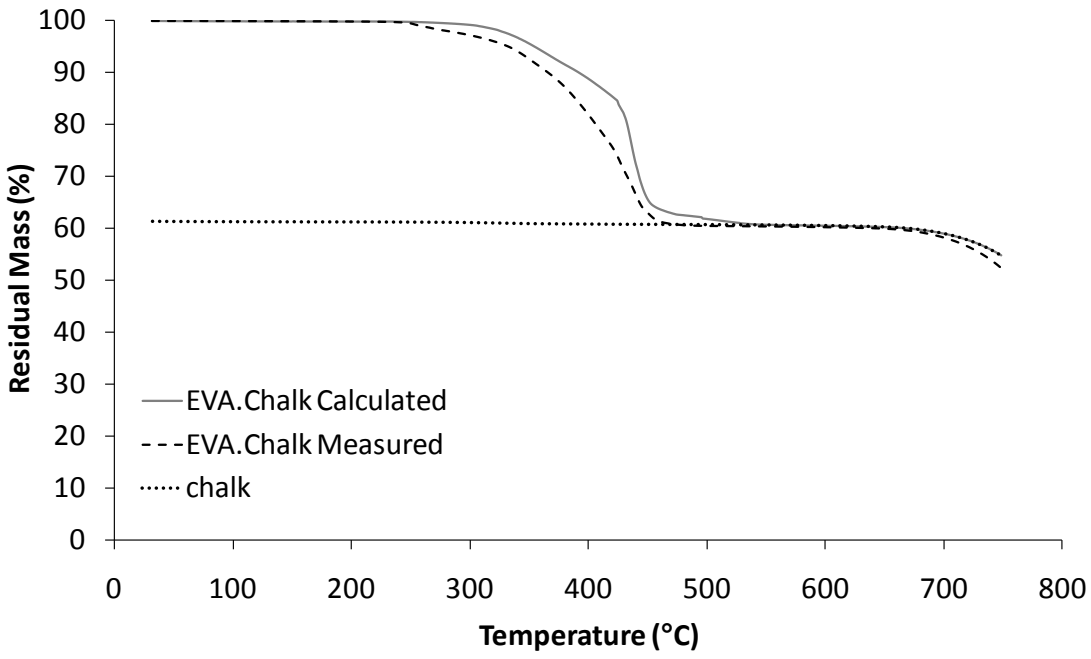


**Figure 69: Calculated and measured thermal decomposition by TGA of EVA compound (EVA.chalk) filled with calcium carbonate**

Figure 69 shows that calcium carbonate begins to thermally decompose at about 650°C compared with the thermal decomposition of a 60% calcium carbonate filled EVA compound based on the formulation shown in Table 5. The full thermal decomposition of calcium carbonate is shown in Figure 55 in section 4.2.4. Figure 67 shows that when the polymers used in the compound are thermally decomposed individually each of them has totally volatilised below 550°C. Therefore the measured mass loss in Figure 69 between the temperatures 250°C and 450°C is likely to be due to

the thermal degradation of the polymers. The slow mass loss between about 450°C and 550°C seen in Figure 67 is due to decomposition of residual carbonaceous char. Figure 69 shows that the addition of chalk causes the polymers to decompose without forming the more stable char above 450°C. This may be caused by the high proportion of calcium carbonate preventing a stable char structure from forming. The remaining residue of 60% of the original mass at 600°C is exactly what is expected because the calcium carbonate accounted for 60% of the original mass and does not begin to thermally decompose until about 650°C. The EVA compound does indeed show a mass loss starting at about 650°C and corresponding with the temperature at which mass loss was measured for the calcium carbonate. This two step thermal decomposition is exactly what would be expected with the calcium carbonate acting as a diluent filler with no active fire retardant effect. A calcium carbonate filled EVA therefore provides a good model for decomposition of a compound containing an essentially inactive filler in terms of active fire retardant effects and can be used to make comparisons with compounds containing mixtures of huntite and hydromagnesite or other mineral fire retardants.

Figure 69 also shows the calculated mass loss profile of a calcium carbonate filled EVA compound compared to the measured mass loss profile. The measured mass loss profile shows that the onset of decomposition occurs earlier than expected from calculation. This shows that there must be some interaction between the components causing the earlier decomposition.

McGarry *et al*[8] showed that EVA forms a carbonaceous skin during decomposition. Deacetylation was shown to be completed by 380°C with the formation of a protective carbonaceous skin. The skin provided a protective layer retarding the degradation of the underlying polymer. Addition of ATH to EVA was shown to cause the skin to rupture due to the evolution of water destroying the layer or the high loading level of the ATH preventing the layer from forming a coherent barrier. This destruction of the barrier lead to an increased rate of degradation of the EVA compared to the unfilled EVA.

In the case of calcium carbonate filled EVA, shown in Figure 69, water evolution disrupting the carbonaceous char layer cannot be the cause of the increased rate of degradation, however the high level of calcium carbonate may be having an effect on the formation of a coherent carbonaceous barrier allowing the underlying polymer to decompose at a faster rate.

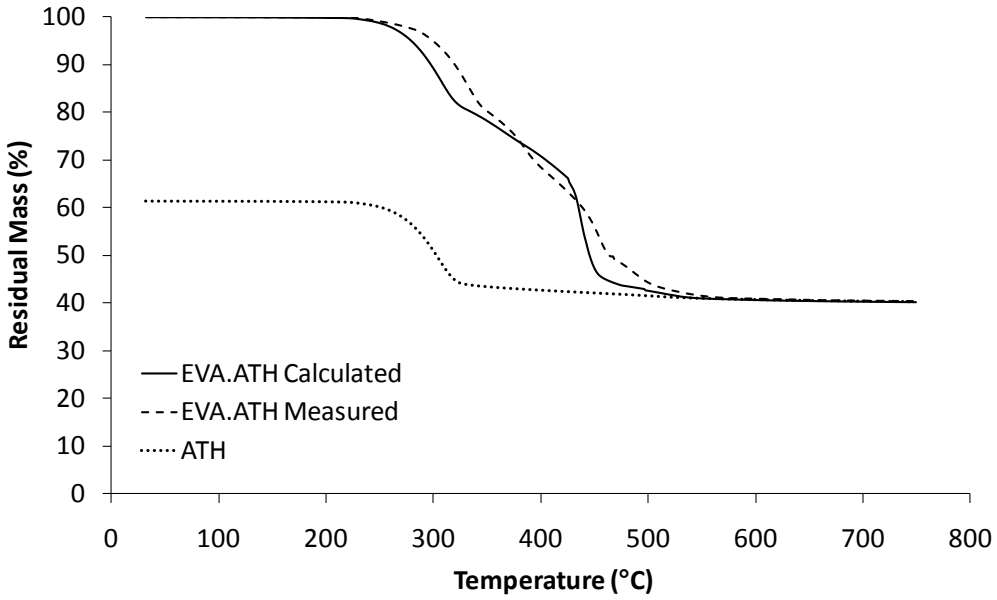


**Figure 70: Calculated and measured thermal decomposition by TGA of EVA compound (EVA.ATH) filled with ATH**

Figure 70 shows a comparison of the calculated mass loss profile of an ATH filled EVA compound compared to the measured mass loss profile. Initially the measured mass loss profile shows a later mass loss than calculation predicts. The onset of decomposition of ATH has been shown to occur at about 180 - 200°C (see section 4.5). When ATH is incorporated into a polymer the initial mass loss of the ATH will not be registered since the released water will become entrapped within the polymer matrix as bubbles. The water vapour in the bubbles will not be released (and therefore register as a mass loss) until the polymer surrounding the bubble decomposes to the point that the bubble bursts releasing the water vapour, or the viscosity of the polymer reduces to the point that the water vapour can move through the polymer to the

surface. Therefore the actual mass loss associated with the thermal decomposition of the ATH appears to occur at a higher temperature.

Between about 380°C and 430°C the measured mass loss becomes greater than calculated. This is probably due to disruption of the carbonaceous skin by release of the entrapped water vapour through the surface of the polymer as discussed by McGarry *et. al.*[8]. Above 430°C the mass loss again becomes less than calculated; at this stage it is possible that the residual aluminium oxide is providing a protective layer over the remaining polymer and slowing its decomposition.

Figure 71 shows that the thermal decomposition of a magnesium hydroxide filled EVA becomes separated into two stages as compared to the apparent single stage expected from calculation. This two stage mechanism has been reported[156,157] previously. The first stage of decomposition has been reported to be due to the loss of the vinyl acetate groups as acetic acid, and the dehydration of the magnesium hydroxide, the second stage is due to the decomposition of the residual polymer.

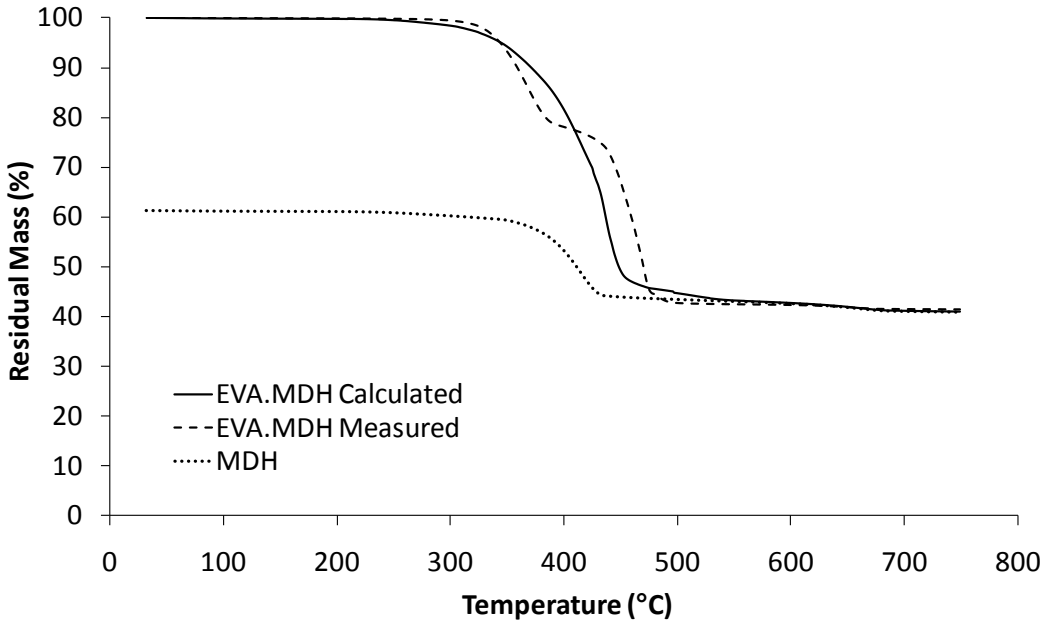


**Figure 71: Calculated and measured thermal decomposition by TGA of EVA compound (EVA.MDH) filled with magnesium hydroxide**

Initially the mass loss of the compound is slightly less than expected from calculation; however at about 340°C the mass loss becomes greater than expected. At this temperature the magnesium hydroxide decomposes rapidly, the bubbles containing

the water vapour may well be breaking the surface of the polymer. This would disrupt any carbonaceous skin that may have formed and the breaking bubbles would also expose more polymer surface to the radiant heat causing an increase in the rate of degradation and mass loss. At temperatures above 430°C the mass loss is less than expected by calculation. At these temperatures the magnesium hydroxide has almost completely decomposed therefore the lower than expected mass loss at these temperatures must be due to some action of the magnesium oxide residue in the decomposing polymer. The residue may be acting as a protective inorganic layer slowing the degradation of the remaining polymer.

Figure 72 shows that aluminium hydroxide loses its water at a lower temperature than the acetic acid loss from EVA. Clearly when ATH begins to decompose the polymer will be molten but not yet decomposing rapidly. Therefore the initial water released will be likely to become entrapped as bubbles within the molten polymer leading to a lower than expected mass loss as seen in Figure 70.

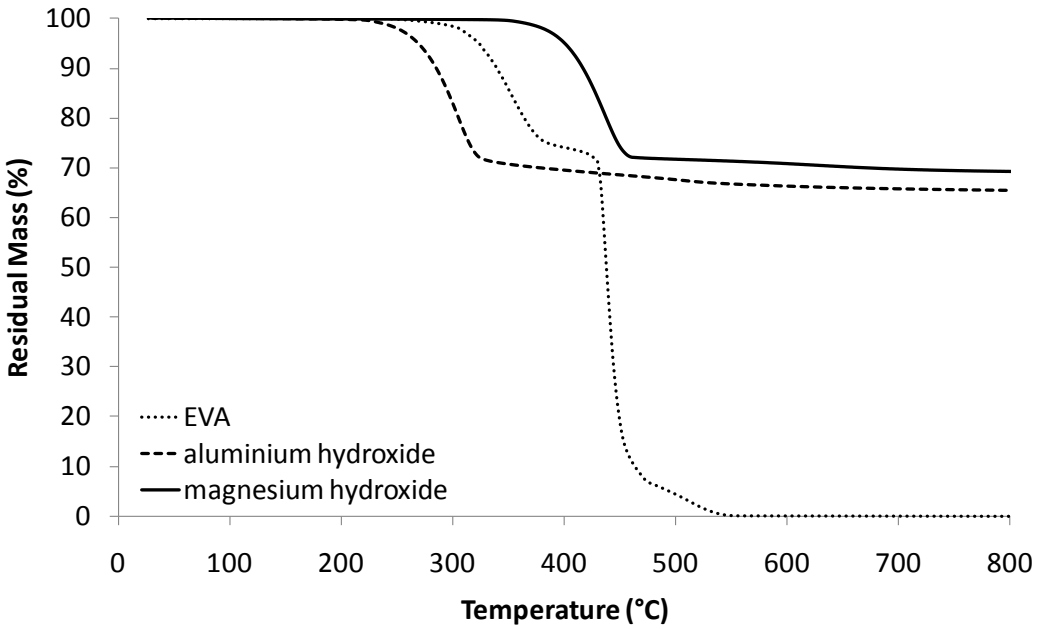


**Figure 72: Comparison of the thermal decomposition measured by TGA of aluminium hydroxide, magnesium hydroxide and EVA**

However, the release of water from magnesium hydroxide occurs at a higher temperature than the release of acetic acid from EVA. It is possible that the release of

water from the magnesium hydroxide has a greater influence on disrupting the char layer than the water from ATH because it is released over the same temperature range that the char provides momentary protection to the underlying polymer. This could explain the measured mass loss occurring at a lower temperature than calculated from proportional summation of the components as shown in Figure 71.

Figure 73 shows the thermal decomposition of an EVA compound filled with hydromagnesite. It shows that measured mass loss starts to occur at about 260°C, well above the expected initial decomposition temperature of hydromagnesite i.e the decomposition of the hydromagnesite appears to be delayed. This apparent delay in decomposition may be due to entrapment of the released water within the polymer matrix as discussed above for the decomposition of the ATH filled compound.

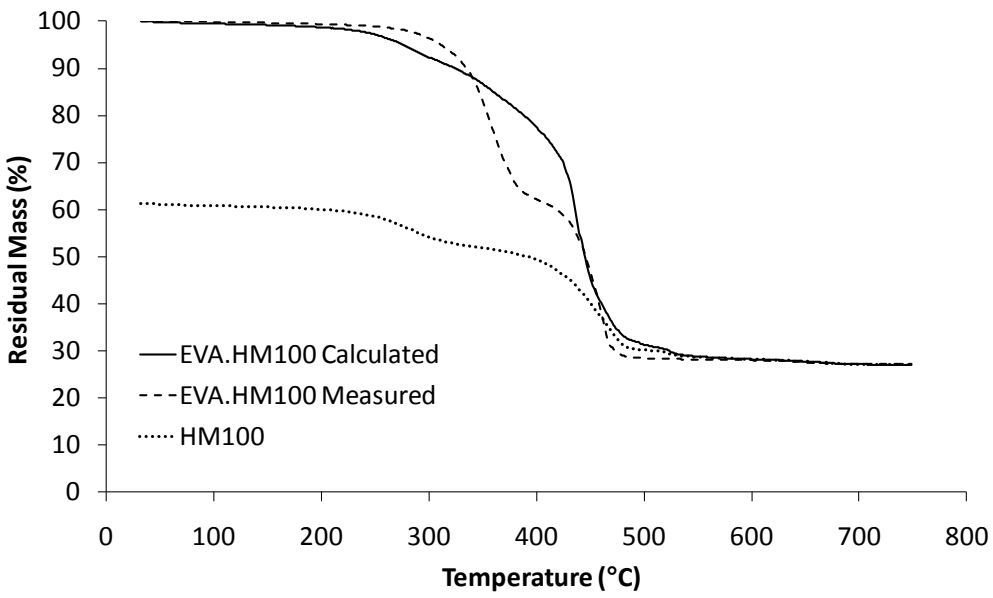


**Figure 73: Calculated and measured thermal decomposition by TGA of EVA compound (EVA.HM100) filled with hydromagnesite**

At about 340°C the calculated and measured mass loss profiles crossover showing that actual decomposition is faster at this stage than calculation would suggest. The work of McGarry *et. al.*[8] which discussed the formation of a carbonaceous skin layer on the surface of EVA compound helps to explain why the measured decomposition rate of the hydromagnesite filled compound switches from being lower than expected to

higher than expected at about 340°C. Up until 340°C the decomposition rate is lower than expected due to the entrapment of the water released from the hydromagnesite within the polymer matrix. At about 300°C the compound starts to lose mass as the polymers start to decompose and form the protective carbonaceous skin layer. At about 340°C it is likely that water release from the hydromagnesite begins to disrupt the protective layer formed following chain stripping of the decomposing EVA. This leads to an increased rate of decomposition compared to the calculated mass loss as the underlying polymer is exposed to the radiant heat and directly attacked by oxygen in the air.

The crossover point in the decomposition of ATH filled EVA (Figure 70) was measured at about 380°C. The fact that the temperatures are similar could indicate that this is the temperature required for the entrapped water vapour to generate enough pressure to break through the surface char layer disrupting its protective nature.

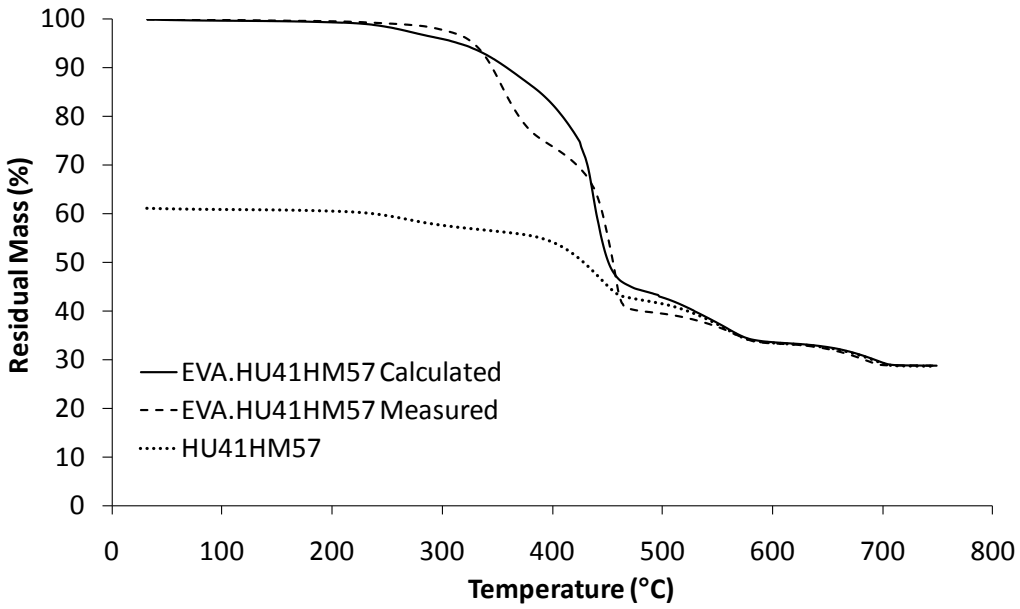


**Figure 74: Calculated and measured thermal decomposition by TGA of EVA compound (EVA.HU41HM57) filled with a mixture of huntite and hydromagnesite**

Figure 74 shows that a blend of huntite and hydromagnesite gives much the same performance compared to calculation as the pure hydromagnesite. However instead of

remaining at a constant mass at temperatures above 550°C the decomposition of the compound shows a further two stages of decomposition. The polymer has completely decomposed by about 500°C, therefore the calculated and measured mass loss profiles become very close above this temperature as all that remains to decompose is the huntite.

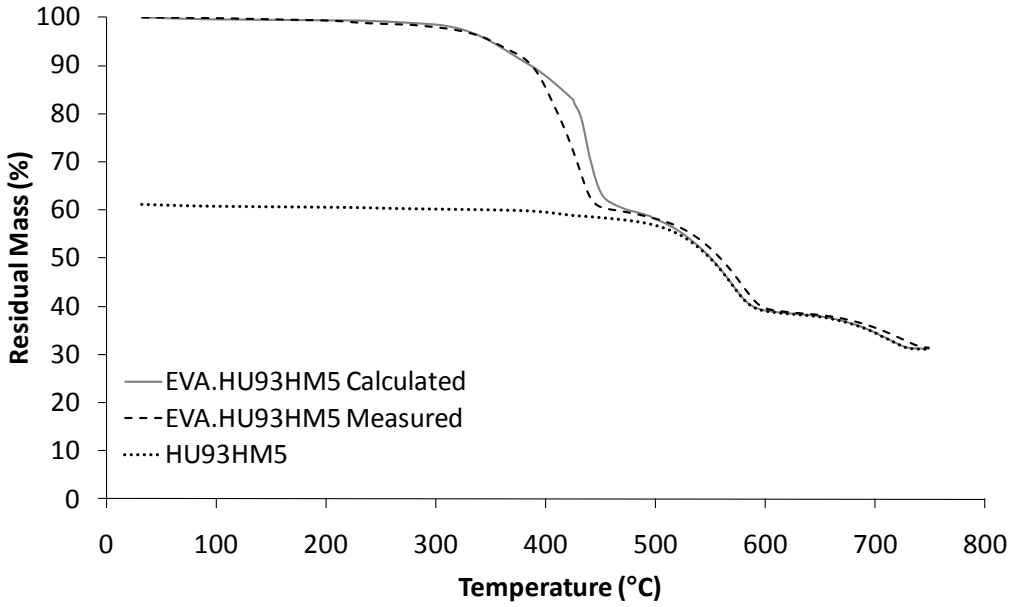


**Figure 75: Calculated and measured thermal decomposition by TGA of EVA compound (EVA.HU93HM5) filled with almost pure huntite**

Figure 75 shows that a very high proportion of huntite (93%) in the mixture with hydromagnesite gives a measured mass loss profile much closer to the calculated profile below 390°C than that of compounds containing hydromagnesite, ATH or chalk. There is no delayed mass loss due to water vapour entrapment since the huntite does not begin to decompose until about 450°C. Also, the huntite does not cause early mass loss on the same scale as the calcium carbonate filled compound (Figure 69). At about 390°C the rate of decomposition does become higher than predicted by calculation. This may be due to the small amount of hydromagnesite present giving off carbon dioxide and disrupting the surface carbonaceous skin, or it could be due to the high

loading level of huntite having an effect on the integrity of the char layer or perhaps catalysing char oxidation.

The compound shows a mass loss leaving about 60% of the original mass at about 470°C followed by a further two mass losses at higher temperature corresponding to the decomposition of huntite. This indicates that most of the polymer has probably decomposed before the huntite starts to have any active fire retardant effect through endothermic release of carbon dioxide. This is a criticism that has been made of huntite by other researchers[121,122,133] and lead to an assumption that huntite is nothing more than a diluent filler. This point will be discussed in more detail as the work presented in this thesis shows that huntite plays a very important role in fire retardancy where blends of huntite and hydromagnesite are used.

Figure 76 compares how huntite, hydromagnesite, ATH, MDH and calcium carbonate affect the decomposition of an EVA compound. Since the decomposition of calcium carbonate does not occur in the same temperature range as the decomposition of the polymers this compound can used as a reference point for comparing the effects of the other additives.

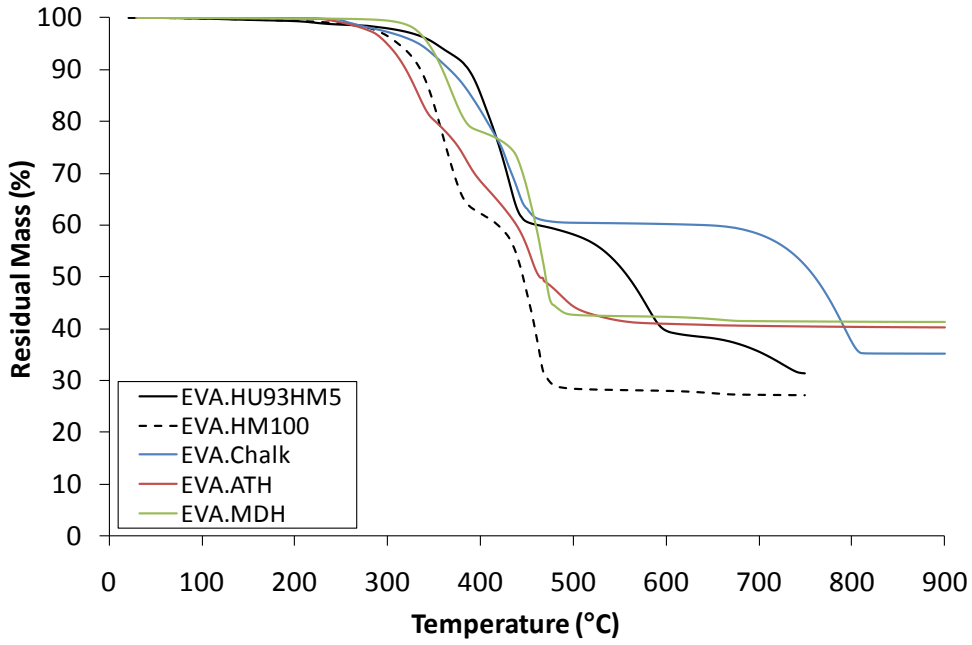


**Figure 76: Thermal decomposition by TGA of EVA compounds filled with huntite, hydromagnesite, ATH, MDH, and calcium carbonate**

ATH has the effect of reducing the temperature at which the compound begins to lose mass compared to the calcium carbonate filled compound. The earlier mass loss is likely to be caused by the decomposition of the ATH which begins to evolve water at about 180 - 200°C, much below the temperature at which the polymer begin to lose mass. This effect is also seen in the compound containing pure hydromagnesite, the water loss from the mineral contributes to compound losing mass at a lower temperature compared to the chalk filled compound.

The magnesium hydroxide increases the temperature at which the initial mass loss is measured as compared to the chalk filled sample. Magnesium hydroxide begins to decompose at about 330°C, corresponding closely with the temperature at which the polymers begin to lose mass. The close correspondence between the temperature at which endothermic decomposition of the magnesium hydroxide initiates and the temperature at which the polymers begin to lose mass means that the rate of polymer decomposition is reduced compared to the sample filled with inert calcium carbonate.

It is interesting to note that the sample containing a high proportion of huntite has the effect of increasing the temperature at which initial mass loss is observed compared to the sample containing calcium carbonate. This shows that the huntite is having an effect not seen in compound filled with calcium carbonate. As seen in Figure 41 in section 4.1, huntite particles have a plate like structure. It is possible that alignment of these particles is slowing the rate of volatilisation of the decomposing polymer chains. This is an idea that will be discussed in more detail in later sections.

## 5.2 Flammability studies using the cone calorimeter and limiting oxygen index

### 5.2.1 Effect of mineral ratios on oxygen index

The effect of the ratio of the two minerals, huntite and hydromagnesite, on limiting oxygen index has been studied. Kirschbaum reported[122] that increasing the proportion of hydromagnesite in a mixture of huntite and hydromagnesite from 0% up to 40% of the total by mass increases the oxygen index of the polymer compound in which the mixture is used. He also reported that increasing the proportion of hydromagnesite any further has no further significant benefit in terms of increased oxygen index. Table 6 shows the results of oxygen index testing on compounds made to the formulation shown in Table 5 these results follow almost exactly the trend described by Kirschbaum. There is only a small increase in the oxygen index as the proportion of hydromagnesite in the mixture is increased from 50 – 100%, but there is a much more significant effect as the hydromagnesite proportion is increased from 5 to 50%.

| Sample | Oxygen Index |
|---|---|
| HU93HM5 | 24.5 |
| HU43HM50 | 28.0 |
| HU41HM57 | 29.0 |
| HU24HM67 | 29.5 |
| HM100 | 29.5 |
| ATH | 30.0 |

Table 6: Effect of huntite/hydromagnesite ratio on limiting oxygen index

The fact that the oxygen index value of an ATH filled compound (Table 6) is very similar to that the compounds filled with mixtures of huntite and hydromagnesite (with hydromagnesite content greater than 50%) suggests that huntite must be having some fire retardant effect. If huntite has no active fire retardant effect (as suggested by some authors[121,122,133]) then hydromagnesite must be almost twice as effective as

ATH. The EVA compound containing HU43HM50 contains only half the quantity of hydromagnesite as there is ATH in the ATH filled compound but the LOI value is only 2 percentage points lower. Clearly hydromagnesite is no more effective than ATH because the compound containing HM100 has an LOI of 29.5% as compared to 30.0% for the ATH filled compound. Therefore, the huntite portion of the mixture of huntite and hydromagnesite must be providing some kind of fire retardant action that has not been previously identified.

### 5.2.2 Consideration of errors in heat release measured in the cone calorimeter

In order to study the effectiveness of both huntite and hydromagnesite, and to try and answer the question of what part huntite plays in fire retardancy, cone calorimetry has been used. However, before discussing the results from the cone calorimeter in detail it is worth considering how the cone calorimeter measures heat release and how endothermically decomposing additives may introduce errors into these results.

The oxygen consumption principle is used to calculate heat release from measurements made using the cone calorimeter[34]. This principle uses the value of 13.1 $kJg^{-1}$[35] as an average for the heat released per kilogram of oxygen consumed. Using the oxygen consumption principle means that heat release values from cone calorimeter measurements are not direct measurements of heat, but calculations of the theoretical amount heat released based on oxygen consumption. No account is taken in these calculations of whether the heat is released into the environment or absorbed by other processes such as the endothermic decomposition of a mineral filler such as hydromagnesite. It has been shown[158] that estimates can be made for the size of these errors using the heat of combustion of the polymer and the decomposition enthalpy of the minerals. The following discussion is focussed only on the endothermic processes occurring during the decomposition of a mineral filler.

An estimate of the heat of combustion of a composite containing an endothermically decomposing mineral can be calculated using the following equation:

$$\Delta H_{composite} = \Delta H_{filler} W_{filler}\% + \Delta H_{c,polymer} W_{polymer}\%$$

Where $\Delta H_{filler}$ is the decomposition enthalpy of the mineral filler, $\Delta H_{c,polymer}$ is the heat of combustion of the polymer and $W_{filler}\%$ and $W_{polymer}\%$ are the weight fractions of the filler and polymer in the composite.

Using the estimated heat release for the composite and comparing this with the heat release from the polymer weight fraction alone a value for the error in heat release ($\Delta$HR%) using the oxygen consumption principle can be calculated using the following equation:

$$\Delta HR\% = \frac{\Delta H_{c,polymer} W_{polymer}\% - \Delta H_{composite}}{\Delta H_{c,polymer} W_{polymer}\%} \text{ x } 100$$

These equations have been used to estimate the error in heat release reported from the cone calorimeter for increasing loading levels of aluminium hydroxide, magnesium hydroxide, huntite, and hydromagnesite (Table 7).

| Mineral Wt% | 0 | 25 | 50 | 60 | 70 | 80 | 90 | 95 | 100 |
|---|---|---|---|---|---|---|---|---|---|
| ΔH, $Al(OH)_3$ - (ATH) | 0 | 0.325 | 0.65 | 0.78 | 0.91 | 1.04 | 1.17 | 1.235 | 1.3 |
| ΔH, $Mg(OH)_2$ - (MDH) | 0 | 0.3625 | 0.725 | 0.87 | 1.015 | 1.16 | 1.305 | 1.3775 | 1.45 |
| ΔH, $Mg_3Ca(CO_3)_4$ - (Huntite) | 0 | 0.2475 | 0.495 | 0.594 | 0.693 | 0.792 | 0.891 | 0.9405 | 0.99 |
| ΔH, $Mg_5(CO_3)_4(OH)_2 \cdot 4H_2O$ - (Hydromagnesite) | 0 | 0.245 | 0.49 | 0.588 | 0.686 | 0.784 | 0.882 | 0.931 | 0.98 |
| ΔH, Polyethylene | -43.28 | -32.46 | -21.64 | -17.31 | -12.98 | -8.66 | -4.33 | -2.16 | |
| ΔH, Polyethylene + $Al(OH)_3$ | -43.28 | -32.14 | -20.99 | -16.53 | -12.07 | -7.62 | -3.16 | -0.93 | |
| ΔH, Polyethylene + $Mg(OH)_2$ | -43.28 | -32.10 | -20.92 | -16.44 | -11.97 | -7.50 | -3.02 | -0.79 | |
| ΔH, Polyethylene + $Mg_3Ca(CO_3)_4$ | -43.28 | -32.21 | -21.15 | -16.72 | -12.29 | -7.86 | -3.44 | -1.22 | |
| ΔH, Polyethylene + $Mg_5(CO_3)_4(OH)_2 \cdot 4H_2O$ | -43.28 | -32.22 | -21.15 | -16.72 | -12.30 | -7.87 | -3.45 | -1.23 | |
| ΔHR%, Polyethylene + $Al(OH)_3$ | 0.00 | 1.00 | 3.00 | 4.51 | 7.01 | 12.01 | 27.03 | 57.07 | |
| ΔHR%, Polyethylene + $Mg(OH)_2$ | 0.00 | 1.12 | 3.35 | 5.03 | 7.82 | 13.40 | 30.15 | 63.66 | |
| ΔHR%, Polyethylene + $Mg_3Ca(CO_3)_4$ | 0.00 | 0.76 | 2.29 | 3.43 | 5.34 | 9.15 | 20.59 | 43.46 | |
| ΔHR%, Polyethylene + $Mg_5(CO_3)_4(OH)_2 \cdot 4H_2O$ | 0.00 | 0.75 | 2.26 | 3.40 | 5.28 | 9.06 | 20.38 | 43.02 | |

**Table 7: Estimated error in heat release rates measured using oxygen consumption methods due to endothermic decomposition of mineral fillers**

It can be seen that as the loading level of the filler increases the error in heat release measured by oxygen consumption ($\Delta HR\%$) increases exponentially. For mineral filler fire retardant applications a loading level of 50 – 65% is common. Higher loading levels are used but this can be detrimental to the mechanical properties and processability of the composite. Therefore the error that can be expected in a typical fire retarded

polymer formulation containing a mineral fire retardant is in the region of 2.5 – 5%. If it is known that the mineral filler has totally decomposed, a correction to the total heat of combustion calculated from cone calorimeter measurements may be justified.

These calculations have been taken further[158] to give the following equation as a proposal for modifying the rate of heat release data generated during cone calorimetry.

$$HRR = MLR\left[EHC - \Delta H_{filler}\left(\frac{W_{filler}}{W_{polymer} + W_{filler}\chi_{H_2O}}\right)\right]$$

Where MLR and EHC are the mass loss rate and the effective heat of combustion of the composite measured during combustion on a cone calorimeter. $\chi_{H2O}$ is a term for the mass fraction of water produced when 1 mol of ATH or MDH decomposes to release *n* mol of water.

$$\chi_{H_2O} = \frac{nM_{H_2O}}{M_{filler}}$$

It takes into account that part of the mass loss measured during combustion in the cone calorimeter is due to water loss from the filler not combustion of the polymer.

It has been suggested[158] that this equation should be used to correct the rate of heat release against time graphs that are often used to present the data from cone calorimeter testing. One obvious assumption that has been used is that the mass loss rate and decomposition enthalpy of the filler remains constant during the entire period of composite combustion. Clearly this is not the case in reality. ATH for example is likely to have a much greater effect on heat release in the early stages of the fire due to its low decomposition temperature. Huntite that has a higher decomposition temperature is likely to have a greater effect later in the fire when higher temperatures are reached. A mixture of huntite and hydromagnesite with its several stages of decomposition over a wide temperature range will have varying effects as the fire progresses.

While it is acknowledged that measurements of heat release using the oxygen consumption method are subject to error due to the use of endothermically

decomposing fillers it is thought that this method cannot accurately compensate for the changing contribution of the filler during the fire and especially cannot compensate for the multistage decomposition of a mixture of minerals such as huntite and hydromagnesite. It may be valid when applied to the total heat release if it is known that complete decomposition of the filler has occurred, but at the loading levels that are typically used (60%) the error is approximately 3 – 5% in polyethylene and depending on the filler used. For these reasons no attempt will be made to correct cone calorimeter data in the current work. Its value is in refining the value of heat release rate to compensate for the systematic error associated with the use of oxygen depletion calorimetry for mineral filler fire retardants. These differences may be more apparent when trying to correlate mineral filler and non-mineral filler fire retarded polymer behaviour in real fires, or in standard tests which do not use oxygen depletion calorimetry to calculate heat release.

### 5.2.3 Effect of mineral ratios on combustion in the cone calorimeter

Averages of three repeats on the cone calorimeter (at a heat flux of 50 $kWm^{-2}$) of EVA compounds based on the formulation shown in Table 5 are shown in Figure 77. This shows how the ratio of huntite to hydromagnesite affects the burning characteristics. The heat release rate curves are characteristic of a char or residue forming material. When a char forms it slows the combustion of the underlying polymer leading to a heat release rate that slows as the fire progresses.

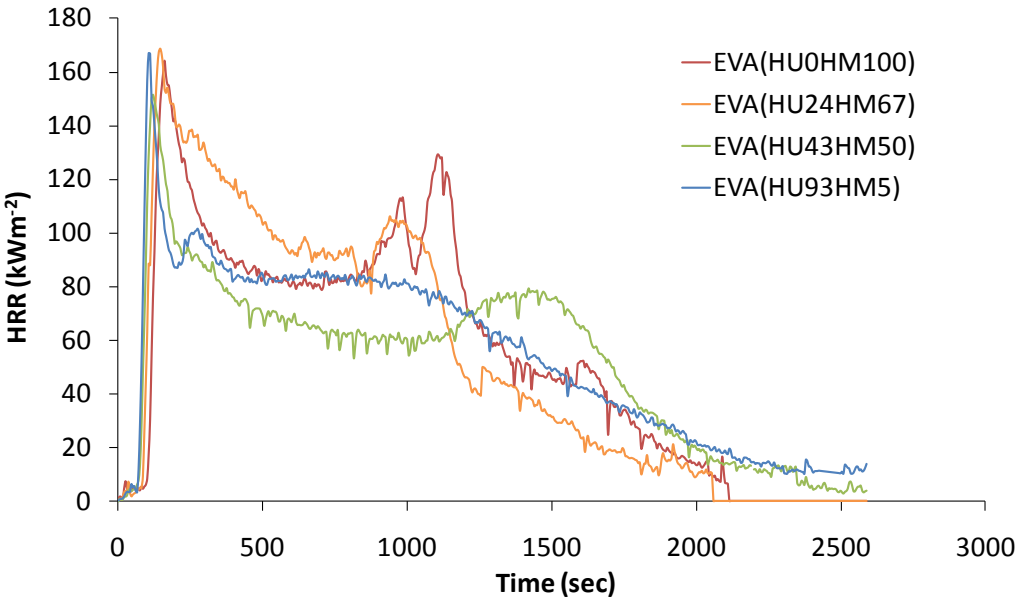


Figure 77: Effect of huntite:hydromagnesite ratio on the rate of heat release

Each sample shown in Figure 77 gives an initial peak in rate of heat release on ignition, believed to result from the ignition of acetic acid, followed by a declining rate of heat release dependant on the ratio of huntite to hydromagnesite. The initial peak is caused when the build up of combustible volatiles above the decomposing sample ignites. This excess of volatiles quickly burns off and the heat release rate becomes steadier as decomposition of the polymer feeds a constant rate of fuel to the flame. In each case a second peak is also observed prior to the final decline in heat release and extinction of the flame. The second peak is decreased in magnitude as the ratio of huntite in the mixture is increased. Increasing the huntite ratio also has the effect of increasing the time taken to reach the second peak due to the slower burning of the sample. The

sample containing almost pure huntite showed a much less distinct second peak although it did occur at an earlier time, breaking the trend for increased time to reach the second peak with increasing huntite content. It was also observed that a higher hydromagnesite content produced a much less stable residue that had a tendency to move and collapse in the later stages of burning. This movement and collapse of the residue is linked to the second peak in heat release rate. As the residue collapses it exposes flammable material trapped beneath the residue causing the rate of heat release to increase. Compounds containing a higher proportion of huntite formed a more stable and stronger residue, this means there was no sudden heat release as the structure collapses, simply a steady release of volatiles through gaps between the particles that form the residue. Therefore huntite is providing physical reinforcement of the residue in the later stages of the fire that is contributing to the fire retardant effect of this mixture of minerals. These differences in the residue, its structure and formation, will be analysed in detail in section 5.2.5.

A comparison of the rates of heat release of EVA compounds filled with a blend of huntite and hydromagnesite with ATH, magnesium hydroxide and chalk is shown in Figure 78.

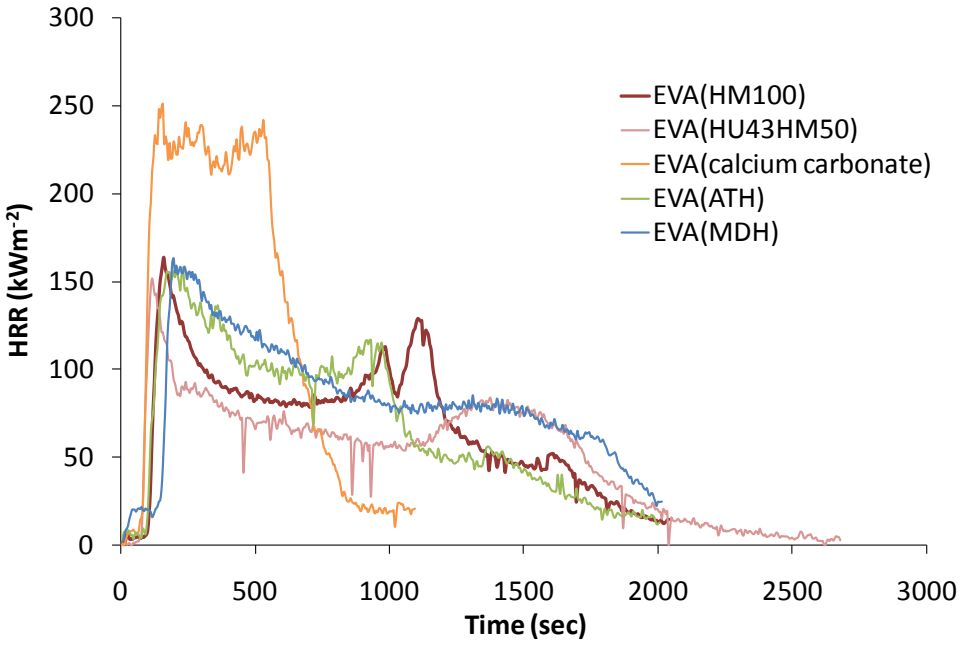


**Figure 78: Comparison of the effect of ATH, MDH, Chalk and a mixture of huntite and hydromagnesite on the rate of heat release**

Clearly the chalk filled compound has a high rate of heat release and a short burning time as would be expected for a compound containing no active fire retardant materials. Replacement of the chalk with ATH, MDH, hydromagnesite or the blend of huntite and hydromagnesite reduced the rate of heat release over the entire burning period. The hydromagnesite filled compound behaves in a very similar manner to the ATH filled compound, both show an initial peak in rate of heat release followed by a second fairly sharp peak associated with movement and collapse of the residue. The compound filled with a blend of huntite and hydromagnesite has a lower rate of heat release than the ATH or hydromagnesite filled compounds for most of the burning time showing that the fact that almost half of the hydromagnesite has been replace by huntite is beneficial. As discussed above, use of a mixture of huntite and hydromagnesite leads to a stronger more stable char which did not collapse towards the end of the test period and gave a longer slower burn.

The heat release characteristics of the magnesium hydroxide filled compound were quite different to the ATH or hydromagnesite filled compounds. The compound shows a much slower reduction in rate of heat release following the initial peak. It was quite clear that the mechanism of formation of the residue from this compound was different to that of the ATH and hydromagnesite filled compounds. This will be discussed in detail in section 5.3.

Table 8 summarises the data from the cone calorimeter at an applied heat flux of 50 $kWm^{-2}$. It shows the effect of the ratio of huntite and hydromagnesite on fire retardant properties in comparison to ATH, MDH and chalk.

| Sample Reference | Time to ignition | Peak HRR | Average HRR | Time to flame out |
|---|---|---|---|---|
| | (sec) | ($kWm^{-2}$) | ($kWm^{-2}$) | (sec) |
| | | | | |
| HM100 | 101 | 168 | 89 | 1883 |
| HU24HM67 | 93 | 162 | 73 | 1702 |
| HU41HM57 | 88 | 168 | 71 | 2175 |
| HU43HM50 | 81 | 154 | 56 | 2253 |
| HU93HM5 | 78 | 174 | 67 | 2359 |
| | | | | |
| ATH | 98 | 169 | 84 | 2007 |
| MDH | 125 | 163 | 88 | 1931 |
| Chalk | 81 | 256 | 133 | 1067 |

**Table 8: Summary of cone calorimeter results**

There is a trend of increasing time to ignition with increasing hydromagnesite content. This is probably due to the endothermic decomposition of hydromagnesite near the surface of the sample in the early stages of the test. As the heat flux is applied to the sample the first reaction of hydromagnesite is to endothermically release water vapour. This will delay the ignition time by reducing the heat energy absorbed by the polymer and therefore reducing the rate of emission of flammable decomposition products. Once the water vapour breaks through the surface of the polymer it also has the effect of diluting the gas phase with water vapour increasing the amount of time needed for these vapours to reach the concentration required for combustion to occur. It was observed that bubbles formed near the surface a short time after the heat flux from the cone heater was applied to the sample. At this stage the bubbles did

not break the surface. This observation is consistent with the apparent increased temperature at which initial mass loss occurs when TGA mass loss profiles are compared with the mass loss profile calculated from the decomposition of the individual components, as discussed in section 5.1.2. The hydromagnesite decomposes but the bubbles become entrapped within the polymer matrix, therefore the mass loss in not recorded in a TGA test until the bubbles break the surface at a higher temperature. The bubbling effect was observed in all samples regardless of the huntite to hydromagnesite ratio. These bubbles are likely to be due to decomposition of hydromagnesite near the surface of the polymer and also the initial stages of decomposition of the polymer, releasing acetic acid. Following bubble formation a black skin formed on the surface of the sample. In each case the black skin broke immediately before or upon ignition of the sample. This is a very similar to the observation made by McGarry *et al*[8] that during the decomposition of EVA, in a TGA instrument or Purser furnace, a protective skin forms which then breaks down to allow combustion of the underlying material.

The time to ignition for the ATH filled compound is similar to the times measured for the samples containing higher proportions of hydromagnesite. This suggests that the mechanisms of ATH and hydromagnesite are similar, and that the endothermic release of water has an effect on increasing time to ignition.

The black skin layer appeared to be very coherent across the whole surface. The fact that it is so coherent is probably what leads to its break down. It traps water vapour and polymer decomposition products beneath it until it is no longer strong enough to withstand the pressure being exerted by these gases. At that point the skin splits releasing a high concentration of decomposition gases which immediately ignite. This also explains why the magnesium hydroxide filled compound has a longer time to ignition. Magnesium hydroxide releases its water at a higher temperature than ATH or hydromagnesite, therefore the skin layer will be disrupted at a higher temperature.

The chalk filled sample gave a time to ignition similar to that of the compounds containing higher levels of huntite. Since chalk does not decompose until about 600°C it can be considered inert during the initial stage of the fire. Its only function is as a

diluent reducing the amount of combustible polymer within the test piece. The similar time to ignition to the huntite filled sample suggests that during initial ignition the huntite, which begins to decompose at about 450°C, also acts only as a diluent filler.

The effect of the ratio of huntite to hydromagnesite shows a trend towards reducing peak HRR with increasing hydromagnesite content. The peak in heat release rate immediately follows ignition, as shown in Figure 77. It is caused when the build up of flammable gases above the sample ignites. These gases are likely to contain a high proportion of acetic acid from the initial decomposition of the EVA and water vapour from the hydromagnesite. Therefore the observation that higher proportions of hydromagnesite reduce the peak heat release rate is consistent with the idea that the endothermic release of water vapour from the hydromagnesite is the controlling factor in the initial stages of ignition and combustion. The ATH filled compound (Table 8) shows a similar peak HRR to the compounds containing higher hydromagnesite content; again this suggests the similar mechanism of ATH and hydromagnesite. The chalk filled compound (Table 8) shows a much higher peak HRR than any of the blends of huntite and hydromagnesite, including the compounds containing very high proportions of huntite. This shows that huntite is not simply acting as a diluent filler, there must be some action that is reducing peak heat release rate as compared to the chalk filled compound. It is also interesting to note that the average heat release rate over the duration of the test is reduced with increasing huntite content. Therefore the hydromagnesite portion of the blend is having the largest positive effect in the initial stages of ignition, but the huntite portion must be having an effect in the later stages, reducing the average heat release rate.

Huntite does not begin to thermally decompose until about 450°C, as discussed in section 5.1.1, this is above the temperature at which most of the polymer has decomposed and has lead some researchers[121,122,133] to conclude that huntite is simply an inert filler in terms of fire retardancy. However, given the fact that it appears to be having an effect on the average rate of heat release this notion needs reconsideration. In the cone calorimeter the test is carried out on horizontally mounted flat plaques of material subjected to a heat flux from above. Therefore any non combustible residue will remain in place. As the polymer compound burns and the

hydromagnesite decomposes, a layer of magnesium oxide and huntite will form. It has been shown[33] that a 50kWm$^{-2}$ heat flux from a cone calorimeter will raise the surface temperature of a ceramic plate, placed where the sample sits, to about 610°C. This temperature is well in excess of the initial decomposition temperature of huntite and therefore some decomposition of this mineral is expected. Even though all of the polymeric material may have decomposed in the upper layers of the sample, the endothermically decomposing huntite will still absorb heat and reduce heat transfer to the underlying polymer. The carbon dioxide released from this decomposition will also dilute the flammable volatiles feeding into the flame from the underlying polymer. This effect will work particularly well in the cone calorimeter due to the fixed radiant heat flux and the horizontal orientation of the samples. However, it is also likely to have an effect in real fire situations where the heat flux is high, either due to the flame above the material or other radiant heat within the area of the material.

Although the trend in both peak rate of heat release and average rate of heat release is related to the ratio of huntite and hydromagnesite, it appears that the optimum ratio for reduction of both measures of heat release rate is an approximately 50:50 mixture of the two minerals showing the importance of both minerals in controlling different stages of the fire.

The ATH filled sample again behaved quite similarly to the samples containing a high hydromagnesite content. The chalk filled sample gave the highest average HRR of all the samples tested, again confirming that the huntite proportion is having more than just a diluent effect on fire properties.

Flame out shows a trend of reducing with increased hydromagnesite content, and therefore increasing with huntite content. This is consistent with the effect that huntite has on reducing the average rate of heat release. As the material burns more slowly it takes longer to consume the same amount of fuel.

From these observations it seems clear that the hydromagnesite content has a role to play in the initial stages of the fire. It helps to increase time to ignition and time to peak heat release rate. However the huntite content has a positive effect in the later stages of the fire by reducing the average HRR over longer periods and extending the

time to extinction therefore meaning it is slowing the burning of the compound after ignition has taken place.

It was also noticed that the repeatability of the samples containing the mixtures of huntite and hydromagnesite (Figure 79) was much better than that of the samples containing ATH (Figure 80). This can be explained through the mechanism of burning. The samples containing huntite and hydromagnesite showed a consistent mechanism of residue formation and the residue remained intact during the test. When the ATH filled samples combusted, a residue layer formed which sometimes remained intact and sometimes broke and collapsed at apparently random times. This exposed the underlying polymer to the heat flux resulting in a peak in rate of heat release as the freshly exposed polymer ignited.

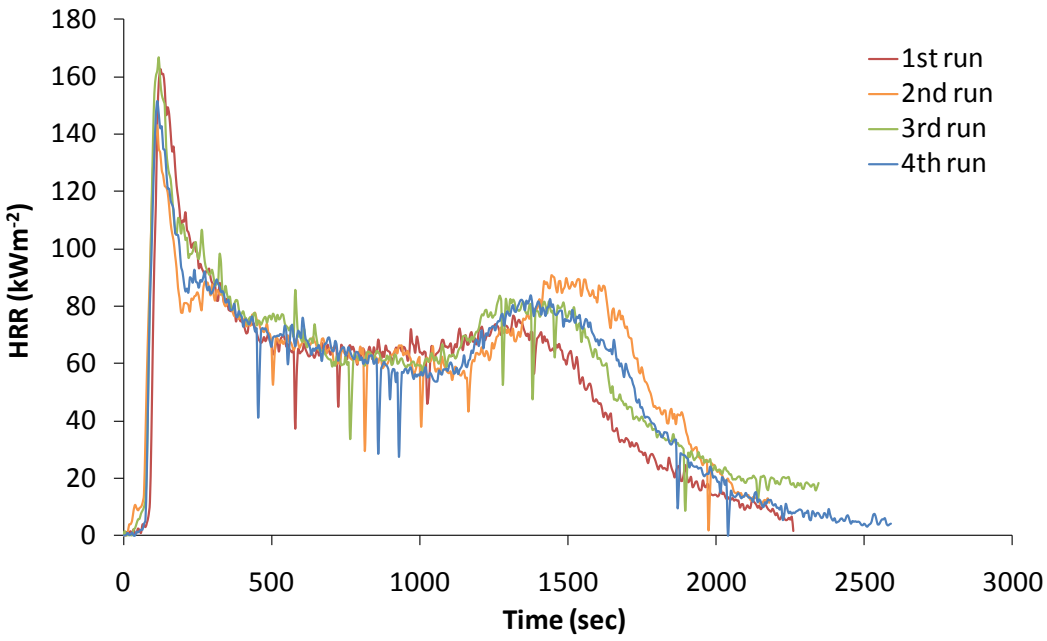


Figure 79: Repeatability of HRR measurements of EVA(HU43HM50)

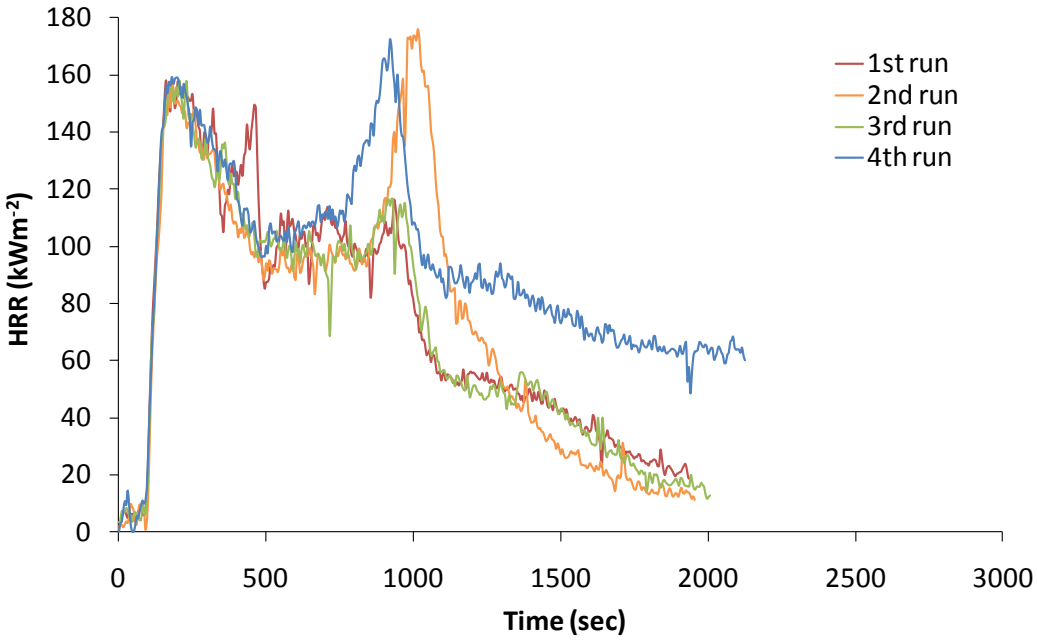


**Figure 80: Repeatability of HRR measurements of EVA(ATH)**

The trends discussed above can be summarised by plotting the fire growth rates (FIGRA) and average heat release rates against the ratio of huntite to hydromagnesite in the mixtures. FIGRA is a value calculated by dividing the peak rate of heat release by the time taken to reach the peak rate of heat release[32,33]. It therefore gives a measure of the speed at which the fire initially grows. Figure 81 shows how the FIGRA value indicates an increase in the fire growth rate as the ratio of hydromagnesite in the mixture with huntite is decreased. This supports the idea that endothermic release of water and carbon dioxide from hydromagnesite is important in the early stages of the fire. When the mixture contains 100% hydromagnesite the fire growth rate is similar to that of ATH, as hydromagnesite is increasingly replaced with huntite the fire growth rate increases to become closer to that of the chalk filled compound.

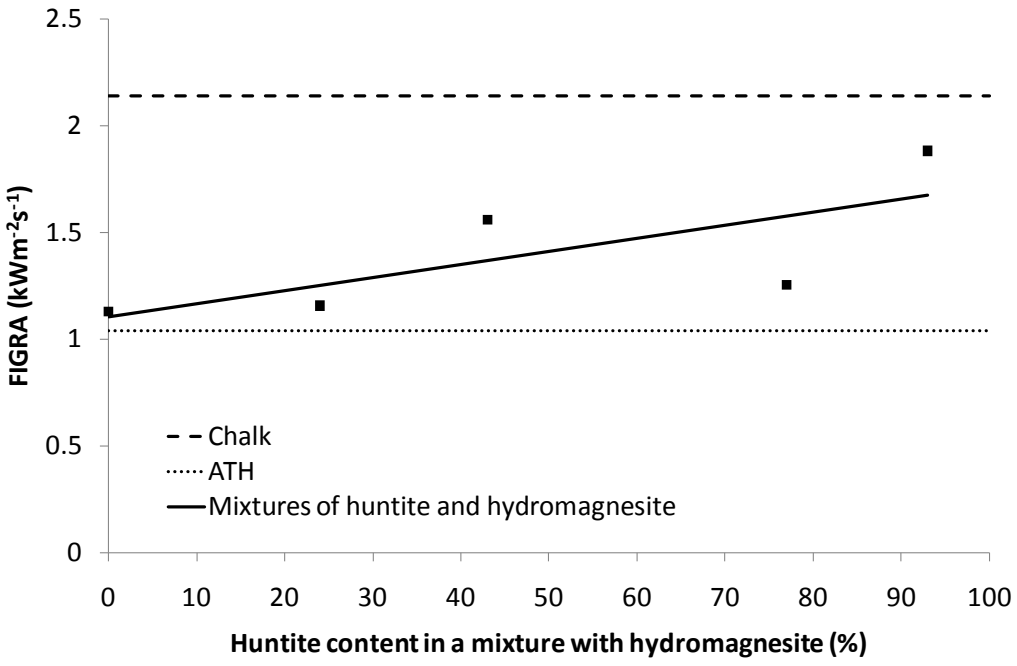


Figure 81: Effect of the ratio of huntite to hydromagnesite on FIGRA

Figure 82 also supports the idea that hydromagnesite is important in the early stages of the fire. It shows that as the hydromagnesite content of a mixture of huntite and hydromagnesite is reduced, the time to ignition reduces from being close to that of an ATH filled compound to being close to that of a chalk filled compound.

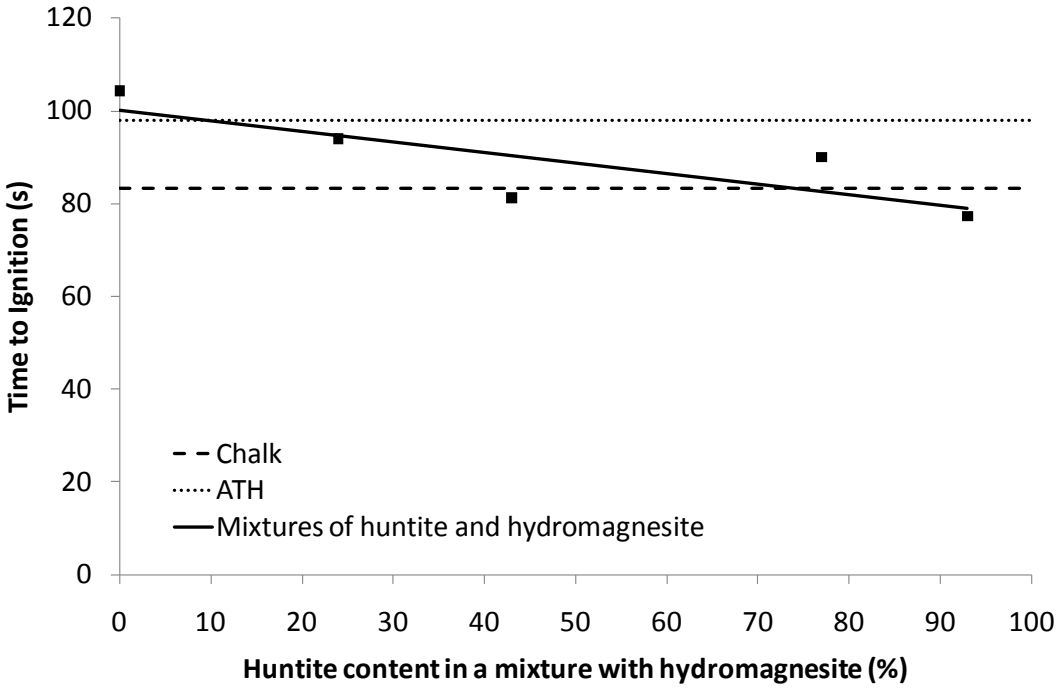


**Figure 82: Effect of the ratio of huntite to hydromagnesite on time to ignition**

Figure 83 shows how the average rate of heat release is reduced as the ratio of huntite in the mixture with hydromagnesite is increased. In the compound containing only hydromagnesite the average rate of heat release is similar to that of ATH, but as the ratio of huntite is increased the average rate of heat release decreases. Together with Figure 81 and Figure 82 this shows that hydromagnesite's main fire retardant action is in increasing the time to ignition and reducing the fire growth rate in the early stages of combustion, while huntite's main fire retardant action is in slowing the average rate of heat release over longer periods later in the fire.

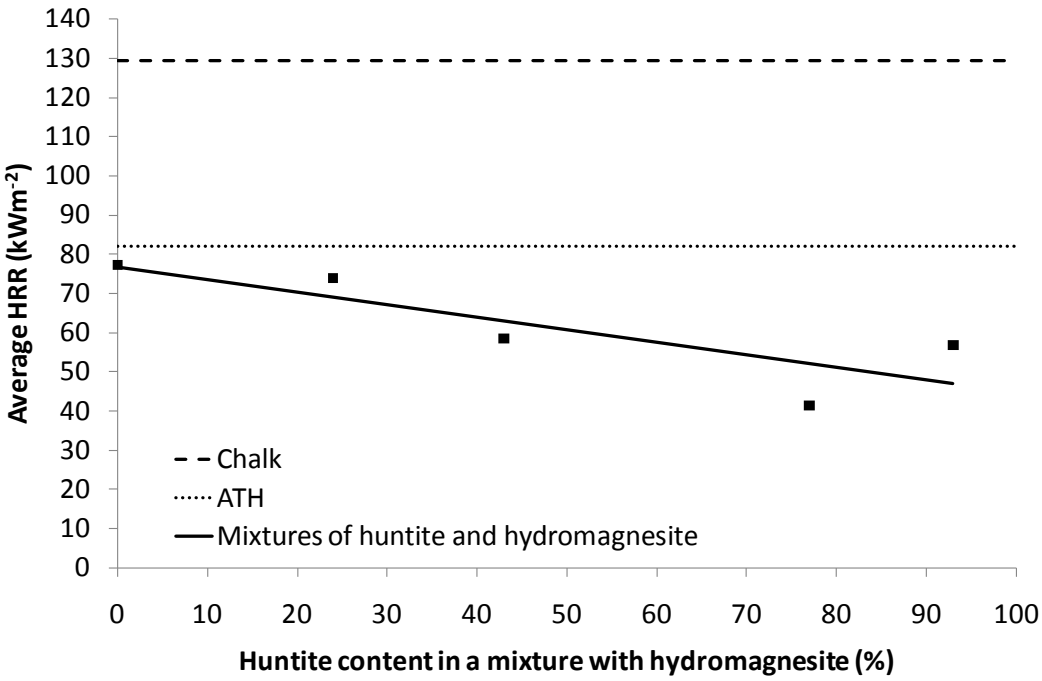


Figure 83: Effect of the ratio of huntite to hydromagnesite on average rate of heat release

The total heat release measured during combustion in the cone calorimeter is an indication of how completely the combustible content of the test material has burned. If a fire retardant causes the polymer to form a char a reduction in total heat release would be measured because less of the carbon content is oxidised. However, as can be seen in Figure 84 the total heat released during combustion of the samples containing mixtures of huntite and hydromagnesite did not vary significantly and was very close to that of the chalk filled compound. This means that the action of these mixtures is in slowing down the combustion of the polymeric material rather than preventing complete combustion or causing significant quantities of the polymer to form a char.

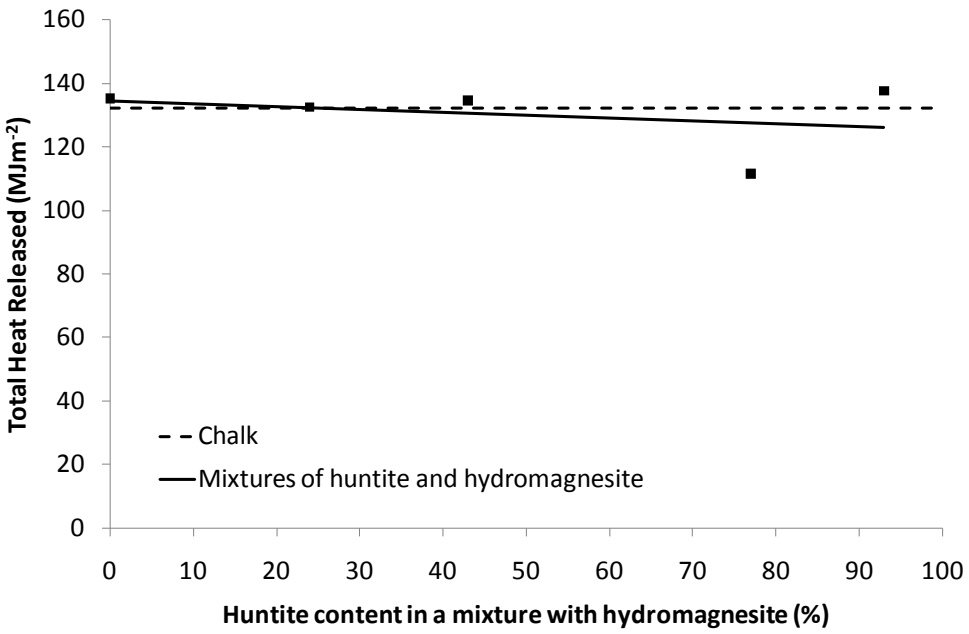


Figure 84:Effect of the ratio of huntite to hydromagnesite on total heat released

### 5.2.4 Effect of cone heat flux

Figure 85 - Figure 91 show how the radiant heat flux influences the rate of heat release. Unsurprisingly the time to ignition is increased as the heat flux is reduced making direct comparison of the heat release rate graphs more complicated. For this reason the rate of heat release is plotted against time since ignition, rather than time since the start of the test as in previous sections. However, the time to ignition is a very important factor and will affect the burning characteristics once ignition has occurred. If a material is exposed to the same heat flux for a longer period while it resists ignition (a good thing in fire retardancy terms) it will have absorbed more heat so the peak rate of heat release would be expected to be higher. In the following examples the longer time to ignition is caused by exposing the sample to a lower applied heat flux resulting a slower rate of polymer degradation, therefore the total heat energy absorbed at a longer ignition time is not necessarily greater. For these reasons the time to ignition for each sample is recorded in the legend of each graph so as not to lose the information.

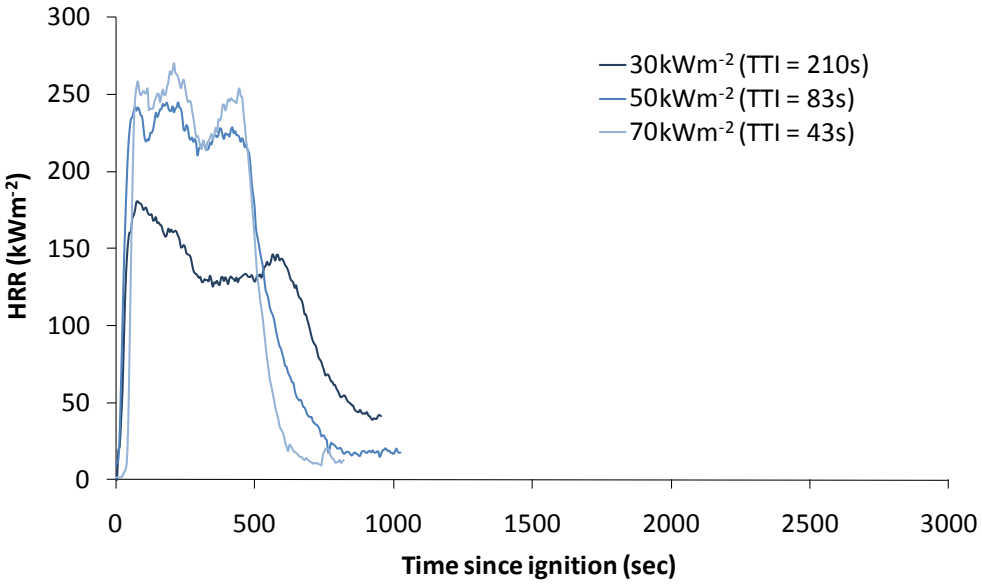


Figure 85: HRR at varying heat fluxes of EVA containing chalk

Figure 85 shows how the rate of heat release for a chalk filled compound is affected by the radiant heat flux. There is a large increase in rate of heat release as the heat flux is increased from 30 $kWm^{-2}$ up to 50 $kWm^{-2}$, however, there is less difference between the rates of heat release between 50 $kWm^{-2}$ and 70 $kWm^{-2}$. Chalk has no active fire

retardant properties; therefore, the increase in the rate of heat release between heat fluxes of 30 $kWm^{-2}$ and 50 $kWm^{-2}$ is entirely due to the increased rate of polymer decomposition induced by the increased radiant heat flux. The smaller increase in rate of heat release between the heat fluxes of 50 $kWm^{-2}$ and 70 $kWm^{-2}$ indicates that the rate of polymer decomposition is less affected despite the further increase in heat flux.

It is also very clear that the time to ignition is significantly affected by the applied heat flux. Reducing the heat flux from 70 $kWm^{-2}$ to 50 $kWm^{-2}$ almost doubles the time to ignition; however reducing the heat flux from 50 $kWm^{-2}$ to 30 $kWm^{-2}$ caused an increase of about 250% in the time to ignition. A lower heat flux will lead to a lower rate of decomposition of the polymer, increasing the time that it takes to reach the critical concentration of combustible gases. The slower decomposition also means that the gases have a longer time to diffuse, again adding to the time it takes to reach the critical concentration required for ignition. These two factors affect time to ignition; hence the relationship between heat flux and time to ignition will not be linear. This relationship is roughly constant for all of the fire retardant fillers examined, see Table 9. In each case reducing the applied heat flux from 70 $kWm^{-2}$ to 50 $kWm^{-2}$ roughly doubled the time to ignition while reducing the applied heat flux from 50 $kWm^{-2}$ to 30 $kWm^{-2}$ increased the time to ignition by about 250 – 300%. While the absolute values of time to ignition are affected by the type of fire retardant filler, these ratios do not appear to be closely linked to it.

| Sample | Increase in time to ignition between heat fluxes of 70 and 50 $kWm^{-2}$ | Increase in time to ignition between heat fluxes of 50 and 30 $kWm^{-2}$ |
|---|---|---|
| EVA.Chalk | 193% | 253% |
| EVA.ATH | 181% | 231% |
| EVA.HM100 | 219% | 287% |
| EVA.HU24HM67 | 213% | 264% |
| EVA.HU43HM50 | 203% | 270% |
| EVA.HU77HM18 | 225% | 252% |
| EVA.HU93HM5 | 179% | 306% |

Table 9: Effect of applied heat flux on time to ignition

The ATH filled sample (Figure 86) shows a sharpening and intensifying of the initial peak in rate of heat release with increasing heat flux. The greater heat flux will cause faster decomposition of the polymer, therefore a greater quantity of flammable volatiles are produced in a shorter period of time. This leads to a shorter time to ignition as the critical concentration of gases required for ignition is reached sooner. A higher heat flux will also cause the excess of flammable gases to combust more rapidly than they would at a lower heat flux; therefore the peak sharpens and intensifies.

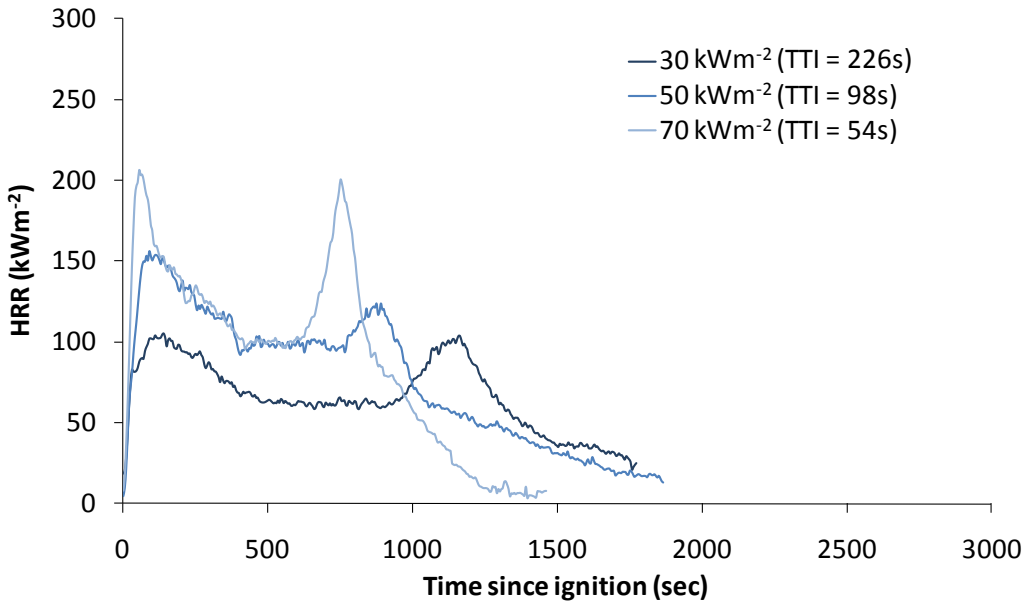


Figure 86: HRR at varying heat fluxes of EVA containing ATH

It is also very evident that the second peak in rate of heat release also intensifies and sharpens significantly with increasing heat flux. As discussed previously this second peak is associated with movement and collapse of the residue. At higher radiant heat fluxes the rate of polymer decomposition is higher and therefore a larger quantity of decomposition gases may become entrapped within the residue as they are not able to diffuse through the residue any more rapidly than at lower heat fluxes. Therefore when the gases are released by collapse of the structure there is a sudden sharp increase in the supply of fuel to the flame which causes a larger second peak in the rate of heat release. A similar effect can be seen in the samples containing huntite and hydromagnesite (Figure 87 - Figure 91) but the second peak is less sharp, particularly in

the compounds containing a higher proportion of huntite. The platy nature of huntite may well be stabilising the residue and slowing the diffusion of the gases to the flame.

The samples filled with mixtures of huntite and hydromagnesite (Figure 87 - Figure 91) show similar behaviour patterns to the ATH filled compounds. They show an increasing sharpness and intensity of the initial peak of heat release as the radiant heat flux is increased. The compounds filled with higher proportions of hydromagnesite (Figure 87 and Figure 88) have rates of heat release, at a heat flux of 50 $kWm^{-2}$, that are roughly half way between those measured at 30 $kWm^{-2}$ and 70 $kWm^{-2}$. As the proportion of huntite in the mixture approaches (Figure 89) and exceeds (Figure 90 & Figure 91) 50%, the rate of heat release at a heat flux of 50 $kWm^{-2}$ becomes close to that measured at 30 $kWm^{-2}$. The example of the chalk filled compound showed that where the filler provides no active fire retardant effect there is a large difference in rate of heat released between these two heat fluxes. The cone calorimeter has been shown[33] to heat the surface of a ceramic board to about 500°C, 610°C, and 700°C when heat fluxes of 30 $kWm^{-2}$, 50 $kWm^{-2}$ and 70 $kWm^{-2}$ are used. It has been shown in section 4.2 that huntite and hydromagnesite go through a series of decompositions commencing at about 220°C and completing at about 750°C. ATH decomposes over a temperature range of about 180°C - 350°C. Therefore a heat flux of 30 $kWm^{-2}$ is more than sufficient to ensure total decomposition of ATH, at higher heat fluxes the decomposition of the ATH will remain the same as at 30 $kWm^{-2}$. As hydromagnesite and huntite have stages of decomposition that occur at higher temperatures these will be activated sooner at the higher heat fluxes. The additional heat flux activates the higher temperature decompositions in the hydromagnesite and huntite which means that it actually becomes more efficient at higher heat fluxes and keeps the rates of heat release closer that which was measured at 30 $kWm^{-2}$.

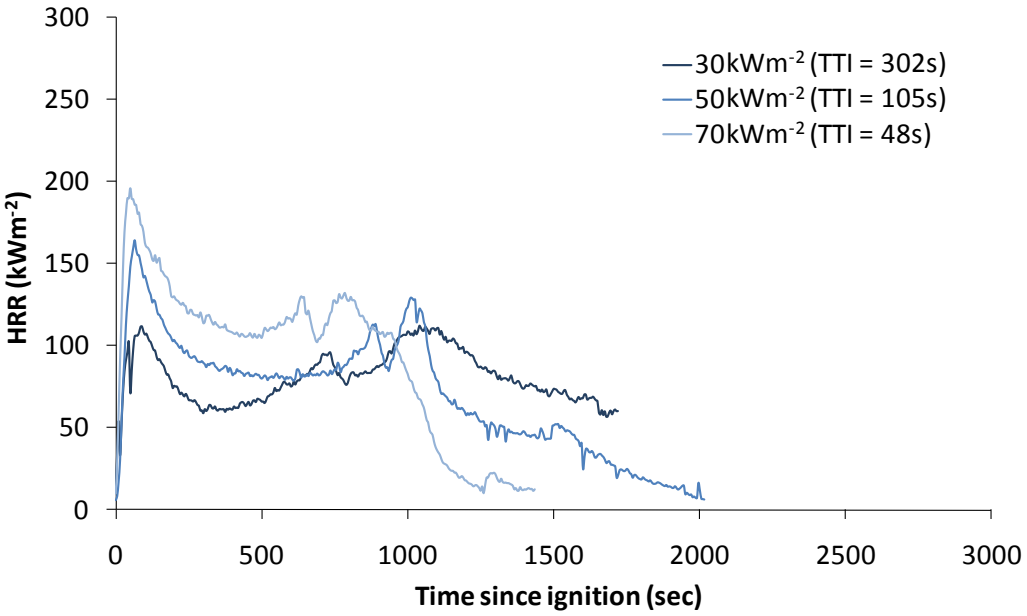


Figure 87: HRR at varying heat fluxes of EVA containing HM100

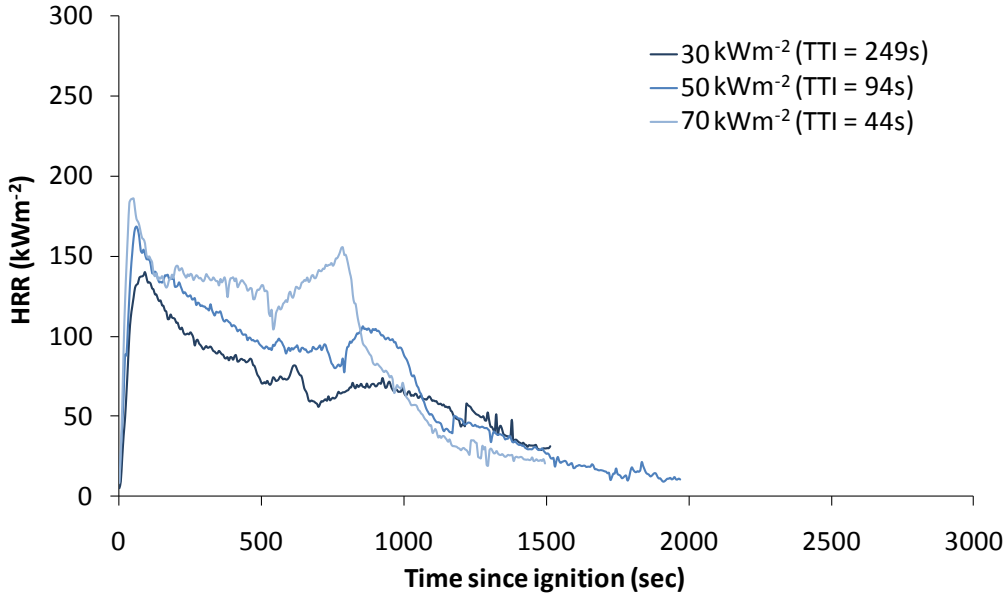


Figure 88: HRR at varying heat fluxes of EVA containing HU24HM67

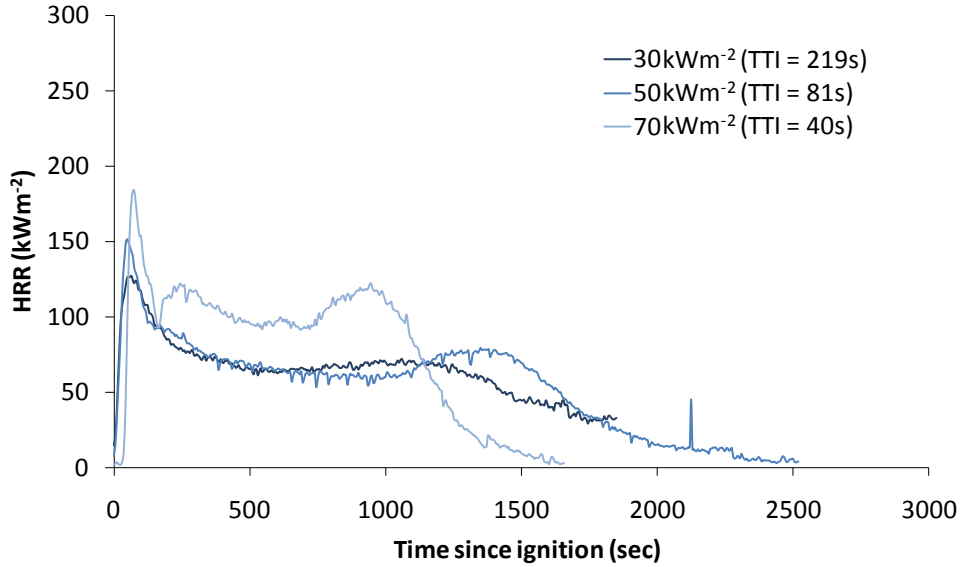


Figure 89: HRR at varying heat fluxes of EVA containing HU43HM50

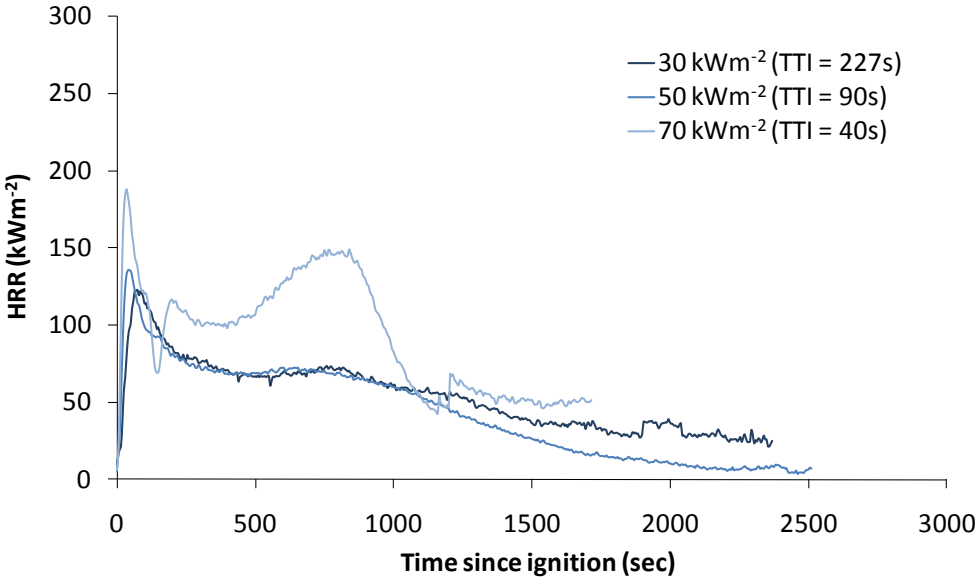


Figure 90: HRR at varying heat fluxes of EVA containing HU77HM18

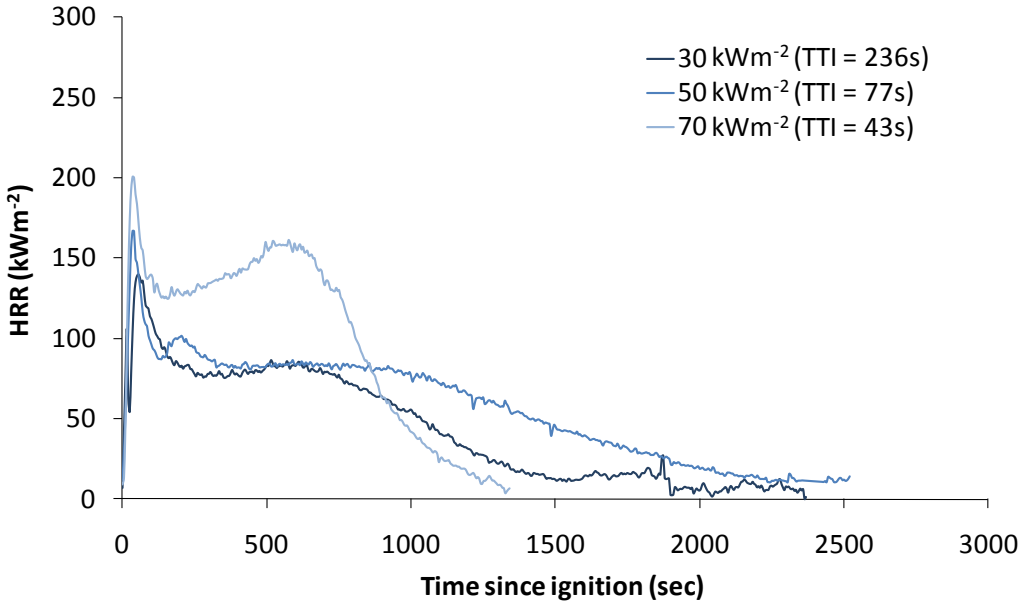


**Figure 91: HRR at varying heat fluxes of EVA containing HU93HM5**

Figure 92 shows the effect of the radiant heat flux on the FIGRA values for EVA containing mixtures of huntite and hydromagnesite in comparison to ATH and chalk. It is clear that there is a linear relationship between FIGRA and heat flux. Again this shows that hydromagnesite is most active during the initial stages of the fire (ignition and initial peak of heat release).

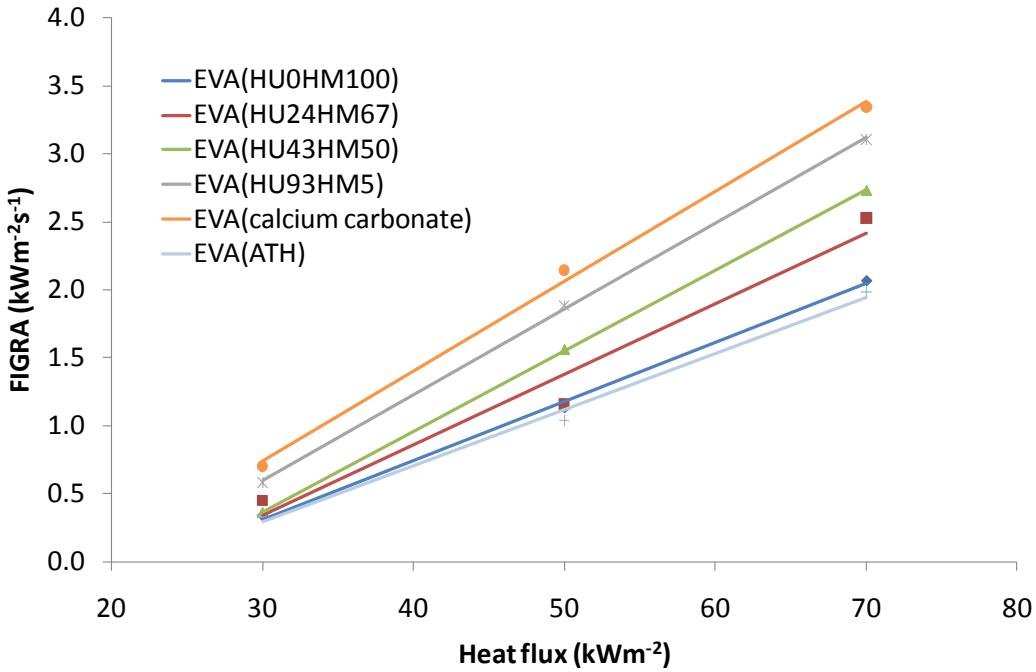


Figure 92: Effect of heat flux on FIGRA

The compounds containing the higher ratios of hydromagnesite gave lower FIGRA values because of their endothermic release of water during the initial decomposition of the polymer. Higher ratios of huntite increase the FIGRA value at each heat flux. There is no evidence that higher heat fluxes lead to early enough decomposition of the huntite to reduce the FIGRA value. If this had occurred a reduction in the gradient of the line between 50 $kWm^{-2}$ and 70 $kWm^{-2}$ would be expected.

Figure 93 shows the effect of the radiant heat flux on the average rate of heat release for EVA containing mixtures of huntite and hydromagnesite in comparison to ATH and chalk. The chalk filled compound shows a steady increase in average rate of heat release as the heat flux is increased, because the chalk offers no active fire retardancy any additional heat flux simply increases the rate of decomposition of the polymer and therefore increases the rate of heat release.

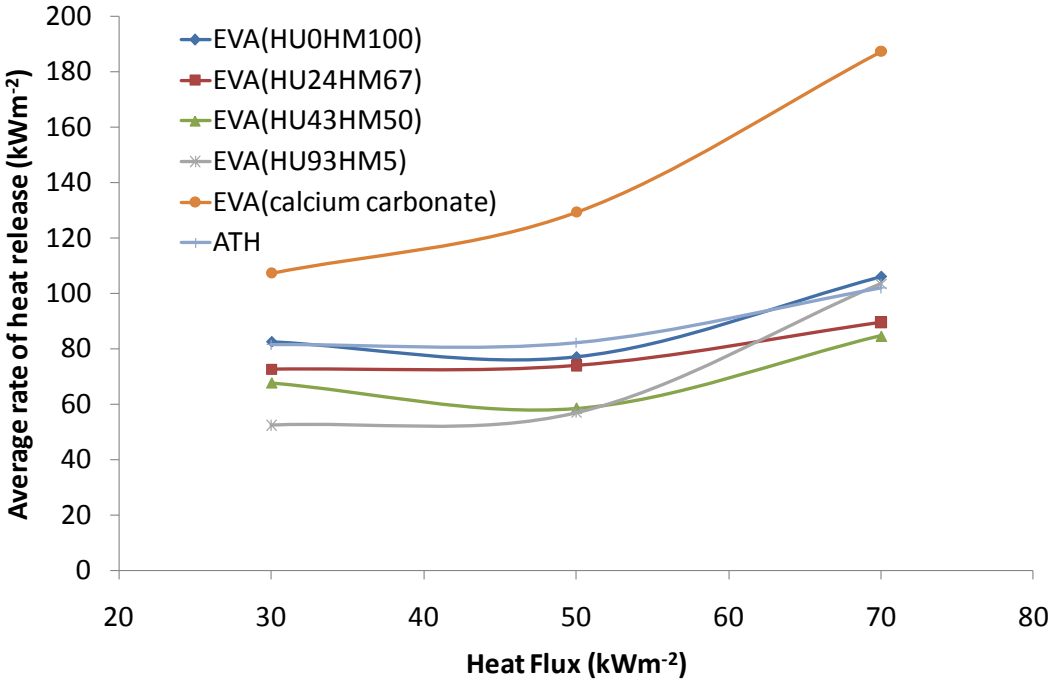


Figure 93: Effect of heat flux on average rate of heat release

In comparison the fire retardant fillers show less of an increase in average rate of heat release as the heat flux is increased. The ATH filled compound and the compound containing only hydromagnesite show very similar behaviour. The compounds containing higher ratios of huntite give progressively lower average rates of heat release, at heat fluxes of 30 $kWm^{-2}$ and 50 $kWm^{-2}$, as the huntite content increases. This is in agreement with the findings presented in section 5.2.3 where increasing proportions of huntite in a mixture with hydromagnesite were shown to reduce the heat release rate at the later stages of the fire. However, at a heat flux of 70 $kWm^{-2}$ the compounds containing higher proportions of huntite become progressively less efficient than expected compared to their performance at lower heat fluxes. The compound containing HU93HM5 had no advantage over ATH or HU0HM100. At lower

heat fluxes (30 $kWm^{-2}$ and 50 $kWm^{-2}$) the physical effects of the platy huntite particles reducing the rate of movement of combustible gases from the solid phase to the flame outweighs the fact that there is less hydromagnesite present to provide cooling and dilution of the flame in the early stages of the fire. Therefore, a lower average rate of heat release results with higher ratios of huntite. At a heat flux of 70 $kWm^{-2}$ the compounds containing higher ratios of huntite became less efficient at reducing the average rate of heat release. At this heat flux the physical action of the huntite alone is not sufficient to reduce the average rate of heat release more than the hydromagnesite.

### 5.2.5 Effect of particle size

Figure 94 shows how the rate of heat release is affected by the particle size of the mixture of huntite and hydromagnesite. The particle size information was supplied by the QA department at Minelco Ltd and was measured using a Malvern Mastersizer 2000. This instrument measures particle size using a laser diffraction technique. The mixtures of huntite and hydromagnesite with a $d_{50}$ particle size of 1.8 µm and 1.0 µm contain approx. 73% hydromagnesite and 20% huntite. The mixture with a $d_{50}$ particle size of 2.9 µm contains approximately 66% hydromagnesite and 22% huntite. The two smaller particle size samples were produced as a single production run on the factory grinding machinery, the larger particle size sample was produced at a separate time. Unfortunately because of the natural variation in the ratios of the minerals and the fact that the machinery's primary purpose is commercial production it was not possible to obtain three particle sizes with exactly the same blend of minerals. Therefore the largest particle size sample was used as the closest available match.

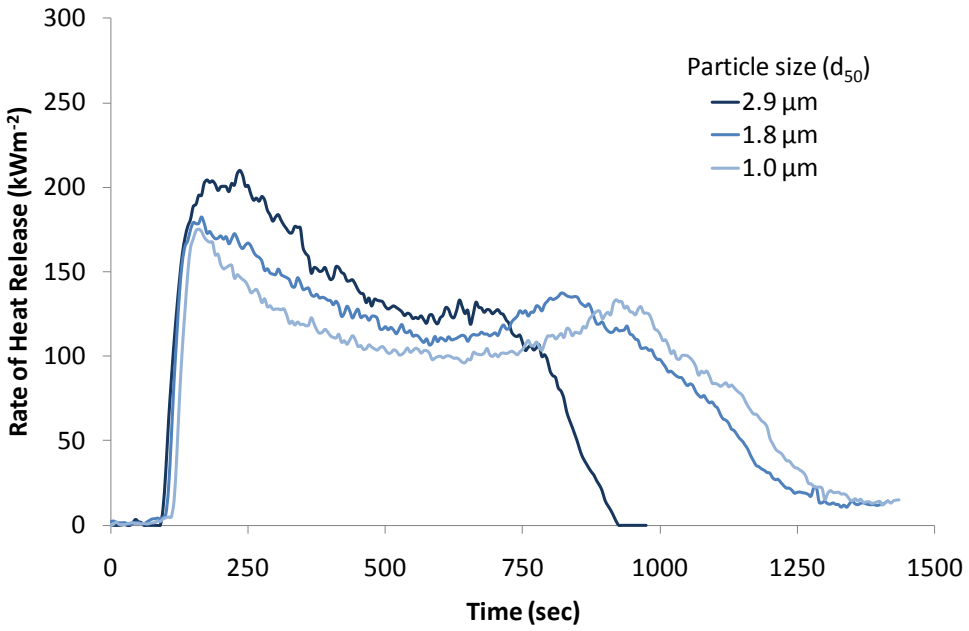


**Figure 94: Effect of particle size of mixture of huntite and hydromagnesite on rate of heat release of an EVA compound**

The effect of particle size is clear; as size is reduced the rate of heat release is also reduced. The smaller particles decompose slightly faster than the larger particles and this effect is large enough to reduce the rate of heat release. Figure 95 shows the thermal decomposition of the two compounds containing the two smaller particle sizes as measured by TGA. Also shown is the mass loss profile calculated by proportionally summing the mass loss profiles of the individual components. The reasons for the differences in the calculated and measured thermal decomposition profiles have already been discussed in detail in section 5.1.2.

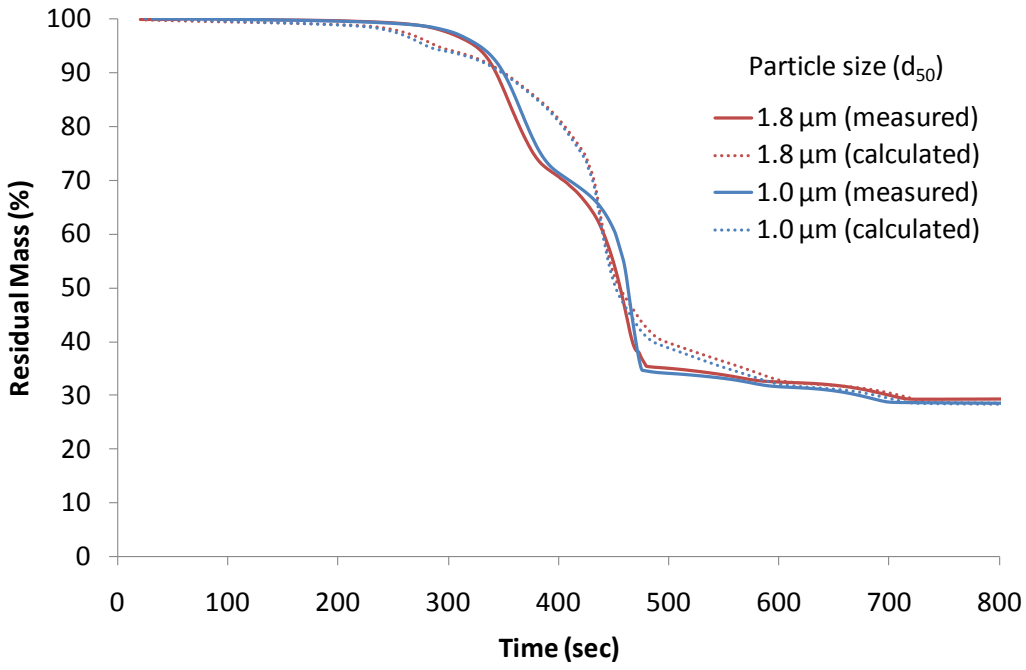


**Figure 95: Thermal decomposition by TGA of EVA compounds containing mixtures of huntite and hydromagnesite at two different particle sizes**

The calculated mass loss profiles show that the EVA compound containing the smaller particle size powder should begin to decompose slightly earlier than that of the compound containing the larger particle size powder. This is because when thermal decomposition of the finer powder begins earlier (see Figure 61). However the earlier decomposition of the mineral means that the endothermic release of water followed by carbon dioxide happens slightly earlier retarding the decomposition of the polymer and diluting the gas phase. The effect can be seen when comparing the measured thermal decomposition of the two compounds. The compound containing the finer powder shows a delayed mass loss at all temperatures compared to that of the

compound containing the coarser powder. The theoretical improvement in fire retardancy shown through measurements made using TGA correspond to the effects in reduction of rate of heat release as measured using the cone calorimeter (Figure 94).

## 5.3 Analysis of the ash residue from the cone calorimeter

So far the effects of huntite and hydromagnesite ratio, particle size and applied heat flux on the rate of heat release have been considered. In order to more fully explain some of the results that have been observed, particularly in relation to the part that huntite plays in fire retardancy, some analysis of the ash residue is necessary.

### 5.3.1 Visual and physical appearance

Visually the ash residue remaining after combustion of the polymeric components of the compounds was complete was very different depending on the huntite/hydromagnesite ratio.

Figure 96 shows the visual differences in the upper surfaces of the residue as the ratio of huntite and hydromagnesite is varied.

**EVA.HU93HM5** **EVA.HU43HM50**

**EVA.HU24HM67** **EVA.HM100**

**Figure 96: Ash from the cone test of samples containing blends of huntite and hydromagnesite**

The ratio of huntite to hydromagnesite is having several noticeable effects:

1. The colour of the ash. Higher hydromagnesite content leads to progressively greyer and eventually black residue indicating that there is more carbon present. Almost pure huntite gives a very white ash indicating that there is very little residual carbon.
2. All the samples clearly show inorganic remains of the skin formed by the decomposition of EVA[8,148] during the initial stages of combustion. This is particularly evident in the compounds containing higher huntite content.

3. The sample containing almost pure huntite shows very little breakage of the skin. Higher hydromagnesite content shows progressively more breakage of the skin and deeper 'cracks' within the sample corresponding to the breaks in the skin. This suggests that when the skin remains intact it provides protection to the material beneath. Where the skin breaks this protection is lost allowing faster degradation of the material below leading to the 'cracks' within the body of the sample.

Figure 97 shows cross sections through the inorganic residue taken from the cone calorimeter.

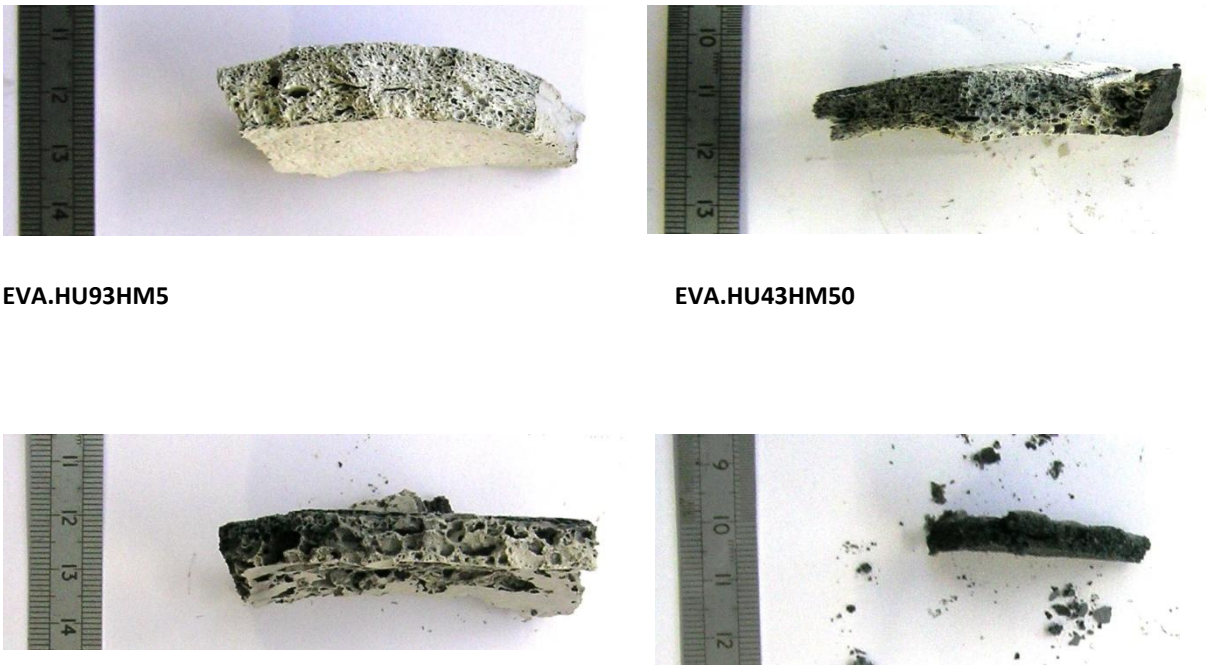

**EVA.HU93HM5** **EVA.HU43HM50**

**EVA.HU24HM67** **EVA.HM100**

**Figure 97: Section through ash of samples containing blends of huntite and hydromagnesite**

Again there are several observations that can be made:

1. The samples all contain bubbles. Higher huntite content samples contained a larger number of small bubbles, while the higher hydromagnesite content samples contained a smaller number of larger bubbles.
2. The colour differences seen on the surface of the residue samples is present throughout the thickness of the sample. Higher huntite gives a whiter residue, while higher hydromagnesite gives blacker residue.

3. Higher huntite content in the samples leads to a thicker residue. The original sample thickness was 6mm. It is therefore clear that the samples containing high levels of huntite have approximately doubled in thickness. The sample containing pure hydromagnesite does not appear to have increased in thickness at all.
4. The strength of the residue is very dependent on the huntite content. The sample containing the highest huntite content was strong enough to easily handle without breaking the residue. The sample containing the highest level of hydromagnesite was very weak. This sample could not be handled without the sample disintegrating.

The final observation that the residue became stronger as the huntite content was increased is something that is difficult to quantify. There are no standardised test methods for measuring the strength of the residue from the cone calorimeter and from experience there are no industry standards either. The response from several industrial contacts has been that the strength of the residue is something that is of interest but it usually assessed objectively in terms of whether particular samples "feel" stronger, or withstand the gentle poking of a finger more robustly than other samples. In many cases the residue from a cone calorimeter test is very weak and loses its integrity simply from the vibrations caused by removing the sample from the holder. In a crude attempt to put some numbers to the strength of the residues a series of samples were removed very carefully from the sample holder after combustion was completed and the residue had cooled. A circular plastic petri dish of 87mm diameter was placed centrally onto the residue and weights were manually added to the dish until the residue collapsed. The recorded weights to cause collapse of the ash are shown in Table 10.

| Ratio of huntite:hydromagnesite | Weight to cause collapse | Notes |
|---|---|---|
| 0:100 | 25g | Difficult to handle without breakage |
| 25:75 | 50g | Difficult to handle without breakage |
| 50:50 | 75g | Handleable with care |
| 75:25 | 140g | Easily handleable |
| Magnesium hydroxide | 25g | Difficult to handle without breakage |
| ATH | 30g | Difficult to handle without breakage |

**Table 10: Strength of residues from the cone calorimeter**

The HRR data, presented in section 5.2.2 suggested that the hydromagnesite had an effect in the initial stages of the fire, increasing time to ignition, and reducing the peak rate of heat release, while the huntite content appeared to reduce the rate of heat release in the later stages of combustion and extend the time of burning. It is now clear the huntite is promoting the formation of a thicker more stable residue which insulates and protects the underlying material more efficiently than the thinner weaker residue of the compounds that contain a higher proportion of hydromagnesite.

Figure 98 shows the ash residue from the compounds containing ATH, magnesium hydroxide and chalk. The reason for the inconsistencies in the HRR measurements of the ATH filled samples (shown in Figure 80) can be seen from these pictures. In some cases the ash residue remained intact throughout the period of combustion giving consistent repeatable results. However, sometimes the upper layer of ash residue was pushed upwards during the combustion collapsing back causing the measurements to be less consistent and repeatable.

**EVA.ATH (intact residue)**

**EVA.ATH (residue that collapsed during test)**

**EVA.MDH**

**EVA.Chalk**

**Figure 98: Residue from cone calorimeter test of samples containing ATH, magnesium hydroxide, and chalk**

The ATH filled samples produced a white residue with a smooth surface similar in colour and texture to the samples containing high levels of huntite. The magnesium hydroxide filled samples produced a very black residue with a cracked surface very similar in colour and texture to the samples containing high levels of hydromagnesite. The chalk filled sample also produced a white smooth residue.

When the residues of the ATH and magnesium hydroxide samples were handled it was immediately noticeable that they were not as strong as the samples containing huntite. The ash crumbled very easily, it was therefore not possible to produce pictures of the cross sections as was done with the previous samples in Figure 97. In order to get some idea of the internal structure of the ash pictures of the undersides of some larger pieces of the ash residue are shown in Figure 99.

**EVA.ATH** **EVA.MDH**

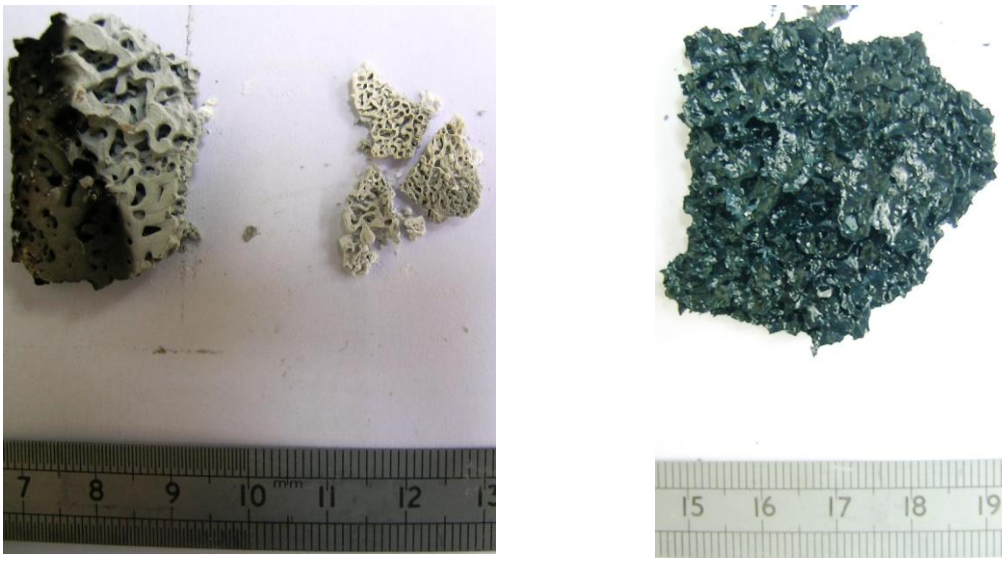


**Figure 99: Internal structure of the residue of samples containing ATH and magnesium hydroxide**

The structure of the residue of both the ATH and MDH filled samples was very different to the foamed structure of the huntite and hydromagnesite filled samples. The ATH filled sample consisted of two distinct layers, although the structure of the layer was very similar to the lower layer. The layers consisted of a network of 'tunnels' and 'pillars'. The upper layer was made of small 'tunnels' and 'pillars' and the lower layer was made up of larger 'tunnels' and 'pillars'. The whole structure was very fragile and immediately collapsed with handling.

The magnesium hydroxide filled sample had a completely different structure. It was not foamed structure, but appeared to consist of a network of ash and voids. The whole structure was very brittle.

The sample containing chalk produced a structure similar to that of the ATH filled sample, this is seen in Figure 100. The residue was slightly stronger than the residue from the ATH filled material but still weak, slightly robust handling quickly reduced the structure to a pile of chalk dust. It was however strong enough to handle carefully and examine the structure. The overall appearance of 'tunnels' and 'pillars' was remarkably similar to that of the ATH filled samples. Sections through the residue (Figure 100) show the visual appearance.

**Figure 100: Internal structure of the residue from samples containing chalk**

### 5.3.2 SEM analysis of the residue

Figure 101 - Figure 103 show low magnification electron microscope images of cross sections of the residues containing varying ratios of huntite and hydromagnesite. In each case it is clear that the bubbles formed during decomposition and combustion of the polymer have been preserved in the inorganic residue.

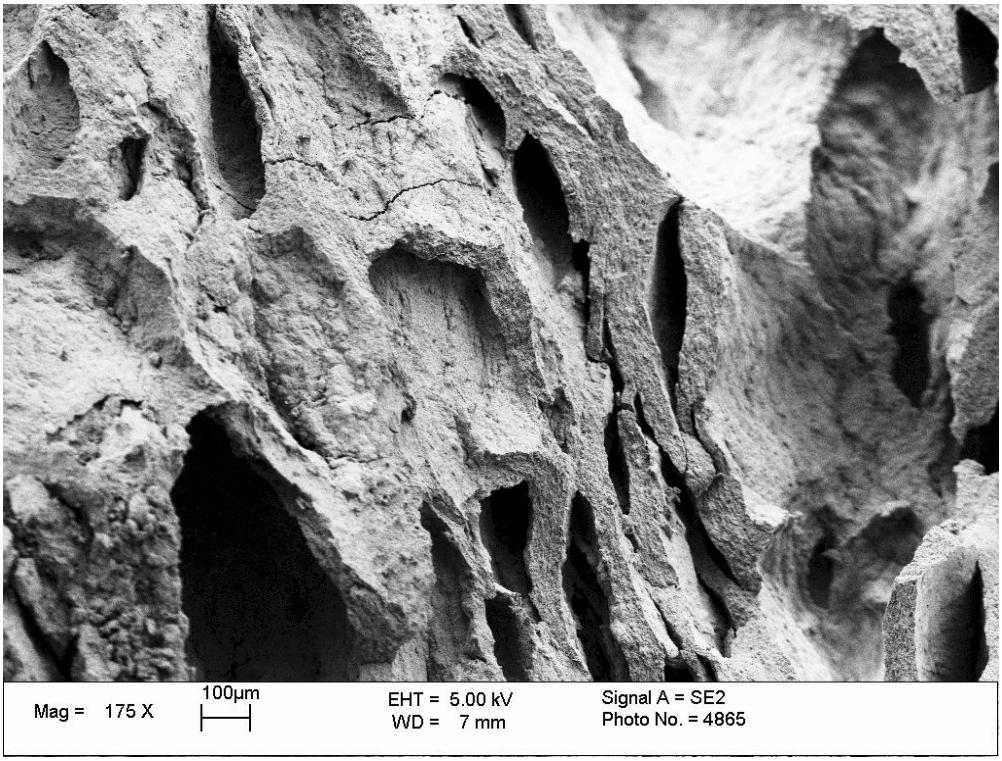


**Figure 101: HU93HM5 Ash Residue**

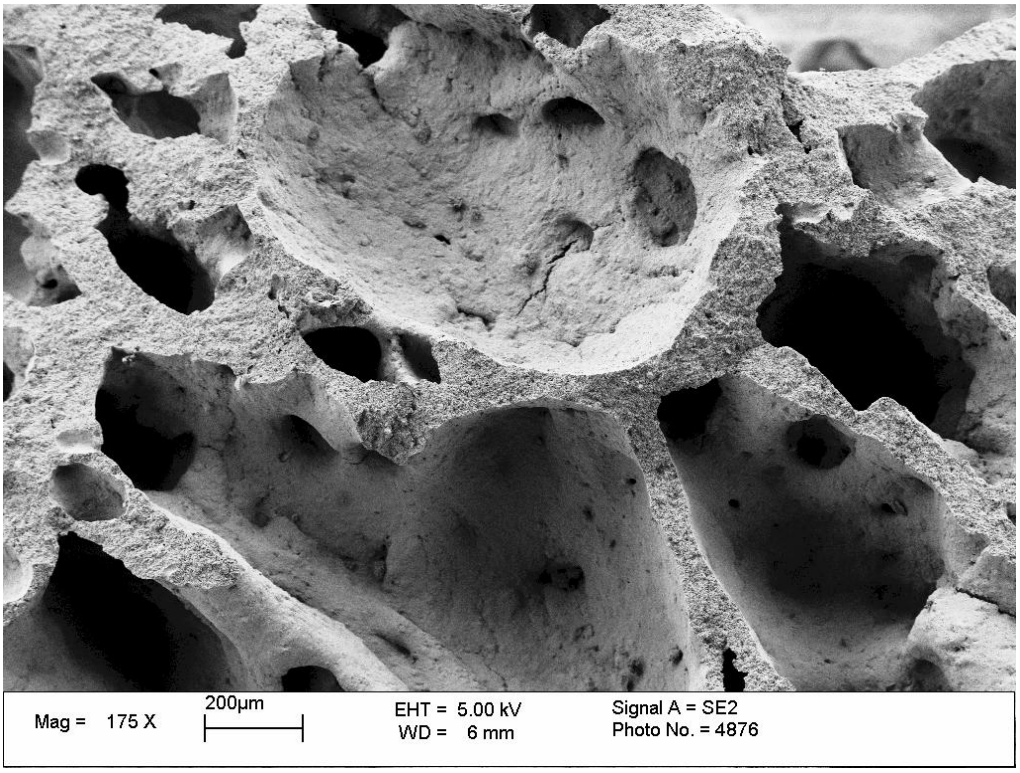


**Figure 102: HU43HM50 Ash Residue**

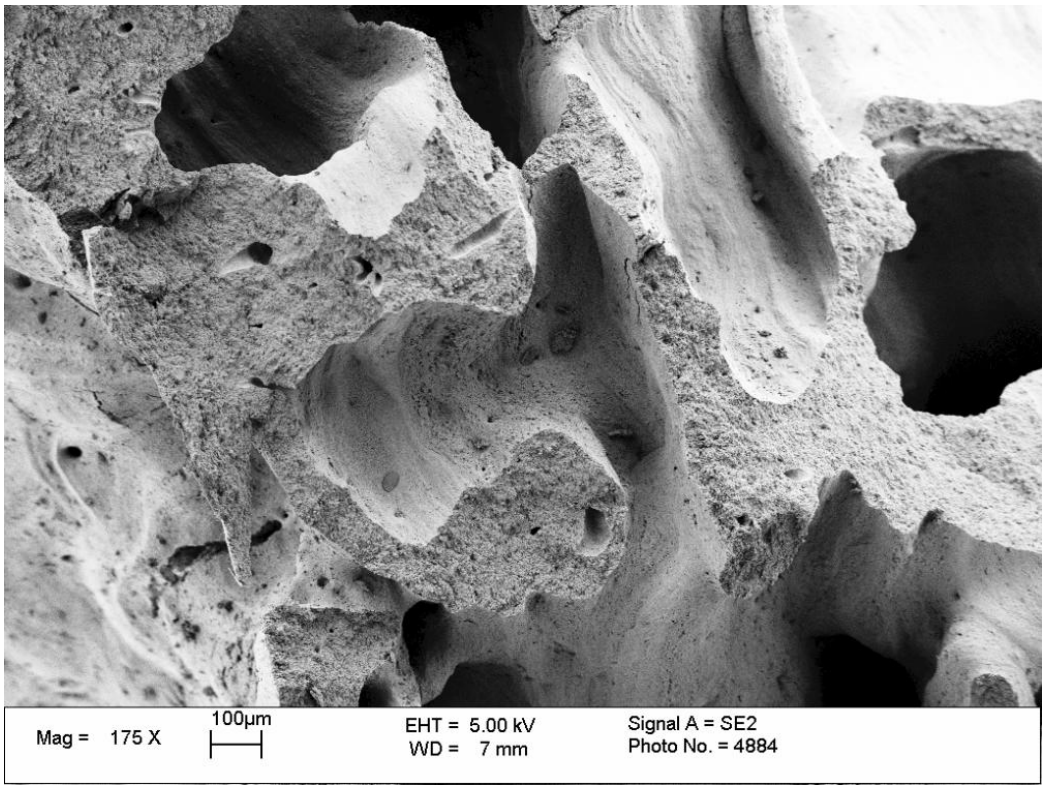


**Figure 103:HU24HM67 Ash Residue**

Figure 104 shows a magnified cross section of part of a bubble wall in Figure 101. It can be seen that the platy huntite particles in the HU93HM5 filled compound have aligned themselves almost completely parallel to one another. Even though the huntite has thermally decomposed due to the heat generated by the combustion of the polymer it has maintained its platy shape. This alignment of the particles around the walls of the bubbles explains the strength of the huntite residue. The particles have aligned parallel to the surface of the bubble as it expanded forming a randomly arranged, overlapping and interlocking, structure of platy particles that has been described variously as being similar in structure to bricks in a wall, leaf mould, papier-mâché, or tiles on a roof. None of these analogies is perfect, but it is easy to envisage the idea of overlapping particles having a strengthening effect.

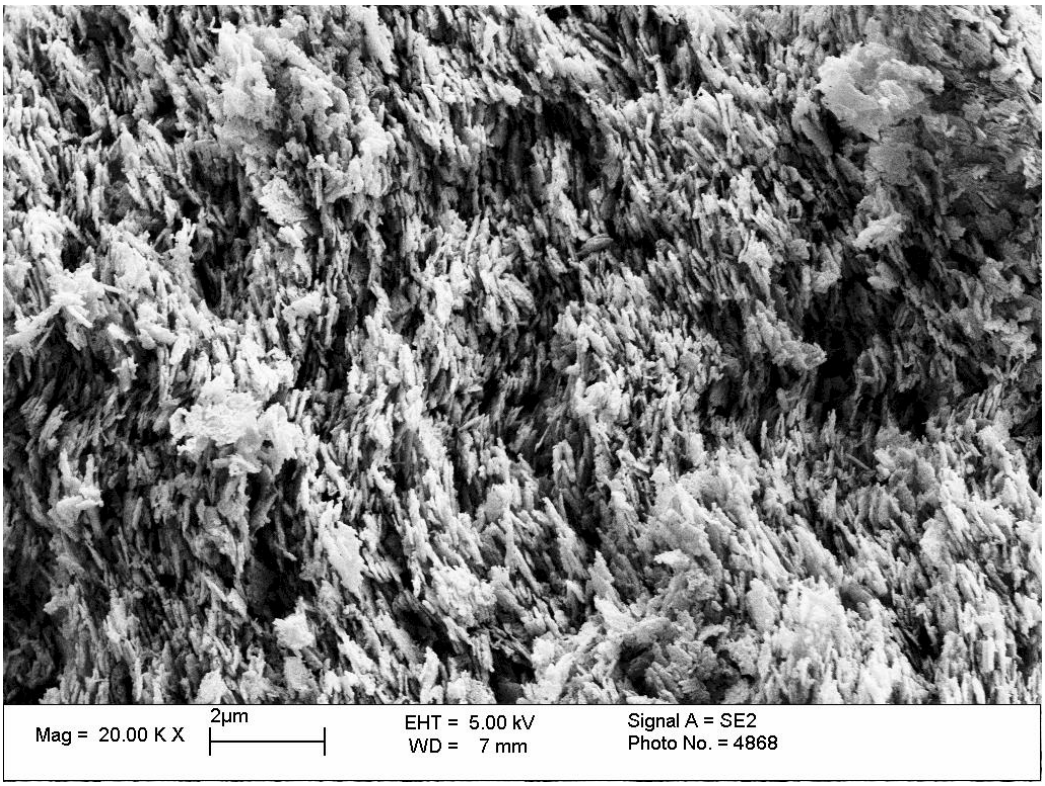


**Figure 104: Cross section of bubble wall (HU93HM5)**

This alignment and overlapping of the particles will help to reduce the rate at which combustible organic decomposition products can migrate to the surface, and therefore to the flame, by creating a tortuous route that the gases must follow. This will starve the flame by restricting the supply of fuel therefore reducing the severity of the fire. The arrangement may also act as an improved radiation shield compared to a totally

random arrangement of particles. This observation of the physical structure of the residue fits with the measurement showing that increased ratios of huntite in a mixture with hydromagnesite gave lower heat release rates in the cone calorimeter.

In Figure 105 the ratio of huntite to hydromagnesite is approximately 43:50. In this case there is clearly a quantity of huntite particles scattered amongst much smaller bead like structures. The bead like structures must therefore be the inorganic residue from the decomposition of the hydromagnesite portion of the original blend.

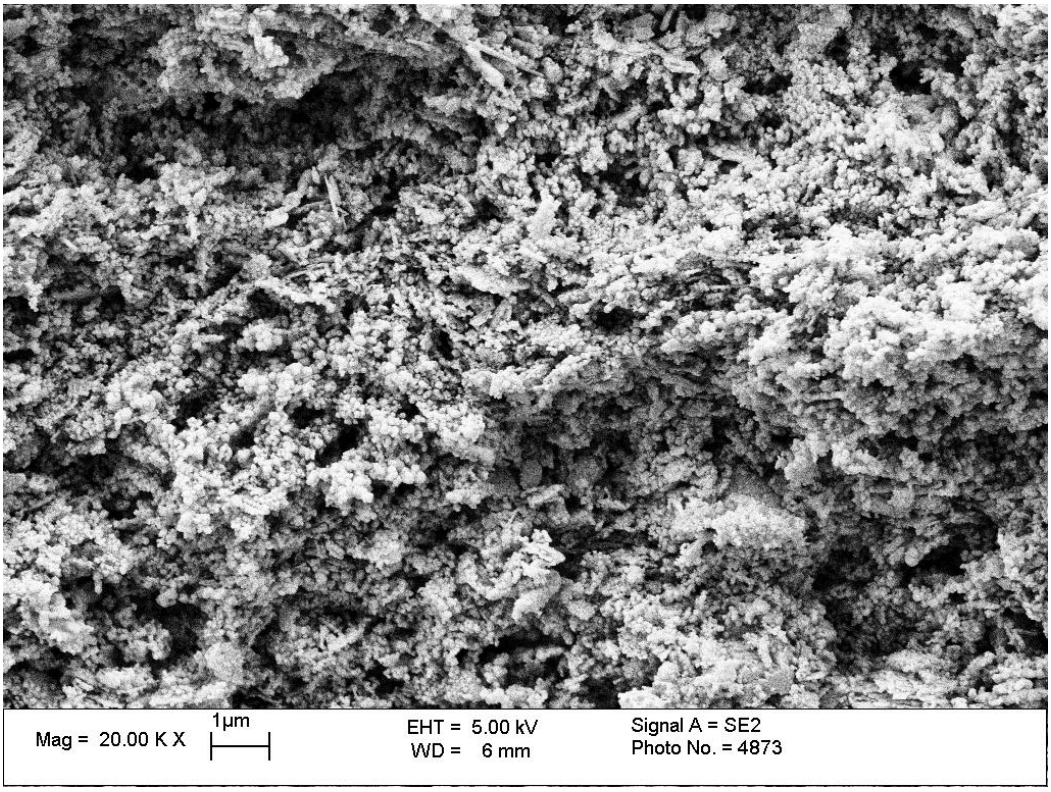


**Figure 105:Cross section of bubble wall (HU43HM50)**

Figure 106 shows that as the ratio of hydromagnesite is increased further the residue becomes dominated by the bead like structures of the hydromagnesite decomposition product. This further explains why a higher ratio of huntite in a mixture with hydromagnesite gives a stronger residue than a higher ratio of hydromagnesite. The beads formed from the decomposed hydromagnesite will easily move over one another and also allow the huntite particles to move against each other when any force is applied to the structure, rather than locking together as the plate like huntite decomposition product is likely to do.

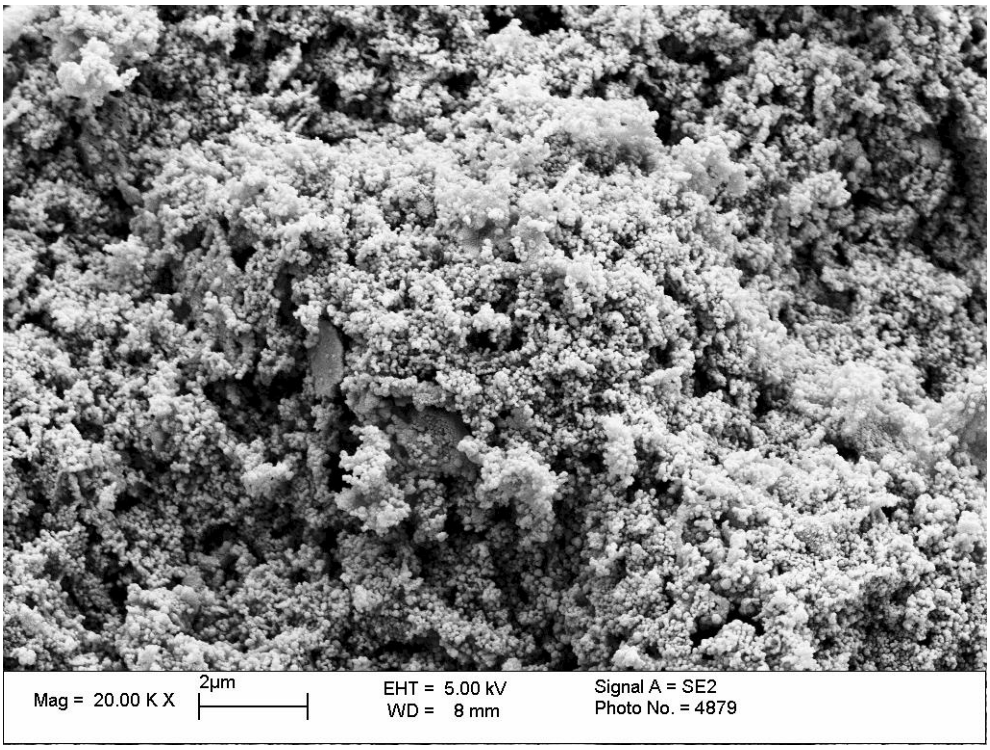


**Figure 106:Cross section of bubble wall (HU24HM67)**

Figure 107 shows the internal surface of a bubble within the residue of the HU93HM5 sample. The huntite particles can be seen positioned parallel to the surface of the bubble. This arrangement of the particles again confirms the reinforcing nature of the huntite decomposition product on the bubble and also its ability to hinder the escape of decomposition gases from the bubble. It is clear that the huntite particles have maintained their platy shape even after combustion of the polymer. However, it can be seen that although the particles have maintained their shape they are no longer solid due to the loss of carbon dioxide during thermal decomposition. Instead they have the appearance of a porous network.

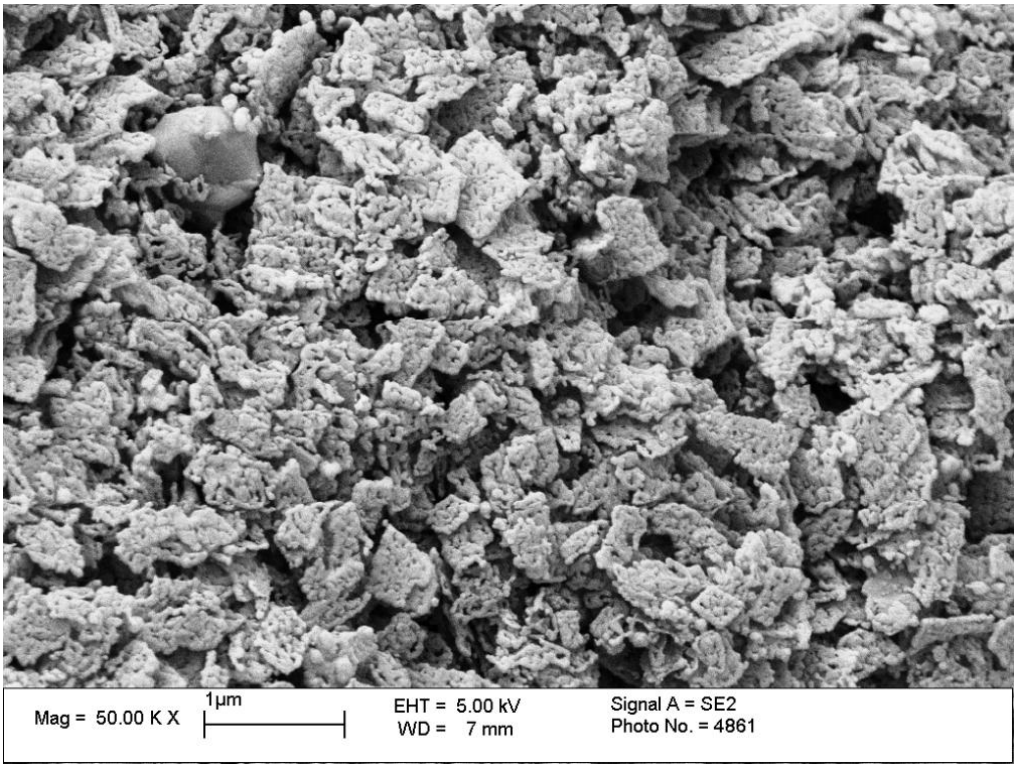


**Figure 107:Internal surface of bubble (HU93HM5)**

Figure 108 shows that when a mixture of huntite and hydromagnesite is used in the compound the huntite particles still maintain their shape and align themselves parallel to the surface of the bubble. However the smaller particles formed from the hydromagnesite decomposition products are interspersed among the decomposed huntite particles.

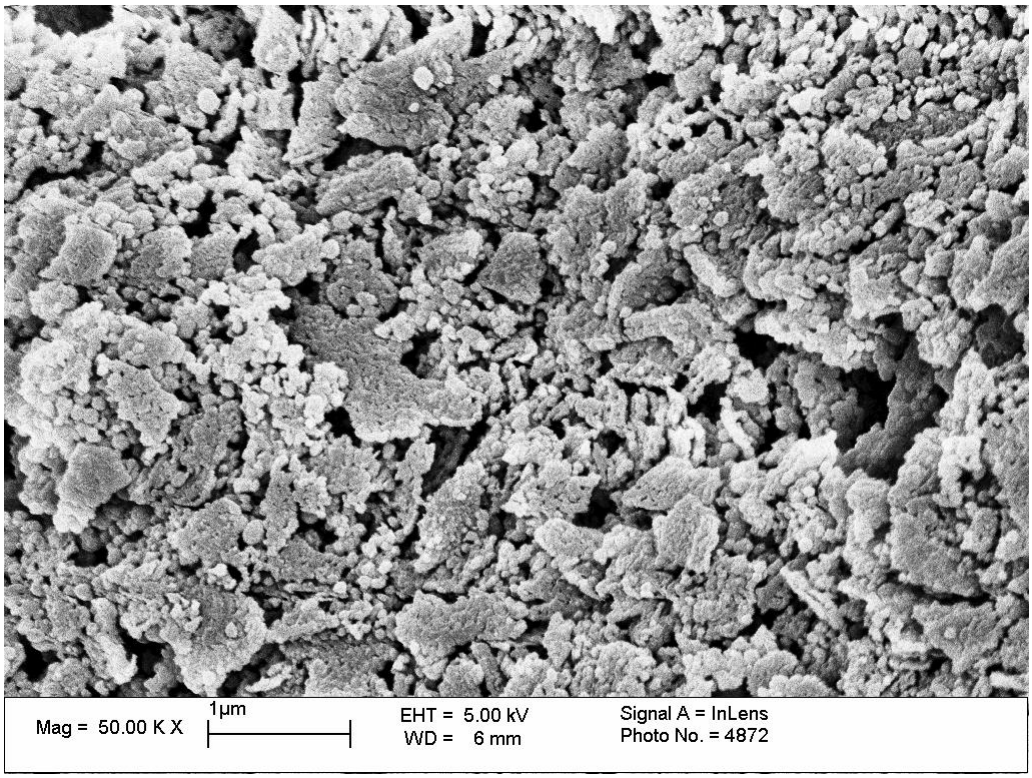


**Figure 108:Internal surface of bubble (HU43HM50)**

Figure 109 shows the internal surface of a bubble within the residue of the compound that contained HM100. The structure of the hydromagnesite decomposition product can be seen in more detail. The internal surface of the bubble consists entirely of the bead like structures that have formed from the hydromagnesite. Clearly this kind of structure will not offer as much strength or hinder the escape of decomposition gases as effectively as the residue containing the overlapping platelets of the huntite decomposition product.

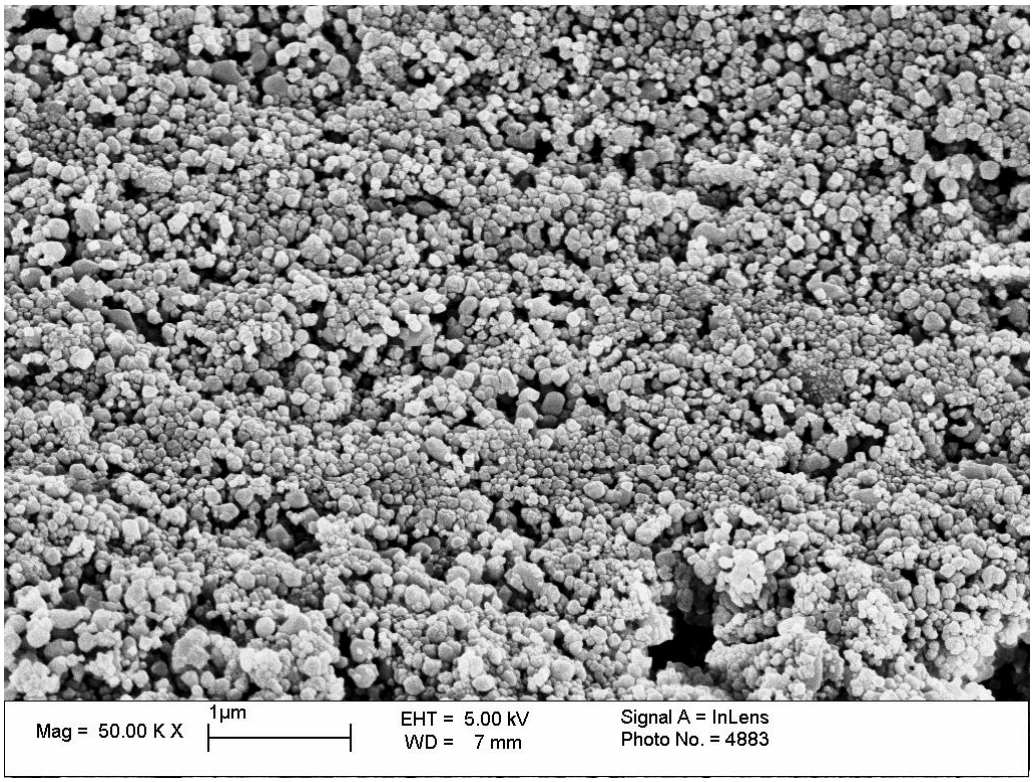


**Figure 109:Internal surface of bubble (HU24HM67)**

Figure 110 shows a higher magnification electron micrograph of the hydromagnesite decomposition product. From this picture it can be seen that most of the particles are less than 100 nm in diameter and that there appears to be no bonding of any kind between the particles.

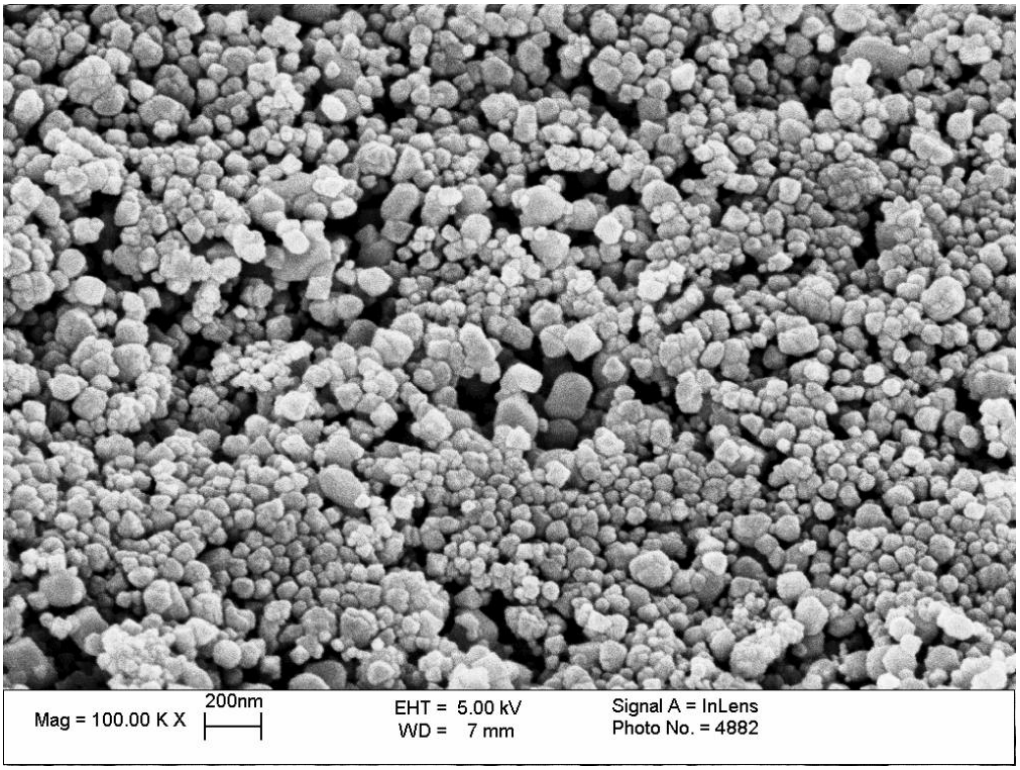


**Figure 110: Internal surface of bubble (HU24HM67) - higher magnification**

The electron micrographs shown in Figure 101 - Figure 110 lead to the conclusion that the huntite decomposition product maintains the original plate like shape of the huntite particle. The platy shape brings a number of benefits through physical interactions with the other particles and with the escaping polymer decomposition products. They physically strengthen the residue meaning that it is less likely to move and collapse during combustion. They also reinforce the foam like structure formed when the hydromagnesite gives off water. This allows the formation of a strong intumescent layer that slows the transfer of heat to the underlying polymer and the

transfer of volatiles from the underlying polymer to the flame. Also during this stage endothermic decomposition of the huntite further reduces heat transfer to the underlying polymer and releases carbon dioxide diluting the combustible gases in the flame.

Hydromagnesite particles are larger than huntite particles before decomposition but during decomposition they disintegrate to form beads of magnesium oxide of less than 100 nm in diameter. Beads will obviously form a weaker residue than one made from aligned plate like particles. They will also act to weaken the residue as higher proportions of them are present in a residue constructed from platy huntite particles.

### 5.3.3 TGA analysis of the ash residue

Because huntite and hydromagnesite go through a number of stages of thermal decomposition over a wide temperature range, TGA analysis of the residue taken from the cone calorimeter may yield information on the maximum temperature reached during combustion.

Mass loss measurements made during cone calorimeter testing (Figure 111) shows that samples containing a higher proportion of hydromagnesite lose more mass than those containing a higher proportion of huntite. This trend is in agreement with the mass loss trend of the compounds during TGA testing (Table 11).

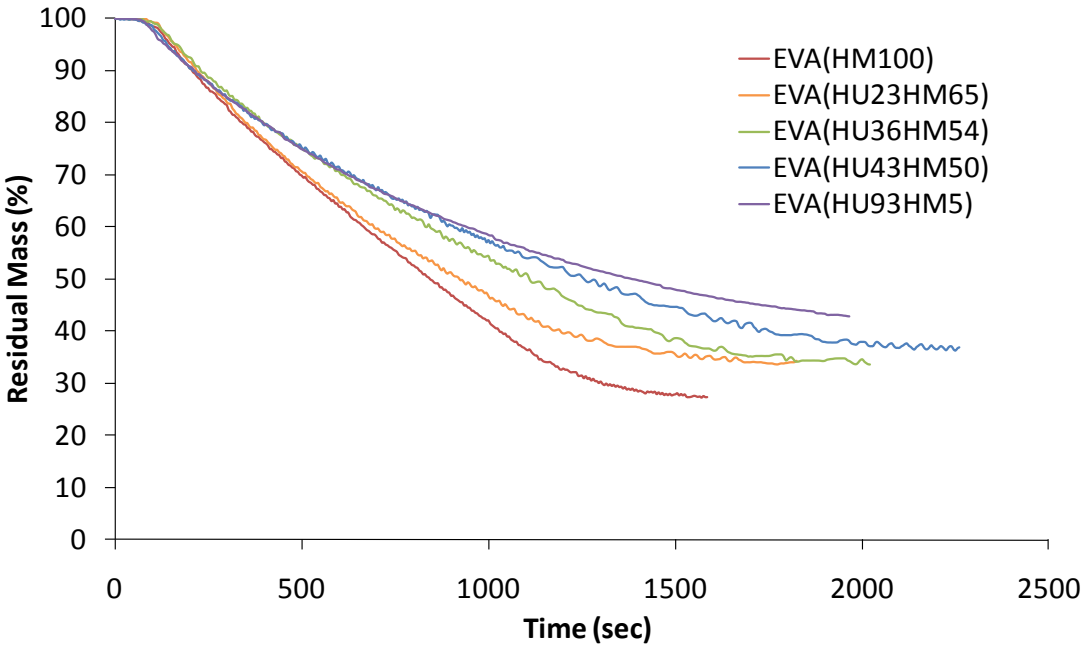


Figure 111: Mass loss during cone calorimeter test

| Sample Reference | Sample Mass Loss (%) | | | Temperature at which TGA mass loss equals cone mass loss (°C) |
|---|---|---|---|---|
| | Cone Calorimeter | TGA (to 750°C) | TGA (to 600°C) | |
| EVA.HM100 | 70.9 | 72.8 (1.9)* | 72.0 (1.1)* | 480 |
| EVA.HU24HM67 | 65.4 | - | 66.5 (1.1)* | 570 |
| EVA.HU41HM57 | 63.8 | 71.1 (7.3)* | 66.5 (2.7)* | 558 |
| EVA.HU43HM50 | 59.6 | 70.6 (11.0)* | 64.6 (5.0)* | 551 |
| EVA.HU93HM5 | 54.6 | 68.5 (13.9)* | 60.3 (5.7)* | 576 |
| EVA.ATH | 58.5 | 59.5 | 59.0 | |
| EVA.MDH | 57.7 | 58.5 | 58.1 | |
| EVA.Chalk | 38.8 | 47.9 | 39.8 | <600 |

* numbers in brackets indicates the difference in mass loss between the TGA and the cone calorimeter

**Table 11: Comparison of mass loss in the cone calorimeter and TGA**

It was shown in section 5.1.2 that complete decomposition of the compounds containing huntite and hydromagnesite, including complete decomposition of both hydromagnesite and huntite had taken place by 750°C. By comparing the mass losses, shown in Table 11, for each sample at 750°C measured by TGA with the total mass losses measured at 50 $kWm^{-2}$ in the cone calorimeter, it can be seen that mass losses are greater in the TGA test and that the effect is more prominent for the samples that contained greater proportions of huntite. This suggests that complete decomposition of huntite has not taken place during combustion in the cone calorimeter.

Since the blends of huntite and hydromagnesite decompose through several stages of mass loss between about 220°C and 750°C the total mass loss measured in the cone calorimeter could be used to estimate the maximum temperature reached during combustion in the cone calorimeter. The temperature at which the mass loss measured by TGA is equal to the total mass loss measured by cone calorimetry provides this estimation.

Mass loss of the ATH and MDH filled samples correlate very accurately between the cone calorimeter and the TGA at both 600°C and 750°C showing that complete decomposition of the mineral must have taken place. This means that no estimation of the maximum temperature reached during combustion can be made for the compounds filled with those minerals, except to say that minimum temperatures of

about 320°C and 450°C must have been reached in order to cause complete decomposition of the ATH and MDH respectively (see Figure 62 in section 4.5). The chalk filled sample shows a very slightly larger mass loss at 600°C and a significantly larger mass loss at 750°C when measured by TGA than the total mass loss measured in the cone calorimeter. This shows that during combustion in the cone calorimeter the chalk filled sample is not likely to have exceeded a temperature of about 600°C because otherwise decomposition of the mineral would have been initiated leading to a larger mass loss.

In order to determine the stage of decomposition that the huntite and hydromagnesite reached during combustion of samples in cone calorimeter testing at 50 $kWm^{-2}$ the ash residue was tested using TGA at a heating rate of 10°$Cmin^{-1}$ in air.

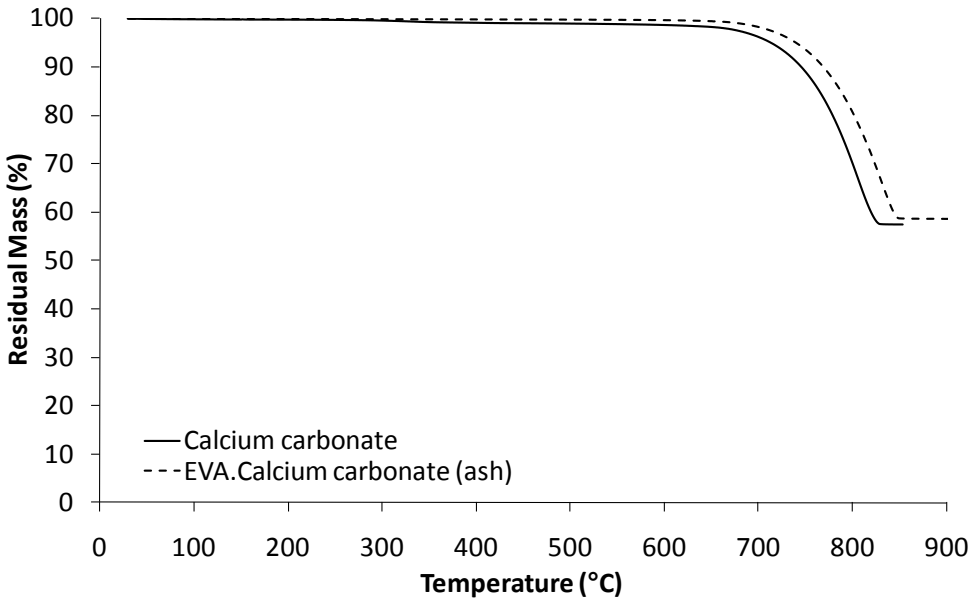


**Figure 112: Thermal decomposition by TGA of chalk in comparison with the ash residue obtained from EVA.chalk**

Figure 112 shows that the mass loss profile measured by TGA of the ash residue from the chalk filled compound was almost identical to the mass loss profile of the chalk alone. This confirms that no decomposition of the chalk occurred during the cone calorimeter testing and therefore the temperature of the compound during

combustion could not have exceeded about 600°C. The colour of the residue was visually consistent with the colour of chalk; therefore it is likely that the residue consists entirely of chalk and no carbonaceous char.

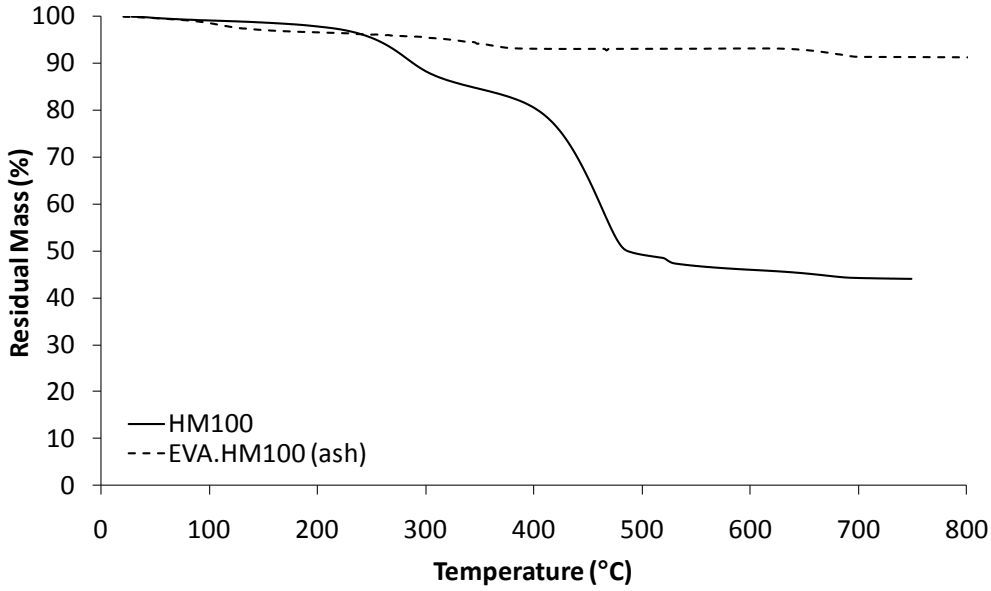


**Figure 113: Thermal decomposition by TGA of HM100 (hydromagnesite) in comparison with the ash residue obtained from EVA.HM100**

Figure 113 shows how the thermal decomposition measured by TGA of the residue obtained from the EVA compound containing pure hydromagnesite compared to the thermal decomposition of the hydromagnesite powder. The hydromagnesite powder shows the characteristic mass loss profile discussed in section 4.2. The residue sample shows a small mass loss at around 100°C which is probably associated with moisture absorbed from the atmosphere in the time between combustion of the compound and testing of the residue. It also shows another small mass loss between the temperatures of 320°C and 380°C. This mass loss does not match with either of the mass losses associated with hydromagnesite. The magnesium oxide residue remaining after the decomposition of hydromagnesite is likely to react with water from the atmosphere to form magnesium hydroxide, the temperature at which this mass loss occurs is consistent with the decomposition of this product. The stages of

decomposition of hydromagnesite up to a temperature of 550°C are no longer present in the ash residue; therefore a minimum temperature of 550°C is likely to have been reached during combustion. Analysis of the sample containing a high proportion of huntite gives further information on the maximum temperature that is likely to have been reached.

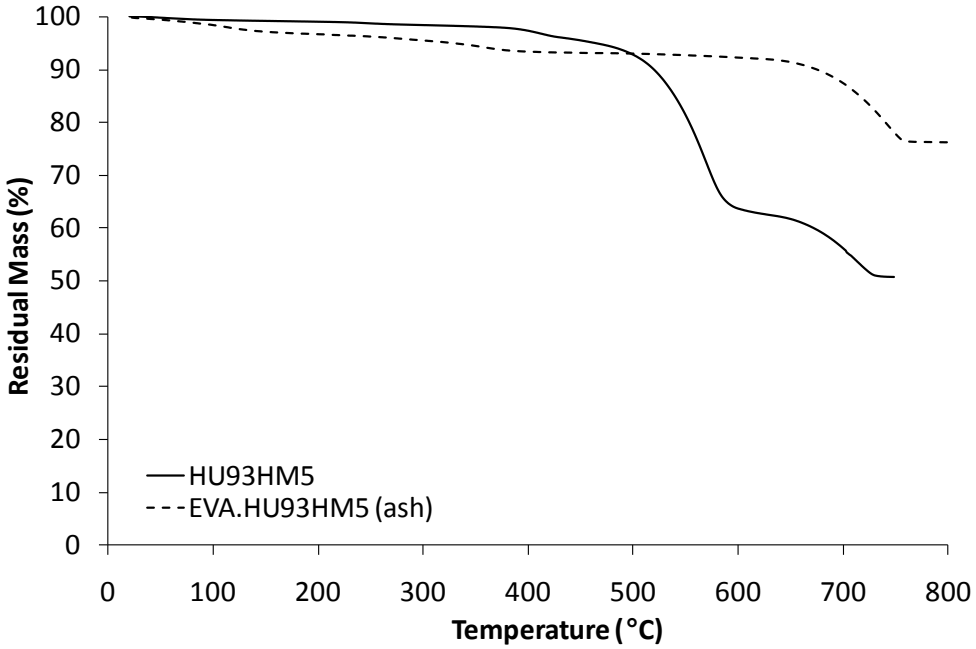


**Figure 114: Thermal decomposition by TGA of HU93HM5 (high huntite) in comparison with the ash residue obtained from EVA.HU93HM5**

Figure 114 shows the thermal decomposition measured by TGA of the residue obtained from an EVA compound containing a high proportion of huntite in a mixture with hydromagnesite compared to the thermal decomposition of the mineral powder. The mineral powder shows the characteristic thermal decomposition discussed in section 4.2 and elsewhere[63,70,71]. Thermal decomposition measured by TGA of the ash residue shows that the initial mass loss between about 400°C and 600°C measured on the mineral powder is no longer present. However the second mass loss occurring above 600°C is present in the mineral powder and the ash residue indicating that the sample did not exceed this temperature during combustion in the cone calorimeter.

This shows that during combustion in the cone calorimeter the huntite has partially decomposed releasing carbon dioxide and leaving magnesium oxide calcium carbonate mixture.

The ash residue again shows a small mass loss at around 100°C which is probably associated with moisture absorbed from the atmosphere. It also shows the other small mass loss at about 350°C also seen in the hydromagnesite sample (Figure 113) and possibly associated with the formation of magnesium hydroxide by reaction of the magnesium oxide with atmospheric moisture.

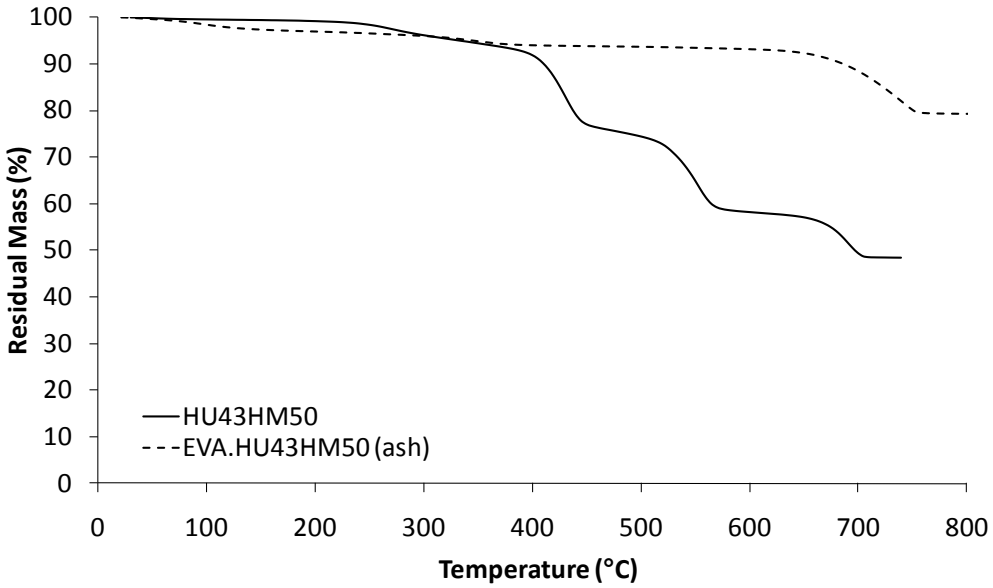


**Figure 115: Thermal decomposition by TGA of HU43HM50 (blend) in comparison with ash residue obtained from EVA.HU43HM50**

Figure 115 shows the thermal decomposition measured by TGA of the ash residue obtained from the EVA compound containing a mixture of huntite and hydromagnesite compared to the thermal decomposition of the mixture of the two minerals alone. The thermal decomposition of the mineral powder shows the characteristic mass loss profile discussed in section 4.2, being a combination of the decomposition of hydromagnesite followed by the decomposition of huntite.

The thermal decomposition measured by TGA of the ash residue again shows the two mass losses at approx. 100°C and 350°C. The sample of ash residue shows that all of the major mass losses associated with the decomposition of hydromagnesite and huntite below 600°C are no longer present. The only mass loss remaining is the higher temperature loss from huntite above 600°C.

These graphs confirm that during cone calorimeter testing the temperature experienced by the combusting material is in the region of 600°C. Therefore hydromagnesite is completely decomposed during the combustion process but huntite is only partially decomposed. This estimate of about 600°C as the temperature achieved during combustion under a heat flux of 50 $kWm^{-2}$ is very close to the figure of 610°C that has been reported[33] as the temperature reached by a non combustible ceramic plate exposed to the same heat flux.

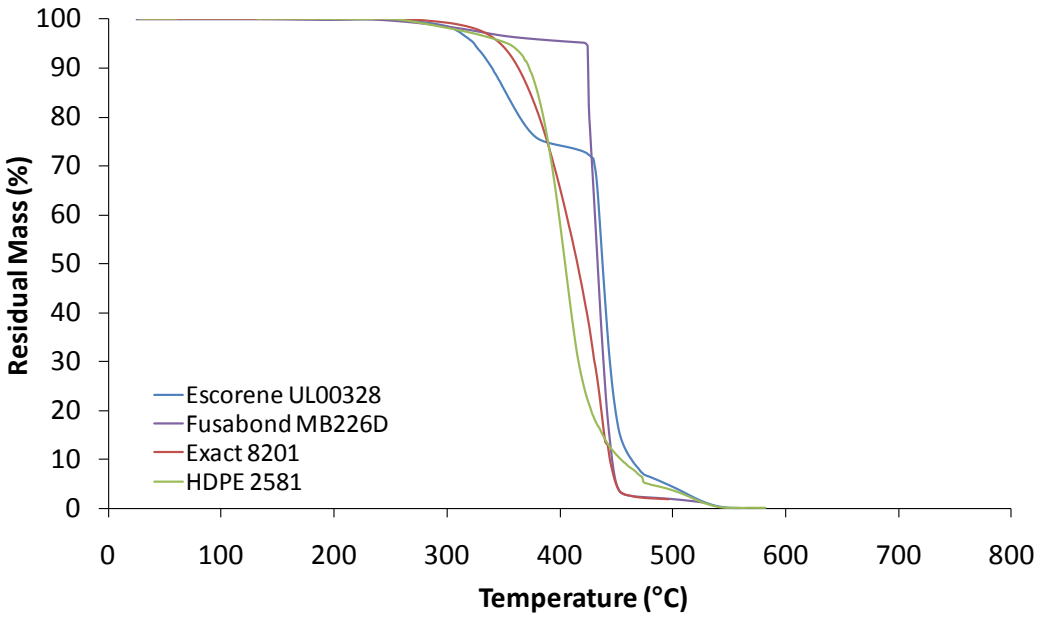


Figure 116: Thermal decomposition by TGA of the polymers used in the EVA compound

Figure 116 shows that all of the polymers used in the compounds for this study completely decompose by about 540°C with maximum decomposition rates between about 400 °C and 440 °C. The initial decomposition of huntite to magnesium oxide and

calcium carbonate occurs between 400°C - 600°C, with the maximum rate of decomposition at about 570°C (Figure 44 in section 4.2). At first sight it appears that huntite should not have much potential as a fire retardant, this suggestion has been reported[121,122,133] several times. However, as the mass of polymer is reduced during combustion an inorganic layer of huntite and magnesium oxide from the decomposed hydromagnesite will build up on the surface of the material. The huntite in this layer will therefore continue to provide additional protection to the polymer beneath by absorbing further heat through endothermic decomposition and release of carbon dioxide into the flame.

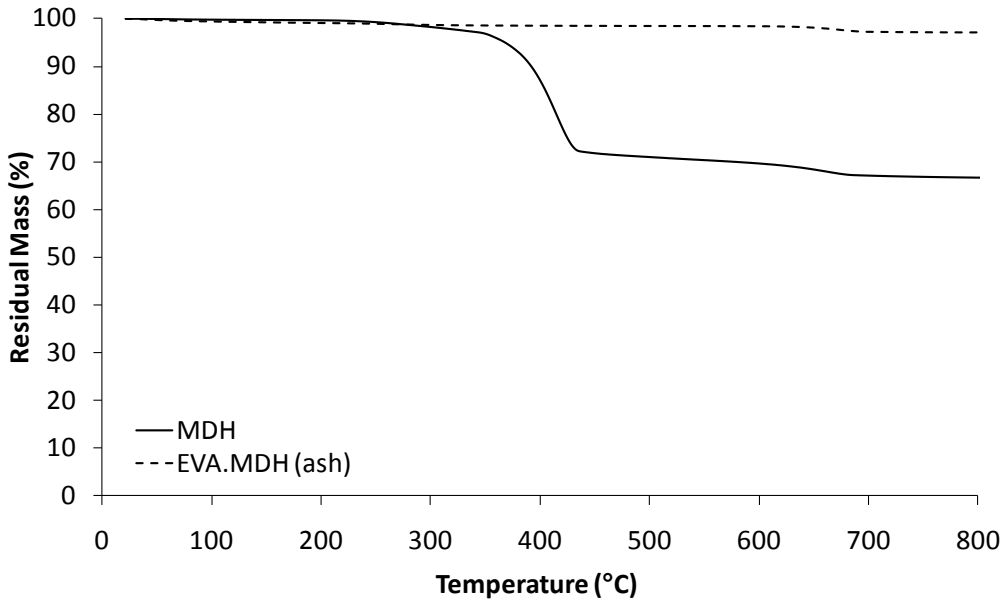


**Figure 117: Thermal decomposition by TGA of magnesium hydroxide in comparison to the ash obtained from EVA.MDH**

Figure 117 shows the thermal decomposition measured by TGA of the ash residue from the magnesium hydroxide filled EVA compound. There is no mass loss between 300°C and 400°C, which is where magnesium hydroxide loses most of its mass, showing that almost complete thermal degradation of the magnesium hydroxide has taken place during combustion in the cone calorimeter. There is a small mass loss in the ash residue measured at just over 600°C which corresponds to a small mass loss

seen in the magnesium hydroxide at the same temperature. Again this indicates that the temperature of the sample during combustion did not exceed 600°C.

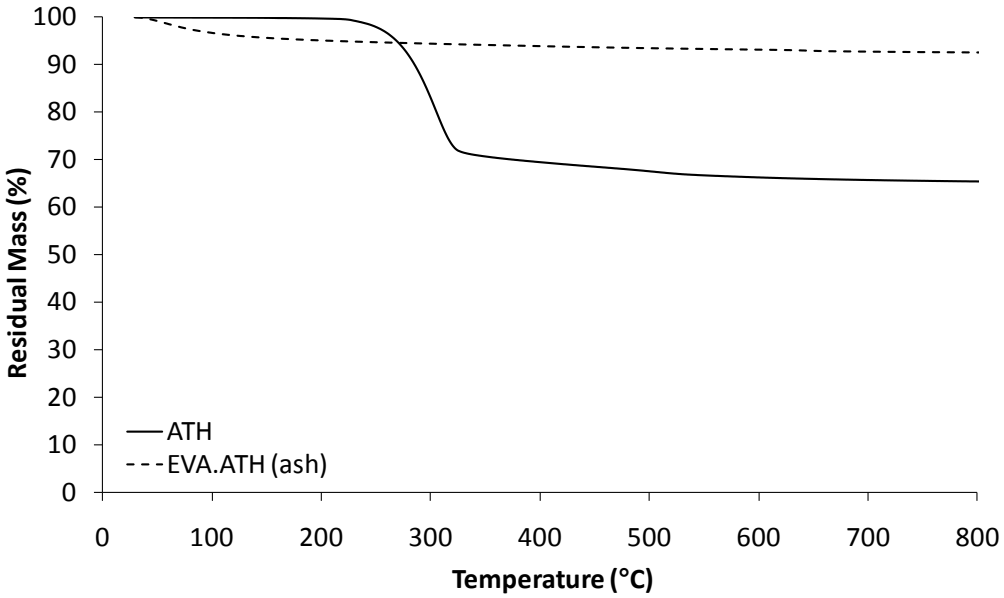


**Figure 118: Thermal decomposition by TGA of ATH in comparison to the ash obtained from EVA.ATH**

Mass loss measured by TGA of the ash residue from the ATH filled sample is shown in Figure 118. The ash residue shows a gradual mass loss over the whole temperature range. There is no rapid mass loss between about 200°C and 300°C as seen with ATH powder indicating that the complete decomposition of ATH has taken place during combustion in the cone calorimeter. It is unclear what the slow mass loss over the temperature range was due to. It is likely to be due to some kind of action that has occurred since the cone calorimeter test such as moisture absorption since the mass loss occurs at low temperatures as well as high temperatures. Therefore the mass loss would not be expected to be due to any products formed during combustion at high temperature.

## 5.4 Summary

It has been shown by TGA that the endothermic decomposition of hydromagnesite coincides with the temperature range at which polymers such as ethylene vinyl acetate and polyethylene thermally decompose. This is a good indicator that hydromagnesite has potential to perform as a fire retardant. Huntite decomposes between about 400°C and 750°C, a temperature range where most of the polymer has completely volatilised. This could be taken as evidence that huntite provides little in terms of useful fire retardant behaviour, however it has been shown that mixtures of huntite and hydromagnesite perform similarly to aluminium hydroxide in measurements involving limiting oxygen index and cone calorimetry. Therefore, huntite is not simply acting as a diluent filler.

TGA analysis of the inorganic residue, remaining after combustion in the cone calorimeter, showed that hydromagnesite was completely decomposed and huntite partially decomposed during combustion. An applied heat flux of 50 $kWm^{-2}$ is sufficient to raise the surface of a sample within the cone calorimeter to about 600°C and the measured partial decomposition of huntite is consistent with this temperature being reached. The partial decomposition of huntite within the ash residue also provides further protection to the underlying polymer and dilutes the flame with additional carbon dioxide.

Electron microscope images of the inorganic residue showed that hydromagnesite decomposes to almost spherical particles of about 100 nm in diameter. The partially decomposed huntite particles were shown to maintain their plate-like structure. Additionally, the partially decomposed huntite particles aligned themselves around the boundaries of the bubbles formed within the polymer during decomposition of the hydromagnesite and the polymer itself. This alignment physically reinforced the residue, making it stronger, and also provides a barrier making escape of the combustible gases from the condensed phase to the flame more difficult.

This combined evidence has been used to show that the endothermic release of water and carbon dioxide from hydromagnesite at temperatures between 220°C and 500°C helps to reduce the initial peak of heat release and increase the time to ignition. It has

also shown that the partial decomposition of huntite at temperatures between 400°C and 600°C helps to reduce the average rate of heat release by providing a physical barrier slowing the release of combustible gases to the flame. The platy huntite particles also help to physically stabilise the residue during the later stages of combustion forming a strong insulating barrier to the underlying polymer.

# 6. Proposed mechanism for the fire retardant behaviour of natural mixtures of huntite and hydromagnesite

It is clear that mixtures of huntite and hydromagnesite are not simply blends of active hydromagnesite and diluent huntite as has been suggested in the past[121,122,133]. The fire retardant mechanism of blends of huntite and hydromagnesite can be split into several subsections. These subsections are: the dilution of the fuel with a non-combustible filler, the endothermic effects of thermal decomposition, the release of water and carbon dioxide, the effects of the inorganic residue.

## 6.1 Dilution of the fuel

Any non-combustible filler will have some fire retardant affect in terms of reducing the total fuel content of a material. In these terms huntite and hydromagnesite are no different from chalk, aluminium hydroxide, magnesium hydroxide or any other non-combustible inorganic filler. Any non-combustible additive will also affect fire properties by altering the heat capacity, thermal conductivity, reflectivity and emissivity of the composite. Huntite and hydromagnesite have heat capacities at 25°C (298 K) of 0.88 and 1.13 $Jg^{-1}K^{-1}$ respectively (see Table 3 in section 2.20). Therefore, making the assumption that the heat capacity remains constant, it can be calculated that to raise huntite and hydromagnesite from 25°C to their decomposition temperatures (400°C for huntite and 220°C for hydromagnesite) takes 330 $Jg^{-1}$ and

220 $Jg^{-1}$ respectively. This is energy that is not heating the polymer, therefore changing its rate of heating.

## 6.2 Endothermic decomposition

The current work has confirmed that the release of water and carbon dioxide from huntite and hydromagnesite is via an endothermic mechanism. It has been reported[159] that the heat capacity of most organic polymers is in the range of 0.9 – 2.1 $JK^{-1}g^{-1}$ at room temperature. Approximations for the heat capacities of a range of polymers from room temperature to the degradation point have been calculated[159] and shown to be in the range of 1.5 – 3.0 $JK^{-1}g^{-1}$. Table 2 in section 2.20 gives values for the heat of decomposition of ATH as 1.3 $kJg^{-1}$. This has lead to the observation[160] that the decomposition enthalpy of ATH is about 1000 times larger than the heat capacity of most organic polymers. Table 2 also reports the decomposition enthalpies of huntite and hydromagnesite as 0.98 $kJg^{-1}$ and 1.3 $kJg^{-1}$ respectively, meaning that the same argument applies to these minerals.

Low density polyethylene has an average heat capacity of about 2.49 $JK^{-1}g^{-1}$ from room temperature to its decomposition temperature at about 450°C[159], meaning that this temperature rise requires about (2.49 $Jg^{-1}$ x 430°C) 1070 J of energy. This is very close to the decomposition enthalpy of the Turkish hydromagnesite, which has been measured at 990 $Jg^{-1}$ from room temperature to about 500°C (Figure 45 in section 4.2). Therefore, in a polymer compound that might contain 40% polymer and 60% hydromagnesite about half of the energy absorbed is used to decompose the mineral rather than heat the polymer. In most situations hydromagnesite is used as a mixture with huntite so the effect from hydromagnesite would be proportionately smaller.

The decomposition of hydromagnesite therefore has a significant effect on reducing the rate of heating and decomposition of the polymer. This has been seen as increases in time to ignition and reductions in initial peaks of heat release as the rate of supply of fuel to the gas phase is reduced. As discussed in section 5.2.2 the heat absorbed by endothermic decomposition of the minerals is not detected by oxygen depletion

calorimetry. However, the affect of the endothermic decomposition on reducing the rate of combustion of the fuel content will be measured.

Huntite decomposes between about 400°C and 750°C and absorbs about 980 $Jg^{-1}$ as it releases carbon dioxide. At the temperature at which huntite begins to decompose polymers such as polyethylene have already almost completely decomposed leading to comments from other authors[121,122,133] that it is little more than a diluent filler in terms of fire retardant action. However, it has been shown in this work that huntite is, at least partially, decomposed during combustion in a cone calorimeter. As the polymer decomposes an inorganic residue remains. Initially the residue may contain decomposition products from hydromagnesite and undecomposed huntite. A heat flux of 50 $kWm^{-2}$ from the cone heater is capable of raising the surface temperature to about 600°C[33]. The fact that samples have reached temperatures in this region has been confirmed using TGA analysis of the residue. Therefore, when the polymer has completely decomposed in the outer layers of a sample but the underlying material still contains organic material, the endothermic decomposition of huntite has the effect of reducing heat energy transfer to the underlying organic material. The intensity of the applied heat flux will influence the degree of degradation of the huntite. In real fire situations this heat flux may be well in excess of the 50 $kWm^{-2}$ used in the cone calorimeter.

The endothermic decomposition of huntite occurs at a higher temperature than hydromagnesite. It therefore begins to have an effect on fire properties at a later stage of the fire. This has been seen in the measurements made using the cone calorimeter as reduced rates of heat release later in the fire. This is a distinct difference from the way in which fire retardant minerals such as aluminium hydroxide or magnesium hydroxide work. Both of these mineral fire retardants are active through endothermic decomposition in the early parts of the fire but have no endothermic mechanism at higher temperature.

### 6.3 Release of water and carbon dioxide

Hydromagnesite has been shown (Figure 50 & Figure 51) to release water between about 220°C and 350°C followed by carbon dioxide between about 350°C and 500°C. This gas has a number of affects on fire retardancy. Initially the release of water vapour at a temperature where the polymer has softened but not significantly decomposed will cause the formation of a foam structure around the particles of hydromagnesite. A foamed or intumescent structure can have an insulating effect, reducing the heat transfer to the underlying layers of polymer. As the temperature rises further the polymer begins to decompose and reduce in viscosity, at this stage the bubbles can break on the surface of the sample opening up further polymer to the radiant heat flux. The negative effect of exposing further polymer to the heat flux and the positive effect of releasing water into the gas phase are competing. During this phase of the fire, hydromagnesite also releases carbon dioxide which again will initially form bubbles within the polymer matrix followed by release into the gas phase. When the water and carbon dioxide enter the gas phase they both have the affect of diluting the flammable decomposition products and therefore reducing the rate of combustion. The heat capacity of both water and carbon dioxide in the flame will also reduce the amount of heat available to further heat the condensed phase. The energy absorbed by the released gases can be estimated by making two assumptions:

1. That the flame temperature reaches 900°C
2. That the mineral decomposes completely and immediately on reaching its decomposition temperature

The energy required to heat the water released from hydromagnesite at 220°C to 900°C can be calculated as 1333 $Jg^{-1}$ and for the carbon dioxide released from the hydromagnesite at 350°C as 424 $Jg^{-1}$. Of course, the assumptions made are not completely realistic because the total volume of water and carbon dioxide are released over a range of temperatures, not at a single temperature. This does however allow a rough estimate to be made of the relative importance of the stages of the mineral decomposition in terms of fire retardancy.

As explained previously huntite begins to decompose at about 400°C, after most of the organic polymer has decomposed. However, the huntite residue remaining on the

upper layers of the sample will continue to dilute the gas phase with carbon dioxide, therefore slowing the rate of combustion in the flame.

### 6.4 Accumulation of inorganic residue

As the mass of polymer is reduced through decomposition and combustion an inorganic residue remains. Again, assuming that hydromagnesite completely and instantly decomposes on reaching its decomposition temperature, it can be calculated that the resulting magnesium oxide would absorb 353 $Jg^{-1}$ of energy to raise its temperature to 600°C. This provides some degree of protection to the underlying polymer. As the combustion progresses the composition of the residue changes. During the initial period of polymer decomposition hydromagnesite endothermically decomposes emitting water and carbon dioxide which form as bubbles surrounding the particles within the polymer matrix. Hydromagnesite completely decomposes during polymer combustion leaving a magnesium oxide residue of bead like structures (Figure 110). Huntite has been shown to have a plate like morphology (Figure 41). Extensional stress within the polymer matrix around the expanding bubbles causes the huntite particles to align in the direction of stress (i.e. parallel to the surface of the bubbles). This can been seen from the electron micrographs of the ash residue (Figure 101 - Figure 110). This alignment of the huntite particles creates a physical barrier to gases escaping from the decomposing polymer. This slows the release of fuel to the flame and provides another mechanism by which huntite reduces the rate of heat release in the later stages of the fire. Neither magnesium hydroxide nor aluminium hydroxide have a similar morphology to huntite, therefore this mechanism of fire retardancy is something that neither metal hydroxide offers. As the huntite particles endothermically decompose later in the fire they maintain their plate like structure giving the residue increased physical strength compared to hydromagnesite, aluminium hydroxide or magnesium hydroxide.

Compounds containing mineral fillers such as huntite and hydromagnesite, aluminium hydroxide or magnesium hydroxide have a tendency to swell in the early stages of the fire as water is released from the mineral and forms a foam within the softened

polymer. During the later stages of the fire, compounds containing either high proportions of hydromagnesite in a blend with huntite, or simply containing aluminium hydroxide or magnesium hydroxide, have a tendency to collapse as the mass of organic material reduces and there is little strength within the residue to maintain the structure. The platy nature of the huntite particles leads to stronger residues, meaning that the foamed structure formed during the initial stages is maintained throughout the burning period and beyond. This means that the insulation provided by the foamed structure is maintained throughout the burning period when a sufficiently high proportion of huntite is present in the mixture with hydromagnesite.

## 6.5 Summary

There are clearly a number of factors contributing to the fire retardant behaviour of mineral filler types of fire retardants. Some of these are easier to quantify than others. The total heat absorbed by the filler and its decomposition products can be estimated by summing the affects of heat capacity of the filler prior to decomposition, heat of decomposition, heat capacity of the residue after decomposition and heat capacity of the gases evolved during decomposition. The heat capacities and heats of decomposition are known quantities (Table 2 and Table 3).

Because the decomposition of endothermic fillers such as ATH, or huntite and hydromagnesite, are not simple the assumption has been made that complete decomposition occurs at the onset temperature. Of course this does not happen in the real world, but as no attempt has been made to measure how the heat capacity changes during decomposition of the minerals this is a necessary step. It also allows the assumption to be made that the water or carbon dioxide is also completely released at one temperature, which again does not happen in reality. It is also assumed that the heat capacity of the materials remains constant, at the values quoted in Table 3, over the heating range. Applying these assumptions the heat absorbed by the filler up to its decomposition temperature can be calculated, as can the heat absorbed by the mass of residue from the decomposition temperature up to

600°C, and the heat absorbed by the mass of released gases from the decomposition temperature up to 900°C. These figures are shown in Table 12

| | Hydromagnesite | Huntite | Aluminium Hydroxide | Magnesium Hydroxide |
|---|---|---|---|---|
| Heat capacity (J $g^{-1}$ $K^{-1}$) | 1.13 | 0.88 | 1.2 | 1.33 |
| Decomposition Temperature (°C) | 220 | 400 | 180 | 300 |
| Energy absorbed by the filler during heating from 25 °C to decomposition temperature (J $g^{-1}$) | 220 | 330 | 186 | 366 |
| Energy absorbed during endothermic decomposition (J $g^{-1}$) | 1300 | 980 | 1300 | 1450 |
| Energy absorbed by the residue during heating from the decomposition temperature to 600 °C (J $g^{-1}$) | 151 | 87 | 211 | 193 |
| Energy absorbed by the released gases during heating from the decompostion to 900°C in the flame (J $g^{-1}$) | 417 | 193 | 488 | 365 |
| **Total energy absorbed (J $g^{-1}$)** | **2088** | **1590** | **2185** | **2374** |

**Table 12: Estimated total heat absorbed by mineral fillers during combustion**

Using these figures the relative contribution of each stage to the total heat absorbed by the fillers has been calculated and is shown in Table 13.

| | Hydromagnesite | Huntite | Aluminium Hydroxide | Magnesium Hydroxide |
|---|---|---|---|---|
| Filler before decomposition | 11% | 21% | 9% | 15% |
| Endotherm | 62% | 62% | 59% | 61% |
| Residue | 7% | 5% | 10% | 8% |
| Released gases | 20% | 12% | 22% | 15% |

**Table 13: Relative contribution of each stage of decomposition to the total heat absorbed by the filler**

It can be seen that in each case the greatest contribution to the heat absorbed comes from the endothermic decomposition. The total heat absorbed before decomposition of the filler occurs is obviously influenced by the decomposition temperature, as well as the heat capacity, of the filler. The total heat absorbed by mixtures of huntite and hydromagnesite can be calculated by proportionally summing the values for the two individual minerals. It is clear that the total heat absorbed by these mixtures will be less than that absorbed by aluminium hydroxide or magnesium hydroxide. However, as discussed earlier in this chapter, heat absorbed by the filler is not the only fire retardant mechanism at work with these fillers. Mixtures of huntite and hydromagnesite form a stronger inorganic residue than that formed by aluminium hydroxide or magnesium hydroxide. The platy morphology of the huntite particles also hinders the escape of combustible gases. The huntite helps to maintain the foam

structure, formed in the polymer by the decomposition of the hydromagnesite, providing a higher degree of insulation than suggested by calculations based simply on heat capacity of the residue.

# 7. Conclusions

The main aim of this work was to understand the thermal decomposition mechanisms of huntite and hydromagnesite from a source in Turkey and to use this understanding to explain the contribution to fire retardant behaviour of each mineral in EVA filled with mixtures of these minerals. The published literature concluded that hydromagnesite decomposed endothermically, releasing water and carbon dioxide. Some authors also concluded that due its high temperature of decomposition, huntite was little more than a diluent filler. This explanation was unsatisfactory as it did not explain why mixtures of these minerals performed equally or better, in terms of fire retardant behaviour, than commonly used aluminium hydroxide.

## 7.1 Chemical composition and thermal decomposition of hydromagnesite

Hydromagnesite, $Mg_5(CO_3)_4(OH)_2{\cdot}4H_2O$, decomposes through a mechanism that depends on the rate of heating, this is linked to the partial pressure of carbon dioxide surrounding the particle. Between 220°C and 350°C it loses approximately 15% of its mass through release of water vapour. Water vapour is evolved from the loss of four molecules of water of crystallisation and from the decomposition of a single hydroxide group. The decomposition of the four carbonate groups, with an associated mass loss of a further 41%, is highly dependent on the partial pressure of carbon dioxide. It is also dependant on the rate of heating because at faster heating rates the partial pressure of the self generated carbon dioxide will be higher because there is less time for it to diffuse away from the particle. High rates of heating cause the carbonate to recrystallise at 520°C forming a more thermally stable structure which then decomposes at a higher temperature. At a heating rate of 1°Cmin$^{-1}$ complete decomposition of the carbonate group has occurred by 450°C, at a heating rate of

30°Cmin$^{-1}$ this temperature has increased to 580°C. In a fire situation it is likely that the recrystallisation at 520°C will occur because of the high heating rates involved. Also, because the hydromagnesite particles are encapsulated within a polymer the carbon dioxide released during decomposition will remain close to the particle surface raising its partial pressure.

The decomposition of hydromagnesite has been shown to be endothermic which is beneficial for fire retardancy. However, there is a small exotherm associated with the recrystallisation of magnesium carbonate at 520°C. Because it is small and overlaps with the endothermic decomposition of huntite it is unlikely to have any negative influence on the fire retardant mechanism of mixtures of these minerals.

Comparison of the mass losses associated with the thermal decomposition of magnesium carbonate, and magnesium hydroxide show that the mass losses associated with hydromagnesite are of the same magnitude that would be expected from of 4:1 mixture of the two minerals (compensating for the 4 water molecules present in hydromagnesite). However, the temperatures at which the mass losses occur vary significantly. This means that hydromagnesite is not simply a hydrated mixture of magnesium carbonate and magnesium hydroxide. It has its own unique crystalline structure incorporating the elements of magnesium carbonate and magnesium hydroxide in a 4:1 ratio.

## 7.2 Chemical composition and thermal decomposition of huntite

Huntite, $Mg_3Ca(CO_3)_4$, endothermically decomposes through release of carbon dioxide. Between 400°C and 630°C it loses 38% of its mass, this correlates to the decomposition of three carbonate groups associated with the three magnesium ions. Between 630°C and 750°C it loses a further 12% of its mass which correlates with the decomposition of the final carbonate group associated with the calcium ion.

Comparison of the mass losses associated with the thermal decomposition of magnesium carbonate and calcium carbonate shows that the mass losses associated with huntite are of the same magnitude that would be expected from a 3:1 mixture of

the two minerals, but the temperatures at which the mass losses occur vary significantly. This shows that huntite is not simply a mixture of magnesium carbonate and calcium carbonate. It has its own unique crystalline structure incorporating the elements of magnesium carbonate and calcium carbonate in a 3:1 ratio.

### 7.3 Fire retardant behaviour of mixtures of huntite and hydromagnesite

The limiting oxygen index of an EVA compound, shown in Table 5, containing ATH gives an oxygen index of 30% compared to 28% for a similar compound containing the same total loading of a mixture of huntite and hydromagnesite with 50% hydromagnesite content. A compound containing the same loading level of 100% hydromagnesite gave an LOI of 29.5% showing that hydromagnesite is almost equally effective as ATH in increasing the oxygen index. Therefore, in mixtures the huntite portion must be having a fire retardant effect that compensates for the lower hydromagnesite loading level.

Hydromagnesite is active in the initial stages of the fire, increasing time to ignition and reducing the initial peak of heat release, during combustion in a cone calorimeter. The endothermic release of water from hydromagnesite slows the rate of heating of the polymer between about 220°C and 350°C, therefore increasing the time that the polymer takes to reach ignition. The release of water vapour creates a foamed structure which increases the insulation effect to the underlying polymer. Water vapour and carbon dioxide from the decomposition of hydromagnesite are released into the flame when degradation of the polymer reduces its viscosity to the degree at which the bubbles can move through the polymer or the degradation of polymer causes the bubbles near the surface to burst.

Huntite is active later in the fire, reducing the average rate of heat release and increasing the time to extinction. The platy huntite particles align parallel to the walls of the bubbles formed by the hydromagnesite decomposition gases. This alignment physically hinders the release of volatile decomposition gases from the polymer into the flame, starving it and slowing the rate of combustion.

As the fire progresses an inorganic residue forms that maintains the foamed structure formed in the early stages of the fire. The platy huntite particles reinforce this structure meaning there is less collapse of the material in mixtures that contain a higher proportion of huntite. Even though the polymer that originally surrounded the huntite particles may have completely decomposed the huntite will thermally decompose, between about 400°C and 750°C, due to the radiant heat from the cone heater (or in real fire situations from the radiant heat of the wider fire). The endothermic decomposition of huntite reduces the heat transfer to the underlying polymer and feeds carbon dioxide into the flame diluting the combustible gases.

The strength of the inorganic residue is dependent on the huntite content. The platy shape of the particles is maintained, even after decomposition of the mineral, reinforcing the residue. Hydromagnesite particles decompose to bead like particles less than 100 nm in diameter which weakens the structure.

Grades of mixed huntite and hydromagnesite with smaller average particle sizes are more effective at reducing the rate of heat release measured by the cone calorimeter due to the slightly earlier and faster decomposition of the particles.

As the heat flux in the cone calorimeter is increased from 30 $kWm^{-2}$ to 50 $kWm^{-2}$ to 70 $kWm^{-2}$ the FIGRA values of mixtures of huntite and hydromagnesite increases linearly meaning that more complete decomposition of huntite at a higher heat flux does not influence the early stages of the fire. However, its platy morphology and endothermic decomposition between 400°C and 750°C mean that it is effective at reducing the heat release rate in the later stages of the fire. Hydromagnesite has a greater affect on increasing time to ignition and reducing the initial peak in rate of heat release thereby reducing FIGRA values at all three heat fluxes through endothermic release of water and carbon dioxide.

In summary the fire retardant action of mixtures of huntite and hydromagnesite comes from a combination of the actions of the two minerals. Huntite is certainly not the inert diluent that has been claimed by some in the past.

# 8. Further work

This thesis has provided a step forward in the understanding of the fire retardant mechanisms of huntite and hydromagnesite. However, as with most scientific work, it does not provide all the answers. Outlined here are some areas that require further work in order to take the next step forward.

The work presented within this thesis was conducted using a formulation based on polyolefins and ethylene vinyl acetate. These polymers were chosen as they represent the type of polymers that are commonly used in one section of the wire and cable industry: the LSOH or low smoke zero halogen sector. PVC is still widely used in the wire and cable industry. It has been criticised for its release of halogenated acid gases, and large quantities of smoke, however it is a very versatile polymer. Mixtures of huntite and hydromagnesite would be well suited to use in this polymer. The decomposition mechanism may well be changed because of reaction between the acid gas and the carbonate mineral which would release the carbon dioxide earlier than expected from the thermal decomposition alone. This may also reduce the quantity of acid gas released into the atmosphere, which could be seen as beneficial but may also increase flammability by reducing the quantity halogen radicals in the flame.

A mixture of huntite and hydromagnesite is only one method of improving fire retardant behaviour. Mixtures of these minerals with other fire retardants that work through other mechanisms may produce synergistic effects that need to be investigated. It has been shown that huntite particles align around bubbles formed during decomposition of the polymer and the hydromagnesite. With a little imagination this structure could be thought of as a brick wall with no cement. If a material could be found that would fill the gaps between the huntite particles and act as cement to the huntite bricks the release of combustible gases may be slowed even further. This may also lead to further mechanical strengthening of the inorganic

residue which can be of benefit in some applications. Materials that could be investigated for this purpose would include low melt glasses which would flow and vitrify between the particles, or zinc borate which again may flow and form a glassy borate between the particles.

There are also many other fire retardant additives such as zinc stannates, phosphorus containing fire retardants, halogenated fire retardants, nitrogen containing fire retardants, etc. etc. which may all have as yet unknown synergies with huntite and hydromagnesite.

Due to limitations with the available equipment no measurements of smoke were possible for this work. A study of the contribution of both huntite and hydromagnesite on smoke production would be beneficial.

# 9. References

1. Brydson J. The Chemical Nature of Plastics, in Anonymous Plastics Materials. Oxford, Butterworth-Heinemann, 1999, pp 19-42

2. Fox B. Fundamentals of Polymers. Proceedings: Flame Retardancy and Flammability of Polymers and Textiles, University of Leeds, June 2008

3. Brydson J. Poly (vinyl acetate) and its derivatives, in Brydson J, editor. Plastics Materials. Oxford, Butterworth-Heinemann, 1999, pp 386-397

4. ASTM E176-08 Standard Terminology of Fire Standards. 2008

5. Beyler CL, Hirschler MM. Thermal decomposition of polymers, in DiNenno PJ, editor. SFPE Handbook of Fire Protection Engineering. Massaschusetts, Quincy, 2002, pp 110-131

6. Hirschler MM. Chemical aspects of thermal decomposition of polymeric materials, in Grand AF, Wilkie C, editors. Fire Retardancy of Polymeric Materials. New York, Marcel Dekker, 2000, pp 27-80

7. DiBlasi C. The Burning of Plastics, in Troitzsch J, editor. Plastics Flammability Handbook. Munich, Hanser, 2004, pp 47-132

8. McGarry K, Zilberman J, Hull TR, Woolley WD. Decomposition and combustion of EVA and LDPE alone and when fire retarded with ATH. Polymer International 2000;49:1193-1198

9. Maurin MB, Dittert LW, Hussain AA. Thermogravimetric analysis of ethylene-vinyl acetate copolymers with Fourier transform infrared analysis of the pyrolysis products. Thermochimica Acta. 1991;186:97-102

10. Maurin MB, Pang JWC, Hussain MA. Thermogravimetric analysis of ethylene-vinyl acetate copolymer with dynamic heating rates. Thermochimica Acta. 1992;209:203-207

11. Razuvaev GA, Troitskii BB, Chochlova LV, Dubova ZB. Thermal degradation of ethylene-vinyl acetate copolymer. Journal of Polymer Science: Polymer Letters Edition. 1973;11:521-523

12. Karlsson L. The burning process and enclosure fires, in Troitzsch J, editor. Plastics Flammability Handbook. Munich, Hanser, 2004, pp 33-46

13. Dufton PW. Fire - Additives and Materials. Rapra, 1995

14. Price D, Anthony G, Carty P. Introduction:Polymer combustion, condensed phase pyrolysis and smoke formation, in Horrocks AR, Price D, editors. Fire Retardant Materials. Cambridge, Woodhead Publishing, 2001, pp 1-28

15. Lewin M, Weil ED. Mechanisms and modes of action in flame retardancy of polymers, in Horrocks AR, Price D, editors. Fire Retardant Materials. Cambridge UK, Woodhead Publishing, 2001, pp 31-68

16. BS ISO EN 4589-1 Plastics - Determination of Burning Behaviour by Oxygen Index: Part 2 Ambient Temperature Test. 1999

17. ASTM D2863 Measuring the Minimum Oxygen Concentration to Support Candle-Like Combustion of Plastics (Oxygen Index). 2008

18. Fenimore CP, Martin FJ. Candle-type test for flammability of polymers. Modern Plastics. 1966;44:141-148 & 192

19. Fenimore CP, Martin FJ. Flammability of polymers. Combustion and Flame. 1966;10:135-139

20. Cullis CF, Hirschler MM: The Combustion of Organic Polymers. London, Oxford University Press, 1981

21. BS EN ISO 4589-3 Plastics - Determination of burning behaviour by oxygen index - Part 3: Elevated-temperature test. 1993

22. Cornish EH: Materials and the Deisgner, ed 1st. Cambridge, Cambridge University Press, 1987

23. Addison OMS Cabling System - Fire Performance Standard. www.addison tech.com/cabling system catalog en download/addison/Fiber%20performance%20standard.pdf, accessed 07/02/2009

24. ASTM D635-10 Standard test method for rate of burning and/or extent and time of burning of plastics in a horizontal position. 2010

25. ASTM D3801-10 Standard test method for measuring the comparative burning characteristics of solid plastics in a vertical position. 2010

26. BS 2782-1: Method 140A Determination of the Burning Behaviour of Horizontal and Vertical Specimens in Contact with a Small Flame Ignition Source. 1992

27. BS 476-15 Fire Tests on Building Materials and Structures. 1993

28. ISO 5660-1 Fire Tests on Building Materials and Structures. 1993

29. ASTM E 1354 - 08 Heat and Visible Smoke Release Rates for Materials and Products Using an Oxygen Consumption Calorimeter. 2008

30. Paul K. Uses of the Cone Calorimeter. Cellular Polymers. 1993;12:433-460

31. Paul KT. Cone calorimeter: Initial experiences of calibration and use. Fire Safety Journal 1994;22:67-87

32. Schartel B, Bartholmai M, Knoll U. Some comments on the use of cone calorimeter data. Polymer Degradation and Stability. 2005;88:540-547

33. Schartel B, Hull TR. Development of fire-retarded materials - Interpretation of cone calorimeter data. Fire and Materials. 2007;31:327-354

34. Babrauskas V. Development of the cone calorimeter - A bench-scale heat release rate apparatus based on oxygen consumption. Fire and Materials. 1984;8:81-95

35. Huggett C. Estimation of rate of heat release by means of oxygen consumption measurements. Fire and Materials. 1980;4:61-65

36. BS EN ISO 13943 Fire Safety Vocabulary. 2000

37. Bourbigot S, LeBras M. Flame Retardant Plastics, in Troitzsch J, editor. Plastics Flammability Handbook. Munich, Hanser, 2004, pp 133-172

38. ASTM E662-09 Standard test method for specific optical density of smoke generated by solid materials. 2009

39. BS 6401 Method for measurement, in the laboratory, of the specific optical density of smoke generated by materials. 1983

40. BS EN ISO 5659-2 Plastics - Smoke Generation Part 2: Determination of Optical Density by a Single-Chamber Test. 2006

41. Weil ED, Levchik SV. Flame Retardants in Commercial Use or Development for Polyolefins. Journal of Fire Sciences. 2008;26:5-43

42. Weil ED, Levchik S, Moy P. Flame and Smoke Retardants in Vinyl Chloride Polymers - Commercial Usage and Current Developments. Journal of Fire Sciences. 2006;24:211-236

43. Lu S, Hamerton I. Recent developments in the chemistry of halogen-free flame retardant polymers. Progress in Polymer Science. 2002;27:1661-1712

44. Bolger R. Flame retardant minerals bromine issue smoulders on. Industrial Minerals. 1996:29-39

45. Beard A: Flame Retardants - Frequently Asked Questions, The European Flame Retardants Association (EFRA)

46. Kandola BK. An Overview of Flame Retardancy. Proceedings: Flame Retardancy and Flammability of Polymers and Textiles, University of Leeds, June 2008

47. Georlette P, Simons J, Costa L. Halogen-Containing Fire-Retardant Compounds, in Grand AF, Wilkie CA, editors. Fire Retardancy of Polymeric Materials. New York, Marcel Dekker, 2000, pp 245-284

48. Weil ED. Synergists, Adjuvants, and Antagonists in Flame-Retardant Systems, in Grand AF, Wilkie CA, editors. Fire Retardancy of Polymeric Materials. New York, Marcel Dekker, 2000, pp 115-145

49. Laoutid F, Bonnaud L, Alexandre M, Lopez-Cuesta J-, Dubois P. New prospects in flame retardant polymer materials: From fundamentals to nanocomposites. Materials Science and Engineering: R: Reports. 2009;63:100-125

50. Laoutid F, Ferry L, Leroy E, Lopez Cuesta JM. Intumescent mineral fire retardant systems in ethylene–vinyl acetate copolymer: Effect of silica particles on char cohesion. Polymer Degradation and Stability. 2006;91:2140-2145

51. Kim S. Flame retardancy and smoke suppression of magnesium hydroxide filled polyethylene. Journal of Polymer Science Part B: Polymer Physics. 2003;41:936-944

52. Horn WE. Inorganic Hydroxides and Hydroxycarbonates: Their Function and Use as Flame-Retardant Additives, in Grand AF, Wilkie CA, editors. Fire Retardancy of Polymeric Materials. New York, Marcel Dekker, 2000, pp 285-352

53. Hancock M, Rothon RN. Principle Types of Particulate Fillers, in Rothon RN, editor. Particulate Filled Polymer Composites. Shrewsbury, Rapra Technology Ltd, 2003, pp 53-100

54. Rothon RN. Effects of Particulate Fillers on Flame Retardant Properties of Composites, in Rothon RN, editor. Particulate Filled Polymer Composites. Shrewsbury, Rapra Technology Ltd, 2003, pp 263-302

55. Rothon RN: Particulate-Filled Polymer Composites. Shrewsbury, Rapra Technology, 2003

56. Rothon RN, Hornsby PR. Flame retardant effects of magnesium hydroxide. Polymer Degradation and Stability. 1996;54:383-385

57. Green J. Calcination of precipitated $Mg(OH)_2$ to active MgO in the production of refractory and chemical grade MgO. Journal of Materials Science. 1983;18:637-651

58. Brett NH, MacKenzie KJD, Sharp JH. The thermal decomposition of hydrous layer silicates and their related hydroxides. Quarterly Reviews of the Chemical Society. 1970;24:185-207

59. Hornsby PR, Watson CL. A study of the mechanism of flame retardance and smoke suppression in polymers filled with magnesium hydroxide. Polymer Degradation and Stability. 1990;30:73-87

60. Hornsby PR, Watson CL. Mechanism of Smoke Suppression and Fire Retardancy in Polymers Containing Magnesium Hydroxide Filler. Plastics and Rubber Processing and Applications. 1989;11:45-51

61. Hornsby PR, Watson CL. Magnesium Hydroxide - a Combined Flame Retardant and Smoke Suppressant Filler for Thermoplastics. Plastics and Rubber Processing and Applications. 1986;6:169-175

62. Durin-France A, Ferry L, Cuesta JL, Crespy A. Magnesium hydroxide/zinc borate/talc compositions as flame-retardants in EVA copolymer. Polymer International. 2000;49:1101-1105

63. Beck CW. Differential Thermal Analysis Curves of Carbonate Minerals. American Mineralogist. 1950;35:985-1013

64. Todor DN: Thermal Analysis of Minerals. Kent, England, Abacus Press, 1976

65. Sawada Y, Uematsu K, Mizutani N, Kato M. Thermal decomposition of hydromagnesite $4MgCO_3 \cdot Mg(OH)_2 \cdot 4H_2O$. Journal of Inorganic and Nuclear Chemistry. 1978;40:979-982

66. Sawada Y, Uematsu K, Mizutani N, Kato M. Thermal decomposition of hydromagnesite $4MgCO_3 \cdot Mg(OH)_2 \cdot 4H_2O$ under different partial pressures of carbon dioxide. Thermochimica Acta. 1978;27:45-59

67. Sawada Y, Yamaguchi J, Sakurai O, Uematsu K, Mizutani N, Kato M. Thermal decomposition of basic magnesium carbonates under high-pressure gas atmoshpheres. Thermochimica Acta. 1979;32:277-291

68. Sawada Y, Yamaguchi J, Sakurai O, Uematsu K, Mizutani N, Kato M. Thermogravimetric study on the decomposition of hydromagnesite $4MgCO_3 \cdot Mg(OH)_2 \cdot 4H_2O$. Thermochimica Acta. 1979;33:127-140

69. Sawada Y, Yamaguchi J, Sakurai O, Uematsu K, Mizutani N, Kato M. Isothermal differential scanning calorimetry on an exothermic phenomenon during thermal decomposition of hydromagnesite $4MgCO_3 \cdot Mg(OH)_2 \cdot 4H_2O$. Thermochimica Acta. 1979;34:233-237

70. Ozao R, Otsuka R. Thermoanalytical investigation of huntite. Thermochimica Acta. 1985;86:45-58

71. Faust GT. Huntite, A New Mineral. American Mineralogist. 1953;38:4-24

72. Barbieri M, Calderoni G, Cortesi C, Fornaseri M. Huntite, A mineral used in antiquity. Archaeometry. 1974;16:211-220

73. Kangal O, Güney A. A new industrial mineral: Huntite and its recovery. Minerals Engineering. 2006;19:376-378

74. Anthony JW, Bideaux RA, Bladh KW, Nichols MC. Handbook of Mineralogy. http://www.handbookofmineralogy.org/pdfs/hydromagnesite.pdf, accessed 14/04/2009

75. Anthony JW, Bideaux RA, Bladh KW, Nichols MC. Handbook of Mineralogy. http://www.handbookofmineralogy.org/pdfs/huntite.pdf, accessed 14/04/2009

76. Georgiades GN, Larsson BJ, Pust C. Huntite-hydromagnesite production and applications. Proceedings: 12th Industrial Minerals Congress 1996 :57-60

77. Stamatakis MG, Renault RW, Kostakis K, Tsivilis S, Stamatakis G, Kakali G. The hydromagnesite deposits of the Atlin area, British Columbia, Canada, and their industrial potential as a fire retardant. Bulletin of the Geological Society of Greece, Proceedings of the 11th International Congress, Athens 2007 ;37

78. Simandl G, Simandl J, Debreceni A. British Columbia Hydromagnesite-Magnesite Resources: Potential Flame Retardant Material. www.em.gov.bc.ca/DL/GSBPubs/GeoFldWk/2000/Simandl_p327-336.pdf accessed 03/06/2008

79. Simandl GJ, Simandl J. Hydromagnesite in British Colombia, Canada. http://www.em.gov.bc.ca/DL/GSBPubs/Paper/P2004-2/P2004-2-13.pdf accessed 03/06/2008

80. Botha A, Strydom CA. Preparation of a magnesium hydroxy carbonate from magnesium hydroxide. Hydrometallurgy. 2001;62:175-183

81. Teir S, Eloneva S, Fogelholm C, Zevenhoven R. Fixation of Carbon Dioxide by Producing Hydromagnesite from Serpentine. Applied Energy. 2009;86:214-218

82. Frost RL, Hales MC, Locke AJ, Kristof J. Controlled Rate Thermal Analysis of Hydromagnesite. Journal of Thermal Analysis and Calorimetry. 2008;92:893-897

83. Haurie L, Fernández AI, Velasco JI, Chimenos JM, Ticó-Grau JR, Espiell F. Synthetic Hydromagnesite as Flame Retardant. A Study of the Stearic Coating Process. Macromolecular Symposia. 2005;221:165-174

84. Haurie L, Fernández AI, Velasco JI, Chimenos JM, Lopez Cuesta J, Espiell F. Synthetic hydromagnesite as flame retardant. Evaluation of the flame behaviour in a polyethylene matrix. Polymer Degradation and Stability. 2006;91:989-994

85. Haurie L, Fernandez AI, Velasco JI, Chimenos JM, Lopez-Cuesta JM, Espiell F. Effects of milling on the thermal stability of synthetic hydromagnesite. Materials Research Bulletin. 2007;42:1010-1018

86. Haurie L, Fernández AI, Velasco JI, Chimenos JM, Lopez Cuesta J, Espiell F. Thermal stability and flame retardancy of LDPE/EVA blends filled with synthetic hydromagnesite/aluminium hydroxide/montmorillonite and magnesium hydroxide/aluminium hydroxide/montmorillonite mixtures. Polymer Degradation and Stability. 2007;92:1082-1087

87. Winchell AN, Winchell H: Elements of Optical Mineralogy (Part II). New York, John Wiley, 1951

88. Robie RA, Hemingway B. Heat-Capacities at Low-Temperatures and Entropies at 298.15 K of Nesquehonite, $MgCO_3 \cdot 3H_2O$, and Hydromagnesite. American Mineralogist. 1972;57:1768-1781

89. Palache C, Berman H, Frondel C: Dana's System of Mineralogy, ed 7. New York, John Wiley, 1951

90. Bariand P, Cesbron FP, Vachey H, Sadrzadeh M. Hydromagnesite from Soghan, Iran. The Mineralogical Record. 1973;4:18-20

91. Dana JD. Mineralogical Contributions. American Journal of Science. 1854;17:78-88

92. Rogers AF. Crystallography of Hydromagnesite. American Journal of Science. 1923;6:37-47

93. Murdoch J. Unit Cell of Hydromagnesite. American Mineralogist. 1954;39:24-29

94. White WB. Infrared Characterization of Water and Hydroxyl Ion in the Basic Magnesium Carbonate Minerals. The American Mineralogist. 1971;56:46-53

95. Akao M, Iwai S. The hydrogen bonding of hydromagnesite. Acta Crystallographica Section B. 1977;33:1273-1275

96. Akao M, Maruma F, Iwai S. The crystal structure of hydromagnesite. Acta Crystallographica Section B. 1974;30:2670-2672

97. Downs RT, Hall-Wallace M. The american mineralogist crystal structure database. American Mineralogist. 2003;88:247-250

98. America mineralogist crystal structure database. http://rruff.geo.arizona.edu/AMS/amcsd.php, accessed 19/11/11

99. XtalDraw. www.geo.arizona.edu/xtal/group/software.htm, accessed 19/11/11

100. Padeste C, Oswald HR, Reller A. The thermal behaviour of pure and nickel-doped hydromagnesite in different atmospheres. Materials Research Bulletin. 1991;26:1263-1268

101. Botha A, Strydom C. DTA and FT-IR analysis of the rehydration of basic magnesium carbonate. Journal of Thermal Analysis and Calorimetry. 2003;71:987-996

102. Khan N, Dollimore D, Alexander K, Wilburn FW. The origin of the exothermic peak in the thermal decomposition of basic magnesium carbonate. Thermochimica Acta. 2001;367-368:321-333

103. Nahdi K, Rouquerol F, Trabelsi Ayadi M. $Mg(OH)_2$ dehydroxylation: A kinetic study by controlled rate thermal analysis (CRTA). Solid State Sciences. 2009;11:1028-1034

104. Inglethorpe SDJ, Stamatakis MG. Thermal decomposition of natural mixtures of hydromagnesite and huntite from Kozani, Northern Greece. Mineral Wealth. 2003:7-18

105. Ramsdell LS. Presentation of the Roebling Medal to Walter F. Hunt. American Mineralogist. 1958;43:334-335

106. Graf DL, Bradley WF. The crystal structure of huntite, $Mg_3Ca(CO_3)_4$. Acta Crystallographica. 1962;15:238-242

107. Dollase WA, Reeder RJ. Crystal structure refinement of huntite, $CaMg_3(CO_3)_4$, with X-ray powder data. American Mineralogist. 1986;71:163-166

108. Riederer J. Recently identified Egyptian pigments. Archaeometry. 1974;16:102-109

109. Eremin K, Stenger J, Huang J, Aspuru-Guzik A, Betley T, Vogt L, Kassal I, Speakman S, Khandekar N. Examination of pigments on Thai manuscripts: the first identification of copper citrate. Journal of Raman Spectroscopy. 2008;39:1057-1065

110. Patel P, Hull TR, McCabe RW, Flath D, Grasmeder J, Percy M. Mechanism of thermal decomposition of poly(ether ether ketone) (PEEK) from a review of decomposition studies. Polymer Degradation and Stability. 2010;95:709-718

111. Liodakis S, Antonopoulos I. Evaluating the fire retardation efficiency of diammonium phosphate, ammonium sulphate and magnesium carbonate minerals on Pistacia lentiscus L. Environment Identities and Mediterranean Area, 2006 ISEIMA '06 First international Symposium on. 2006:35-39

112. Liodakis S, Antonopoulos I, Agiovlasitis IP, Kakardakis T. Testing the fire retardancy of Greek minerals hydromagnesite and huntite on WUI forest species Phillyrea latifolia L. Thermochimica Acta. 2008;469:43-51

113. Liodakis S, Antonopoulos I, Tsapara V. Forest fire retardancy evaluation of carbonate minerals using DTG and LOI. Journal of Thermal Analysis and Calorimetry. 2009;96:203-209

114. Liodakis S, Agiovlasitis IP, Antonopoulos I, Stamatakis MG. Fire retarding performance of hydromagnesite on forest species from a wildland/urban interface area in Athens. Forest Ecology and Management. 2006;234:S126-S126

115. Liodakis S, Antonopoulos I, Kakardakis T. Evaluating the use of minerals as forest fire retardants. Fire Safety Journal. 2010;45:98-105

116. Bensalem A, Chang W, Fournier A, Kallianos G, Paine J, Podraza K, Schleich D, Seeman J. Smoking Article Wrapper Having Filler of Hydromagnesite / Magnesium Hydroxide and Smoking Article made with said Wrapper. US Patent 5,979,461. 1999

117. Bensalem A, Chang W, Fournier JA, Kallianos AG, Paine J, Podraza K, Schleich D, Seeman J. Hydromagnesite / Magnesium Hydroxide Fillers for Smoking Article Wrappers and Methods for making Same. US Patent 5,927,288. 1999

118. Alternative FR filler for rubber and plastics. Plastics and Rubber Weekly. 1988:10

119. Mineral Fire Retardant Filler Suppresses Smoke. European Plastics News. 1988;15:40

120. Mineral Filler is Flame Retardant, Smoke Suppressor. Modern Plastics International. 1990;20:10/2

121. Kirschbaum GS. Huntite/hydromagnesite - Mineral Flame Retardants as Alternative and Complement to Metal Hydroxides. Proceedings: Flame Retardants ’98, London. 1998:151-161

122. Kirschbaum G. Minerals on Fire: Flame Retardants Look to Mineral Solutions. Industrial Minerals. 2001:61-67

123. Clemens ML, Doyle MD, Lees GC, Briggs CC, Day RC. Non-Halogenated Flame Retardant for Polypropylene. Proceedings: Flame Retardants ’94, Manchester. 1994:193-202

124. Basfar AA, Bae HJ. Influence of Magnesium Hydroxide and Huntite Hydromagnesite on Mechanical Properties of Ethylene Vinyl Acetate Compounds Cross-linked by DiCumyl Peroxide and Ionizing Radiation. Journal of Fire Science. 2010;28:161-180

125. Rigolo M, Woodhams RT. Basic magnesium carbonate flame retardants for polypropylene. Polymer Engineering & Science. 1992;32:327-334

126. Kandola BK, Pornwannachai W. Enhancement of Passive Fire Protection Ability of Inorganic Fire Retardants in Vinyl Ester Resin Using Glass Frit Synergists. Journal of Fire Science. 2010;28:357-381

127. Geoffrey C. Fire-retardant additives and their uses. 1991;Patent EP 0420302

128. Jachimi R. Intumescent one-component sealant. 1997;Patent US 5594046

129. Nguyen DT, Langille KB, Veinot DW, Bernt JO. Compound of intumescent powder and thermoplastic material. 2004;Patent US 6790893 B2

130. Seii U, Katsuji T. Fire retardant and fire resistant ethylene-propylene-diene copolymer composition and low voltage fire resistant wire/cable. 2007;Patent JP 2007169415

131. Shoichiro N. Fire resistant silicone resin composition and low voltage fire resistant cable. 2005;Patent JP 2005171191

132. Spano VW. Passive fire protection. 1997;Patent US 5643661

133. Morgan AB, Cogen JM, Opperman RS, Harris JD. The effectiveness of magnesium carbonate-based flame retardants for poly(ethylene-co-vinyl acetate) and poly(ethylene-co-ethyl acrylate). Fire and Materials. 2007;31:387-410

134. Staveley LAK, Linford RG. The heat capacity and entropy of calcite and aragonite, and their interpretation. The Journal of Chemical Thermodynamics. 1969;1:1-11

135. Anderson CT. The Heat Capacities of Magnesium, Zinc, Lead, Manganese and Iron Carbonates at Low Temperatures1. Journal of the American Chemical Society. 1934;56:849-851

136. Touré B, Lopez-Cuesta J, Benhassaine A, Crespy A. The Combined Action of Huntite and Hydromagnesite for Reducing Flammability of an Ethylene-Propylene Copolymer. International Journal of Polymer Analysis and Characterization. 1996;2:193-202

137. Mitzlaff M, Troitzsch J. Building, in Troitzsch J, editor. Plastics Flammability Handbook. Munich, Hanser, 2004, pp 227-432

138. Toure B, Cuesta JL, Gaudon P, Benhassaine A, Crespy A. Fire resistance and mechanical properties of a huntite/hydromagnesite/antimony trioxide/decabromodiphenyl oxide filled PP-PE copolymer. Polymer Degradation and Stability. 1996;53:371-379

139. Wagner ER, Joesten BL. Halogen-modified impact polystyrenes: Quantification of preflame phenomena. Journal of Applied Polymer Science. 1976;20:2143-2155

140. Briggs C, Rutherford A, SPE. Unique Flame Retardant Filler for Pe and Other Cable Compounds. Proceedings Antec ’90, Dallas, 1990:1216-1221

141. Briggs CC. Ultracarb: The natural flame retardant. Paper presented at the Fillers and Additives in Plastics '91 European Technical Conference, held 9-10 October, 1991, Lund, Sweden. 1991:20

142. Briggs CC, Bhardwaj B, Gilbert M. Flame Retardant PVC Cable Compounds using Huntite-Hydromagnesite. Proceedings Filplas ’92, Manchester 1992

143. Briggs CC. Reduced Hazard Flame Retardant PVC Compounds. Proceedings PVC ’93, Brighton, 1993

144. Briggs CC, Day RC, Gilbert M, Hollingbery LA. Optimising Fire Properties for Plasticised PVC Compounds. Proceedings PVC ’96, Brighton, 1996:269-280

145. Briggs CC, Hollingbery LA, Day RC, Gilbert M. Optimising fire properties of plasticised poly(vinyl chloride) compounds. Plastics rubber and composites processing and applications. 1997;26:66-77

146. BS 7655 Specification for insulation and sheathing materials for cables. 2000

147. Laoutid F, Gaudon P, Taulemesse J-, Lopez Cuesta JM, Velasco JI, Piechaczyk A. Study of hydromagnesite and magnesium hydroxide based fire retardant systems for ethylene–vinyl acetate containing organo-modified montmorillonite. Polymer Degradation and Stability. 2006;91:3074-3082

148. Hull TR, Quinn RE, Areri IG, Purser DA. Combustion toxicity of fire retarded EVA. Polymer Degradation and Stability. 2002;77:235-242

149. Ashton HC. Fire Retardants, in Xanthos M, editor. Functional Fillers for Plastics. Weinheim, Wiley-VCH Verlag, 2005, pp 285-315

150. Hemingway B, Robie RA. Heat-Capacities at Low-Temperatures and Entropies at 298.15 K of Huntite, and Artinite. American Mineralogist. 1972;57:1754-1767

151. Xiong Y. Experimental determination of solubility constant of hydromagnesite (5424) in NaCl solutions up to 4.4 m at room temperature. Chemical Geology. 2011;284:262-269

152. Kiselev AV, Lygin VI. Electron-microscopic study of the porous structure of magnesium hydroxide and its changes under thermal treatment. Russian Chemical Bulletin. 1959;8:388-394

153. Conesa JA, Marcilla A, Font R, Caballero JA. Thermogravimetric studies on the thermal decomposition of polyethylene. Journal of Analytical and Applied Pyrolysis. 1996;36:1-15

154. Vasile C, Costea E, Odochian L. The thermoxidative decomposition of low density polyethylene in non-isothermal conditions. Thermochimica Acta. 1991;184:305-311

155. Huang J, Lu W, Yeh M, Lin C, Tsai I. Unusual thermal degradation of maleic anhydride grafted polyethylene. Polymer Engineering & Science. 2008;48:1550-1554

156. Wang Z, Qu B, Fan W, Huang P. Combustion characteristics of halogen-free flame-retarded polyethylene containing magnesium hydroxide and some synergists. Journal of Applied Polymer Science. 2001;81:206-214

157. Li Z, Qu B. Flammability characterization and synergistic effects of expandable graphite with magnesium hydroxide in halogen-free flame-retardant EVA blends. Polymer Degradation and Stability. 2003;81:401-408

158. Zhang J, Wang X, Zhang F, Richard Horrocks A. Estimation of heat release rate for polymer–filler composites by cone calorimetry. Polymer Testing. 2004;23:225-230

159. Stoliarov SI, Safronava N, Lyon RE. The effect of variation in polymer properties on the rate of burning. Fire and Materials. 2009;33:257-271

160. Hull TR, Witkowski A, Hollingbery LA. Fire retardant action of mineral fillers. Polymer Degradation and Stability. 2011;96:1462-1469